KONINKLIJKE NEDERLANDSE AKADEMIE VAN WETENSCHAPPEN

PROCEEDINGS

SERIES B

PHYSICAL SCIENCES

VOLUME LXIII - No. 3

NORTH-HOLLAND PUBLISHING COMPANY - AMSTERDAM - 1960

The complete Proceedings consist of three Series, viz.:

SERIES A: MATHEMATICAL SCIENCES

SERIES B: PHYSICAL SCIENCES

SERIES C: BIOLOGICAL AND MEDICAL SCIENCES

Articles for these Series cannot be accepted unless formally communicated for publication by one of the members of the Royal Neth. Academy of Sciences.

The Royal Society celebrates its tercentenary in July, 1960. To mark the occasion a series of special articles has been written by eminent scientists describing, often at first hand, progress in some various fields of science in which United Kingdom research is contributing to world knowledge. Lord Hailsham, who is Lord Privy Seal and Minister for Science in Mr. Harold Macmillan's Government has written this foreword to the series.

It is with great pleasure that the Royal Netherlands Academy of Sciences publishes this foreword and also some of the articles in sign of esteem for the Royal Society and a mark of sympathy for its tercentenary.

M. W. Woerdeman,
President of the Royal Netherlands Academy of Sciences

BRITAIN's CONTRIBUTION TO THE MODERN AGE OF SCIENCE

BY

LORD HAILSHAM

Lord Privy Seal and Minister for Science

For three hundred years the Royal Society has been the natural focus of scientific opinion, and a continuous source of encouragement and initiation in the development of scientific research. It is therefore particularly appropriate that their tercentenary celebrations should be marked by the publication of a series of authoritative articles on British scientific achievements. The development of science is a field in which I have been concerned as a Minister over the past two years, and will be yet more deeply concerned in the future. I am therefore particularly glad to contribute a foreword to this series of articles.

It would be difficult to overrate the importance of science in our national life. In industry and agriculture, in peace and in war it is trite, but never superfluous, to remind ourselves that survival depends on our scientific achievement. But, I would stress today that man does not live by bread alone. British contributions to science are part of our national culture and science itself is actually and potentially a great source of spiritual and intellectual enrichment in the modern world.

One Of Several Partners

The appointment by the Government of a Minister for Science implies a fresh recognition of these truths. But the Minister is there not to control and direct scientists, but to help them by advocating the needs of the scientists and the sciences inside and outside the Government.

For the Government is only one of several partners. The others include the teaching profession, the universities, industry, agriculture, and, of course, the scientists in all vocations who are most conspicuously represented in our national life by the Royal Society. It is through the co-operation of all these that we may look for the continuous advancement of scientific knowledge and improved application of it for the national good.

Hailsham

This article is one of a series specially written by leading scientists in Britain to mark the 300th anniversary of the Royal Society in July, 1960. The Royal Society—or to use its full title, "The Royal Society of London for the Promotion of Natural Knowledge"—received its first Charter from King CHARLES II, who also described himself as its founder and patron . . .*).

CRYSTALLOGRAPHY

ACHIEVEMENTS IN X-RAY CRYSTALLOGRAPHY

BY

SIR LAWRENCE BRAGG, F.R.S.

Director of the Royal Institution, London, the scientific body made famous by Michael Faraday

(Communicated at the meeting of February 27, 1960)

X-ray crystallography is the deduction of the arrangement of atoms in various types of substances, and particularly in crystals, by studying the manner in which these substances scatter a beam of X-rays. It became possible when the German scientist VON LAUE discovered X-ray diffraction by a crystal in 1912. The rays from a Röntgen Ray tube were limited to a narrow beam by passing them through a fine hole, and when this beam fell on a crystal, and the scattered rays were recorded by a photographic plate, the photographs showed a symmetrical pattern of spots. VON LAUE correctly interpreted this effect as due to the "diffraction" of X-ray waves by the regular pattern of atoms in the crystal.

This discovery was a crucial event in the history of science. In addition to proving conclusively that X-rays were electromagnetic waves like light, and leading to the study of the characteristic X-ray wavelengths emitted by the elements which played a key part in subsequent research into atomic structures, it made it possible to analyse the structure of matter in a new and very powerful way.

Optical Grating Principle

The effect is due to the same principle which governs the production of spectra by a diffraction grating. An optical grating consists of a number of fine lines ruled regularly on a glass or metal plate. When light falls on such a grating, each line scatters a wavelet. In certain directions, depending on the spacing of the grating and the wavelength of the light, the wavelets combine so that their crests and troughs coincide, and in

*) The other articles of this series published by the Royal Netherlands Academy of Sciences, appeared in the following journals: this Proceedings, p. 221; Proceedings C, Biological and Medical Sciences, Vol. LXIII, No. 3, p. 286; Verslag van de Gewone Vergadering der Afdeling Natuurkunde, Deel LXIX, No. 2, pag. 29.

these directions a strong beam of light is scattered. In other directions there is no such fit, the waves cancel each other's effects, and there is no scattered beam. This is the principle of "Interference" enunciated by the famous THOMAS YOUNG in the first years of the 19th century, who first clearly demonstrated the wave nature of light. Many of the most beautiful colours in nature, such as the iridescent sheen on some beetles, the blue of a butterfly's wing or a jay's feather, the play of colour in mother-of-pearl or, more strikingly, in an opal, are not due to pigments, but to interference.

There is therefore no new optical principle in X-ray diffraction, but there is a contrast in emphasis. An optical grating is used to analyse light. Because of wavelength differences, red light consisting of the larger waves and blue light of the shorter waves, the grating diffracts each wavelength in characteristic directions. A very simple pattern of regular lines in the grating is used to analyse a complex spectrum consisting of many different wavelengths.

Monochromatic Beam

In X-ray analysis, on the other hand, we wish to analyse the grating. The simplest possible spectrum is used, in fact a monochramatic X-ray beam consisting of a single wavelength. This falls on a complex grating composed of atoms arranged in some kind of regular pattern in three dimensions. The aim is to deduce the atomic arrangement from the directions and intensities of the scattered beams or "spectra".

It would be out of place to outline the rather complicated geometry of the effect in this article. It may perhaps suffice to say that every variation of atomic pattern produces a characteristic pattern of X-ray diffraction which we can calculate, so by observing the latter we can deduce the former.

Conditions Precisely Right

One point may be noted. Nature has been kind to us in arranging that the scale of dimensions is just right. X-ray waves are about 1,000 times shorter than light waves, and their wavelength is of the same order of magnitude as the distance between atoms in crystals. This is precisely the right condition for the interference of the waves scattered by the different atoms in the crystal, which are regularly arranged like soldiers drawn up on parade or the pattern of a wall-paper.

This new art of X-ray analysis is so important because it has cast a flood of light on problems in many branches of science. Chemists are able to tell us the proportions of the elemental atoms which build up chemical compounds. In some cases, in particular in the case of the compounds of the element carbon, they can discover which atom is linked to which. But X-ray analysis goes further; it gives us a map or blueprint of the structure, with each atom in its correct place, so that we

can see how it is surrounded by its neighbours and how far away they are. Just as a blueprint explains to an engineer how a machine works, so this map makes it possible for the scientist to understand why bodies possess their properties and how they interact with each other.

Fantasy Realised

In "The Ethics of the Dust", Ruskin explained to his class of young ladies what fascinating patterns they would find if only they had a way of magnifying a speck of dust so much that they could see the patterns of its building stones or atoms. We are now able to realise his fantasy.

Scientists in all countries have made contributions to the art of X-ray analysis, but it can be claimed that the United Kingdom has played a leading part. The first analyses were made in the U.K., and up to the present a large proportion of the major advances in applying it to increasingly complex problems have had their origin in British laboratories. In reviewing the structures which have been analysed, we can play a kind of "animal, mineral, and vegetable" game, though these are not quite the categories we want. The convenient ones are – Inorganic (oxides, salts, minerals), Organic (the compounds of carbon), Metallic (metals and alloys), and finally Biological (the vast molecules which play a part in life processes).

The First Analyses

Most of the first structures to be analysed were inorganic, because they were simple. The first of all was the structure of rocksalt, or sodium chloride NaCl, shown in Figure 1, where the two types of sphere show the position of the centres of sodium (Na) and chlorine (Cl) atoms. Innocent though this structure may appear, it caused something like a

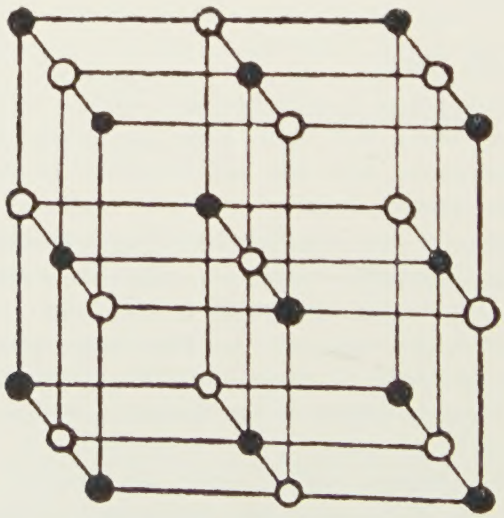

Fig. 1. The structure of rock salt (sodium chloride).

minor chemical revolution. A cornerstone of chemistry is the conception of the molecule, the basis of Dalton's atomic theory. The vast numbers of different chemical compounds are built from comparatively few elements. Dalton postulated that each pure compound is composed of identical molecules, each molecule being a small family party of various atoms united together as a group. For instance, sodium chloride was held to be composed of molecules each containing one atom of sodium and one of chlorine. But, looking at the structure in Figure 1, where is the molecule? Each sodium atom (Na) is surrounded equally by six chlorine atoms (Cl), and each chlorine atom by six sodium atoms, in a kind of three-dimensional chessboard pattern, and there is nothing to indicate that one sodium is particularly linked to one chlorine.

A Hard Fight

The answer, as is now realised, is that the structure is composed of charged atoms or ions, sodium being positive and chlorine negative. It is the electrical attraction of these opposite charges which holds the structure together, and of course each positive tends to be surrounded by negatives, and vice versa. The equality in numbers of sodium and chlorine atoms comes, not from pairing of one sodium with one chlorine, but because the electrical charges must balance. So there is no molecule; it is as if we had found that the numbers of ladies and gentlemen at dinner parties is generally equal and falsely concluded they were all necessarily married couples, instead of realising that it was because each lady liked to have a gentleman on either side, and vice versa. It was a hard fight to get the idea accepted. I remember well how we were begged by the chemists to find some inclination, however slight, of a sodium atom to the chlorine to which it properly belonged!

The idea of inorganic compounds being composed of ions has given a new slant to inorganic chemistry. It has its most striking application in the structure of the minerals. The most common elements, which form by far the greatest proportion of the Earth's crust, are oxygen, silicon, and aluminium. Sand, for instance, is mostly silica or quartz, a substance made up of silicon and oxygen in such a way that there are twice as many oxygen ions as silicon ions. These are highly charged ions with strong attractions. Silicon is always surrounded by four oxygen atoms at the corners of a tetrahedron, aluminium by six at the corners of an octahedron, (like two pyramids joined base to base), or sometimes by four like silicon. The framework of the common minerals, the silicates, is a kind of fabric of these tetrahedra and octahedra linked by the oxygen atoms at their corners.

Like Patterns of Knitting Stitches

We may compare these two types to the purl and plain stitches in knitting, which in suitable combinations can produce such complex

patterns on garments. The tetrahedra are the strongest stitches, and it can be seen at once that there must be four main types of pattern which can be built with them. They can either be separate, or they can be joined corner to corner in a long string, or they can be joined by three corners to make sheets, or by all corners to make a three-dimensional framework (see Figure 2).

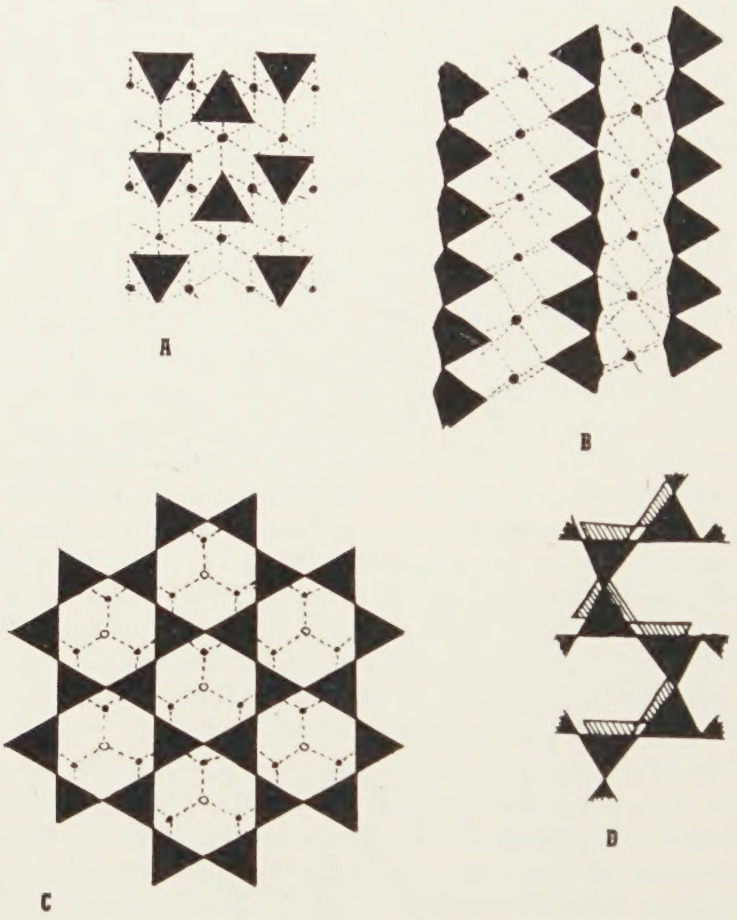

Fig. 2. Schematic representation of the main silicate structures. (a) Isolated groups. (b) Chains. (c) Sheets. (d) Three-dimensional frameworks.

These are precisely the four great families of silicate minerals. The first is represented by the dense olivines (the jewel peridot is an olivine), the second by such fibrous minerals as asbestos, the third by mica and the minute spangles which form clay, the last by the felspars of which the pink or grey opaque crystals in a granite are an example.

Complexity Resolved Into Order

These minerals, and others like them, are held together by strong forces and hence have a high melting point, and they are relatively light;

hence, as the Earth cooled, they came to the top and form the crust on which we live. A knowledge of structure has turned complexity into order and simplicity. The dynamics of the structures were elucidated by the American scientist Linus Pauling but the main story of the silicates was worked out in the United Kingdom.

If the idea of the molecule was found to be inappropriate in inorganic compounds, it received ample vindication when organic compounds came to be analysed by X-rays. These compounds are for the main part composed of carbon, oxygen, nitrogen and hydrogen. The atoms are bound together by links which are strong and which are localised, as if each atom had places in its surface to which another atom could be bolted. The groups of atoms so linked together into a chemical molecule

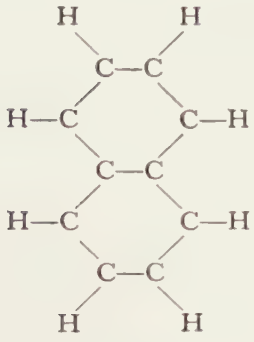

Naphthalene, $C_{10}H_8$

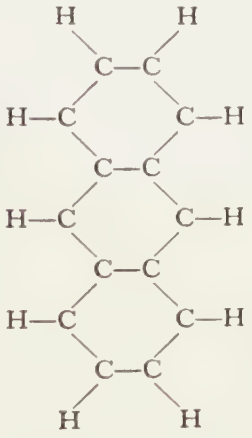

Anthracene, $C_{14}H_{10}$

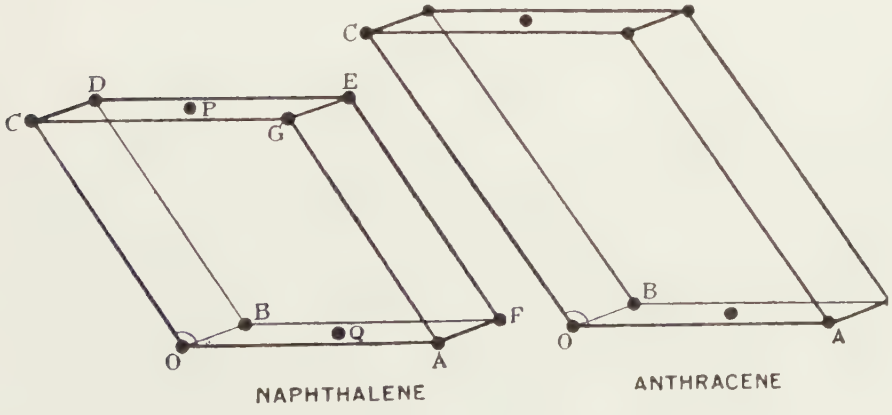

Fig. 3. Naphthalene and anthracene.

are bound by comparatively weak forces to neighbouring molecules, hence they can be regarded as separate entities in a real molecular sense. This is in contrast to the inorganic compounds which form a continuous structure of alternating positive and negative ions.

Rapid Development

The analysis of organic compounds began with my father's work on naphthalene and anthracene illustrated in Figure 3. Organic chemists had shown that the former of these consisted of two benzene rings and the latter of three benzene rings fused together. The distance between carbon atoms had been ascertained from the structure of diamond. The "unit cell" or box containing each pattern element of a crystal can be directly found by X-ray analysis, and my father was able to show that the box on the left could just contain two naphthalene molecules, that on the right two anthracene molecules, of the form postulated by organic chemistry. X-ray analysis of organic compounds developed rapidly after this start, at first in the main confirming and making precise the pictures of organic molecules deduced by the methods of stereo-chemistry, and latterly discovering molecular structures which had hitherto defied chemical analysis. In contrast to this start, Figures 4 and 5 show two

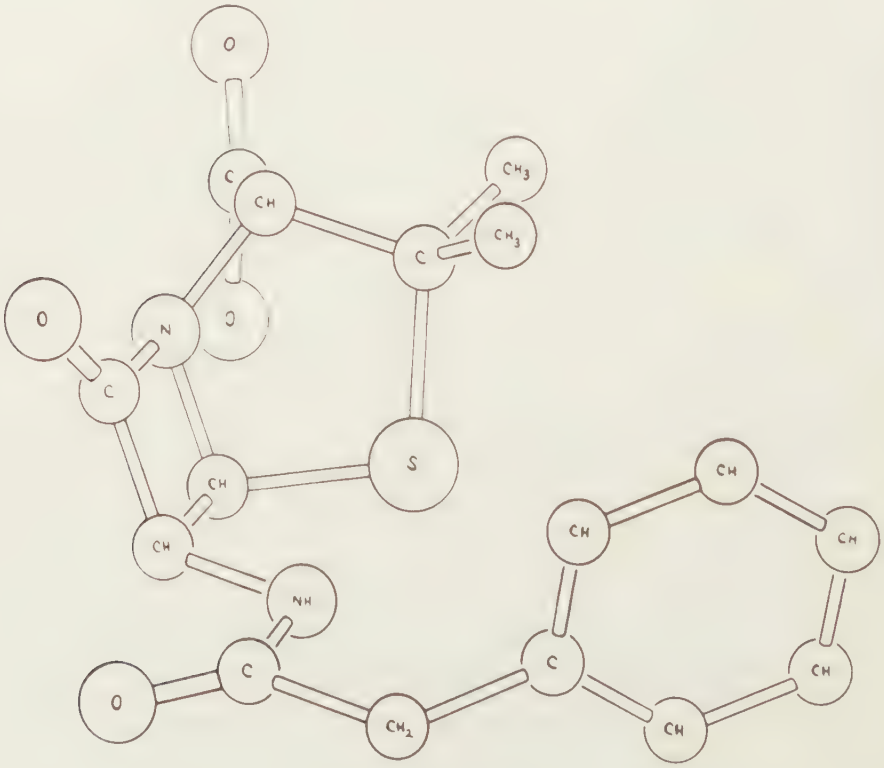

Fig. 4. Penicillin.

recent triumphs, the positions of the atoms in the molecules of penicillin and vitamin B12, determined by Mrs. Hodgkin, F.R.S., and her colleagues, by X-ray analysis in her Oxford Laboratory.

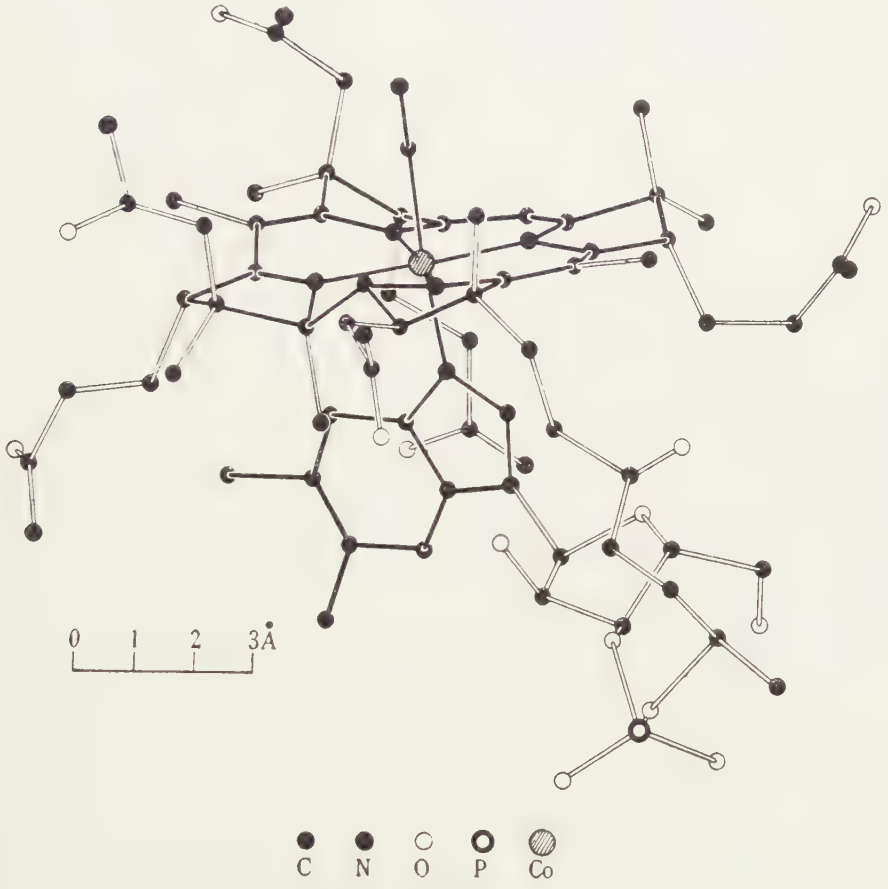

Fig. 5. Vitamin B_{12}.

The story of the compounds between metals, or alloys, is very fascinating and involves quite new ideas. The basis of Dalton's atomic hypothesis was the law governing the definite proportions in which atoms combine to form compounds. This gave rise to the conception of family parties of atoms, the molecules, which we have seen to have been misleading in inorganic compounds but appropriate to organic compounds. In alloys, the law of combining proportions no longer holds. When one metal is alloyed with another—for instance, zinc with copper—a series of different structures is formed, depending upon the proportions of zinc and copper in the alloy. Each structure is not characterised, however, by a definite ratio of the two elements; on the contrary, it exists over a certain range of proportions which is often quite extensive.

Reason Is Clear

The reason for this is clear if we consider the peculiar nature of a metal. A metal atom is characteristically electropositive, that is to say it has one or more electrons which are very easily detached from the atom leaving it a positive ion. When metal atoms come together to form a metal structure, these loosely-held electrons cease to belong to individual atoms and become a continuous electron sea with the positive ions embedded in it. The structure is held together by the electrostatic attraction between the positive ions and the enveloping negative electron sea. There are no bonds between atoms; that is why a metal can be distorted without breaking.

No Law Of Combining Proportions

The same conception explains the non-existence of a law of combining proportions. There is no longer a need to balance the numbers of positive and negative atoms as in an inorganic crystal, because each atom brings with it its own balancing charge in the electrons it contributes to the structure. We may liken it to one of those parties of the type where the number and balance of the guests is not of prime importance because each brings his own supply of drink. An important factor in determining the phase structure is the ratio of the number of electrons to the number of atoms. When zinc is added to copper, each zinc atom brings two electrons with it, while the copper has one, so the electron-atom ratio is increased. The phase structure, at first simple, assumes more complex forms as the amount of zinc increases. Scientists in many countries contributed to this story, but the work on complex alloys by Bradley in Manchester, and on the influence of the electron-atom ratio by Hume-

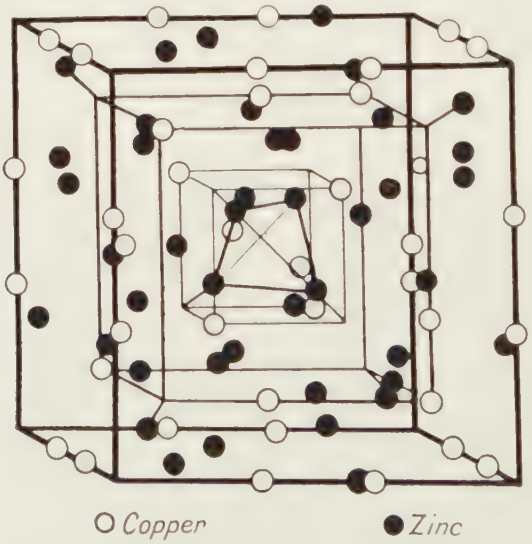

Fig. 6. Brass, an alloy of copper and zinc.

Rothery in Oxford, was outstandingly important. Figure 6 shows an example of Bradley's analysis.

A Separate Class

Biological molecules are essentially organic compounds like those already described, but they are conveniently considered in a separate class because of their size and complexity. The molecule of haemoglobin, for instance, which colours our blood red and has the task of conveying oxygen from our lungs, which absorb it when we breathe, to the muscles and other parts of the body where it is needed, has a molecular weight of 68,000 and contains about 12,000 atoms. Protein molecules, of which haemoglobin is an example, are for the most part composed of carbon, oxygen, nitrogen, and hydrogen, like all organic compounds, and also contain a few atoms of special kinds such as sulphur.

It appears that each type of protein molecule has a specific task to perform. It may be quite a simple one, like that of carrying oxygen, but the complexity of the molecule may be ascribed to the need to do this task at just the right place and in just the right way. We are reminded of the contrast between the simple letter delivered at our door, and the complex of delivery van and postman, and indead all the organisation behind them, to ensure that the letter reaches the right address.

Carriers Of The Hereditary Factor

A whole group of proteins called enzymes is concerned with the various chemical tasks in our bodies. Another group of biological molecules comes under the heading of "nucleic acid". It appears to be their task to act as the templates on which new protein is manufactured, and as the types of protein made determine the nature of the organism, they are the carriers of the hereditary factor in a parent which decides the nature of its offspring.

The successful application of X-ray analysis to the study of these biological molecules is one of the romances of modern science. A vast amount of brilliant research on their constitution had been done by chemical techniques; the X-ray work is based on this foundation, but it has performed its typical function of giving precision to the picture. An account of the biological implications of the results is given in another article of the present series, so examples will not be given here. I will restrict myself to saying how thrilling it has been to see that X-ray analysis can be applied to such very complex bodies.

Protein Structure Analysed

The leading X-ray group in the country has been the research unit directed by Perutz and Kendrew in Cambridge and supported by Britain's Medical Research Council. Their work has resulted in the first successful analysis of a protein structure by Kendrew, the myoglobin molecule

which acts as a store-house of oxygen in muscle. It would have been almost inconceivably difficult to tackle a molecule containing 3,000 atoms (myoglobin is about one-quarter the size of haemoglobin) by the X-ray techniques which had served for simple molecules.

Success has been attained owing to a discovery by Perutz that certain heavy atoms such as mercury, iodine, or gold, could be chemically attached to specific points of each molecule without disturbing the crystal structure.

A Massive Assault

It is relatively easy to discover the positions in the structure of these heavy marker atoms, which scatter the X-rays far more powerfully than the light atoms of the organic complex. By noting the differences which they cause to the X-ray diffraction, it is possible to apply an analysis which reveals the protein structure.

It is a massive frontal assault. Vast numbers of measurements have to be made, and the results are fed into electronic computers which perform in a few seconds calculations which would take as many weeks if done by human agency. The results are just now coming off the production line, and it is a very exciting time.

Another extremely important success of the Cambridge unit was the establishment of the structure of nucleic acid by Crick and his American colleague Watson. This structure, which will also be described elsewhere, has suggested a fascinating mechanism for the processes of heredity.

Why is this so important? It is again a question of the precise picture. The functions of these molecules must be dependent upon their geometry. They must just so fit each other that the right parts are brought into conjunction, and can interact chemically. We may hope to understand such processes when we know the structure—we may hope to see how the enzymes act, why vitamins are necessary, what hormones do, why certain substances are poisonous. As in other and simpler realms of X-ray analysis, we can confidently hope that a new flood of light will be cast by this new knowledge.

This article is one of a series specially written by leading scientists in Britain to mark the 300th anniversary of the Royal Society in July, 1960. The Royal Society—or to use its full title, "The Royal Society of London for the Promotion of Natural Knowledge"—received its first Charter from King CHARLES II, who also described himself as its founder and patron . . .*).

PHYSICS

ACCURATE MEASUREMENT OF TIME

BY

LOUIS ESSEN,

a senior scientist at Britain's National Physical Laboratory. He built the first atomic clock using caesium atoms at this Laboratory

(Communicated at the meeting of February 27, 1960)

Our domestic clocks can be set right to within one second by means of the six "pips" broadcast by the British Broadcasting Corporation, and more accurate clocks used for scientific purposes can be set to about one-hundredth of a second by means of special time signals from the Royal Greenwich Observatory.

The very ease with which clocks can be set in this way may conceal the complex processes involved in establishing the accurate time scale on which the signals are based.

The Solar Day

Any process which is repeated in a regular manner can be used to indicate the passage of time, but the regular movements of the bodies of the solar system are so inescapably obvious that they have been adopted for this purpose from the earliest times until the present day. In particular, the rotation of the Earth on its axis gives the solar day, which is divided by means of clocks into hours, minutes and seconds.

Although the solar day which governs our daily routine is such an obvious choice as the astronomical unit of time, it possesses two marked disadvantages: it is not of equal value throughout the year, and it cannot be measured very precisely.

Anyone who has seen a star moving across the field of a telescope will realise how much more precisely the passing of a star can be timed as it

*) The other articles of this series published by the Royal Netherlands Academy of Sciences, appeared in the following journals: this Proceedings, p. 210; Proceedings C, Biological and Medical Sciences, Vol. LXIII, No. 3, p. 286; Verslag van de Gewone Vergadering der Afdeling Natuurkunde, Deel LXIX, No. 2, p. 29.

crosses a point vertically overhead; and in practice stellar observations are used to determine the sidereal day, which is the time of rotation of the Earth relative to the fixed stars. This is then converted, from a knowledge of the length of the year, into the mean solar day.

A number of other corrections for known irregularities of the Earth's rotation are also made, and the clocks which supply the time signals are adjusted to keep in time with a hypothetical day based on current and past astronomical measurements and corrected to give a unit as nearly as possible uniform throughout the year.

It is important to notice that astronomical time serves two quite different purposes – it gives the time of day, which is required for civil and some scientific purposes, and also furnishes a scale of time on which the duration of events can be measured. It thus supplies the answers to the questions "What time is it?" and "How long does it take?" Most scientific work is concerned with the second question, and modern developments, particularly in the field of radio, often require a very exact measurement of extremely short events.

Quartz Clocks

When we are concerned with short events such as the time of one oscillation of a radio wave, it is more convenient to speak of the number of times the event is repeated in a second, that is to say, its frequency. The frequency of the transmitter at Droitwich, England, for example, is 200,000 cycles per second, and the frequency of television transmitters is in the region of 100,000,000 cycles per second.

Transmitting stations each operate in a narrow band of frequencies and, if they are not to interfere, they must keep strictly within this band. The accurate measurement and control of frequencies is essential if full use is to be made of the radio frequency spectrum available. Frequencies cannot be measured easily in terms of pendulum clocks, and a new form of clock, the quartz clock, was developed. A common form of this consists of a ring of about five centimetres diameter cut from a natural quartz crystal, and maintained in vibration by a radio valve at a frequency of 100,000 cycles per second.

The frequency depends mainly on the dimensions of the quartz ring, but can be pulled a little by the electrical circuit so as to have exactly its nominal value. Radio valves can be used as a reduction gear to give an electrical impulse for every 100,000 vibrations, and these "seconds" impulses can operate an ordinary clock dial. The quartz clock thus gives a time scale which is sub-divided into very small fractions of a second and yet can extend for a number of years. This time scale provided by quartz clocks and astronomical observations of the stars enables intervals of time to be measured with an accuracy of one part in 100,000,000 (1×10^{-8}).

The fine sub-divisions of the quartz clock time scale can be displayed on the screen of a cathode ray oscilloscope, and the duration of a single event can be measured by generating sharp electrical impulses at the beginning and end of the event and applying them to the scale on the oscillosope. If, however, the event is repetitive, the frequency of repetition can be measured more simply and accurately by making fuller use of the properties of electronic circuits, which can be made to carry out the arithmetical processes of addition, subtraction, multiplication and division of frequencies.

To take a very simple example, suppose the frequency to be measured is 99,999 c/s. This frequency is subtracted from the 100,000 c/s of the standard, leaving a frequency of one c/s, which appears as a variation of the electrical current taken by the valve. This slow variation can be timed by very simple means with an accuracy of one per cent. The overall accuracy of the comparison is thus one-hundredth of a cycle in 100,000 cycles, that is one part in 10,000,000.

Elaborations of this simple technique enable any frequency to be measured in terms of a standard quartz clock with an accuracy of one part in 10,000,000,000. Such a fantastic accuracy is actually required in scientific work and also in technical applications. The accuracies required in these applications have thus advanced well beyond the accuracy with which the astronomical unit of time can be determined. This is not because astronomers have not made full use of technical improvements, but because of fundamental limitations placed by the solar system itself and of gaps in our knowledge of some of the complexities of its movements.

The Atomic Clock

Although quartz clocks can be used with the required accuracy, it is no longer adequate to calibrate them by means of the rotation of the Earth. This difficulty has been overcome by using as a standard of time another event which is regularly repeated in nature. This is the radio wave generated by an atom when its electron arrangement is changed slightly from one stable condition to another. The frequency of the wave is defined by one of the most fundamentally important relationships in physics and is simply proportional to the difference in the energy of the atom in the two states.

It should be emphasised that we are concerned here only with small changes in the atom, and not with the disruption of the central core, with resulting radioactive radiation. The changes of energy are minute compared with the "atomic energy" liberated when the atom is disrupted. Within this range of minute energy changes the larger differences give rise to radiation at a high frequency which appears as visible light.

The sodium lamps used for street lighting represent a practical appli-

cation of visible atomic radiation. There is no technique for comparing the frequency of this radiation with a quartz clock, and it cannot therefore be used as a standard of frequency or time. A smaller difference in energy gives rise to radiation at a lower frequency which falls in the range of radio waves, and this frequency can be measured by a quartz clock by means of the techniques described above. The actual frequency measurement is not difficult, but there are many practical difficulties arising from the weakness of the radiations and from the need to observe them without introducing disturbing effects which cause a slight shift of the natural atomic frequency. To overcome these difficulties, one of the most advanced experimental techniques is used; and of the many atoms or molecules which could be used theoretically the caesium atom has proved to be the most suitable.

Magnetic Effects

Consider the structure of this atom. It consists of a heavy central nucleus surrounded by 55 electrons, 54 of which are arranged in stable groups with a single electron surrounding them. This outer electron and the nucleus itself are spinning, and the spins can be in either the same or in opposite directions. The transition from one condition to another is accompanied by the emission of a radio wave having, according to recent measurements, a frequency of 9,192,631,770 cycles per second. This happens to be in the range of frequencies used for radar during World War II, and corresponds to a wavelength of about three centimetres. It is a very convenient value from the point of view of electronic circuits.

In order to understand how the atomic clock works, it is necessary to consider also the magnetic effects of the spinning electron. A spinning electric charge produces a magnetic field, and the atom therefore behaves as a small magnet the polarity of which is reversed when the spin is reversed. If, therefore, the atoms are passed through a non-uniform magnetic field they will be deflected in opposite directions according to which of the two states they are in.

Atoms in the two states can be separated by the arrangement of apparatus shown in Figure 1, all the parts being enclosed in a very high vacuum. Atoms leaving the oven travel in straight lines until they are deflected by the magnets. Atoms in opposite states are deflected along paths such as 1 and 2 and are selected by the central slit. Those selected are deflected farther in the same direction, away from the detector.

An Important Feature

In the part of the path between the two magnets an alternating field is now applied, and when this has the correct strength and frequency the atoms in the low energy state absorb energy from the field and jump to the high energy state. At the same time those in the high energy state are induced to emit radiation at their natural frequency and jump to the

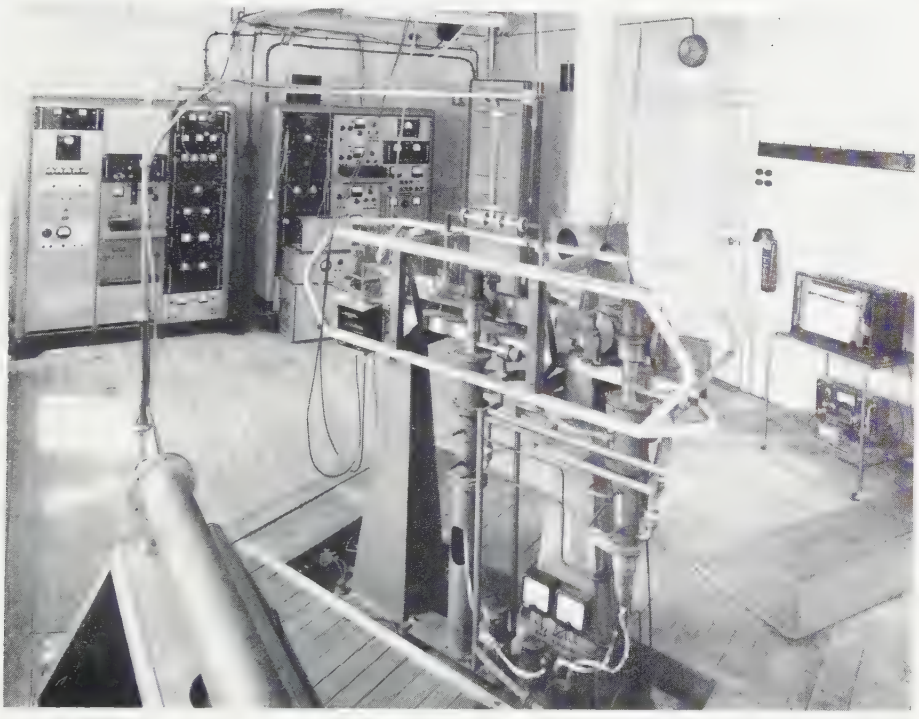

This photograph of the atomic clock shows (centre) the first caesium beam chamber, in use since 1955. The long vertical tube behind it houses the new more accurate caesium standard. To the left are the electronic circuits associated with the caesium standard. In the left foreground is the small self-contained caesium standard.

low energy state. Many of the atoms thus change their state and therefore the direction of their magnetisation. They are then deflected in the opposite direction by the second magnet and reach the detector, where they are converted into an electrical current which can be measured by well-known techniques.

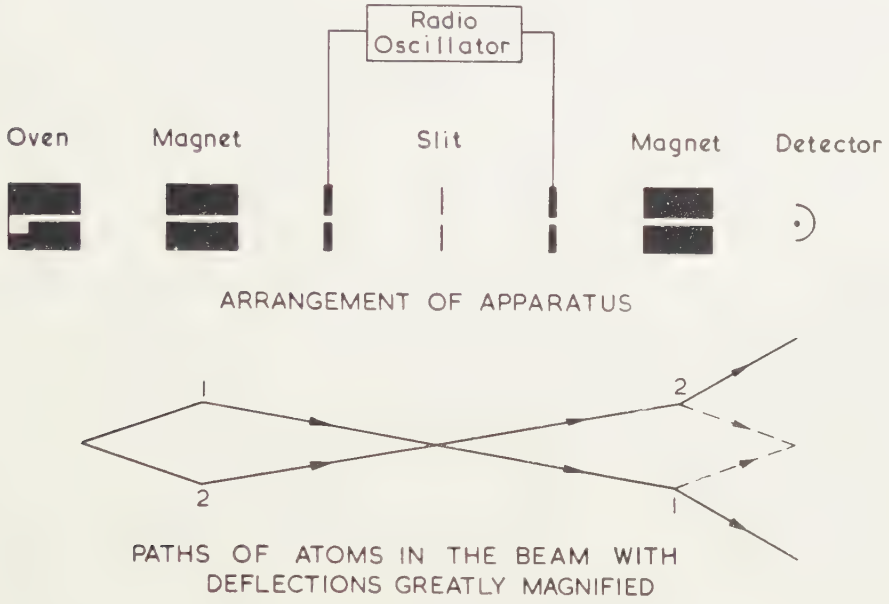

Fig. 1.

The important feature of the atomic standard is the extraordinary sharpness of this effect: it is only when the frequency of the radio oscillator corresponds almost exactly to that of the atoms that transitions from one state to the other occur. In practice, the frequency is varied slowly and set to give a maximum atomic beam current, and this setting can be made with an accuracy of one part in 10,000,000,000. The sharpness depends only on the length of time which the atoms spend in the field producing the transitions. In the present equipment, which is five feet (1.524 m) long, this is rather less than a thousandth of a second. A new clock which is being built at the National Physical Laboratory is 17 feet (5.182 m) long, and will give a still greater precision.

When the radio oscillator has been set to the atomic frequency it is used to calibrate the quartz clocks, or in sophisticated versions of the equipment it can be made to adjust the clocks automatically so that they keep in step with the atomic radiation.

Problem Greatly Simplified

Thus, instead of making the clocks keep in step with the Earth, which turns on its axis once in 86,400 seconds and revolves once round the

sun in roughly 30,000,000 seconds, we now make them keep in step with the atom which makes roughly 10,000,000,000 vibrations in one second. This change enables the unit of time to be defined much more accurately and conveniently and also much more quickly, in a few minutes instead of a few years.

The problem of time measurement has thus been greatly simplified. When it took at least a year to set the quartz clocks in terms of astronomical time, it was necessary to keep these clocks operating under very stable uniform conditions for periods of years. Elaborate precautions had to be taken to ensure this continuity of operation, safeguards being incorporated for such emergencies as the failure of the electrical supplies. It had to be assumed, morevoer, that the clock continued to gain or lose by the amount indicated by earlier measurements; and as it is known that even the best quartz clocks are subject to erratic changes, it was customary to employ a number of clocks at each installation. The atomic clock enables the quartz clock to be calibrated or directly controlled in a few minutes, and there is no longer any need for continuity except over the time interval being measured. For most purposes this is relatively short, and it is only long in astronomical work such as the measurement of the time of rotation of the earth in terms of atomic time. (Figure 2).

The standard of time differs from those of length and mass in one important respect: it can, as explained at the beginning of this article, be made available over wide areas by means of radio time signals. In

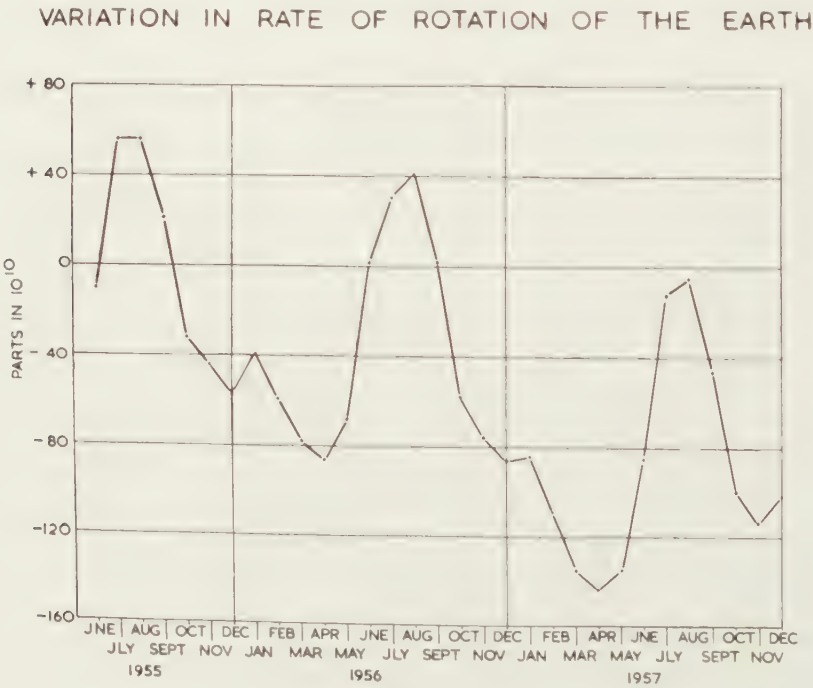

Fig. 2.

exactly the same way standard frequencies can be made available by controlling the frequency of the transmitter. Thus Droitwich, which has the convenient round number value of 200 kc/s, is often used for this purpose, and in addition, for more accurate work, a special service of transmissions with the call sign MSF is sent from the Rugby, England, station by the Post Office on behalf of Britain's National Physical Laboratory. These operate on frequencies of 60 kc/s, 2.5 Mc/s, 5 Mc/s and 10 Mc/s, and since 1955 they have been measured in terms of the caesium atomic standard.

In Many Countries

In this way the great accuracy of this standard has been used for precise time measurements in many different countries. One use of the transmissions has been to compare the frequencies of the atomic standards in the United Kingdom with those in the United States of America, Canada and Switzerland. The very close agreement between them, in spite of the fact that they have been made quite independently and have many differences in detail, gives strong justification for the use of the caesium resonance as a standard.

The thoughtful person will still ask how we know that the atomic frequency is constant. How do we know that it is the speed of the rotation of the Earth, and not the atomic frequency, which has changed slightly during the last few years? The answer is that there is at present no theoretical reason by which a change in the atomic frequency could be explained, and all experiments that have been made have failed to reveal any change.

On the other hand, there are a number of possible explanations for a small change in the period of rotation of the Earth. As with all standards of measurement, there is no means of knowing positively that it is constant. It is simply the most constant thing we know of, and if anything better is found then that will become the new standard.

SILICON TETRACHLORIDE TREATED PAPER IN THE PAPER CHROMATOGRAPHY OF PHOSPHATIDES

IIa. MECHANISM OF THE CHROMATOGRAPHY OF EGG PHOSPHATIDES

BY

H. G. BUNGENBERG DE JONG AND J. TH. HOOGEVEEN

(Communicated at the meeting of December 19, 1959)

1. *Introduction*

In part I of this series we have dealt with the preparation of "acid" and "neutralized $SiCl_4$-treated paper", properties of these papers, and an example of their use in following a fractionation of a phosphatide mixture [1]. In the present paper we shall first deal with the chromatography on $SiCl_4$-treated paper of a single phosphatide (sections 3–8), for which we have chosen lecithin (phosphatidyl choline) [1]. Subsequently the chromatography of a mixture of phosphatides (egg phosphatides) will be examined.

2. *Methods*

In the present study we use exclusively Schleicher and Schüll paper no 2043*b*, 17 × 27 cm, and follow the directions given in Part I for their preparation with $SiCl_4$ [1]. By means of a self-filling capillary pipette (of about 5 mm^3 capacity) the lecithin solution is brought up on the starting points. Chromatography is performed with di-isobutylketone—acetic acid—H_2O (50:25:5 by volume) in a dark room at constant temperature (20°), with the large slitfeeding apparatus described in a former communication [2]. After drying, the chromatogram is stained with the Acid Fuchsin—$UO_2(NO_3)_2$ – 0.01 N HCl staining solution described in former communications [3], [4]. After drying once more the spots are outlined with a pencil.

3. *Experiments in which* 0.12 % *lecithin spots are applied at increasing distances from the slit*

In these experiments nine 0.12 % spots (5 mm^3) were applied on a line drawn from a point on the lower end of the paper sheet, 10 mm from the left hand boundary, to a point 20 cm above the lower end and 10 mm to the left of the right hand boundary. The first and ninth spot lie 25 mm from the left and right hand sides of the paper, while the mutual distance of the spots (in horizontal direction) is 15 mm. 5 mm of the sheet dips through the slit in the feeding tube. Thus the distance of the first spot to the slit is 1.5 cm, of the ninth spot 17.5 cm, while the distance between spots is 2 cm measured in the vertical direction. The

[1] We thank Dr. G. J. M. HOOGHWINKEL for putting a solution of pure lecithin (column fraction) dissolved in chloroform-methanol (4:1) to our disposal.

front was allowed to ascend to a line drawn on the paper 20 cm from the lower margin, or 19.5 cm from the immersion line.

In total four such chromatograms were made, namely with acid $SiCl_4$-treated paper of different ages (fig. 1 and 2) and with neutralized $SiCl_4$-treated paper of different ages (fig. 3 and 4). Fig. 1–4 have in common that the transported spots do not lie on a straight line through the

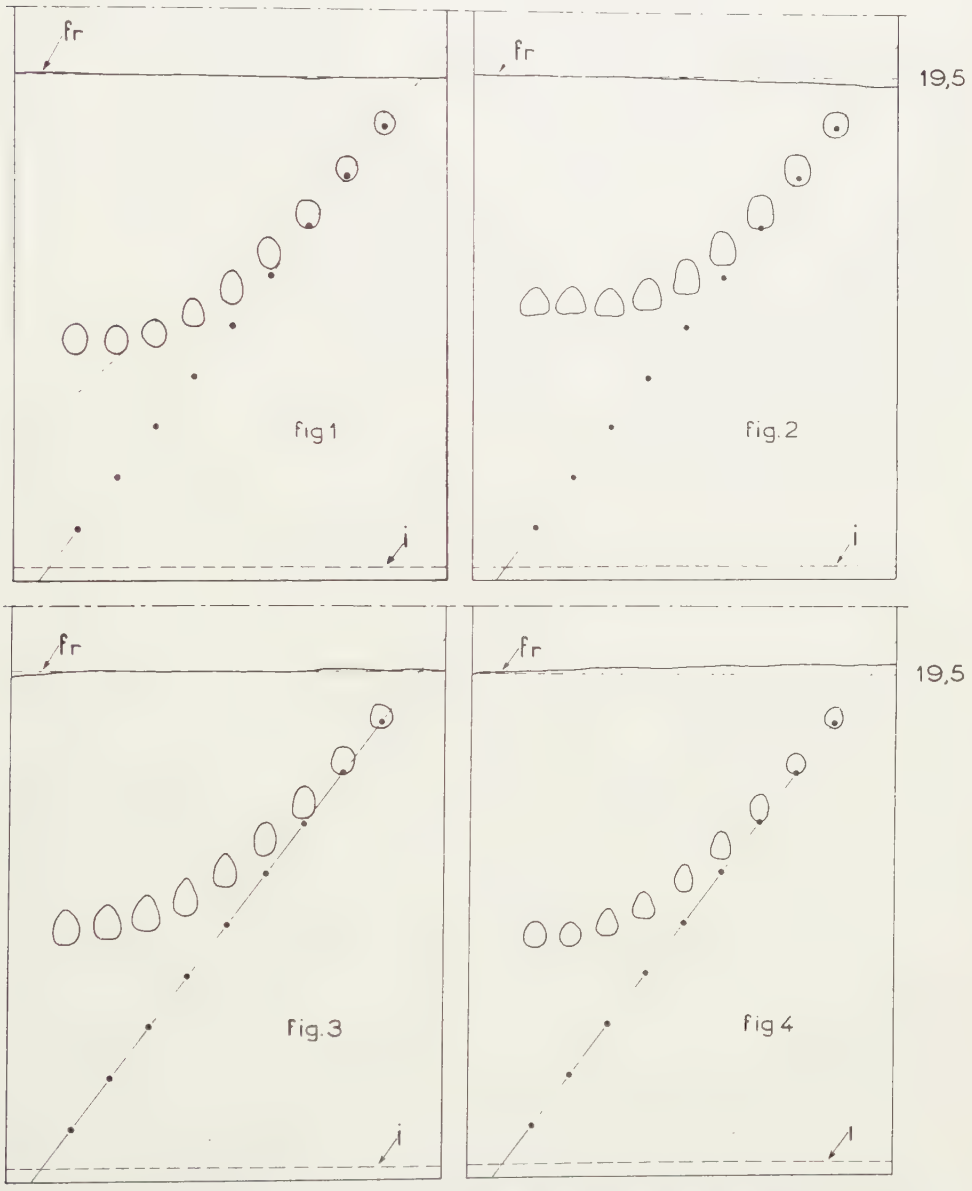

Figs. 1–4. Chromatograms of lecithin provided with nine starting points on a sloping line. The front (fr) has risen 19.5 cm above the immersion line (i). Acid (figs. 1 and 2) and neutralized (figs. 3 and 4) $SiCl_4$-treated paper of different age has been used (fig. 1 = 4 hrs; fig. 2 = 47 hrs; fig. 3 = 2 days and fig. 4 = 72 days after preparation respectively).

intersection point of the frontline with the line through the starting points (compare for instance the broken line drawn in fig. 1). Any straight line through this intersection point, between frontline and the line through the starting points, represents a definite R_f-value. It should be evident that R_f-values (which are constant in the case of ideal partition chromatography) are in our case not at all constant.

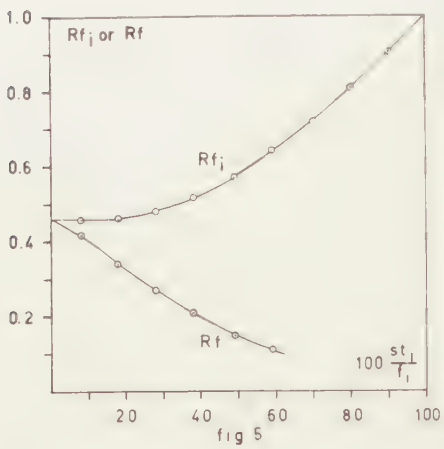

fig 5

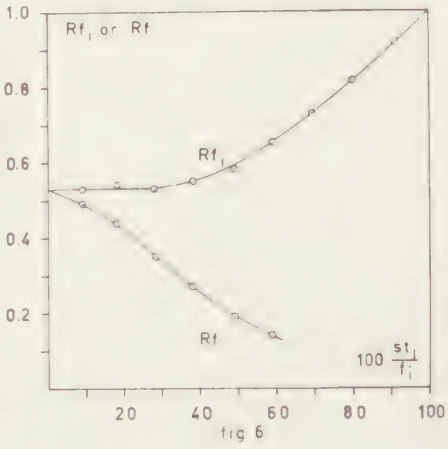

fig 6

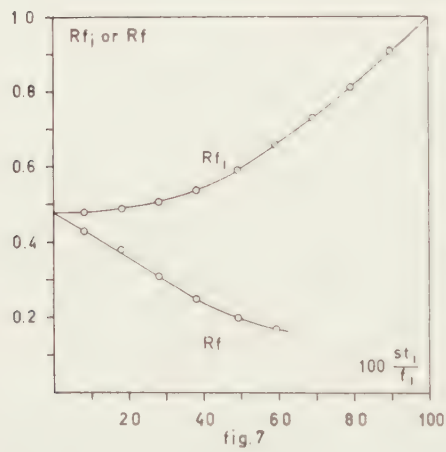

fig.7

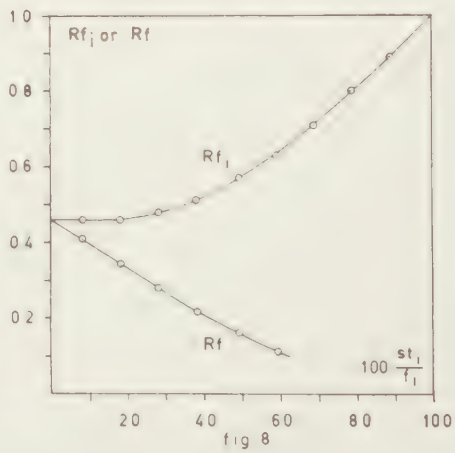

fig 8

Figs. 5–8. R_f and R_{f_i} as a function of $100\frac{st_i}{f_i}$ calculated from the chromatograms of figs. 1–4).

The fact that the curves through the transported spots approximate a horizontal level on the left side of the paper indicates that the position of the transported spots becomes more and more independent of the position of the starting point, the lower the latter is situated.

Table I and fig. 5–8 illustrate the above statements. The symbols used have the following meaning.

$$\text{“}R_f\text{”} = \frac{a_{st}}{f_{st}} = \frac{\text{distance of spot to starting line}}{\text{distance of front to starting point}}$$ [1])

$$\text{“}R_{f_i}\text{”} = \frac{a_i}{f_i} = \frac{\text{distance of spot to immersion line}}{\text{distance of front to immersion line}}$$

$100\frac{st_i}{f_i}$ = distance starting point immersion line as a percentage of the distance front-immersion line.

TABLE I

“R_f” and “R_{f_i}” as a function of $100\frac{st_i}{f_i}$

	FIG	Spot number, reckoned from left to right					
		no 1	no 2	no 3	no 4	no 5	no 6
“R_f”	1	0.42	0.34	0.27	0.21	0.15	0.11
	2	0.49	0.44	0.35	0.27	0.19	0.14
	3	0.43	0.38	0.31	0.25	0.20	0.17
	4	0.41	0.34	0.28	0.22	0.16	0.11
“R_{f_i}”	1	0.46	0.46	0.48	0.52	0.57	0.64
	2	0.53	0.54	0.53	0.55	0.58	0.65
	3	0.48	0.49	0.51	0.54	0.59	0.66
	4	0.46	0.46	0.48	0.51	0.57	0.63
$100\frac{st_i}{f_i}$		8	18	28	38	49	59

Inspecting the first four rows of the Table we see clearly that a characterisation of chromatographic displacement by an “R_f” value would be quite inadequate. On each row this value decreases rapidly with increasing distance of the starting point from the immersion line.

However, as rows 5–8 of the Table may show, the value of “R_{f_i}”. is within the experimental error the same for the first, the second and practically for the third starting point. The location of the starting point has become unimportant here. For higher starting points the value of “R_{f_i}” increases. As can be seen from the definition of “R_{f_i}” given above, its value must reach the value 1.00 (at $100\frac{st_i}{f_i} = 100$) when the starting point lies at the front itself. From the definitions given of “R_f” and “R_{f_i}” it also follows that both will be equal when $100\frac{st_i}{f_i} = 0$, that is, when the starting point coincides with the immersion line. The “R_f” curves in fig. 5–8 therefore start where the horizontal part of the “R_{f_i}” curves intersect the ordinate. To calculate “R_f” values for the 7th, 8th and 9th spot would be useless as the displacements of the spots are too small here to be measured with any accuracy. The further course of the R_f curves to the right therefore remains unknown.

Figures 5–8 demonstrate that “R_f”-values nowhere approach a constant

[1]) It would perhaps be better to use here the symbol “$R_{f_{st}}$“, rather than R_f. The suffix st indicates that distances are reckoned from the starting point.

value, but that "R_{f_i}" is practically constant when the front has passed sufficiently high above the starting point.

The results suggest that a gradient is present in the composition of the mobile phase on the paper. The horizontal part of the "R_{f_i}" curve may denote a particular composition of the mobile phase at which the upward migration of lecithin reaches its maximum velocity, relative to the velocity of the front.

4. *The occurrence of a gradient in the mobile phase wetting the paper*

In the next following communication this subject will be studied in detail. For the time being it will suffice to demonstrate the existence of a gradient in a single case. In the example given below a sheet (17×27 cm) of "acid"-$SiCl_4$-treated Schleicher and Schüll no. 2043*b* was used. The sheet had been in air for 163 hrs., a period sufficient to ensure that all HCl formed during preparation has left the paper. The immersion line, and parallel to it lines 4.5; 9; 13.5; 18 and 22.5 cm above the immersion line were drawn on the paper beforehand. In the large slitfeeding apparatus this sheet was run with the customary mobile phase until the front reached the line drawn at 22.5 cm above the immersion line. The sheet was taken out of the apparatus and was cut into five strips along the pencil lines. As the strips were cut they were allowed to drop into wide flasks, each containing 50 ml. of distilled water. The weight of these flasks with their stoppers should be known beforehand. All these manipulations were accomplished in as short a time as possible. (20 seconds) to prevent evaporation losses. The flasks were now weighed so that the weight of the wetted strips became known. Extraction of the strips was accomplished by standing overnight. Two aliquots of 20 ml. of the extract were titrated with NaOH. We calculated the weight of

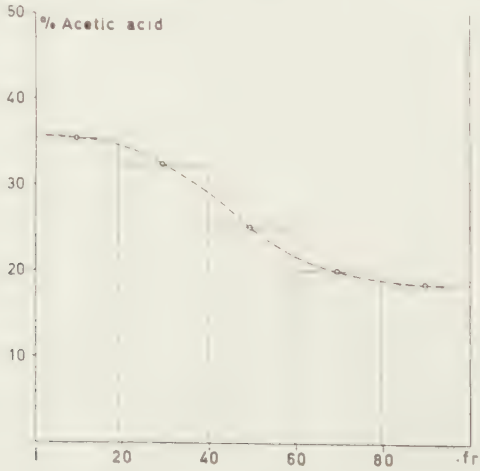

Fig. 9. Gradient in the mobile phase wetting the paper (variation of weight percentage of acetic acid in the mobile phase). Abscissa: Percentages of the distance between front (fr) and immersion line (i).

acetic acid originally present in each strip. The strips themselves were then dried. The difference in weight of the wetted and dry strip gave us the weight of the mobile phase present in each strip. We finally calculated the mean acetic acid content in weight per cent of the mobile phase in each of the five strips. The results are given in fig. 9. We observe that the mean acetic acid concentration in the mobile phase diminishes distinctly when we move upwards in the paper, from 35.5 % in the lowest

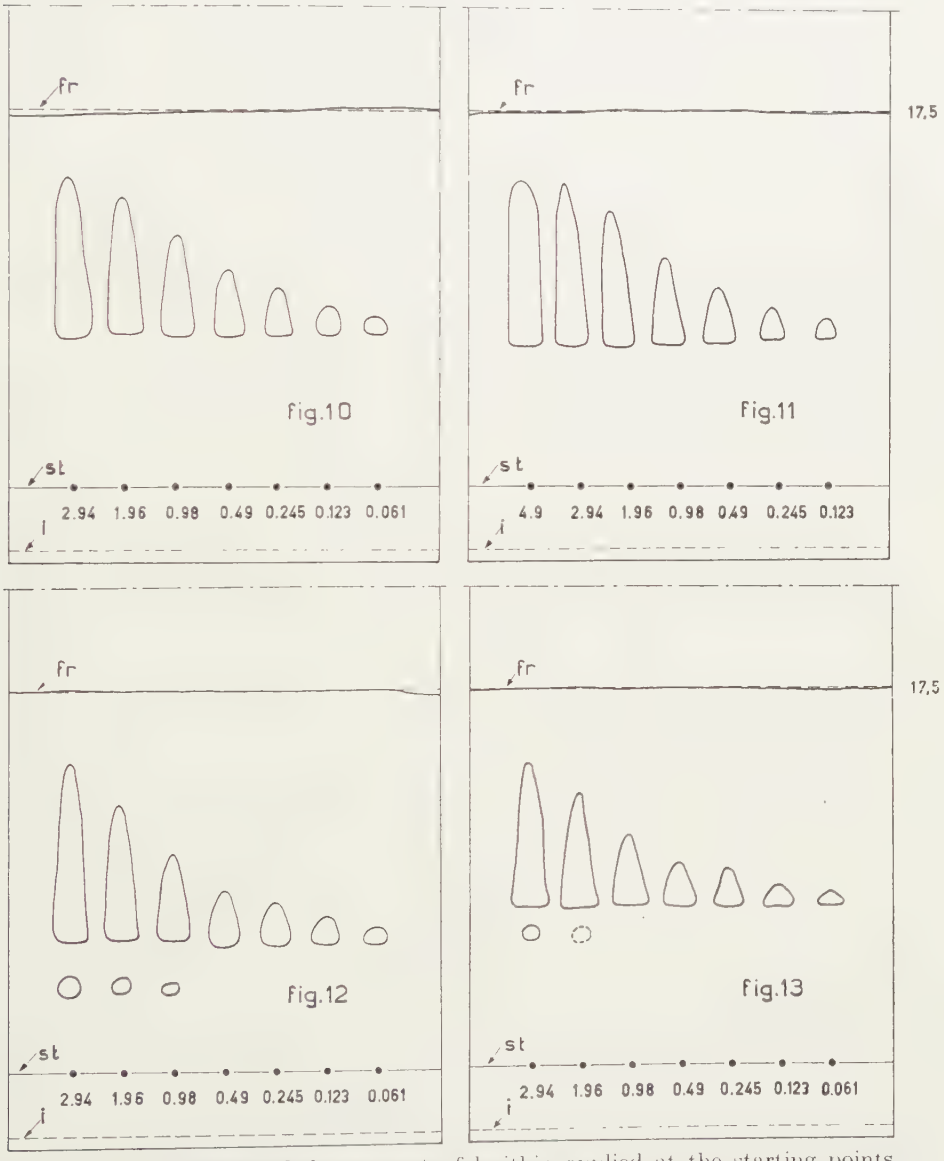

Figs. 10-13. Influence of the amount of lecithin applied at the starting points (figures below the starting points give concentrations of the lecithin solution of which 5 mm³ has been applied). Neutralized $SiCl_4$-treated paper (figs. 10 and 11) of different age (fig. 10 = 2 days); fig. 11 = 73 days) and acid $SiCl_4$-treated paper of different age (fig. 12 = $\frac{1}{2}$ hour; fig. 13 = 44 hours) has been used.

strip, to 18.4 % in the highest strip. The gradient in the paper is given approximately by the broken curve.

5. *Influence of the concentration of the lecithin solution applied on the starting line*

a) Qualitative results

In these experiments the same pure lecithin fraction was used as in section 3. Various dilutions of the stock solution were made with $CHCl_3$-methanol (80:20) ranging from 4.9 to 0.061 %. As always, 5 mm^3 solution was applied on the paper, so the amount of lecithin varied from 245γ to 3γ.

The starting line was drawn 2.5 cm above the immersion line and the front was allowed to ascend 17.5 cm above the immersion line. Four kinds of paper were used, namely neutralized $SiCl_4$-treated paper of different age (fig. 10 and 11) and acid $SiCl_4$-treated paper of different age (fig. 12 and 13). The chromatograms have in common that with increasing amounts of lecithin applied on the paper,

a) the area of the transported spot increases considerably,
b) the lower margin of the spots in each figure lie on a nearly horizontal line,
c) the gain in area of the spot is due to some broadening but mainly to increase in length in upward direction, whereby the spots acquire a roughly triangular shape. With very large amounts of lecithin the top of the triangle becomes definitely rounded (see left spot on fig. 11),
d) small spots are evenly stained, with the same intensity as the lower part of the triangular spots. In the latter the colour intensity increases in upward direction, the more so as the total length of the triangular spot increases.

A discussion of points a–d, together with the results mentioned in the next paragraph will follow in section 6.

The small spots appearing below the lecithin spots to the left of the chromatograms in fig. 12 and 13 are discussed in paragraph c.

b) Spot area as a function of the lecithin concentration in the solution applied on the starting line

With a planimeter the areas of the spots were measured on the chromatograms given in the figures 10–13. The results have been given in Table II. In column 6 the mean area of the spots has been given. By taking the mean areas, the errors made in outlining the spots and in measuring the area are minimized. The logarithm of the mean area is plotted in fig. 14 against the logarithm of the lecithin concentration of the solution applied on the starting line.

It appears that the points approximate a straight line drawn at a slope of 0.65. Since this slope is about 2/3, the area of the spot appears to increase with roughly the 2/3 power of the amount of lecithin applied.

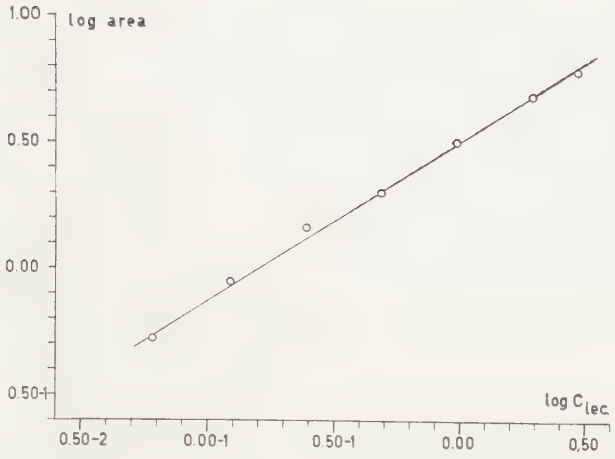

Fig. 14. Double-logarithmic plot of spot area in relation to lecithin concentration applied.

TABLE II

Spot area (cm^2) as a function of lecithin-concentration

lec. conc. %	fig. 10	fig. 11	fig. 12	fig. 13	mean area
0.061	0.61	0.57	0.53	0.42	0.53
0.123	0.89	0.99	0.92	0.78	0.90
0.245	1.58	—	1.55	1.31	1.48
0.49	2.41	2.07	1.97	1.67	2.03
0.98	3.79	3.29	3.19	2.77	3.26
1.96	5.75	5.05	4.83	4.36	5.00
2.94	7.07	6.18	6.65	5.42	6.33
4.9	—	7.68	—	—	—
nature of paper and age	neutr. 2 days	neutr. 72 days	acid $\frac{1}{2}$ hr.	acid 44 hrs.	—

c) Decomposition (slight) of lecithin on acid $SiCl_4$-treated paper

On the figs. 12 and 13, where acid papers have been used, below the lecithin spot a small spot may be observed at the highest concentrations of the lecithin. This small spot is not observed on the figs. 10 and 11 which refer to neutralized papers. Since these spots are stained with Acid Fuchsin-$UO_2(NO_3)_2$ they correspond to a phosphatide containing one positively charged froup and one negatively charged group [3, 4]. This phosphatide must have been formed from the lecithin by the HCl present in the paper. From the distance between the base of the lecithin spots and these small spots, it seems likely that some lysolecithin has been formed.

The HCl contents of the paper diminishes in air, so it is to be expected that in fig. 12 (spots applied $\frac{1}{3}$ hour and chromatography begun $\frac{1}{2}$ hour after preparation of paper) more lyso-lecithin is formed than in fig. 13 (chromatography 44 hours after preparation of paper). This is confirmed by the fact the in fig. 12 a spot is visible at 2.94, 1.96 and 0.98 % lecithin, whereas in fig. 13 the spot at 2.94 % is not very pronounced and that at 1.96 % is only faintly discernible.

A comparison of the area and intensity of staining of the lysolecithin spot at 2.94 % lecithin with the lecithin spot at 0.061 % indicates that during the total time of contact of the lecithin with the paper (about 3 hrs.) in fig. 12 about 2 %

and in fig. 13 about 1 % of the lecithin present has been converted to lysolecithin.

In the figures 1 and 2, also referring to acid $SiCl_4$-treated papers below the lecithin spots no other spots are visible. This is understandable, since here a very dilute lecithin solution (0.12 %) was applied. The lysolecithin spots would here correspond to a concentration in the order of 0.002 % or less, far below the linit of visible staining of lecithin, which lies between 0.03 and 0.01 % [4].

When acid papers are used for the separation of a phosphatide mixture these results should be taken into account. When the total lecithin concentration is relatively high, a faint spot of lysolecithin does not allow the conclusion that lysolecithin was present originally. A second chromatogram should be run on neutralized paper. When no lysolecithin spot is obtained here, the spot on the acid paper was probably due to hydrolysis. We may expect that on acid paper a similar decomposition of cephalin occurs; again we should compare chromatograms on acid and on neutralized paper.

d) Change in chromatographic properties of $SiCl_4$-treated papers

The chromatograms figs. 1, 2, 12 and 13 have been run on acid $SiCl_4$-treated papers which belong to one batch.

Therefore they are really comparable and conclusions may be drawn about the effects of ageing. Comparing fig. 1 and fig. 2, it appears that the horizontal level reached on the left side of the chromatogram is situated higher after 47 hours than after 4 hours. A comparison of fig. 12 and fig. 13 yields the same conclusion, since the horizontal line corresponding to the base of the spots lies higher on a chromatogram made 44 hours after instead of $\frac{1}{2}$ hour after the $SiCl_4$ treatment. Change of acid $SiCl_4$-treated paper is probably due to a gradual loss of HCl from the paper (compare section 4 in Part I of this series [1]). The question whether neutralized $SiCl_4$-treated paper also changes over time cannot be answered from our experiments regarding horizontal levels (fig. 3 and fig. 4) and base lines (figs. 10 and 11). The reason is that the neutralized papers represented in fig. 3 and fig. 10 belong to one batch and those in fig. 4 and fig. 11 belong to another. From other experiments we have the impression that rapid changes, as they occur in acid papers, do not occur in neutralized papers.

6. *Mechanism of the chromatographic displacement of lecithin*

The results in section 3 indicate that a gradient in the composition of the mobile phase wetting the paper may play an important role. The occurrence of a gradient has been demonstrated in section 4.

When one tries to obtain a chromatogram with di-isobutylketone alone as the mobile phase, lecithin practically does not move from the starting spot. With acetic acid alone lecithin moves practically with the front. These observations permit two alternative hypotheses regarding the mechanism of chromatographic displacement. The possible mechanisms are:

1) partition chromatography, with an R_f-value which is very small with di-isobutylketone, and equal to unity with acetic acid.
2) adsorption chromatography, in which lecithin is not eluted by di-isobutylketone and completely by acetic acid.

The chromatography of lecithin with our mobile phase (with di-isobutylketone and acetic acid as main constituents) does not have the characteristics of partition chromatography, but must be interpreted as

a kind of *adsorption chromatography in which a gradient in the composition of the mobile phase plays an essential part*. The results both of section 3 and section 5 are in accordance with this hypothesis.

There will be a characteristic composition in the gradient at which lecithin is eluted with a maximal rate. In upward direction the acetic acid / di-isobutylketone ratio decreases, as a result of which the elution rate becomes ever smaller. This explains why in the figures 1–4 (section 3) the spots lie on a curve which tends to reach a horizontal level to the left, indicating that particular composition within the gradient at which the elution rate is maximal.

If we were concerned here with adsorption chromatography, without a gradient in the mobile phase, the lecithin spots would show tailing in downward direction, while the concentration of lecithin in the spot would be highest near the top of the spot. The presence of a gradient will have two effects:

A) The spot is continually eluted at its base (because the elution rate here becomes a maximum).

B) The eluted lecithin moves upward and is adsorbed higher up in the spot. But because in upward direction the elution rate strongly diminishes, the concentration of lecithin will increase more strongly in upward direction than when no gradient was present.

Point A) is in good agreement with our observation that whatever the amount of lecithin applied, the lower margin of the transported spots will always lie on the same horizontal level. (see point b, section 5, paragraph a).

Point B) is in agreement with the fact that the colour intensity of the spot increases in upward direction, the more so as the total length of the triangular spot increases (point d, section 5, paragraph a). The remaining points in section 5) paragraph a) are easily explained. If it is true that we are concerned with adsorption chromatography, a larger amount of lecithin must necessarily lead to an increase of the spot in area (point a). The characteristic triangular shape (point c) results partly from point A (nearly flat base) partly from the fact that the starting spots are circular in shape. As the mobile phase, moving vertically through the centre of the spot, transports a maximum amount of lecithin, the migrated spots must necessarily have a peak (provided the amount of lecithin applied is large enough).

The spot areas increase less than proportionally with the amount of lecithin applied. (Section 5, paragraph *b*). This follows from the fact that in a large spot the lecithin concentration at the top is higher than in a small spot.

7. *Influence of the ascension height of the front*

In this section a number of chromatograms will be run in the same apparatus (the large slit-feeding apparatus) one after the other, and

allowing the mobile phase to ascend to increasing heights. As freshly prepared acid $SiCl_4$ treated paper changes its chromatographic properties markedly over the period of the experiment (one workday) neutralized $SiCl_4$-treated paper was used instead. Five sheets of one batch, each provided with nine starting points on an oblique line, were run the day after their preparation. The front ascended 4.5, 9.5, 14.5, 19.5, and 24.5 cm above the immersion line.

The chromatograms obtained are reproduced in the figures 15–19,

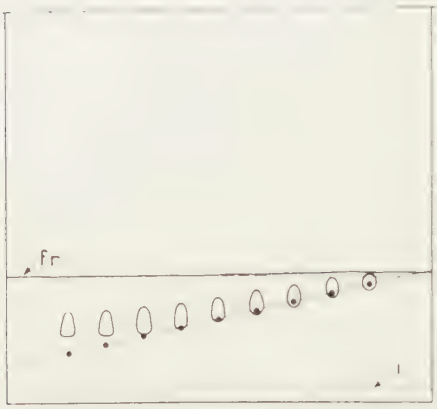

Fig. 15

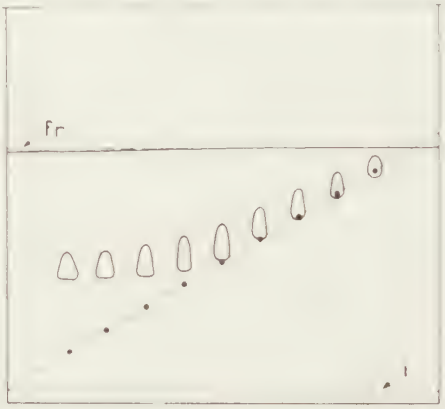

Fig. 16

Figs. 15–16. Chromatograms of lecithin on neutralized $SiCl_4$-treated paper, with nine starting points on sloping lines. On each, starting point 5 mm³ af a 0.11% lecithin solution has been applied. The front has risen approximately 4.5 and 9.5 cm above the immersion line.

which are quite similar to the figures 1–4. Figure 15 shows that the mechanism whereby the spots reach a practically horizontal level ("asymptote") on the left side of the chromatograms is already effective at the beginning of the ascension of the mobile phase in the paper. For each of the chromatograms, graphs could be obtained in which "R_f" and "R_{f_1}" are plotted as a function of $100\frac{s_1}{f_1}$, and these graphs would be similar to those of the figures 5–8. Attention should, however, be drawn to the effect of the ascension height of the front.

In fig. 20 we have plotted for the first four spots of each chromatogram, a_{st} = distance "centre" of the spot to starting point, against f_{st} = distance of front to starting point.

We observe that

1) for each starting point a separate curve results,
2) no curve goes through the origin,
3) excepting the curve corresponding to spot no. 1, none of the curves is a straight line.

If the R_f-value was an adequate expression to characterize the chromatographic displacement of lecithin on $SiCl_4$-treated paper we should

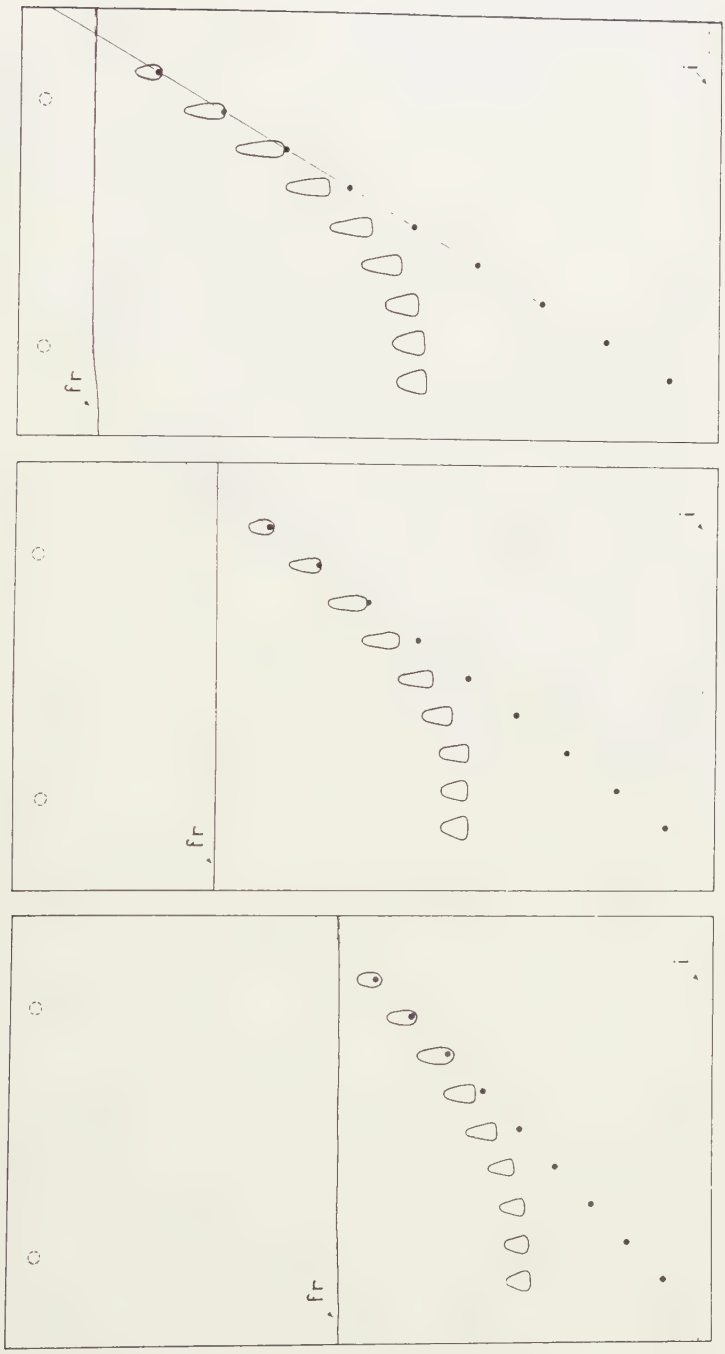

Figs. 17–19. Chromatograms of lecithin on neutralized $SiCl_4$-treated paper, with nine starting points on sloping lines. On each starting point 5 mm^3 of a 0.11% lecithin solution has been applied. The front has risen approximately 14.5, 19.5 and 24.5 cm above the immersion line.

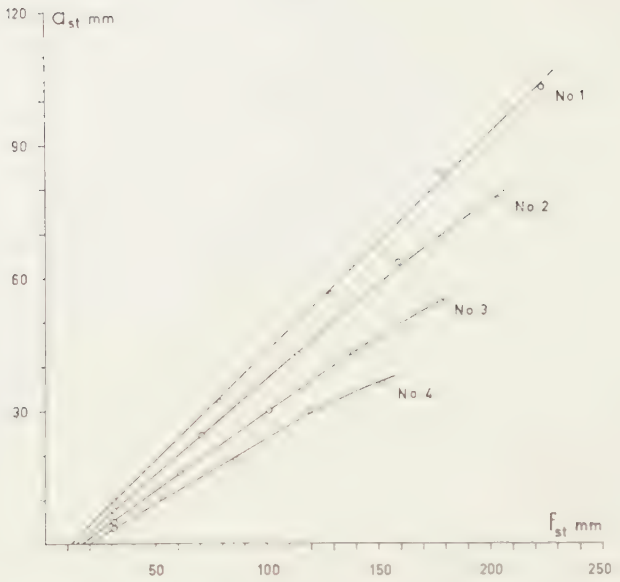

Fig. 20. a_{st} plotted against f_{st}, for the spots no 1 (left) to no 4 on the chromatograms figs. 15–19.

TABLE III

"R_f" calculated for the spots migrated from starting points no 1 (left)–4

Chromatogram figure	"R_f" (calculated from spot centre)			
	no 1	no 2	no 3	no 4
15	0.33	0.24	0.16	0.11
16	0.41	0.35	0.26	0.20
17	0.43	0.37	0.30	0.22
18	0.46	0.40	0.31	0.25
19	0.46	0.38	0.30	0.24

TABLE IV

"R_{f_1}" calculated for the spots migrated from starting points no 1 (left)–4

Chromatogram figure	"R_{f_1}" (calculated from spot centre)				"R_{f_1}" (calculated from spot base)			
	no 1	no 2	no 3	no 4	no 1	no 2	no 3	no 4
15	0.56	0.54	0.58	0.60	0.47	0.48	0.48	0.54
16	0.51	0.51	0.52	0.55	0.46	0.47	0.47	0.55
17	0.50	0.50	0.51	0.54	0.47	0.47	0.49	0.52
18	0.50[5]	0.50	0.50[5]	0.54	0.48	0.48	0.48	0.52
19	0.48	0.48	0.49	0.49	0.46	0.47	0.47	0.50

TABLE V

Distance from immersion line to horizontal line through basis of the two left spots ("asymptote") and to the front ("front")

Chromatogram figure	"asymptote" in m.m.	"front" in m.m.	$R_{f_i} = a_i/f_i$	Ascension time in minutes	$f_i/\sqrt{t}$
15	21.5	45.5	0.47	12	13.1
16	44	94	0.47	45	14.0
17	68	144	0.47	99	14.5
18	94	194	0.48	181	14.4
19	113	243	0.47	290	14.3
			mean 0.47		mean 14.1

find for the four starting points one and the same straight line through the origin. The slope of this line would be equal to R_f.

Figure 20, and also the "R_f" values in the columns 2–5 of Table III, lead to the same conclusion as section 3, namely that we are far from the conditions of partition chromatography.

The columns 2–5 of Table IV give "R_{f_i}" values (as defined in section 3). measured from the "centre" of the spots. Excluding a chromatogram with a very small ascension height of the front (fig. 15; $f_i = 4.5$ cm), the values of "R_{f_i}" for the first three spots are quite close.

The spots on the chromatograms fig. 15–19 are not round but triangular. The location of the base of a spot is in these cases characteristic, while that of the "centre" is not. (See sections 5 and 6). It is better therefore

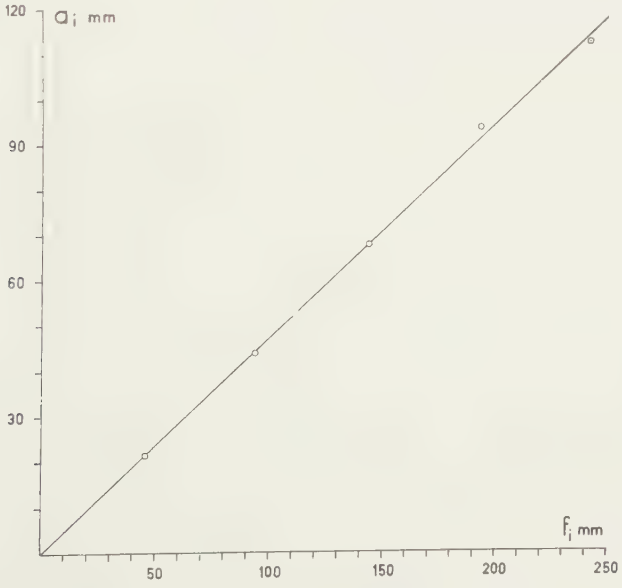

Fig. 21. "Asymptote" (a_i) as a function of "front" (f_i).

to calculate "R_{f_i}" values from spot-bases (a_i then is taken the distance spot base to immersion line). This has been done in the columns 6–9 of the Table IV. The "R_{f_i}" values for the starting points nos. 1 and 2 (and even for starting point no. 3 approximately) are now constant within experimental errors. This includes the chromatogram with the very low ascension height (fig. 15). Thus on all five chromatograms the spots which migrated from starting points nos. 1 and 2 lie practically on the asymptote. The mean distances from spot base to immersion line, and the mean distances front-immersion line, are given in Table V in the columns "asymptote" and "front" respectively. They have been plotted in fig. 21 and appear to lie reasonably well on a straight line. The slope of this line is R_{f_i}, (without quotation marks) which quantity is to be defined as follows

$$R_{f_i} = \frac{a_i}{f_i} = \frac{\text{distance asymptote to immersion line}}{\text{distance front to immersion line}}$$

In a given apparatus (here the large slit-feeding apparatus) R_{f_i} is a characteristic constant for the chromatography of lecithin on neutralized $SiCl_4$-treated paper. The last column of the table shows that the ascension height of the front is proportional to the square root of time.

The results in this section (the fact that R_{f_i} is independent of front-height) mean that the composition of the mobile phase at which the elution of lecithin occurs with maximum velocity lies always at the same fraction of the ascension height above the immersion line.

8. *Comparison with the chromatography of lecithin on untreated paper*

In a former communication similar experiments as in the preceding section were reported, with the difference that untreated Schleicher and Schüll 2043*b* was used [5]. The results were similar to those obtained in fig. 21 with neutralized $SiCl_4$-treated paper, a_i being proportional to f_i, but the slope of the straight line through the origin is somewhat higher ($R_{f_i} = 0.65$).

The similarities and differences in the chromatography with untreated and $SiCl_4$-treated papers still await further investigation. In one of the following communications of this series experimental evidence will be brought forward to demonstrate the existence of a gradient in untreated paper too. The question will be discussed whether or not this gradient is equal in the two cases.

(To be continued)

SILICON TETRACHLORIDE-TREATED PAPER IN THE PAPER CHROMATOGRAPHY OF PHOSPHATIDES

IIb. MECHANISM OF THE CHROMATOGRAPHY OF EGG PHOSPHATIDES

BY

H. G. BUNGENBERG DE JONG AND J. TH. HOOGEVEEN

(Communicated at the meeting of December 19, 1959)

9. *Chromatography of a mixture of lecithin, lysolecithin and sphingomyelin on $SiCl_4$-treated paper. Influence of the total concentration*

a) Discussion of the chromatograms

Having studied in the preceding sections the chromatography of one single phosphatide (lecithin), we now proceed in this and the next sections with the chromatography of mixtures of phosphatides. The aim is to see whether the characteristics found with lecithin also apply to other phosphatides and in how far complications arise by the mutual interference of spots.

In the present section we start from the same stock solution of lecithin (L)+lysolecithin (LL)+sphingomyeline (S) as used in Part I of this series [1]). The concentrations of the components in the mixture are not exactly known, but it is certain that they are distinctly different, namely L > LL > S. By dilution with the solvent (chloroform:methanol = 80:20) solutions were made ranging from 0.25 % to 2 % total concentration.

We proceeded in the same way as in section 5, and obtained the chromatograms given in figs. 22–24. If these chromatograms are compared with the analogous chromatograms on which only lecithin was applied (figs. 10–11) we observe for each row of spots in principle the same consequences of the increase in concentration. A new phenomenon, not evident in figs. 10–11, is the appearance of an incision in the base of the spot. This incision is never present at the base of the lower row of spots, which belong to lysolecithin.

Thus lysolecithin behaves in all points a–d summed up in section 5, paragraph a, as lecithin when present alone on the paper. The mechanism

[1]) We thank Dr. G. J. M. HOOGHWINKEL for putting to our disposal this stock solution. It has been made by column chromatography (crude separation of total egg-phosphatides with an aluminum oxyde column and thereafter separation with a silicic-acid column). Some fractions of the silicic-acid column were mixed; only lecithin, lysolecithin and sphingomyelin are present in the mixture. After evaporation it was dissolved in $CHCl_3$-methanol (80:20).

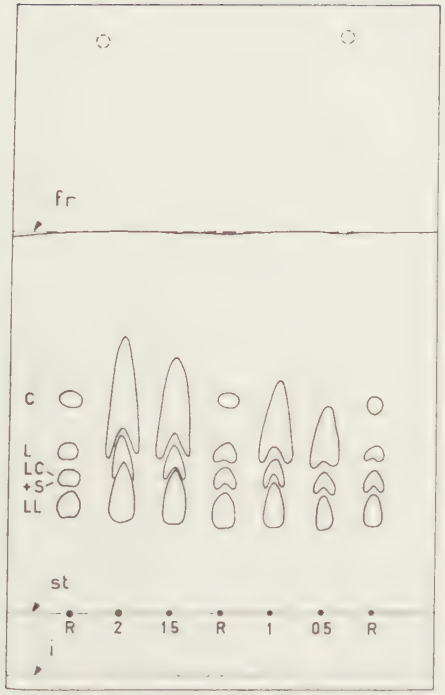

Fig. 22

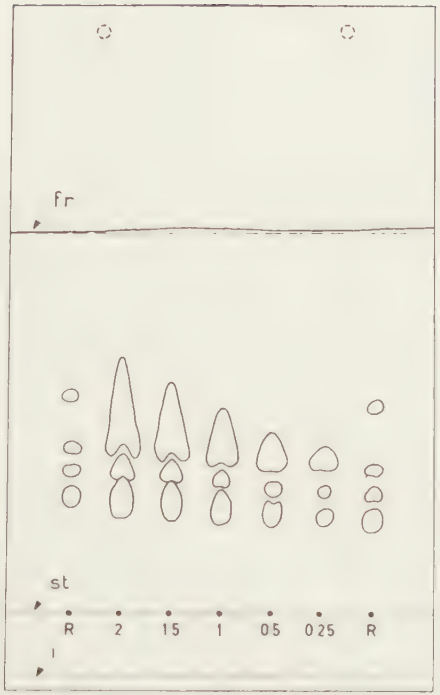

Fig. 23

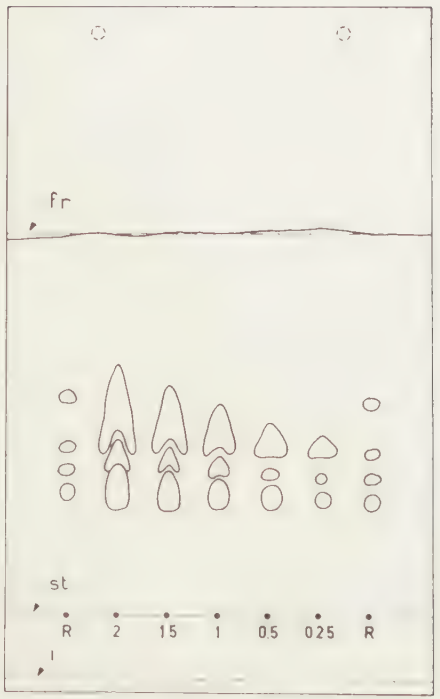

Fig. 24

Figs. 22–24. Chromatography of a mixture of lecithin (L), lysolecithin (LL) and sphingomyelin (S). Influence of the total concentration (in %). Neutralized $SiCl_4$-treated paper (fig. 22) and acid $SiCl_4$-treated paper (figs. 23 and 24) of different age (fig. 22 — 4 days; fig. 23 — 4 hours and fig. 24 — 48 hours) has been used. At R 5 mm^3 of the 0.5% reference mixture has been applied.

of the chromatography of lysolecithin is thus the same as was discussed for lecithin in section 6 (adsorption chromatography in combination with gradient elution). The difference is only that the particular composition of the mobile phase necessary to reach the maximum elution rate for lysolecithin is found at another point of the gradient, lower on the paper.

The spots higher up in the figs. 22–24 have a flat or rounded base only at low total phosphatide concentration, at higher concentrations (from 1 % on in fig. 23 and 24 and already from $\frac{1}{2}$ % on in fig. 22) the base of the spots shows an incision. As the incision has about the shape of the top of the spot below it, one must assume that at a certain stage of the chromatography the spots must have made contact but are now drifting apart. This is supported by the fact that at high total phosphatide concentration this contact is still present. Compare in figs. 22–24 the lower and middle spot at 2 % total concentration.

The above can also be explained in terms of adsorption chromatography combined with gradient elution (section 6). There is no reason for the lower row of spots (lysolecithin) to show incisions because there are no other spots below it. Thus these spots have a more or less flat base and the increase in area with increase of the concentration takes place in upward direction. When its top meets the base of the middle spot, lysolecithin (which here is strongly adsorbed) displaces the phosphatide of the middle spot (which at the base is relatively weakly adsorbed). The top of the middle spot in the same way displaces the phosphatide at the base of the upper spot. As the displacements are necessarily the least at the left and right of the base, the two rounded off lobes at either side of the incision will be displaced least and thus will tend to remain on one horizontal line. We see that this line for the upper spots goes through the second reference spot (second from above) and thus the upper spots belong to lecithin. Similarly the corresponding line for the middle spots goes through the third reference spot and thus represents sphingomyeline.

b) Dependence of the area of the spots on the total phosphatide concentration

We have argued in section 6 that the area of the lecithin spot should increase with a power lower than one when the lecithin concentration is increased. This expectation fits in with the results mentioned in section 5. One should expect that the same will hold for each of the spots of

[1]) In fig. 23 the base of the lower spots lie on a line slightly sloping upwards to the left. But it is seen that the line connecting the lower spot of the reference mixture also shows the same sloping upwards to the the left. As all four spots of the reference mixture lie higher at the left of the chromatogram than at the right, the cause of this phenomenon does not reside with our mixture of three phosphatides. During its rise the front remained horizontal. A possible cause might be an occasionally occuring temperature gradient in the dark room. The complication shown in fig. 23 is rare, since the lines connecting the reference spots as a rule proceed nearly horizontally.

a phosphatide mixture, at least when the spots are sufficiently free.

We have measured with a planimeter the spots in the figs. 22, 23 and 24 and have given the results in Table VI. We are of course interested whether we find here the same simple relation (log area as a linear function of log concentration) as was found for lecithin in section 5. When in the case of fig. 22 the logarithm of the area is plotted against the logarithm of the total concentration it is seen that here irregularities are present (for instance the area of lecithin at 0.5 % lies far too high). As in this figure we have only 4 concentrations one of which cannot be trusted, we shall not take the mean of the figs. 22, 23 and 24. Therefore we shall only consider the mean areas of the figs. 23 and 24, in each of which figures 5 total concentrations are represented.

TABLE VI

Spot area (cm^2) of lecithin, sphingomyelin and lysolecithin in dependence on total phosphatide concentration

Spots of:	Total conc. %	Spot area			Mean area of figs. 23 and 24	Slope of regression line in fig. 25
		fig. 22	fig. 23	fig. 24		
Lecithin	0.25	—	0.92	0.68	0.80	0,63
	0.5	2.03	1.38	1.25	1.31[5]	
	1	2.77	2.03	1.77	1.90	
	1.5	3.58	2.75	2.28	2.51[5]	
	2	3.94	3.21	2.87	3.04	
Sphingomyelin	0.25	—	0.21	0.17	0.19	0,63
	0.5	0.50	0.30	0.22	0.26	
	1	0.55	0.39	0.50	0.44[5]	
	1.5	0.69	0.58	0.50	0.54	
	2	0.88	0.63	0.77	0.70	
Lysolecithin	0.25	—	0.36	0.32	0.34	0,62
	0.5	0.79	0.61	0.59	0.60	
	1	1.15	0.90	0.75	0.82[5]	
	1.5	1.54	1.03	1.11	1.07	
	2	1.84	1.24	1.33	1.28[5]	
nature of paper and age		neutr. 4 days	acid 4 hrs.	acid 48 hrs.		

The mean areas are given in column 6. The logarithms of the mean areas have been plotted in fig. 25 against the logarithm of the total phosphatide concentration. The straight lines through the points are the calculated regression lines. They appear to have nearly the same slopes, see column 7. We find thus a similar behaviour for the three phosphatides of our mixture. As these slopes (0.63; 0.63; 0.62) are smaller than unity, the areas of the spots of all three components of the phosphatide mixture

increase less than proportional with the applied amounts. This shows that partition chromatography does not apply here. The results are precisely what is to be expected when we have adsorption chromatography operated by gradient elution (see section 6). That the slopes found here are very near to those in the case when lecithin is present alone (0.65: see fig. 14), shows that at the close of the chromatography no great disturbances have persisted resulting from displacement effects in the early stages.

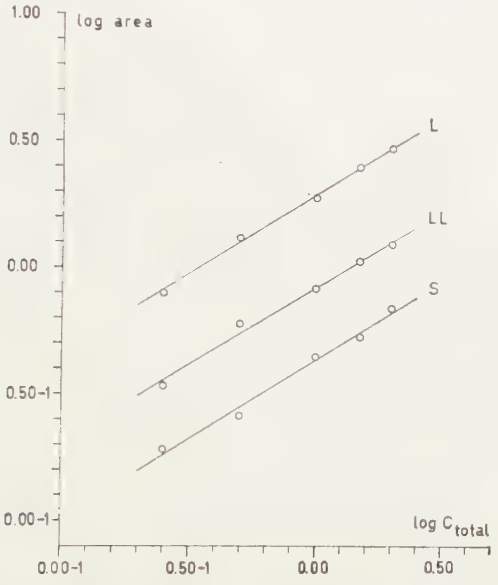

Fig. 25. Dependence of the logarithm of the mean spot areas, from figs. 23 and 24, on the logarithm of the total concentration of the phosphatide mixture.

10. *Chromatography of a mixture of cephalin, lecithin, their lysoproducts and sphingomyelin. Influence of the total concentration*

a) Discussion of the chromatograms

The mixture of the five above mentioned phosphatides, which at 0.5 % total concentration in preceding sections served as "reference mixture", was used here as 3.5; 3; 2.5; 2; 1.5; 1 and 0.5 % solution in chloroform-methanol (80:20). We proceeded in the same manner as in section 9 and obtained the chromatograms given in fig. 26 (neutralized $SiCl_4$-treated paper, 3 days old) and in figs. 27 and 28 (acid $SiCl_4$-treated papers, $\frac{1}{2}$ and 32 hrs. old respectively). Though five components are present we obtained only four spots, because the lysocephalin and sphingomyelin spots coincided. (See Part I of this series). The sequence of the spots reckoned from upper to lower is cephalin(C)—lecithin(L)—lysocephalin + sphingomyelin(LC + S)—lysolecithin(LL). The results are analogous to those in section 9, in which a mixture of L, S and LL was investigated. Here too with an increase of the total concentration the spots increase in area

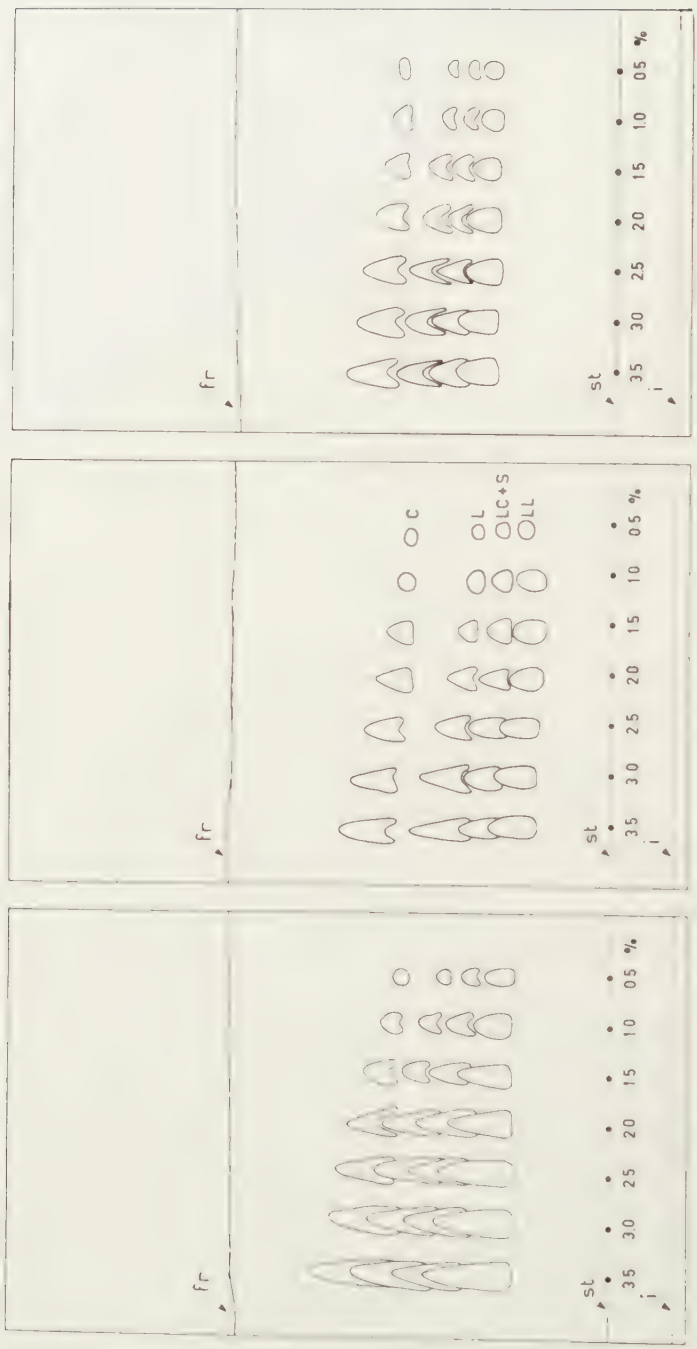

Fig. 26

Fig. 27

Fig. 28

Figs. 26-28. Chromatography of a mixture of cephalin (C), lecithin (L), their lysoproducts (LC and LL), and sphingomyelin (S). Influence of the total concentration (in %). Neutralized SiO_2-treated paper (fig. 26) and acid SiO_2-treated paper (figs. 27 and 28) of different age (fig. 27 — $\frac{1}{2}$ hour; fig. 28 — 32 hours) has been used.

in upward direction. Once more the spots on the lower row (LL) have a flat or rounded base, all bases on one horizontal line.

The spots on the three higher rows (LC + S; L and C) have (except at low concentration) an incision in the base. On each row the lower limit of the lobes on either side of the incision tends to remain on the same horizontal line as the base of the free spot at low concentration (see below paragraph c). We refer to section 9 for an explanation of these phenomena (adsorption chromatography, combined with gradient elution).

The same generalizations hold when L is present alone (section 5, figs. 10–13), and when L, S and LL are present in a mixture of the three (section 9, figs. 22–24). The base (or when incisions are present and no disturbances occur, the lower limit of the lobes at either side of the incision) of each phosphatide spot occupies a particular zone in the gradient of the mobile phase on the paper.

b) Dependence of spot area on the total phosphatide concentration

In order to investigate the relation between spot and concentration, the areas of the C, L, LC + S and LL spots were measured (see Table VII).

If the logarithm of the spot area is plotted against the logarithm of the total concentration we do not obtain the simple result as in the preceding section. The points lie much more irregularly distributed than in fig. 25. Because strong penetrations of spots occur, the chromatogram in fig. 26 is least trustworthy. We therefore give only the slopes of the calculated regression lines for the chromatograms in fig. 27 and fig. 28:

fig. 27	C = 0.95 ;	L = 0.90 ;	LC + S = 0.56;	LL = 0.57
fig. 28	C = 0.88 ;	L = 0.79 ;	LC + S = 0.72;	LL = 0.67
mean:	$C = 0.91^5$;	$L = 0.84^5$;	LC + S = 0.64;	LL = 0.62

Taking the mean slopes as representative, we may compare them with the slopes found for L when present alone = 0.65; (see section 5, fig. 14) and for L, S and LL applied as mixture: L = 0.63; S = 0.63 and LL = 0.62 (section 9, fig. 25). Only the mean slopes corresponding to the lower rows of spots LL and LC + S on the chromatograms of figs. 27 and 28 are of the same order of magnitude. The mean slope corresponding to the third row of spots (L) is distinctly higher. Since the mean slope corresponding to the upper rows of spots (C) has a still higher value, possibly in the chromatography of the reference mixture a disturbing factor enters, which is the more effective when the number of spots below the spot considered is higher.

This factor may result from the similarity of the partial concentrations of the components. From the spot areas one estimates roughly

$$C : L : LC + S : LL = 1:1:1:2.5.$$

With an increase of the total concentration, all four spots and most of all the lower spots will be considerably extended in upward direction. Considerable interpenetration of spots will thus occur during the beginning stages of chromatography.

Compare fig. 26, in which, starting with a total concentration of 2.5 %, the four spots still form a closed group. It is not surprising that strong disturbances must occur in such cases.

In the case of chromatography of the lecithin + sphingomyelin + lysolecithin, studied in the preceding section, the situation is much more favourable. Here the highest row of spots belongs to the predominating component (L) and the second row of spots belongs to the component (S) present in the smallest concentration.

If the amount of the phosphatide mixture applied is increased, the L spots will considerably increase in area. Since above L there is no other row of spots, this does not lead to disturbances.

TABLE VII

Spot area (cm^2) of cephalin, lecithin, lysocephalin + sphingomyelin and lysolecithin as a function of total phosphatide concentration

Total conc. %	cephalin			lecithin		
	fig. 26	fig. 27	fig. 28	fig. 26	fig. 27	fig. 28
0.5	0.33	0.26	0.31	0.31	0.24	0.24
1	0.54	0.37	0.52	0.50	0.52	0.38
1.5	0.89	0.70	0.74	0.63	0.53	0.62
2	1.11	1.02	0.99	1.24	0.77	0.76
2.5	1.41	1.09	1.25	1.44	1.01	0.85
3	1.69	1.27	1.58	1.51	1.30	0.98
3.5	1.66	1.47	1.57	1.80	1.43	1.04
Total conc. %	lysocephalin + sphingomyelin			lysolecithin		
	fig. 26	fig. 27	fig. 28	fig. 26	fig. 27	fig. 28
0.5	0.38	0.32	0.26	0.71	0.42	0.43
1	0.69	0.58	0.39	1.26	0.82	0.66
1.5	0.91	0.74	0.61	1.54	1.08	0.82
2	1.32	0.72	0.62	1.94	0.99	1.15
2.5	1.12	0.90	0.86	2.45	1.15	1.31
3	1.35	1.05	0.88	2.77	1.22	1.31
3.5	1.31	0.90	1.06	2.98	1.39	1.56

From the fact that the slopes of the L, S and LL lines in fig. 25 are practically equal, it must be concluded that the disturbance due to penetration of the top of the LL spots into the base of the S spots, similarly of the top of the spots into the base of the L spots, during the early stages of chromatography, have practically disappeared at the time the chromatography was stopped.

c) The location of the lower limit of the lobes of the three upper spots on the chromatograms

We said in paragraph *a* that the lower limit of the lobes of incised spots tend to remain on the same horizontal line as the base of the free spot at low concentration.

When the figs. 26–28 are examined more closely we see that the lower limit of these lobes lie on lines sloping more or less upward to the left. This means that these lobes too are pushed upward as a result of the disturbance caused by the spots below. Thus when we use the position of the lower limit of the lobes for calculating R_{f_1}, we will find too high a value for R_{f_1}.

11. *Chromatography of a mixture of cephalin, lecithin, their lysoproducts and sphingomyelin to increasing heights of the front*

We use the same reference mixture as already employed in section 10. Its components will in the following be abbreviated to C (cephalin); L (lecithin); S (sphingomyelin); LC (lysocephalin) and LL (lysolecithin). For reasons discussed in section 7 we used neutralized $SiCl_4$-treated paper. Five sheets of one batch, each provided with nine starting points on an

oblique line, were run the day after their preparation in the large slit-feeding apparatus, 5 mm³ of the 0.5 % solution of the reference mixture was applied on the starting points. The chromatograms obtained are reproduced in the figures 29–33.

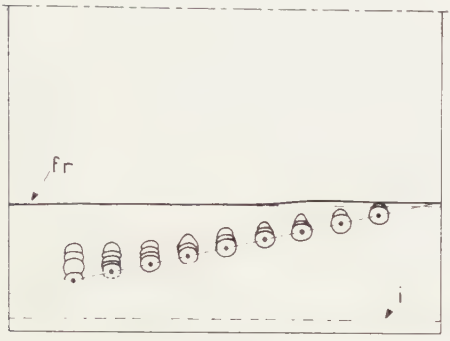

Fig. 29

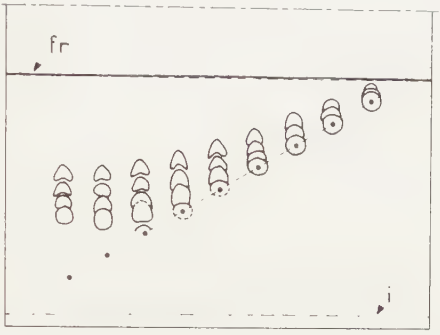

Fig. 30

Figs. 29–30. Chromatograms of the reference mixture on neutralized $SiCl_4$-treated paper; nine starting points on sloping lines. The front has risen approximately 4.5 and 9.5 cm above the immersion line.

On each of the figures we may observe from right to left what happens when the distance front-starting place increases. It is seen that first a closed group of spots is formed (fig. 29), then the upper spot (C) detaches itself from the group, and successively the second (L) and the third spot (CL+S), after which the fourth spot (LL) is free too.

TABLE VIII

Distance from immersion to horizontal line through base of the two left spots ("asymptote") and to front ("front")

Spot	fig.	"asymptote" (a_l) in mm	"front" (f_l) in mm	R_{f_l} (= a_l/f_l)	
Cephalin	30	51.5	93	0.55	
	31	83	144	0.58	mean:
	32	111.5	193.5	0.58	**0,57**
	33	139	244.5	0.57	
Lecithin	30	45.5	93	0.49	
	31	70.5	144	0.49	mean:
	32	93	193.5	0.48	**0,48**
	33	113.5	244.5	0.46	
Lysocephalin + Sphingomyelin	30	40	93	0.43	
	31	62	144	0.43	mean:
	32	79	193.5	0.41	**0,42**
	33	97	244.5	0.40	
Lysolecithin	30	33	93	0.35	
	31	50.5	144	0.35	mean:
	32	65	193.5	0.34	**0,35**
	33	82.5	244.5	0.34	

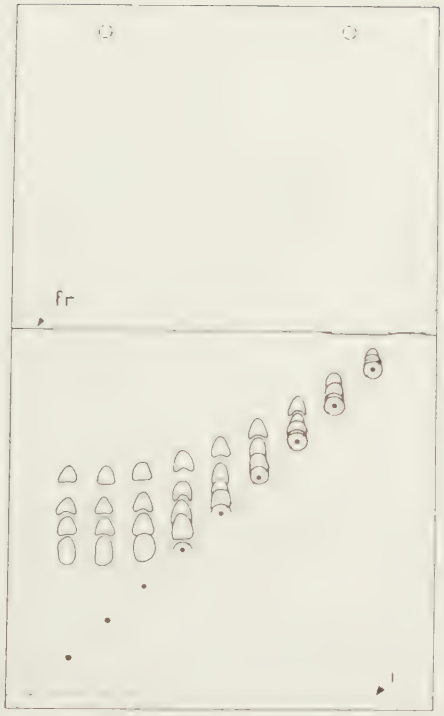

Fig. 31

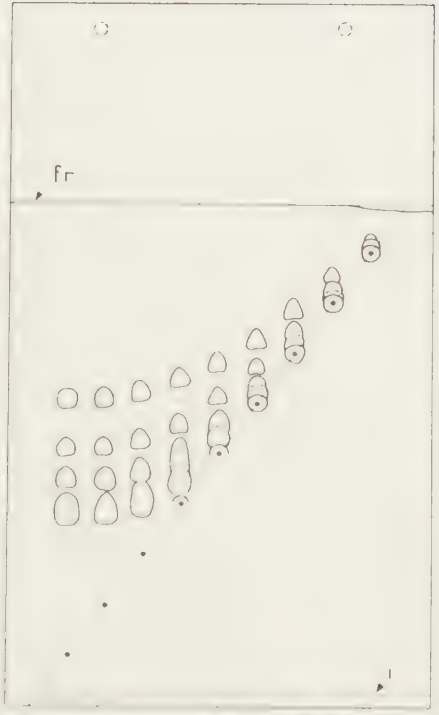

Fig. 32

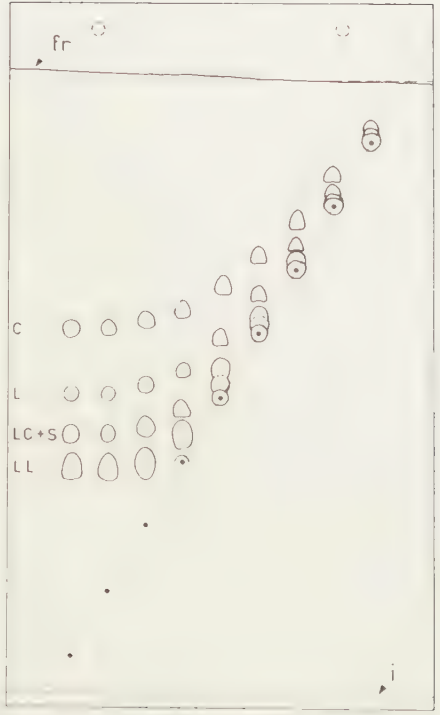

Fig. 33

Figs. 31–33. Chromatograms of the reference mixture on neutralized $SiCl_4$ treated paper, with nine starting points on sloping lines. The front has risen approximately 14.5, 19.5 and 24.5 cm above the immersion line.

In the closed group the three upper spots have incisions at the base. When a spot has just detached itself from the group, moving upwards, it still shows the incision at the base. The incision gradually disappears when the spots drift farther apart, the base becoming flat. We have already explained the formation of an incision at the base of the spots in sections 9 and 10. The results in these sections led to the conclusion that the mechanism of the chromatography of cephalin, lysocephalin and sphingomyelin (not separated) and of lysolecithin is the same as discussed for lecithin in section 6. This conclusion is confirmed by the results shown in the figures 29–33. We see here clearly that for each of the components (C; L; LC+S and LL) of the mixture, the same applies as was found in Section 7, see figs. 15–19, for lecithin when present alone.

It is observed that to the left on the figures 30–33 the place of the transported spots becomes independent of the starting place. Thus R_f values have no sense here and the chromatography is not a partition chromatography.

The four levels which on each of the figs. 30–33 the C, L, LC+S and LL spots tend to reach, must then indicate characteristic compositions within the gradient of the mobile phase, at which the transport velocity upward has reached its maximum value. Assuming that the two groups of spots nearest the left-hand margin of the chromatograms lie already on these limiting values, we may investigate the position of these four levels as a function of the position of the front.

The mean distances between spot bases and immersion line (a_i) and between front and immersion line (f_i) are given in columns 3 and 4 of Table VIII. They have been plotted in fig. 34.

If we inspect column 5 of the Table, we see that for each spot the values of R_{f_i} lie close together. The value 0.55 for cephalin on the first row is very probably an error, for it appears that in fig. 34 the three higher situated points appertaining to C lie practically on a straight line through the origin.

The R_{f_i} values for LL are equal within the experimental errors, so that we may consider a_i to be practically proportional to f_i. (Compare the lower straight line drawn in fig. 34). One would expect that for the two spots in between, the points would lie on straight lines through the origin too. If we inspect, however, column 5 of the Table, the R_{f_i} values for L, and similarly for LC+S, we get the impression that here a systematic decrease of R_{f_i} with increase of f_i is present, which just exceeds the experimental errors. Hence the L and the LC+S curves in fig. 34 are probably not straight lines through the origin, but they proceed in a slightly convex manner. When L is present alone, we obtained a straight line through the origin (compare fig. 21). This suggests that the slight curvature of the L and LC+S curves in fig. 34 is connected with the fact that here a mixture of phosphatides has been applied on the starting points.

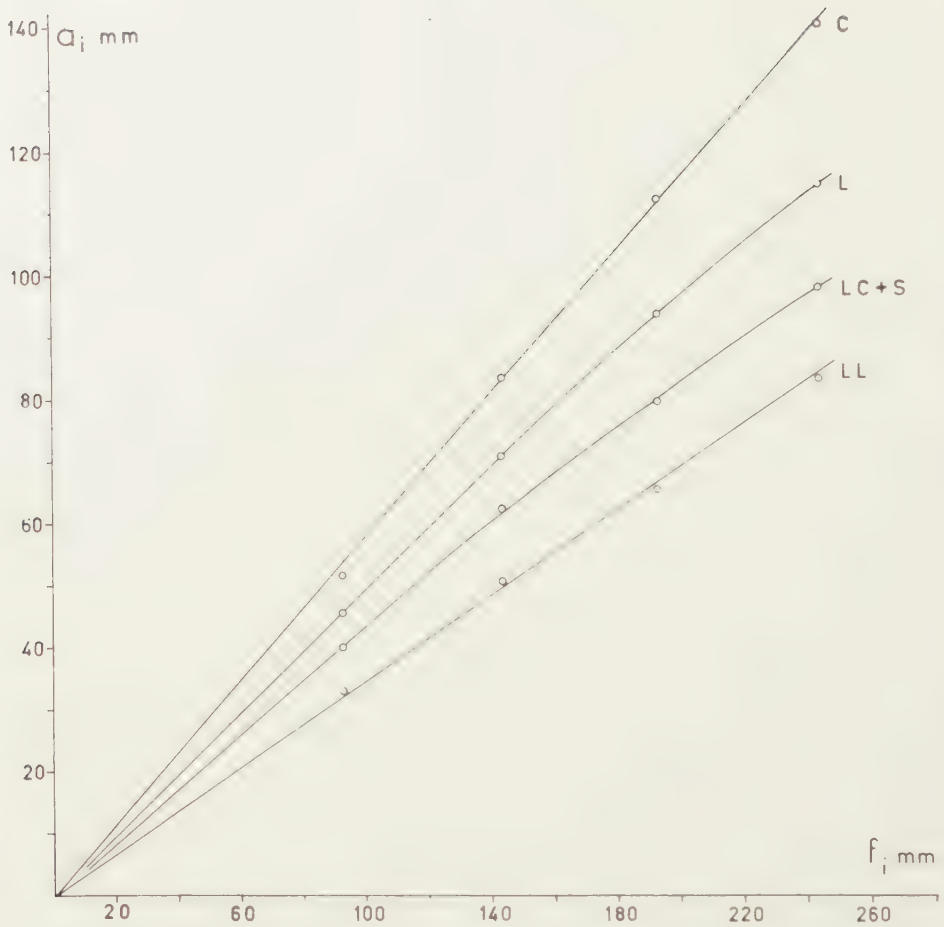

Fig. 34. The values of a_i, for the four separate phosphatides on the chromatograms of the figures 29–33, plotted against f_i.

This may be connected with the fact already mentioned, namely that chromatography of a mixture of phosphatides begins with the formation of a closed group of spots (compare fig. 29). As a result the spots do not move freely and the lower situated cause incisions in the base of the higher situated spots.

The upper spot (C) soon detaches itself from the group. This may explain that the curve through the last three C points is within the experimental error a straight line through the origin. It takes a longer time before the L spot detaches itself from the remaining closed group and a still longer time before the LC + S spot comes free. As long as they are in the closed group they must lie too high and only gradually their position on the chromatogram will take the place where they should be, if the phosphatide considered were the only phosphatide present.

We must still give an explanation why the LL points do (practically) lie on a straight line through the origin. This may be due to the fact

that it occupies the lowest place in the closed group of spots formed at low f_i values. There is no spot below it, so it cannot be pushed upwards. The base will from the beginning lie at that point of the gradient which is characteristic for maximum elution rate (relative to the rate of the front). We may thus explain that the curves for C and LL in fig. 34 are practically straight lines through the origin, and that the curves appertaining to the spots (L and LC+S), which in the beginning were "compressed" in between the upper (C) and the lower spot (LL), are slightly curved.

The results in this section may be summed up in two points:

1) Each of the four spots reaches its maximum elution rate relative to that of the front at a characteristic composition of the gradient. Because R_{f_i} is independent of the front height the above-mentioned characteristic compositions are found (practically) always at the same fractions of the ascension height of the front above the immersion line.
2) In the chromatography of a mixture of phosphatides the spots lying in between the upper and lower may show an apparently too high R_{f_i} at a relatively low front height. In this case the front should rise more than 15 cm above the immersion line, if the correct R_{f_i} values are to be obtained.

12. *Summary*

1. The chromatography of lecithin alone, and of mixtures of egg phosphatides, has been investigated with the aid of a large slit-feeding apparatus, using 17 × 27 cm sheets of $SiCl_4$-treated Schleicher and Schüll no. 2043*b*, and di-isobutylketone – acetic acid – H_2O (50:25:5 by volume) as mobile phase.

2. Two types of chromatograms have been run:

A) Sheets provided with nine starting points on equal distances on a sloping line, intersecting the front on the paper, while on each starting point 5 mm^3 of a dilute solution of lecithin or mixture of egg-phosphatides was applied.

B) Sheets provided with nine equidistant starting points on a horizontal line; the concentration of the 5 mm^3 solution applied was increased for the successive starting points.

3. When lecithin alone is applied on chromatograms of type A mentioned sub 2, the migrated spots are situated on a curve, in such a way that the spots which have migrated from the lowest starting points reach a practically horizontal line (asymptote).

4. Since a straight line cannot be drawn through the intersection point of front and sloping line and through all spots, R_f values (in the ordinary sense) are not constant.

5. The quotient of distance a_i of the asymptote mentioned sub 3 to the immersion line (i), divided by the distance f_i of the front to the immersion line, is independent of the ascension height of the front. It is proposed to denote this quotient with the symbol $R_{f_i} = a_i/f_i$.

6. The results suggest that a gradient is present in the mobile phase and that the asymptote may indicate a particular composition of the mobile phase at which the upward migration of lecithin reaches its maximum velocity, relative to the velocity of the front.

7. The existence of a gradient has been demonstrated. The acetic acid concentration in the mobile phase wetting the paper markedly decreases in upward direction.

8. When a mixture of egg phosphatides is applied four spots are obtained: C = cephalin (upper); L = lecithin; LC + S = lysocephalin + sphingomyelin (not separated) and LL = lysolecithin (lower).

9. When this mixture is applied on chromatograms of type A mentioned sub 2, the spots are now situated on four curves, each practically reaching a horizontal level (asymptotes). The four asymptotes denote the particular compositions in the gradient at which the upward migration of C, of L, of LC + S and of LL reaches their maximum velocity relative to the front.

10. Here too the R_{f_i} of the four spots is indepent of the ascension height, provided the ascension height is chosen high enough. At relatively low ascension heights the R_{f_i} values for the two middle spots are found slightly too high (see below sub 16).

11. Chromatograms of the type B mentioned sub 2 may serve to investigate the influence of increasing amounts of phosphatides applied at the starting points.

12. With lecithin alone, it is found that

a) the area of the transported spots increases less than proportionally with the amount applied (slope of line in a double logarithmic plot 0.65).

b) the lower margin of the spots lies on a nearly horizontal level; the increase in area is due mainly to an increase in length, whereby the spots acquire a roughly triangular shape.

c) In the triangular spots the lecithin concentration increases in upward direction.

13. In principle the same is found when a mixture of phosphatides is applied. However, complications may occur by mutual hindrance of the spots. The lower spot always has a flat base, but higher situated spots may show an incision at the base, or even at high total concentration the spots may form a closed group. In cases in which the mutual disturbance is slight, the lines obtained by plotting the log (area) against

the log (total concentration) have a slope about equal to the slope obtained for lecithin alone.

14. A discussion of the results sub 12) and 13), combined with the results concerning the importance of a gradient in the mobile phase (points 3–11), leads to a picture of the mechanism of the chromatography of egg phosphatides with our mobile phase. It is to be considered as adsorption chromatography operating with gradient elution.

15. The characteristic place of a spot on the chromatogram is the location of its base (here the elution rate has reached its maximum) and not the location of its centre. Hence in calculating $R_{f_i} = \frac{a_i}{f_i}$ one should take for a_i the distance of the spotbase to the immersion line.

16. In the early stages of the chromatography of a mixture of phosphatides a closed group of spots is formed. The question why the spots lying in between the upper and lower spots show slight deviations from R_{f_i} = constant, when the front height is but small (see point 10), has been answered.

17. Acid $SiCl_4$-treated paper shows a slight hydrolytic activity. This paper, when freshly prepared, distinctly changes its chromatographic properties over time. For this reason the experiments concerning the independence of R_{f_i} with regard to the front height (mentioned sub 5 and 10) have been performed on neutralized $SiCl_4$-treated paper.

Department of Medical Chemistry,
University of Leyden

REFERENCES

1. Bungenberg de Jong, H. G. and J. Th. Hoogeveen, these Proceedings, Series **B** *63*, 190 (1960).
2. ———— and ————, these Proceedings, Series **B** *63*, 1 (1960).
3. ———— and G. R. van Someren, these Proceedings, Series **B 62**, 150 (1959).
4. Hooghwinkel, G. J. M., J. Th. Hoogeveen, M. J. Lexmond and H. G. Bungenberg de Jong, these Proceedings, Series **B 62**, 222 (1959).
5. Bungenberg de Jong, H. G. and J. Th. Hoogeveen, these Proceedings, Series **B** *63* 15 (1960).

QUANTITATIVE ASPECTS OF THE TRICOMPLEX STAINING PROCEDURE.

THE STAINING OF LECITHIN SPOTS APPLIED ON CHROMATOGRAPHIC PAPERS Ia

BY

G. J. M. HOOGHWINKEL AND H. P. G. A. VAN NIEKERK

(Communicated by Prof. H. G. BUNGENBERG DE JONG at the meeting of Jan. 30, 1960)

In earlier papers of this laboratory [1, 2], an indicating reaction for phosphatides containing an acidic group and a basic group carried out by suspending a spot test paper or paper chromatogram in an aqueous staining solution was described. This method was based on the supposition that phosphatides of the acid-base type would stain with an appropriate dye (cationic or anionic) in the presence of a well chosen non- (or weakly) coloured ion (anion or cation), when the latter has a sufficiently strong affinity to the phosphatide and on the other hand only a weak affinity to the dye.

It was known that basic dyes stain the paper itself rather strongly, consequently giving an intensely coloured background, and that most inorganic anions do not have a large affinity for the positive group of the phosphatide. Consequently our choice fell on a staining method for phosphatides of the acid base type using an acid dye and an appropriate cation [1] Earlier investigations on "Reversal of charge spectra" [3] have revealed that among cations the uranyl ion has by far the greatest affinity for the phosphate group, while this cation does not have, a very prominent affinity for carboxyl or sulphate-groups. Using in the staining procedure a dye(anion) containing sulphate groups Acid Fuchsin and uranyl ions (cation) resulted in a successful staining method with a negligeable background staining. If, indeed, the mechanism of the staining method must be considered an affect of Coulomb interactions as proposed for "tricomplex systems" [4], a quantitative relationship based on equivalence between the amount of dye and the amount of phosphatides present is to be expected. For reasons to be discussed later the greater part of the present investigation deals with a tricomplex staining in which instead of Acid Fuchsin is used Edicol Supra Ponceau 4 RS.

To investigate this supposition is necessary to state beforehand the circumstances at which the maximum staining of a certain amount of phosphatide will occur. If indeed this quantitative relationship does occur, it is perhaps also possible to use the method to measure the

concentration of a solution containing an unknown amount of phosphatides.

Methods and materials

A. *Lecithin*

Lecithin was purified from eggs by column chromatographic separation, using Al_2O_3 and SiO_2 columns and as eluent (5,6)methanol-chloroform mixtures.

The lecithin was dissolved in chloroform-methanol (80:20) and shows by paperchromatographic separation on silica-impregnated paper only one spot on the lecithin place. This suggests a high purity. In a $\pm$ 5 % standard solution the nitrogen and phosphorus contents were determined. From the nitrogen contents and phosphorus contents respectively and the lecithin molarity of the approximately 5 % solution is calculated. The nitrogen content indicates a concentration of 63.8 $\pm$ 0.3 m mol/l. The phosphorus contents indicates a concentration of 63.9 $\pm$ 0.6 m mol/l. The ratio P/N = 1.0, assuming the molarities are not different within the experimental errors. The N determination was carried out as a micro Kjeldahl determination. The P content was estimated according to Meijer [11].

For theoretical calculations we use for our standard lecithin solution the molarity of 63.8 m mol if the experiments are carried out with the so-called 5 % lecithin solution.

In other cases we use a so-called 2 % solution; we shall then use a molarity of 25.52 m mol.

B. *General staining procedure for lecithin on filter paper*

Using a capillary pipet with a volume of 4.73 mm^3 a certain amount of lecithin is applied on a filter paper. The lecithin-solutions used are of different concentrations and made in chloroform-methanol 80:20 (v/v). The applied spots will enclose a circular surface having a diameter of about 9 mm.

When the methanol-chloroform is evaporated, the paper strip, containing one or more of such lecithin spots, is suspended in a staining bath The staining bath for general use contains the following ingredients in concentrations as indicated dissolved in destilled water:

0.005 % Acid Fuchsin or Edicol Supra Ponceau 4 RS.
0.2 % Uranyl nitrate.
0.01 n HCl.

After a short time the lecithin spots will be stained red, while the slight background colour is only due to the paper being soaked by the staining solution.

After a fixed time the paper containing the red coloured lecithin spot or spots is dried with some care, between common filter paper and after that with the aid of a stream of warm air.

In most of our experiments the concentration of the uranyl nitrate in the staining bath is 0.2 % and the normality of the hydrochloric acid is 0.01 n. If another uranyl nitrate concentration or another hydrochloric acid normality is used it will be indicated.

C. *The filter paper*

The filter paper used was Schleicher and Schüll 2043*b*, impregnated with silicic acid, as used for paper chromatography (2, 7). The filter paper is divided with a pencil in squares of $1\frac{1}{2}$ by $1\frac{1}{2}$ cm. The lecithin solutions are applied in the middle of a square and the chloroform-methanol is allowed to evaporate for at least 10 minutes before immersing the paper in a staining bath.

It is not necessary to use impregnated papers, but we did so to develop a method for a quantitative evaluation of paper chromatograms on silica-impregnated papers.

Non-impregnated papers give, as we could conclude from some experiments, the same results. However, impregnated papers have a stronger "texture" and so they are easier to manipulate. Moreover the impregnated papers do not desintegrate into fibres as easily as non-impregnated papers.

D. *Capillary pipet*

The lecithin solutions in chloroform-methanol 80:20 (v/v) were applied with a self filling capillary pipet. This pipet has a volume of 4.73 mm^3.

The statistical calculations based on 16 measurements indicate that by using the pipet the volume applied on the paper is 4.73 mm^3, standard deviation $\pm$ 0.12 mm^3.

E. *Elution of the dye from the paper squares carrying the stained lecithin spots*

For measuring the amount of dye present at a spot we have to elute the dye from the paper.

This is possible by using a solution of 50 % tert.-butylalcohol in water containing $^3/_5$ n HCl. This solution is chosen as a result of some experiments in which other solvents were tried as well.

The solution must be acidic because Acid Fuchsin loses its colour in alkaline medium. The dye is not soluble in most organic solvents, so a total or partly aqueous medium is needed. Moreover it is desirable to use a solution in which the lecithin will be soluble, because in that case elution will progress considerably quicker. It was known that aqueous solutions of tert.-butylalcohol (25 % tert.-butylalcohol and higher) are good solvents for phosphatides. The hydrochloric acid in the elution solvents promotes a quicker elution but is not especially required.

Generally we now elute $1\frac{1}{2}$ by $1\frac{1}{2}$ cm squares containing a stained lecithin spot with 5 ml $^3/_5$ n HCl in 50 % tert.-butylalcohol in water.

At the same time a blank determination is carried out. The blank is a $1\frac{1}{2}$ by $1\frac{1}{2}$ cm filter paper square containing no lecithin stained under the same conditions. These blanks are "stained" faintly red due to the dried staining solution soaked up by the paper. To measure the amount of dye that is eluted the extinction of the eluate is determined with a Unicam SP 500 spectrophotometer. The exact eluate extinction only corresponding to the amount of the dye linked to the lecithin is not obtained by substracting the total blank extinction value but by substracting only 70 % of this value. This point will be discussed later (see experimental part sub 5).

F. *The use of Edicol Supra Ponceau 4 RS*

In the course of these investigations it became evident that the Acid Fuchsin preparation we used contained quite a number of substances other than Acid Fuchsin also having a red colour. In this respect we examined a series of Acid Fuchsin preparations of various manufactures. Our criterium was a paper electrophoretic separation [8] of the components of the commercial dye. Most of them contained 4–6 red coloured components and moreover 3–4 components only visible if viewed under ultra violet light ('chromatolite'). We searched for and found a dye which contains three acidic groups, and without impurities. Edicol Supra Ponceau 4 RS (I.C.I.) was such a dye. A commercial product it proved to be free from impurities upon examination of the electropherogram in visible and in ultra violet light.

For quantitative calculations it was necessary to know the dye content of the commercial dye preparation. For this reason we carried out nitrogen determinations (micro kjeldahl) in the dye. As a result of this determination we could state that Edicol Supra Ponceau 4 RS contains 60.9 % pure dye. The remainder of the commercial product consists of an amount of salts. According to Th. Vickerstaff [6] salts are generally added to a commercial dye as diluent to bring the dye to a standard tinctorial strength for convenient use. In most cases sodium chloride, sodium sulphate or soluble starch are used for this purpose. We did not investigate the kind of diluent added to the Edicol Supra Ponceau 4 RS, because it was of no interest to us [1]).

G. *Physico-chemical properties of the acidic dyes*

To measure the amount of dye present in the eluate of a stained lecithin spot it is necessary first to examine the properties of the dye in the eluting solvent. Both acidic dyes used in this work contain 3 acidic groups as shown in the formulae given below (figure 1).

---

[1]) Complex interactions generally are influenced by the presence of other salts. At the low dye concentration in the staining solution, however, the salt concentration due to impurities in the commercial dye will have practically no influence on the tricomplex staining reaction.

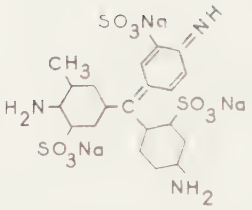

Acid Fuchsin
M=607

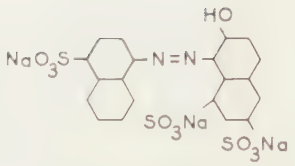

Edicol supra Ponceau 4 RS
M=604

Fig. 1

Using 0.001 % dye solutions in $^3/_5$ n HCl in 50 % tert.-butylalcohol the absorption spectra are determined (see figure 2).

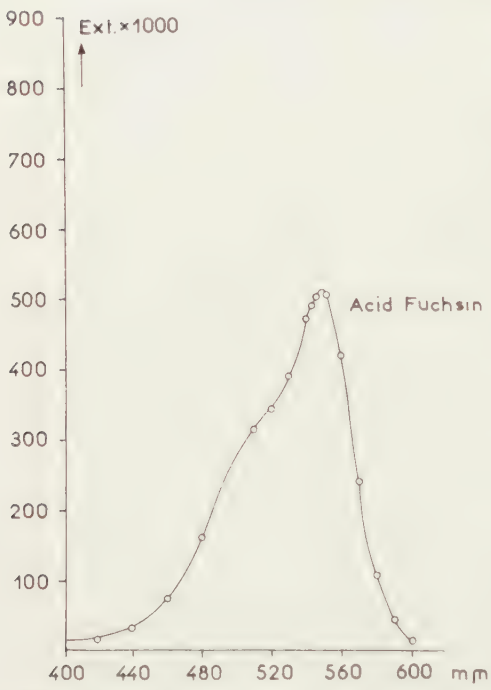

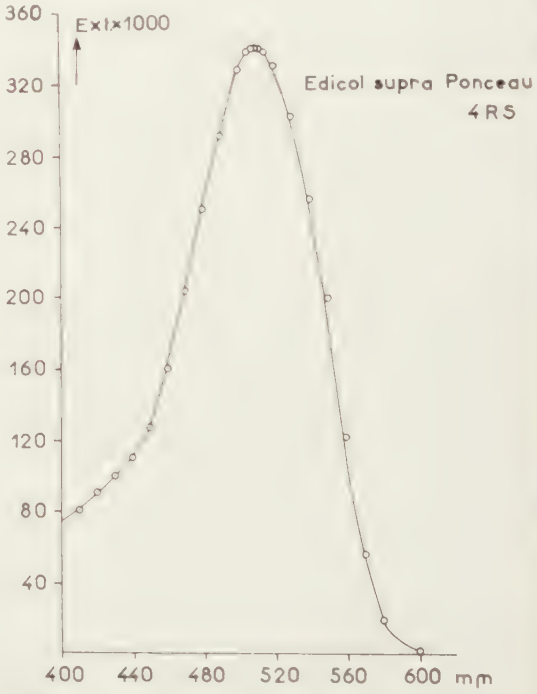

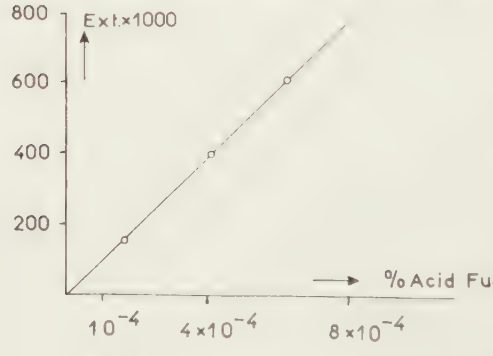

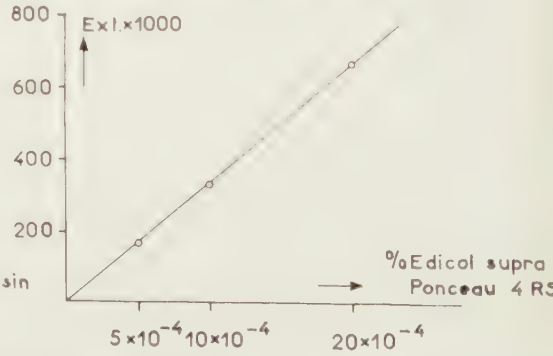

Fig. 2. Absorption spectra and concentration dependence of Acid Fuchsin and Edicol Supra Ponceau 4 RS.

If measured at the maximum absorption wave length we can see that the extinction has a linear dependence of the dye concentration in the eluting solvent. So the dyes do behave according to the law of Lambert–Beer (see figure 2).

The spectrophotometrical determinations are made with a Unicam SP 500 spectrophotometer, using a 1 cm diameter cuvette.

Experimental Results

I. *Some preliminary experiments with Acid Fuchsin*

In our earlier experiments we used the dye Acid Fuchsin (Schuchardt) The staining period was 16 hours. After that the paper was dried as described under methods.

Next the squares of $1\frac{1}{2}$ by $1\frac{1}{2}$ cm were cut out and suspended in an erlenmeyer in exactly 5 ml $^3/_5$ n HCl in 50 % tert.-butylalcohol in water. After closing the erlenmeyer with a stopper the paper has to stay in the solution till all the dye has dissolved in the eluting solvent. With the spectrophotometer the extinction of the eluate is measured at 549 mμ

The following experiment was carried out:

Lecithin solutions of different lecithin concentrations in chloroform-methanol (80:20) were applied on filter paper squares. The staining procedure was performed in 5 fold and after elution of the spots the extinction was measured. The results are shown in figure 3.

The abscissa gives the lecithin concentration in percentages and the ordinate gives the eluate extinctions diminished with 70 % of the blank extinction value.

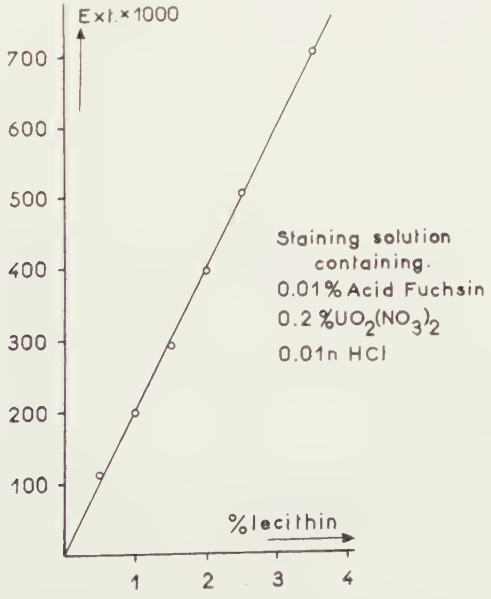

Fig. 3. The eluate extinction of lecithin spots stained with Acid Fuchsin in dependence of the lecithin concentrations.

The straight line which is found suggests the expected linear relationship when between the reacting components a tricomplex system is formed.

The experiments performed using Acid Fuchsin as a dye in the staining bath will not be reported here in detail, because on theoretical grounds this dye (a commercial product) is not suitable for calculations of molecular relations. The reason is that, as already mentioned under methods and meterials, Acid Fuchsin is far from a pure dye. For exact calculations it is necessary to use a pure dye or a commercial dye which does not contain impurities of organic coloured matter. The impurities we eventually can tolerate are the salts which are used as diluents.

Edicol Supra Ponceau 4 RS (see earlier in this paper), is sufficiently pure for general use in this investigation.

II. *The influence of various factors on the staining of lecithin, using Edicol Supra Ponceau 4 RS*

In the following experiments we have tried to search for the optimal staining conditions in order to be able to evaluate some fundamental properties of the staining method under investigation.

The most important factors which determine the results of the staining are:

1. The pH of the staining solution.
2. The immersion time in the staining solution.
3. The concentration of the dye in the staining solution.
4. The concentration of $UO_2(NO_3)_2$ in the staining solution.
5. The influence of lecithin concentration (which leads to the argumentation of using the 70 % blank extinction value as real blank value).

The effect of variations in the pH, dye concentration and duration of immersion in the staining solution are investigated using the dye Edicol Supra Ponceau 4 RS. The uranyl nitrate concentration in the staining solution is fixed at 0.2 %. The effect of the uranyl nitrate concentration is studied using a dye concentration of 0.01 %.

Furthermore, it must be noted, we did not rinse the stained papers after staining and before drying, because we found that quite a considerable amount of dye is lost by rinsing the papers.

Rinsing is prescribed as a manipulation if the staining reaction is used for qualitative purposes, for instance in identification reactions by paper chromatographic separations.

1. Influence of the pH of the staining solution

To examine this effect we carried out some experiments in which we used a 2 % lecithin solution in chloroform-methanol (80:20). A dye concentration of 0.01 % was used. Using different HCl concentrations a pH range between the values 0 and 4 was obtained. The next table gives the results.

TABLE 1

Effect of pH variation on staining intensity

pH of staining solution	A	B	Extinction A–70 % B
	Extinction × 1000 of eluate of lecithin spot	Extinction × 1000 of eluate of blank	
0	120, 123, 122, 120	62, 64, 64, 66	121 — 45 = 66
1	198, 205, 197, 203	43, 43, 43	201 — 30 = 171
2	230, 230, 232, 230	36, 36, 38, 37	231 — 26 = 205
3	221, 215, 222, 220	37, 35, 35	220 — 25 = 195
4	203, 215, 210, 215	37, 37, 39, 39	215 — 27 = 188

The graphic demonstration of the results is given in the next figure:

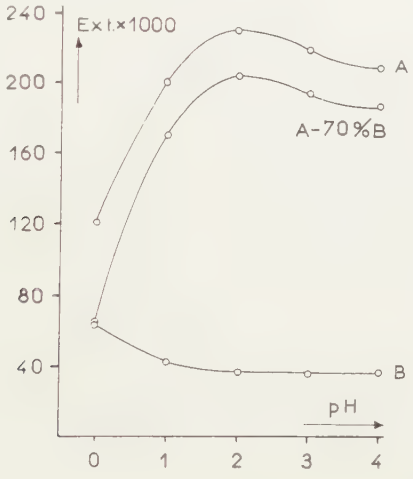

Fig. 4. Extinctions of the eluates obtained from lecithin spots stained in solutions having different pH values.

Using Acid Fuchsin the same experiment was carried out. The result was exactly the same in both cases. So we must conclude that at pH = 2 more dye is bound by the lecithin then at other pH values.

As it is our object to search for the conditions promoting the strongest staining of lecithin, it is necessary for our further experiments to use a staining solution, containing 0.01 n HCl, so that the pH has a value 2.

2. The influence of the staining time

The staining of lecithin spots is carried out with two staining solutions. The first one contained 0.002 % Edicol Supra Ponceau 4 RS, the second one contained 0.01 % of the dye.

The experiment is carried out with 2 and 5 % lecithin solutions. The staining times used are 2, 6, 16 and 40 hours.

In the next table the results are summarised:

TABLE 2

Staining of 5 and 2 % lecithin spots in 0.002 % and 0.01 % Edicol Supra Ponceau 4 RS during respectively 2, 6, 16, 40 hours

Dye concentration 0.002 %	Extinction in eluate (E × 1000)							
Staining time in hours	5 % lec. spot			2 % lec. spot			Blank	
2	58	68	73	65	75	83	11	7
6	122	149	147	155	135	143	10	10
16	340	335	317	166	166	165	6	6
40	435	442	431	169	170	171	7	9
Dye concentration 0.01 %	Extinction in eluate (E × 1000)							
Staining time in hours	5 % lec. spot			2 % lec. spot			Blank	
2	230	270	275	205	216	216	28	27
6	492	472	492	218	217	222	32	34
16	550	557	555	226	225	219	35	35
40	545	541	545	225	226	226	35	35

In Figure 5 gives curves representing the data of table 2.

The mean extinction values of the determinations are diminished with 70 % of the mean extinction values of the blank. Fig. 4 demonstrates clearly what happened, but the experimental points on the curves are mean values of the values mentioned in the table and they are diminished with 70 % of the blank extinction values. (This latter point will be discussed later on).

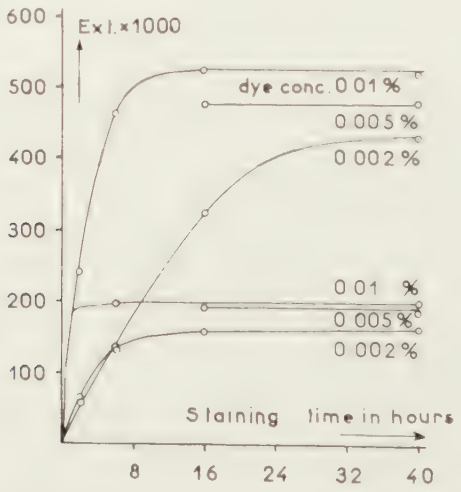

Fig. 5. Relationship between staining time and eluate extinction for two lecithin concentrations in staining solutions containing resp. 0.002, 0.005 and 0.01 % of Edicol Supra Ponceau 4 RS.

It can be seen from the figure that a spot from a low lecithin concentration (2 %) reaches its maximum colour intensity in a shorter staining time than a spot of a higher (5 %) lecithin concentration. Using the 0.002 % dye containing staining solution, the maximum eluate extinction for 5 % lecithin spots is not reached even after 16 hours of staining, while the 2 % lecithin spots in the same staining solution are stained with maximum intensity within 16 hours.

We also carried out a staining experiment using a 0.005 % dye concentration. It must be concluded from this experiment that even in an 0.005 % dye concentration after 16 hours, using 2 and 5 % lecithin spots, the colour intensities have reached their maximum (see the table).

TABLE 3

Eluate extinctions of 2 and 5 % lecithin spots on 1½ by 1½ cm squares using a 0.005 % dye concentration in the staining bath after 16 and 40 hours staining

Staining time in hours	Extinction of eluate × 1000									
	5 % lec. spot			2 % lec. spot			Blank			
16	489	489	485	209	209	213	19	19	17	17
40	493	490	488	203	201	200	15	16		

It must be noted that it is evident that if the staining reaches its maximally possible intensity level the staining is more reproduceable so that the corresponding determination results do not differ considerably. In fact for practical purposes duplo determinations will suffice if the method is carried out under maximum or nearly maximum conditions.

3. Infleunce of the dye concentration of the staining solution

Lecithin spots are stained for 16 hours using staining solutions of different dye concentration. The extinctions are measured of the eluates and given in the next table (mean values of 5 determinations).

TABLE 4

Eluate extinctions of lecithin spots stained in solutions with different dye concentrations

Dye concentration %	Extinction × 1000 diminished with 70 % blank extinction	
	2 % lecithin spots	5 % lecithin spots
0.001	145	225
0.002	162	410
0.005	198	481
0.01	230	530
0.025	253	611

The graphic demonstration of the influence of the dye concentration as given in the above table is demonstrated in the next figure (figure 6).

From both curves the conclusion may be drawn that the amount of dye bounded to the lecithin strives to a maximum.

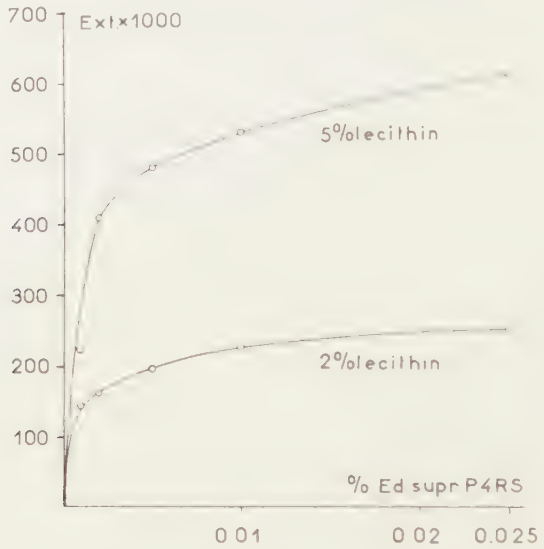

Fig. 6. The dependence is given of the extinction values from eluates of lecithin spots stained during 16 hours in staining solutions containing various dye concentrations.

4. Influence of the uranyl nitrate concentration of the staining solution

Kinetically the staining reaction has to be considered as an equilibrium reaction between 3 components: lecithin (amphion), Edicol Supra Ponceau 4 RS (anions) and uranyl (kations). The amount of lecithin is fixed, as an insoluble phase, while the dye and the inorganic UO_2^{++}, both are soluble and subsequently will determine the equilibrium. As can be seen from figure 4 it is clear that the dye concentration, at a constant uranyl nitrate concentration, determines the maximum amount of dye which can be bound. Figure 5 demonstrates an asymptotic relationship between eluate extinction, which actually means the maximum amount of dye bound, and the dye concentration in the staining solution, again if the wranyl nitrate concentration was fixed at 0.2 % in the staining solution.

From a kinetic point of view it also must be possible to promote a maximum dye uptake by the lecithin if the uranyl nitrate concentration is chosen higher. For this reason lecithin spots on filter paper squares are stained in staining solutions having various $UO_2(NO_3)_2$ concentrations and a constant dye concentration (0.01 % Edicol Supra Ponceau 4 RS). Staining time is 16 hours.

TABLE 5

Eluate extinctions diminished with 70 % of the blank eluate value of 2.5 % lecithin spots on filter papers, stained in staining solutions containing 0.01 % Edicol Supra Ponceau 4 RS and different uranyl nitrate concentrations

Uranyl nitrate concentration %	Extinction of lecithin spot diminished with 70 % of blank-value (E × 1000)
0	40
0.002	157
0.02	232
0.2	295
0.4	317
0.8	330
1.2	324

The next figure (figure 7) gives the graphic demonstration of the above figures.

The result of the last experiment suggests that the highest possible amount of dye that can be taken up the lecithin is expressed by an eluate extinction of 330 (E×1000), this being the value found for a 2.5 % lecithin spot.

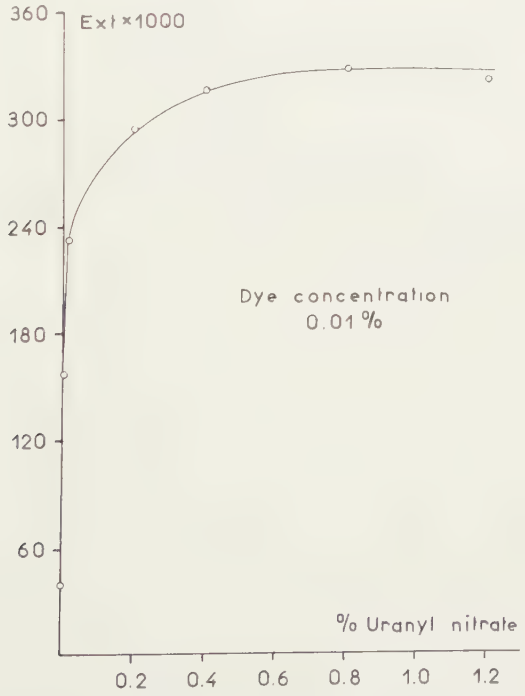

Fig. 7. Dependence of the eluate extinction on the uranyl nitrate concentration of the staining solution.

5. The influence of the lecithin concentration and argumentation of using the 70 % blank eluate extinction as real blank values

To examine the dependence of the staining result obtained by staining lecithin spots, prepared by applying different lecithin solutions, of the concentration it is necessary to perform the reaction using a dye concentration in the staining bath and a staining time such that after finishing the staining procedure equilibrium is reached. For 2 % and 5 % lecithin solutions this equilibrium is reached according to fig. 4, if stained in a staining solution containing 0.005 % or 0.01 % and higher dye concentrations. To be sure of the reproducibility of the reaction we have chosen a dye concentration of 0.01 % Edicol Supra Ponceau 4 RS.

The next table gives the results of an experiment in which lecithin spots of different lecithin concentrations are stained under the conditions as described above.

TABLE 6

Eluate extinctions (E × 1000) of lecithin spots of different concentrations diminished with 70 % of the extinction of the blank eluate (mean values of 5 determinations) stained in 0.01 % Edicol Supra Ponceau 4 RS. Uranyl nitrate concentration 0.2 %.

Lecithin concentration %	Eluate extinction — 70 % blank extinction (E × 1000)
0.5	61
1	111
1.5	157
2	212
2.5	268
3.5	381

The next figure (figure 8) gives the graphic demonstration of the results from the above table.

The same experiment was carried out by cutting out the stained spots. In that way the same line was obtained going through the point zero of the x and y axes. This was one of the arguments that it is justified to diminish the eluate extinction of the spot test square ($1\frac{1}{2}$ by $1\frac{1}{2}$ cm) having a surface of 2.25 cm² with 70 % of the blank extinction value. This 70 % is chosen because of the surface of a $1\frac{1}{2}$ by $1\frac{1}{2}$ cm square which is not occupied by a lecithin spot ($d = 9$ mm, surface 0.636 cm²). If we calculate this factor we see that it will be 2.25 cm² − 0.636 cm² = 1.614 cm². This amount of 1.614 is practically 70 % of the total surface of a $1\frac{1}{2}$ by $1\frac{1}{2}$ cm square. Some more experiments were performed to make sure that this correction factor is to be trusted. Using a different filter paper square made the part of the filter paper not occupied by lecithin 50 %. It was evident that in that case 50 % of the blank value must be subtracted from the extinction values obtained. Moreover, an experiment

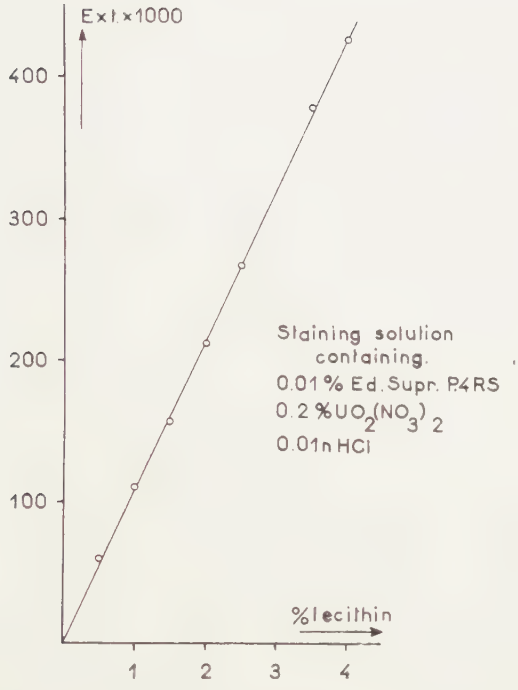

Fig. 8. Dependence of the eluate extinction on the lecithin concentration.

was carried out by applying a triglyceride solution in chloroform-methanol (80:20 v/v) with the same pipet on a filter paper square of $1\frac{1}{2}$ by $1\frac{1}{2}$ cm. By staining this paper and comparing it with a blank, an unstained 9 mm diameter triglyceride spot could be seen on hardly coloured background. Secondly the eluate extinction of this triglyceride spot (which does not stain with the tricomplex staining) was $\pm$ 30 % less than the eluate extinction of the blank.

(To be continued)

QUANTITATIVE ASPECTS OF THE TRICOMPLEX STAINING PROCEDURE

THE STAINING OF LECITHIN SPOTS APPLIED ON CHROMATOGRAHIC PAPERS Ib

BY

G. J. M. HOOGHWINKEL AND H. P. G. A. VAN NIEKERK

(Communicated by Prof. H. G. BUNGENBERG DE JONG at the meeting of Jan. 30, 1960)

DISCUSSION

1. *The composition of the tricomplex*

The theoretical background of the staining method investigated in this paper seems to find a confirmation in the experimental results. Schematically a tricomplex can be pictured as given in this figure.

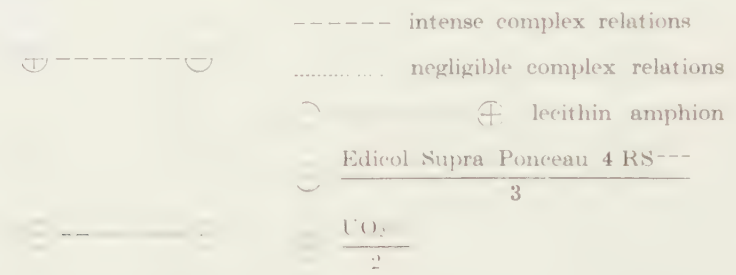

The lecithin molecules are present on the paper in the smectic phase and insoluble in the staining solution. A UO_2^{++} ion will be attracted by means of Coulomb forces by the negatively charged phosphate group of the lecithin and the dye is attracted by means of Coulomb forces by the positively charged quarternary ammonium ion group of the choline residu of the lecithin. If indeed the attraction between the dye ions and the UO_2^{++} ions are negligible then the tricomplex will be formed.

The tricomplex can be given in formula:

$$\text{Lecithin} \cdot \frac{+-(\text{Edicol Supra Ponceau 4 RS})^{---}}{3} \cdot \frac{UO_2^{++}}{2}$$

This molecular formula gives the composition if all charged groups of the lecithin are compensated by dye ions and uranyl ions respectively. If in our experimental results we can find indications that the stained lecithin complex under examination will be composed according to this expectation then we can consider the theoretical starting point as stated by Bungenberg de Jong as confirmed.

From the staining results of certain amounts of lecithin at pH = 2 during 16 hours at different dye concentrations we could conclude that the dye uptake by lecithin tends to reach a maximum. The staining of certain lecithin amounts using different uranyl concentrations gives a clear indication concerning the maximally possible amount of dye taken up by the lecithin. The molecular proportions combined in a stained complex can be calculated from experimental data given in the foregoing paragraphs of this paper.

The amount of lecithin on the spot applied by using the 4.73 mm³ capillary pipet is calculated as follows:

a 5 % lecithin solution is equivalent to 63.8 m mol/l

a 2.5 % lecithin solution is equivalent to 31.9 m mol/l

a 2 % lecithin solution is equivalent to 25.5 m mol/l

4.73 mm³ of the same lecithin solution contains respectively

$$(63.8),\ (31.9) \text{ or } (25.5) \times \frac{4.73}{1000 \times 1000} \text{ m mol lecithin.}$$

These amounts are present at a spot if these are applied with the capillary pipet:

4.73 mm³ of a 5 % lecithin solution thus means 3.02×10^{-4} m mol

4.73 mm³ of a 2.5 % lecithin solution thus means 1.51×10^{-4} m mol

4.73 mm³ of a 2 % lecithin solution thus means 1.21×10^{-4} m mol

The eluates of the stained squares containing the lecithin spots are prepared by extraction of the dye with exactly 5 ml $^3/_5$ n HCl in 50 % tert. butylalcohol.

If the eluate extinction (Ext. × 1000) is given by the value X then the amount of dye in m mol/5 ml can be calculated as follows:

$$\frac{X}{333} \times \frac{5}{100} \times 0.001 \times \frac{60.9}{100} \times \frac{1000}{604.475} \text{ m mol.}$$

Mol. weight of Edicol Supra Ponceau 4 RS = 604.475.

Extinction of a 0.001 % dye solution = 333 (Ext. × 1000).

The purity of the dye is 60.9 %. The eluate volume is 5 ml.

The amount of dye taken up by the lecithin corresponding with an eluate extinction of X is also $15.1\ X \times 10^{-8}$ m mol.

The molecular ratio $\frac{\text{Edicol Supra Ponceau 4 RS}}{\text{Lecithin}}$ shortly E/L is calculated as follows:

5 % lecithin spot $\frac{15\,X \times 10^{-8}}{3.02 \times 10^{-4}} = \frac{5X}{10000}$,

2.5 % lecithin spot $\frac{15\,X \times 10^{-8}}{1.51 \times 10^{-4}} = \frac{10X}{10000}$,

2 % lecithin spot $\frac{15\,X \times 10^{-8}}{1.21 \times 10^{-4}} = \frac{12.5X}{10000}$.

From the results of the staining experiment using a constant uranyl concentration with different dye concentrations and from the experiment using a constant dye concentration and different uranyl nitrate concentrations in the staining bath the molecular ratio $\frac{\text{Edicol Supra Ponceau 4 RS}}{\text{Lecithin}}$ is calculated. The results of the calculations are demonstrated in the next figures:

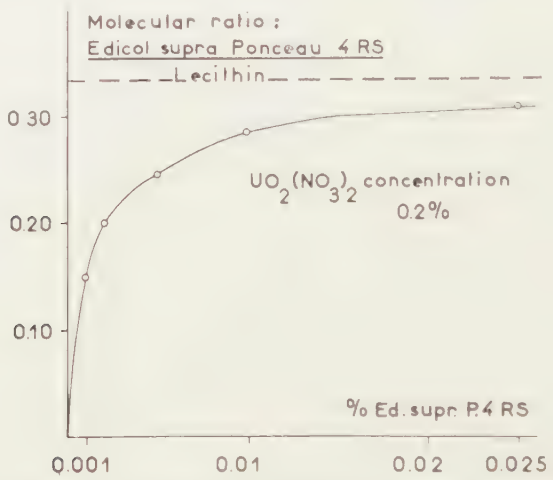

Fig. 9. Molecular ratio E/L in dependence on the dye concentration.

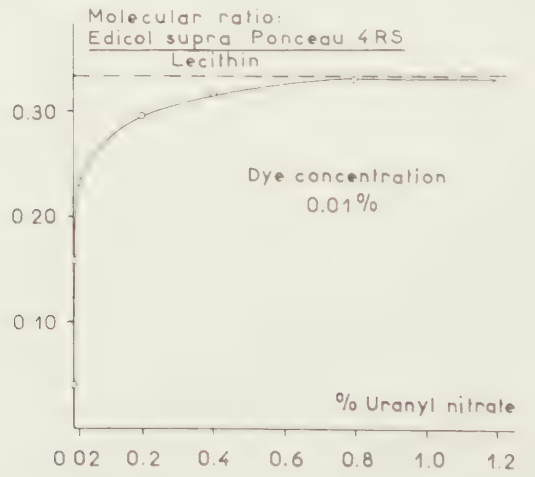

Fig. 10. Molecular ratio E/L in dependence on the uranyl nitrate concentration.

If the tricomplex system were formed exactly as indicated by the stoechiometric composition indicated earlier in this discussion the molecular ratio E/L of 0.33 theoretically is to be expected.

As a matter of fact this is the value for an equivalence of the Coulomb atractions between the ionic partners in this complex. Based on the same argument the molecular ratio: $\frac{\text{uranyl nitrate}}{\text{lecithin}}$ will be 0.50.

If we study the graphical demonstrations in fig. 9 and 10 we see that in both cases the molecular ratio E/L tends to a maximum reaching the value 0.33 in the case of variation of the uranyl-nitrate concentration. This value is not reached in the experiment in which the dye concentration varies but it is evident that the line still tends in the upward direction, so evidently this ratio tends to a limit being without doubt 0.33.

Work is in progress on the experimental evaluation of the equivalence of the UO_2^{++} ion in the tricomplex system. The results indicate that indeed a molecular ratio $\frac{\text{uranyl nitrate}}{\text{lecithin}} = 0.50$ or nearly 0.50 will be reached if the staining conditions are chosen well. (v. NIEKERK and HOOGHWINKEL [10].

2. *Perspectives for the application in quantitative analysis*

The linear proportionality we found between the eluate extinction and lecithin concentration if the staining is carried out at pH = 2, with a dye concentration of 0.01 % and an uranyl nitrate concentration of 0.2 % and a staining time of 16 hours suggests that the method is suitable as a method for the quantitative determination of lecithin.

Moreover, we have strong indications that not only lecithin but also cephalin (phosphatidyl ethanolamine), lyso lecithin and sphingomyelin stain with this method exactly in the same way. If that is true the method is more generally usable and provides a universal method to determine so-called "acid-base" phosphatides. The method will be more simple than other determination methods (Phosphorus, or Nitrogen estimations) and is more specific than those methods. Hence it is a micro-determination which means that only very small amounts of material are necessary to carry out a determination. We used the method to follow the course of column chromatographic separation of phosphatides qualitatively and quantitatively.

Investigations are in progress to use the method for quantitative paper chromatography of egg phosphatides. A paper chromatogram must be stained with the tricomplex method. The satined spots must be cut out and must be eluted with $^3/_5$ n HCl 50 % tert. butylalcohol solvent and the extinctions of the eluates can be measured in a spectrophotometer. Our preleminary experiments indicate that the composition of a mixture of the above-mentioned phosphatides can be determined in a rather accurate way. HOOGHWINKEL and v. NIEKERK [12]).

SUMMARY

1. The experimental conditions necessary to get a maximum staining result of lecithin spots on silicie acid-impregnated filter paper, using the tricomplex staining for phosphatides are examined. Pure lecithin is used as representative for the acid-base type phosphatides. In earlier publications the dye Acid Fuchsin was used. In this paper we used, to get more

exact results, the dye Edicol Supra Ponceau 4 RS (I.C.I.), a dye containing approximately 40 % inorganic salt, but no impurities of organic matter. In most of our experiments the staining solution contains 0.2 % uranyl-nitrate and 0.01 n HCl.

2. The following factors influencing the staining results have been investigated:

a. Hydrochloric acid normality: At 0.01 n (pH = 2) the strongest colour intensity was obtained.

b. Staining time. 2, 8, 16 and 40 hours staining are compared: With a sufficiently high dye concentration a staining time of 16 hours is most suitable.

c. Variations in dye concentration, and the uranyl nitrate concentration: It was demonstrated that maximum staining is obtained if the equilibrium concentrations are sufficiently high. By choosing higher uranyl-nitrate concentrations in the staining solution the maximum staining intensity is reached by lower dye concentrations.

3. The linear relation between eluate extinction and lecithin concentration is established using suitable experimental conditions.

4. Discussed is the theoretical composition of the complex in the case of staining a threevalent dye anion and its experimental approximation. A molecular ratio dye/lecithin = 0.33 is on theoretical grounds to be expected. This value is indeed reached or nearly reached if the experimental conditions are appropriately chosen.

5. The usability of the quantitative method as a general method for the determination of acid-base type phosphatides is discussed. Preliminary results are mentioned concerning investigations being in progress, about the quantitative evaluation of paper chromatograms of a mixture of the above-mentioned phosphatides.

Department of Medical Chemistry,
University of Leyden

REFERENCES

1. Bungenberg de Jong, H. G. and G. R. van Someren, these Proceedings, Series **B 62**, 150 (1959).
2. Hooghwinkel, G. J. M., J. Th. Hoogeveen, M. J. Lexmond and H. G. Bungenberg de Jong, these Proceedings, Series **B 62**, 222 (1959).
3. Bungenberg de Jong, H. G., in A. R. Kruyt, Colloid Science II chapt. IX, 2. Elsevier Publishing Company, inc. 1949.
4. ———, also in Colloid Science II chapt. X, 6
5. Hanahan, D. J., J. Biol. chem. **228**, 685 (1957).
6. Rhodes, D. N. and C. H. Lea, Biochem. J. **56**, 526 (1957).
7. Marinetti, G. V., and Elmer Stotz, B.B.A. **21**, 168 (1956).
8. Hooghwinkel, G. J. M. and F. J. M. Heslinga, to be published.
9. Vickerstaff, Th., The Physical Chemistry of dyeing, Oliver and Boyd (1954).
10. Niekerk, H. P. G. A. van and G. J. M. Hooghwinkel, to be published.
11. Meyer, A. E. F. H., These Proceedings ,series **B 60**, 37 (1957).
12. Hooghwinkel, G. J. M. and H. P. G. A. van Niekerk, to be published.

CONCENTRATION PROFILES IN THREE-COMPONENT REACTION SYSTEMS

BY

W. R. DAMMERS [1])

(Communicated by Prof. J. A. A. KETELAAR at the meeting of February 27, 1960)

Introduction

Some years ago WATERMAN [2] and WEBER [1] proposed an empirical equation describing the composition of reaction systems consisting of one feed component (A) and two product components (B and C). In recent publications on this subject, DE BOER and VAN DER BORG [3, 4] replaced the empirical equation by a theoretical relation between the product concentrations based on a simple kinetic model. The present communication deals with some further aspects of both the empirical and the theoretical relation; in addition, an alternative model is suggested, which is not subject to the limitations inherent in van der Borg's mechanism.

The empirical relation between the product concentrations

Waterman and Weber considered a number of three-component reaction systems, in which at the time $t=0$ only the feed component (A) is present, whereas at $t=\infty$ this component is completely converted into one of the product components (C). Denoting the concentrations (mole or weight fractions) of A, B and C at the time t by z, y and x, respectively, the relation between y and x appeared to be represented satisfactorily by the hyperbolic equation

$$y = \frac{x(1-x)}{a+bx} \tag{1}$$

where a and b are constants depending on the system under consideration and on the reaction conditions applied. In WEBER's thesis [1] this equation has been applied to various catalytic processes. For this purpose, experimental values of y and x are plotted in a rectangular isosceles triangle (Fig. 1) and the y, x curve is fitted to the experimental points with the aid of values for the constants a and b, obtained by a trial-and-error procedure.

---

[1]) Bataafse Internationale Petroleum Maatschappij N.V., The Hague, The Netherlands.

From Weber's examples, the application of equation (1) to catalytic reaction systems seems to be quite successful. However, in view of the absence of numerical information on the standard deviations of a and b, the visual agreement between the curves thus obtained and the experimental data may be somewhat misleading. A more reliable criterion for testing the applicability of the proposed relation might have been achieved by linearizing equation (1):

$$\frac{x(1-x)}{y} = a + bx$$

and evaluating constants a and b (and their standard deviations) by means of an extension of the method of least squares.

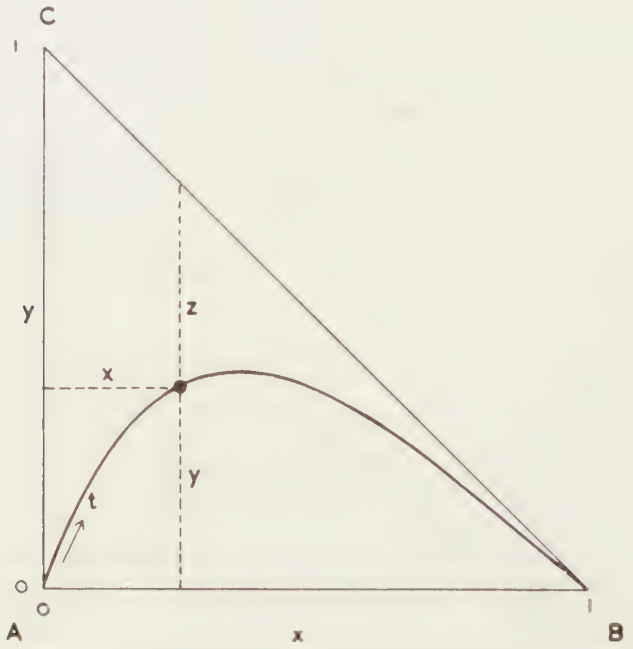

Fig. 1. Graphical representation of equation (1)

Another objection to the application of equation (1) has already been mentioned by Van der Borg [3], when observing that parts of the hyperbolae in Weber's diagrams fall outside the triangle and, consequently, do not satisfy the essential condition

$$x+y \leqslant 1 \tag{2}$$

This weakness of Weber's method is a result of the absence of an adequate physical basis underlying the proposed equation. Constants a and b have no direct physical significance and the adjustment of equation (1) to the experimental points thus readily leads to values for a and b which violate condition (2). This can be illustrated in the following way.

From equation (1) we derive for slope s of the hyperbolae:

$$s = \frac{dy}{dx} = \frac{1-2x}{a+bx} - \frac{bx(1-x)}{(a+bx)^2}.$$

Slopes s_0 at $t=0$ $(x=0)$ and s_1 at $t=\infty(x=1)$ thus are

$$s_0 = \frac{1}{a} \quad \text{and} \quad s_1 = -\frac{1}{a+b}$$

Conversely, we find for constants a and b:

$$a = \frac{1}{s_0} \quad \text{and} \quad b = -\left(\frac{1}{s_0} + \frac{1}{s_1}\right)$$

Since the y, x curves are confined to the region inside the triangle, slopes s_0 and s_1 must fulfil the requirements

(3) $$s_0 \geqslant 0 \quad \text{and} \quad -1 \leqslant s_1 \leqslant 0$$

The conditions for a and b are therefore:

(4) $$a \geqslant 0 \quad \text{and} \quad a+b \geqslant 1$$

Table 1 shows the values of a and b obtained by Weber by applying equation (1) to a number of catalytic processes under various reaction

TABLE 1
Values for constants a and b derived by Weber [1]

reaction system	Fig. No.	a	b	a + b
hydrogenation of linoleic esters	27	0.0065	0.947	0.954
		0.0272	0.886	0.913
		0.0481	0.880	0.928
		0.0950	0.978	1.073
hydrogenation of linoleic esters	28	0.117	0.712	0.829
		0.340	0.398	0.738
		0.340	0.398	0.738
		0.340	0.398	0.738
		0.747	0.128	0.875
		1.66	2.21	3.87
hydrogenation of cottonseed oil	31	0.0108	0.980	0.991
hydrogenation of soybean oil	32	0.0050	1.01	1.015
hydrogenation of linseed oil	33	0.0320	1.05	1.082
hydrogenation of linseed oil	34	0.108	0.985	1.093
chlorination of benzene	35	0.0340	0.922	0.956
chlorination of methane	36	0.0124	0.987	0.999
		0.0922	1.01	1.102
isomerisation of *n*-hexane	37	0.0045	1.30	1.304
isomerisation of *n*-octane	38	0.0175	0.970	0.988
oxidation of paraffin wax	39	0.344	1.43	1.774
		0.164	1.33	1.494
isomerisation of methyl oleate	40	0.129	1.18	1.309
		0.389	0.943	1.332
isomerisation of methyl oleate	41	0.210	1.01	1.220
		0.350	0.804	1.154

conditions. From this Table, the second column of which refers to the graphs in Weber's thesis, it may be seen that about half of the exemples do not satisfy the condition $a-b \geqslant 1$; the corresponding values of a and/or b should therefore be revised.

Limitations of Van der Borg's mechanism

Waterman and Weber developed their empirical relation after observing that most three-component reaction systems could not be described by one of the following kinetic models:

simultaneous first-order reactions

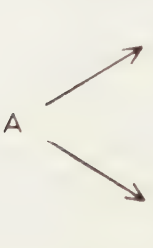

consecutive first-order reactions

It thus seems obvious to start from a mechanism in which both simultaneous and consecutive reactions take place. Restricting the problem to models involving three first-order rate constants, only two models with variable slopes of the y, x curves at $t=0 (x=0)$ are conceivable, viz.

I

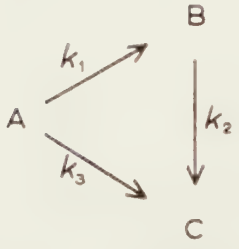

II

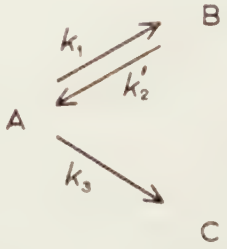

The first model has been discussed in detail by De Boer and Van der Borg [3, 4]; they also successfully applied this mechanism to one of the catalytic reactions considered by Weber (low-temperature hydrogenation of linoleic ester). It can be shown, however, that model I does not apply to all of Weber's examples. A careful mathematical analysis (Appendix 1) reveals that the reaction systems obeying model I can be divided into two separate groups (I*a* and I*b*); the pertinent properties of the systems contained in each of these groups are given in Table 2.

From Table 2 it is seen that reaction systems corresponding to group I*a* yield y, x curves with variable slopes at $t=\infty (x=1)$, but the maximum

TABLE 2

Properties of reaction systems corresponding to model I

	group Ia	group Ib
ratio of rate constants	$\frac{k_2}{k_1+k_3} \geqslant 1$	$0 \leqslant \frac{k_2}{k_1+k_3} \leqslant 1$
slope of y, x curves at $t = 0$ $(x = 0)$	$s_0 = \frac{k_1}{k_3}$	$s_0 = \frac{k_1}{k_3}$
slope of y, x curves at $t = \infty$ $(x = 1)$	$0 > s_1 = \frac{k_1}{k_2} \cdot \frac{k_3}{k_3} \cdot 1$	$s_1 = 1$
maximum concentration of component B	$0 \leqslant y_{\max} \leqslant \frac{s_0}{1+s_0} \cdot \frac{1}{e}$	$\frac{s_0}{1+s_0} \cdot \frac{1}{e} \leqslant y_{\max} \leqslant 1$

concentration of component B does not exceed the value 1/e(=0.368). The systems of group I*b*, on the other hand, can (and usually will) have maximum B concentrations greater than 1/e, but all y, x curves in this group touch the hypotenuse of the triangle at $t=\infty(x=1)$. This implies that reactions in which

$$0 \geqslant s_1 > -1 \quad \text{and} \quad \frac{1}{e} < y_{\max} \leqslant 1 \tag{5}$$

cannot be represented by model I. It may be remarked that most of the isomerisation reactions listed in Table 1 appear to satisfy the properties mentioned in (5); as a consequence, these systems are not amenable to analysis by van der Borg's mechanism.

Discussion of model II

The second model combines the reversible conversion of A into B with the unidirectional side-reaction A $\rightarrow$ C. This mechanism may be valid, for instance, in the case of a "difficult" equilibrium reaction accompanied by destruction of the feed component (e.g. the isomerisation of methyl cyclopentane to cyclohexane, in which the methyl cyclopentane partly decomposes into smaller aliphatic molecules).

The mathematical treatment of model II is given in Appendix 2. For the slopes of the y, x curves at $x=0$ and $x=1$ we obtain:

$$s_0 = \frac{k_1}{k_3} \quad \text{and} \quad s_1 = \frac{k_1+k_2'-k_3}{2k_3} - \sqrt{\left(\frac{k_1+k_2'-k_3}{2k_3}\right)^2 + \frac{k_1}{k_3}} \tag{6}$$

in agreement with the conditions postulated in (3). Introducing s_0 and s_1 as the characteristic constants, we derive from (6):

$$\frac{k_1}{k_3} = s_0\,, \quad \frac{k_2'}{k_3} = (1+s_1)\left(1-\frac{s_0}{s_1}\right), \quad \frac{k_1}{k_2'} = \frac{1}{(1+s_1)\,(1/s_0-1/s_1)}\,. \tag{7}$$

In terms of s_0 and s_1 the relation between the concentrations of components B and C becomes:

$$\left(1-x+\frac{y}{s_1}\right)^{1+s_1} = \left(1-x-\frac{s_1}{s_0}y\right)^{1-(s_0/s_1)} \tag{8}$$

From (8) we calculate for the maximum of the y, x curve:

$$\ln \frac{y_{max}}{s_0} = - \frac{(1+s_1)\ln(1+s_1) - (1-s_0 s_1)\ln(1-s_0 s_1)}{(1+s_1)-(1-s_0 s_1)} . \tag{9}$$

For the extreme cases $s_0 = \infty$ and $s_1 = -1$ equation (9) reduces to the following limiting valus of y_{max}:

$$s_0 = \infty \rightarrow y_{max} = -s_1 \quad \text{and} \quad s_1 = -1 \rightarrow y_{max} = \frac{s_0}{1+s_0} . \tag{10}$$

In Fig. 2 values of y_{max}, calculated from equation (9), are plotted as a function of slope s_1 for various values of slope s_0. This graph shows that y, x curves with $s_1 > -1$ can have maximum y values considerably greater than 1/e. The limitations inherent in model I are therefore not present in model II; from a mathematical point of view, model II thus proves to be more flexible than model I.

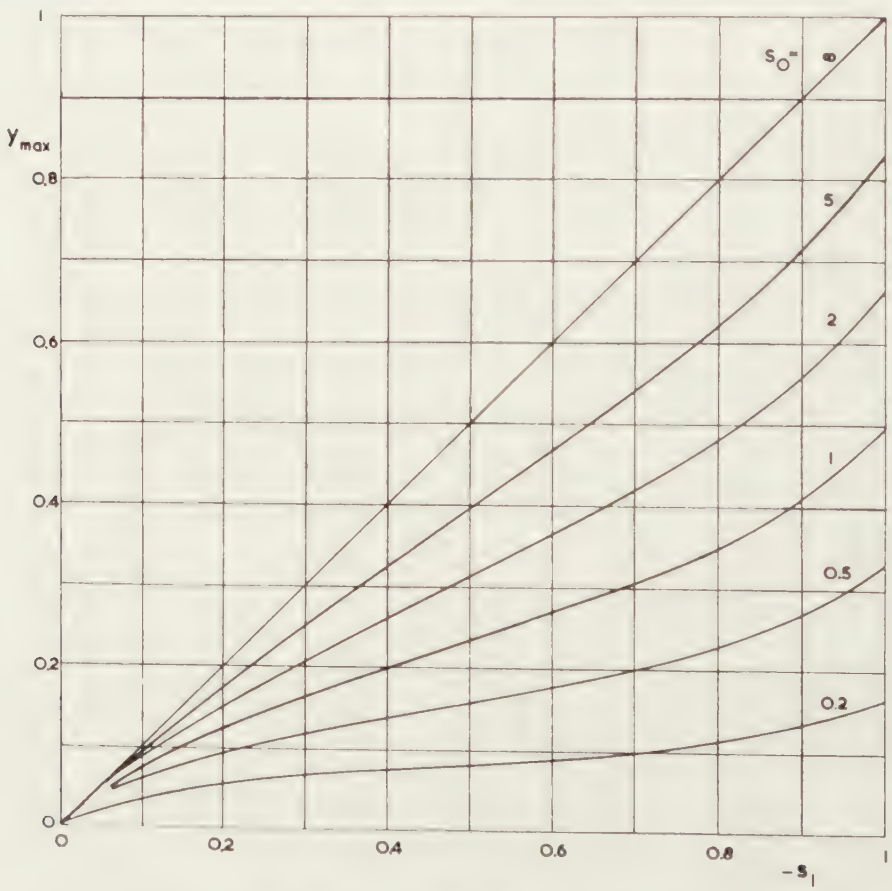

Fig. 2. Maximum concentration of component B in model II as a function of slopes s_0 and s_1

APPENDIX 1: *Mathematical treatment of model I*

The rate equations applying to model I are:

$$\frac{dz}{dt} = -(k_1+k_3)z, \quad \frac{dy}{dt} = k_1 z - k_2 y, \quad \frac{dx}{dt} = k_2 y + k_3 z \tag{11}$$

Integrating these equations with the aid of the conditions

$$x+y+z=1 \qquad \text{and} \qquad t=0,\ z=1$$

we obtain:

$$z = e^{-(k_1+k_3)t} \tag{12}$$

$$y = -\frac{k_1}{k_1-k_2+k_3}\left\{e^{-(k_1+k_3)t} - e^{-k_2 t}\right\} \tag{13}$$

$$x = 1 + \frac{k_2-k_3}{k_1-k_2+k_3}e^{-(k_1+k_3)t} - \frac{k_1}{k_1-k_2+k_3}e^{-k_2 t}. \tag{14}$$

Differentiation of (13) and (14) with respect to t gives:

$$\frac{dy}{dt} = \frac{k_1}{k_1-k_2+k_3}\left\{(k_1+k_3)e^{-(k_1+k_3)t} - k_2 e^{-k_2 t}\right\} \tag{15}$$

$$\frac{dx}{dt} = -\frac{(k_2-k_3)(k_1+k_3)}{k_1-k_2+k_3}e^{-(k_1+k_3)t} + \frac{k_1 k_2}{k_1-k_2+k_3}e^{-k_2 t} \tag{16}$$

Hence

$$\frac{dy}{dx} = \frac{k_1(k_1+k_3)e^{-(k_1+k_3)t} - k_1 k_2 e^{-k_2 t}}{-(k_2-k_3)(k_1+k_3)e^{-(k_1+k_3)t} + k_1 k_2 e^{-k_2 t}}. \tag{17}$$

For $t=0 (x=0)$ this expression is reduced to

$$s_0 = \left(\frac{dy}{dx}\right)_{x=0} = \frac{k_1}{k_3} \tag{18}$$

whereas for $t=\infty (x=1)$ equation (17) becomes indefinite. In order to obtain a value for s_1, numerator and denominator of (17) are multiplied by the factor $\exp(k_1+k_3)t$:

$$\frac{dy}{dx} = \frac{k_1(k_1+k_3) - k_1 k_2 e^{(k_1-k_2+k_3)t}}{-(k_2-k_3)(k_1+k_3) + k_1 k_2 e^{(k_1-k_2+k_3)t}}. \tag{19}$$

Now, if $t=\infty (x=1)$, we must distinguish between the following cases:

$$k_1-k_2+k_3<0 \rightarrow 0 \geqslant s_1 = -\frac{k_1}{k_2-k_3} > -1 \tag{20a}$$

$$k_1-k_2+k_3>0 \rightarrow s_1 = -1 \tag{20b}$$

indicating the existence of two separate groups of reaction systems satisfying model I.

The time t_m at which the concentration of component B attains a

maximum value y_m is calculated from (15) by putting $dy/dt = 0$; we then obtain:

$$t_m = \frac{\ln (k_1 + k_3) - \ln k_2}{(k_1 + k_3) - k_2} = - \frac{\ln k_2 / (k_1 + k_3)}{k_1 - k_2 + k_3}. \tag{21}$$

Substitution of (21) in (13) yields:

$$y_m = \frac{k_1}{k_1 + k_3} \left(\frac{k_2}{k_1 + k_3} \right)^{k_2 / (k_1 - k_2 + k_3)}. \tag{22}$$

Introducing the constants

$$s_0 = \frac{k_1}{k_3} \quad \text{and} \quad q = \frac{k_2}{k_1 + k_3}$$

equation (22) changes into

$$y_m = \frac{s_0}{1 - s_0} \cdot q^{q/(1-q)}. \tag{23}$$

Application of the criteria mentioned in (20) to the second factor at the right-hand side of (23) results in:

$$k_1 - k_2 + k_3 < 0 \rightarrow \quad q > 1 \quad \rightarrow 0 \leqslant q^{q/(1-q)} < \frac{1}{e} \tag{24a}$$

$$k_1 - k_2 + k_3 > 0 \rightarrow \quad 0 \leqslant q < 1 \quad \rightarrow \frac{1}{e} < q^{q/(1-q)} \leqslant 1. \tag{24b}$$

Combining (24) with (23), we finally arrive at the expressions for the maximum y values given in Table 2.

Appendix 2: *Mathematical treatment of model II*

This mechanism gives rise to the following rate equations:

$$\frac{dz}{dt} = -(k_1 + k_3) z + k_2' y, \quad \frac{dy}{dt} = k_1 z - k_2' y, \quad \frac{dx}{dt} = k_3 z. \tag{25}$$

As in Appendix 1, these equations may be integrated to yield expressions for z, y and x as functions of t. However, equations (6)–(9) can be obtained in a more direct way. For this purpose we write:

$$\frac{dy}{dx} = \frac{dy\ dt}{dx/dt} = \frac{k_1 z - k_2' y}{k_3 z} = \frac{k_1 (1 - x) - (k_1 + k_2') y}{k_3 (1 - x) - k_3 y}. \tag{26}$$

For $t = 0 (x = y = 0)$ equation (26) is reduced to:

$$s_0 = \frac{k_1}{k_3} \tag{27}$$

while for $t = \infty (x = 1, y = 0)$ the application of de l'Hospital's rule results in the quadratic equation

$$s_1^2 - \frac{k_1 + k_2' - k_3}{k_3} s_1 - \frac{k_1}{k_3} = 0. \tag{28}$$

In view of condition (3) only the negative root of (28) can be used:

$$(29) \qquad -1 \leqslant s_1 = \frac{k_1+k_2'-k_3}{2k_3} - \sqrt{\left(\frac{k_1+k_2'-k_3}{2k_3}\right)^2 + \frac{k_1}{k_3}} \leqslant 0.$$

In order to integrate (26), this equation is transformed into:

$$(30) \qquad \frac{dy}{dx} = \frac{\frac{k_1}{k_3} - \frac{k_1+k_2'}{k_3}\frac{y}{1-x}}{1-\frac{y}{1-x}}.$$

Introducing the new variable

$$(31) \qquad u \equiv \frac{y}{1-x} \quad \text{with} \quad \frac{dy}{dx} = (1-x)\frac{du}{dx} - u$$

we obtain from (30) and (31)

$$(32) \qquad (1-x)\frac{du}{dx} = \frac{u^2 + \frac{k_1+k_2'-k_3}{k_3}u - \frac{k_1}{k_3}}{u-1}.$$

Since

$$(33) \qquad \frac{k_1}{k_3} = s_0 \quad \text{and} \quad \frac{k_1+k_2'-k_3}{k_3} = s_1 - \frac{s_0}{s_1}$$

equation (32) can be changed into:

$$(1-x)\frac{du}{dx} = \frac{u^2 + (s_1 - s_0/s_1)\,u - s_0}{u-1} = \frac{(u+s_1)(u-s_0/s_1)}{u-1}.$$

Hence

$$\frac{dx}{1-x} = \frac{(u-1)\,du}{(u-s_1)(u-s_0\,s_1)}$$

and thus:

$$(34) \qquad \left(s_1 + \frac{s_0}{s_1}\right)\frac{dx}{1-x} = \frac{1+s_1}{u+s_1}\,du - \frac{1-s_0/s_1}{u-s_0/s_1}\,du.$$

With the boundary conditions

$$t=0,\ x=y=0,\ u=0$$

the integration of (34) yields:

$$-\left(s_1+\frac{s_0}{s_1}\right)\ln(1-x) = (1+s_1)\ln\left(1+\frac{u}{s_1}\right) - \left(1-\frac{s_0}{s_1}\right)\ln\left(1-\frac{s_1}{s_0}u\right).$$

Resubstituting (31) and re-arranging the resulting expression, we finally obtain equation (8). The maximum value of y is easily derived from (26) and (8):

$$\frac{dy}{dx} = 0 \;\rightarrow\; 1-x_m = \frac{k_1+k_2'}{k_1}\,y_m = \left(\frac{1}{s_0} - \frac{1}{s_1} + \frac{s_1}{s_0}\right)y_m.$$

Inserting this value into (8), we arrive at equation (9).

Acknowledgement

The author is greatly indebted to Dr. F. SJENITZER (Bataafse Internationale Petroleum Maatschappij N.V., The Hague), both for initiating the subject discussed in this communication and for his stimulating criticism.

REFERENCES

1. WEBER, A. B. R., Thesis (Delft, 1957) Chapter V.
2. WATERMAN, H. I., Anal. Chim. Acta, **18**, 395 and 498 (1958).
3. BORG, R. J. A. M. VAN DER, Proc. Kon. Ned. Akad. van Wetensch., Series B **62**, 299 (1959).
4. BOER, J. H. DE and R. J. A. M. VAN DER BORG, idem, **62**, 308 (1959).

SOME EARLY ROTALIID FORAMINIFERA. I

BY

C. W. DROOGER

(Communicated by Prof. G. H. R. VON KOENIGSWALD at the meeting of Febr. 27, 1960)

Abstract. Some species of Foraminifera from Paleocene beds of French Guyana are described in detail: *Rotalia hensoni* SMOUT, *R.* cf. *sigali* DROOGER, *Storrsella haastersi* (VAN DEN BOLD), *Lockhartia haimei* (DAVIES), *Smoutina cruysi* n.sp. and *Ranikothalia soldadensis* (VAUGHAN and COLE). Unquestionable representatives of *Lockhartia* are for the first time reported from America. The genera *Smoutina* and *Storrsella* are new. The features of our *R. soldadensis* recommend the distinction of the genus *Ranikothalia*.

A discussion of classification and possible phylogenetic relations of rotaliid Foraminifera is followed by a determination key to the genera.

INTRODUCTION

In a number of borings near the mouth of the Maroni River in the northwestern part of French Guyana (South America), a series of 10–45 metres of hitherto unknown marls and limestones was encountered in between the Quaternary covering and the basement rock. Several samples of the marls were found to contain well-preserved microfaunas (CRUYS, 1959). In addition to about a dozen species of Ostracoda and about an equal number of species of smaller Foraminifera, four species of "larger" Foraminifera were found in variable, but usually high quantities. Especially these larger Foraminifera provide a fairly exact age determination of this Basses Plaines formation as Paleocene, since the species give the possibility of direct correlation with deposits in other parts of Central America and also with some deposits in India and around the Persian Gulf. The age determination is supported by the associations of the smaller Foraminifera (with *Asterigerina texana* (STADNICHENKO), several types of the genus *Boldia*, and representatives of the groups of *Anomalinoides danica* (BROTZEN) and *A. midwayensis* (PLUMMER)), and of the Ostracoda with, as the most common elements, the groups of *Buntonia alabamensis* (HOWE and PYEATT), *Hermanites bassleri* (ULRICH) and *Clithrocytheridea tombigbeensis* (STEPHENSON).

The investigated samples, twelve altogether, come from depths between 25 and 100 m of three of the borings: XF–TP, XF–15 and XF–16 (see fig. 1). A stratigraphic description of the sediments of these borings was published by CRUYS (1959). An account of the entire microfauna will be given by the present author in the near future.

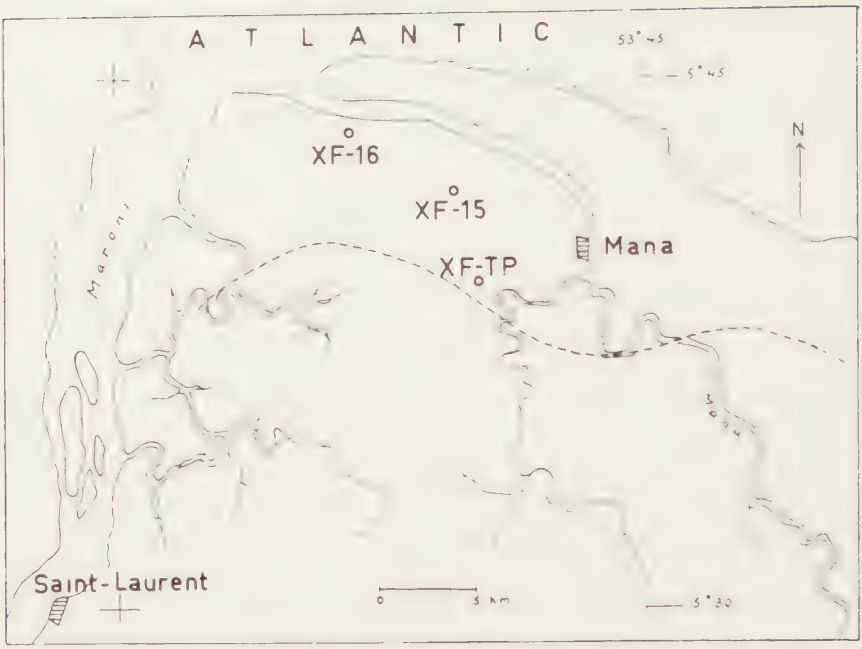

Fig. 1. Sketch map of the Mana region, NW French Guyana, with the location of the investigated borings. The approximate southern limit of extension of the Basses Plaines formation is given as a dashed line (after H. CRUYS, 1959).

Sincere thanks are due to Dr. F. BLONDEL, director, and Dr. P. BUCHOT, chief geologist of the Bureau Minier Guyanais (Paris) for the authorization to publish the details of this fauna, and to Dr. H. CRUYS (Cayenne) for the careful sampling and the necessary field information. Dr. A. H. SMOUT (London) and Prof. W. STORRS COLE (Ithaca, N.Y.) gave valuable advice on some of the species, but they are by no means responsible for the present text and its conclusions.

SYSTEMATIC DESCRIPTION

Only the rotaliid Foraminifera of the Basses Plaines formation will be dealt with. Also two species from the collections of VAN DEN BOLD from the Paleocene–Lower Eocene series of Guatemala and British Honduras will be redescribed. One of these species is represented in the Guyanese material. The family groupings within the Rotaliidea are considered to be too much a matter of conjecture, they have therefore been entirely omitted.

Genus **Rotalia** LAMARCK, 1804

Since the description of various details of the type species, *Rotalia trochidiformis*, by DAVIES (1932), SMOUT (1954) and REISS and MERLING (1958) canal systems and other fine structures are more and more

considered as important features for the disentangling of this heterogeneous group. In our opinion this has thus far not been very successful. As for the literature, various misinterpretations of the canal systems appear to add to the confusion.

At present four generic names are the ones most commonly used: *Rotalia* LAMARCK, *Ammonia* BRÜNNICH (=*Streblus* FISCHER, =*Turbinulina* RISSO) with the type species *Nautilus beccarii* LINNÉ, *Neorotalia* BERMUDEZ with the type species *Rotalia mexicana* NUTTALL, and *Pararotalia* Y. LE CALVEZ with the type *Rotalina inermis* TERQUEM. All these genera are characterized by a trochoid simple spiral. On the dorsal side the whorls are widely evolute, all of them visible, if not covered by excess shell material. Ventrally the last coil surrounds an umbilical mass which continues in the interior towards the first chambers. The ventral side of the sutures is more or less fissured.

The type species of *Rotalia* has a ventral spiral canal around the fissured umbilical mass, whereas such a canal would be absent in *Ammonia (beccarii)*, because the umbilical spiral fissure has not become blocked by calcareous deposits of the later whorls. According to BERMUDEZ (1952, p. 76) the genus *Neorotalia* would differ from *Ammonia* in the appearance of the wall. This wall is vitreous in *Ammonia*, dull and opaque in *Neorotalia*. The latter genus would range from Late Cretaceous to Oligocene, while it is replaced by *Ammonia* from the Oligocene up to recent time (BERMUDEZ, p. 72). *Pararotalia* was considered to be characterized by an areal aperture, i.e. not reaching the base of the apertural face of the final chamber (LOEBLICH and TAPPAN, 1957).

These differences are either dubious or very hard to observe. The appearance of the wall as the main difference between *Ammonia* and *Neorotalia* may very well be due to the state of preservation of the individuals. In general, older and more fossilized specimens tend to have the originally vitreous wall transformed into a wall which is dull and opaque. Moreover, the separation in time of these two types of wall cannot be confirmed by our own observations. Although the majority of older species do possess a dull wall, for instance in part of the individuals of *Rotalia* cf. *sigali* from the Guyanese Paleocene, the wall is vitreous. On the other hand, we frequently observed Neogene specimens, in our opinion belonging to the *Rotalia beccarii* group, in which the wall is opaque.

KAASSCHIETER (1955, 1960) and BATJES (1958) considered *Pararotalia* insufficiently distinct, in as much as the position of the aperture appeared to them a subordinate feature of great individual variation in the Eocene-Miocene group of European species with *Rotalia audouini*, *R. armata*, *R. canui*, *R. inermis*, *R. spinigera* and *R. calvezae*. Actually, the areal aperture is mainly observed in earlier chambers of the individuals. The areal position may be seen as a consequence of the additional basal rim of the septal flap to an originally interiomarginal aperture. Accordingly,

Hofker (1957b) and Reiss and Merling (1958) claim *Neorotalia* to be a synonym of *Pararotalia*.

Also the quoted differences between *Rotalia* and *Ammonia* are hardly useful. First, it is evidently often difficult to observe the exact structure of the spiral canal or fissure, as may be concluded from the discussions by Davies (1932), Barker and Grimsdale (1937), Smout (1954), Reiss and Merling (1958) and Hofker (1958b). The statements are sometimes even contradictory. Actually, the cavities between the central mass, the umbilical free part of the septal flap and the more or less developed umbilical lip of the ventral chamber wall with its additional lamellae, which together form the spiral canal or fissure, are greatly variable in size and shape. Moreover, it is very difficult or even impossible, to decide whether the spiral fissures of fossil specimens are blocked or not, and if blocked, whether this has been done by the animal itself or by a later filling from the outside during fossilisation. This could, for instance, not be decided with certainty for our individuals of *Rotalia hensoni*.

The above discussion seems to be a plea for leaving all species in the single genus *Rotalia*, as it is frequently done. Although submitting to it in this paper we are nevertheless convinced that the genus is heterogeneous.

In the Early Tertiary there are at least two groups included in *Rotalia* s.l. that may be differentiated by the characters of the umbilical mass.

There is the group of *Rotalia trochidiformis*, the type species, in which the umbilical mass is fissured, the grooves being continuous with the more or less developed sutural fissures of the ventral side. There is no deep, open, circular fissure separating the umbilical filling from the surrounding chambers, but the ventral surface of the chambers is confluent with that of the umbilical mass. At least in *R. trochidiformis* the well developed umbilical lips and flaps nearly entirely cut off a series of "astral lobes", which form the described spiral canal and which communicate with the chamber cavities. Also *R. vanbelleni* (see below) clearly belongs to this group of real *Rotalia* species, which group probably was not very great, and may even have been restricted to the Late Cretaceous and Early Tertiary.

In the second group the sutural furrows open into a deep circular fissure, which borders an umbilical mass. This mass is not fissured, though it may superficially consist of a number of welded, rounded knobs, evidently without deep fissures in between. Individuals with one continuous plug, and others with a number of welded bosses, may occur together in a single species and in the same population. The chamber cavities again open at their umbilical ends into the spiral fissure. The umbilical flap (toothplate) is variously developed, possibly absent in several forms. The umbilical lips are also less well developed, overlying spaces that are widely open towards the circular fissure. Often these umbilical tips of the ventral chamber walls may be thickened and imperforate, in extreme

cases resulting in a series of knobs along the spiral fissure. Whether this fissure has been blocked in its deeper parts by secondary deposits formed during life, thus leaving a buried spiral canal, could not be decided in the few sections of *R. hensoni* in our material.

This second group certainly comprises *R. algeriana* Magné and Sigal and *R. primitiva* Cushman and Bermudez from the Late Cretaceous, *R. hensoni* Smout and *R. sigali* Drooger from the Paleocene, and *R. cushmani* Applin and Jordan and *R. orientalis* Cushman and Bermudez from the Eocene, to cite but a few examples among the older species. Apart from the special apertural features, the diagnostic value of which is considered doubtful, the *Pararotalia* group (Loeblich and Tappan, 1957) seems to fit in completely. Probably these groups correspond for the greater part with *Neorotalia*, as Smout (1955) interpreted it, who thought that this was the primitive and persistent stock of the Rotaliidae. Also the group around the Oligo-Miocene *R. mexicana* (=*Neorotalia* Bermudez) is likely to belong here and even part of the still younger group of *Ammonia* species, but in these younger groups the limits with *Rotalia* s.str. become more indistinct. In many of these species the umbilical filling consists of a number of closely set rounded bosses, the exact nature of which has not yet been investigated. Even in the group of *Rotalia beccarii* the umbilical filling may vary from entirely absent to a pattern resembling that in *R. trochidiformis*. It is furthermore quite possible that new lineages added to the confusion, such as forms that may have descended from our *Smoutina* group (see below).

At the moment no simple method can be advanced for a subdivision of *Rotalia* s.l.. The importance of many observations on detailed structure in this group has evidently been overstressed by too rapid generalizations. Detailed re-investigations of nearly all described species are needed. Probably relations and structures will appear to be much more complex than outlined here.

Rotalia hensoni Smout

Pl. 1, fig. 1–6

Rotalia hensoni Smout, 1954, p. 45, pl. 15, fig. 8.

Occurrence. This species was encountered in boring XF–16 only, where it is rare to frequent in several samples. The specimens have a moderate state of preservation.

Description. The dorsal side forms a low cone, usually with not more than two whorls visible, the earlier one of which often forms a slightly more elevated part. Generally only the later sutures are apparent. They are oblique and curved. The ventral side is flattened, occasionally slightly concave, more often somewhat inflated. There is a central plug of variable size, which is mostly entire, but which may show some shallow, fairly

broad depressions. The plug is often strongly protruding and it is limited by a deep circular furrow, which in some "weathered" individuals is of extreme depth. The ventral sutures are radial, somewhat curved, with deep grooves near the umbilicus, which gradually narrow and shallow towards the periphery. Close to this fairly sharp border the sutures are generally flush with the surface and somewhat more curved. The wall of the umbilical part of the chambers is often thickened and imperforate, which gives the test an *Asterigerina*-like appearance. The remainder of the opaque walls is finely perforated. Ventrally six to eight chambers are visible in the last convolution. Usually no external opening could be ascertained, but in a few specimens there is an elongate, basal opening towards the umbilicus, opening into the circular umbilical fissure and the proximal part of the anterior sutural fissure. It is covered by an umbilical lip as an extension of the ventral chamber wall. In broken specimens earlier chambers are seen to have a separate basal intercameral foramen farther towards the periphery.

A small number of sections revealed but few additional details. The septa are clearly double. Buried sutural fissures of earlier whorls were seen to be connected with the circular umbilical fissure.

There are distinct widenings of this umbilical fissure below the lips of the ventral chamber walls. Fairly clear are the communications between the chamber cavities and these widened areas of the spiral fissure, through fairly wide passages in the umbilical flap in anterior direction. The nature of the lime blocking all deeper parts of the spiral fissure could not be checked. It seems to cut off the connections of the earlier chambers and sutural fissures. Hence, it may be extraneous, deposited after death. The umbilical mass appeared to be solid, its furrows being very superficial.

The observed dimensions of the test are:

	XF–16, 81–82 m	86.40 m
diameter	0.30–0.80 mm	0.50–0.90 mm
thickness	0.25–0.35 mm	0.30–0.40 mm

Specific determination. The observed features and dimensions of our specimens very closely agree with those of SMOUT's species of Qatar. Other species resembling our individuals usually differ in minor details, such as a greater number of chambers in the final convolution (*R. cushmani* APPLIN and JORDAN, *R. algeriana* MAGNÉ and SIGAL, *R. sigali* DROOGER). *R. hensoni* clearly belongs to the *Pararotalia-Neorotalia* group.

Age. In Qatar *R. hensoni* is only known from the Paleocene, zone 2.

Rotalia cf. **R. sigali** DROOGER

Pl. 1, fig. 7

Cf. *Rotalia sigali* DROOGER, 1952, Contrib. Cushman Found. Foram. Res., vol. 3, p. 99, pl. 15, fig. 36, 37.

Occurrence. Rare to frequent in XF–15, 62 m and 67.50 m.

Description. Our relatively few and minute specimens (diameter up to 0.25 mm) are of variable state of preservation. Part of them are opaque, showing very few details, others are better preserved with more or less vitreous, distinctly perforated walls. The general shape of the test ranges from planoconvex to biconvex, with the dorsal side most elevated. The dorsal spiral is widely evolute, usually showing more than two coils. The sutures are strongly oblique and slightly curved, commonly somewhat depressed. The periphery is narrowly rounded. The ventral sutures are radial, somewhat curved, and in the later part also depressed. There is a central umbilical mass of greatly variable size, usually consisting of a number of closely set, rounded pustules. It is surrounded by a somewhat irregular depression of variable width and in the most distinct individuals very deep. The visible depth is probably connected with the state of preservation. The circular furrow shows extensions along the sutures, usually not far and rapidly shallowing. The umbilical ends of the ventral chamber walls may bear small knobs. There is a low aperture towards the umbilical end of the base of the final chamber, partly adjoining the spiral fissure. There are seven to twelve chambers in the final coil.

Specific determination. There is a general resemblance with *R. sigali* from Algeria, but the difference in size, the North African forms being larger (up to 0.45 mm) renders a comparison of our few specimens too difficult. The possibility cannot even be precluded that our *R.* cf. *sigali* individuals are small variants of *R. hensoni* of the other samples.

Age. *R. sigali* was described from beds with *Exogyra overwegi*, *Cardita beaumonti* and *Roudaireia drui*, which deposits were considered to be of Danian-Paleocene age, but which, according to other authors, still belong to the Late Maastrichtian (Emberger, Magné, Reyre and Sigal, 1955).

Rotalia vanbelleni (Van den Bold)

Pl. 1. fig. 8. 9

? *Cibicides vanbelleni* Van den Bold, 1946, Contrib. Study Ostracoda, p. 125, pl. 18, fig. 8.

not *Siderolites vanbelleni* (Van den Bold), Brown and Bronnimann, 1957, Micropaleont., vol. 3, p. 31, pl. 1, fig. 4–6, textfig. 5–10.

This species of Van den Bold's Guatemala collections is not represented in our Guyanese material, but since its features were recently misinterpreted by Brown and Bronnimann, it is shortly dealt with in order to complete the type description.

The original material in the collections of the State University of Utrecht consists of only some ten specimens, which are rather ill-preserved. It is occasionally impossible to separate them from the equally indistinct *Asterigerina texana* (Stadnichenko) of the same collection.

Description. The dorsal side is slightly convex, the ventral side fairly high, conical to semiglobular, the periphery narrowly rounded. The ornamentation is variable. The ventral umbilical region is always distinctly fissured, the narrow furrows leaving a number of polygonal to elongated raised structures. There is no distinct circular depression around the umbilical filling, but its fissures are continuous with those of the sutures between the chambers. The depth of these sutural grooves could not be verified; often they are only apparent for a short distance away from the umbilical mass. The remainder of the ventral surface may be smooth, faintly showing the moderately curved sutures and the coarse pores. The other extreme in the variation range, which is more common, shows an ornamentation consisting of pustules, decreasing in size towards the periphery. This ornamentation is seen to begin with double rows of beads along the sutures and then filling more irregularly the remaining surface in between.

The whorls are dorsally widely evolute, but usually only the last few chambers are distinct. The sutures are somewhat limbate, curved and more or less oblique. To a slight ventral ornamentation corresponds a smooth dorsal surface. In these specimens the later sutures, also the spiral one, may be slightly depressed. The central part of this side is obscured by thickening of the wall in these individuals. Commonly the dorsal side is again ornamented with low pustules, which are largest in the central area. On the final chambers the beads may again be present as double rows along the sutures only.

If at all present, the aperture is obscured in our specimens. No sections were made, but in broken individuals the septa appeared to be double. Fissures seem to be restricted to the ventral central mass and the sutural parts directly around it.

Unfortunately, the material of several of Van den Bold's samples had got mixed up, so that it is uncertain whether the described variation is valid for assemblages of single samples.

Specific determination. *R. vanbelleni* evidently does not belong to the group of both previously described Guyanese species. In general features it much better resembles the type species of *Rotalia*, *R. trochidiformis* from the Eocene of the Paris basin. It is specifically different in several details, such as the high ventral side and the surface ornamentation that usually occurs over nearly the entire outer surface.

Regarding description and figures, *Siderolites vanbelleni*, described by Brown and Bronnimann (1957) from Cuban Late Cretaceous deposits is certainly not conspecific with *Rotalia vanbelleni* from Guatemala and British Honduras. There are no indications for the presence of peripheral spines in the individuals of the latter species, and also in other features there is considerable difference as may be seen from a comparison of the descriptions and figures.

Age. Van den Bold recorded his species from several samples of the Paleocene–Lower Eocene series of Guatemala and British Honduras. As for the accompanying fauna of Foraminifera and Ostracoda there is no reason to regard this general age determination as doubtful.

Genus **Storrsella** n.gen.

Type species. *Cibicides haastersi* Van den Bold

Etymology. The genus is named in honour of Prof. W. Storrs Cole (Ithaca, N.Y.), whose numerous well-illustrated papers on larger Foraminifera added substantially to our knowledge.

Diagnosis. Test reversed trochoid with lamellar walls of radial structure. The chamber cavities of the simple spiral are dorsally more involute than ventrally. The umbilical centre of the dorsal side may be ornamented with one or more fused knobs, with some radial canals in between. The ventral umbilical area shows a reticulate pattern of grooves, which continue into those of the sutures. The umbilical mass is entirely fissured; possibly the chamber cavities communicate with these fissures through narrow openings. No distinct, prominent spiral canal was observed, though the presence of an astral furrow in some specimens suggests that umbilical flaps and lips may seperate such a structure. The basal intercameral foramen is median to ventral.

Remarks. This simple genus differs from nearly all others among the Rotaliidea in the reversed trochoid character of the test, in which the chamber cavities are most involute on the dorsal side. It is the main difference from *Rotalia* s.str. (*R. trochidiformis* group). Possibly both genera possess a more or less developed ventral spiral canal consisting of a series of astral lobes. The genus *Fissoelphidium* Smout shows the same fissures in the sutures and the umbilical mass, but these features are found at both sides of this planispiral genus. There is some superficial resemblance with the early Paleocene *Daviesina* species (*D. danieli* Smout, 1954, p. 69, pl. 7, fig. 15–17), which is normally trochoid, however. The reversed trochoid character also occurs in *Laffitteina* Marie (Marie, 1945; Drooger, 1952, who misinterpreted dorsal and ventral sides), but this genus has no fissured umbilical mass, and the intraseptal spaces communicate with the exterior through pores. The resemblance with *Cibicides* Montfort is only superficial.

Probably other species, described as *Cibicides* or *Rotalia*, belong to this new genus. For instance, *R. capdevilensis* Cushman and Bermudez (1947, p. 25, pl. 6, fig. 1–3) from the Lower Eocene of Cuba, has the general appearance of *Storrsella*. Also *Lockhartia roestae* (Visser) from the Campanian-Maastrichtian of Europe (Hofker, 1955a, 1959) shows the reversed trochoid character of our new genus. Too few details of these species are known for a more certain opinion, however.

Storrsella haastersi (Van den Bold)

Pl. 1, fig. 10, pl. 2, fig. 1–12

Cibicides haastersi Van den Bold, 1946, Contrib. Study Ostracoda, p. 125, pl. 18, fig. 9.

Occurrence. This is the most common species in the Guyanese material, occurring in all three borings. It is frequent in nearly all samples, occasionally it is abundant.

Description. The shape of the test shows considerable variation. The dorsal side is more or less convex; usually it is a low cone. It only shows the chambers of the last coil, which are narrow, elongated and curved. They nearly reach the centre, encircling a small, somewhat inflated boss, which may consist of a small number of fused and indistinct, low knobs or granules. The sutures are generally somewhat raised, but at the other end of the observed range of variation they are slightly depressed between the last few chambers.

The ventral side shows greater variation, ranging from convex to flat and even slightly concave. Young specimens are usually plano-convex, adult ones more compressed and ranging from biconvex to concave-convex. At the ventral side the chambers of the last whorl are clearly visible with distinct, curved sutures in between. In well-preserved specimens the sutures are seen to contain fissures, which begin close to the periphery and deepen towards the centre. The fairly wide central area shows an umbilical mass cut down according to a reticulate pattern

---

Plate 1

a, ventral view; *b*, dorsal view; *c*, peripheral view.

Figs. 1*a*, *b*, *c*. *Rotalia hensoni* Smout. XF-16, 86.40 m. × 28.

Figs. 2, 3. *Rotalia hensoni* Smout. Ventral views of specimens showing the ventral-umbilical aperture. XF-16, 81–82 m. × 45.

Fig. 4. *Rotalia hensoni* Smout. Ventral view of a specimen with the last few chambers broken off. In addition to a labial aperture in anterior direction, the separate intercameral foramen can be seen. XF-16, 81–82 m. × 45.

Fig. 5. *Rotalia hensoni* Smout. Horizontal half-section showing the connections of the chamber cavities and the septal fissures with the spiral fissure. XF-16, 81–82 m. × 45.

Fig. 6. *Rotalia hensoni* Smout. Axial half-section showing the deep spiral fissure and the umbilical flaps, lips and openings of some of the chambers. XF-16, 81–82 m. × 45.

Figs. 7*a*, *b*, *c*. *Rotalia* cf. *R. sigali* Drooger. XF-15, 67.50 m. × 90.

Figs. 8*a*, *b*, *c*. *Rotalia vanbelleni* (Van den Bold). Holotype of ? *Cibicides vanbelleni* Van den Bold. Paleocene-Lower Eocene series of Guatemala, Utrecht coll. no. S. 12621. × 45.

Figs. 9*a*, *b*, *c*. *Rotalia vanbelleni* (Van den Bold). Smooth variant. Paleocene-Lower Eocene series of Guatemala. × 45.

Figs. 10*a*, *b*, *c*. *Storrsella haastersi* (Van den Bold). V 134, Paleocene-Lower Eocene series of Guatemala. × 45.

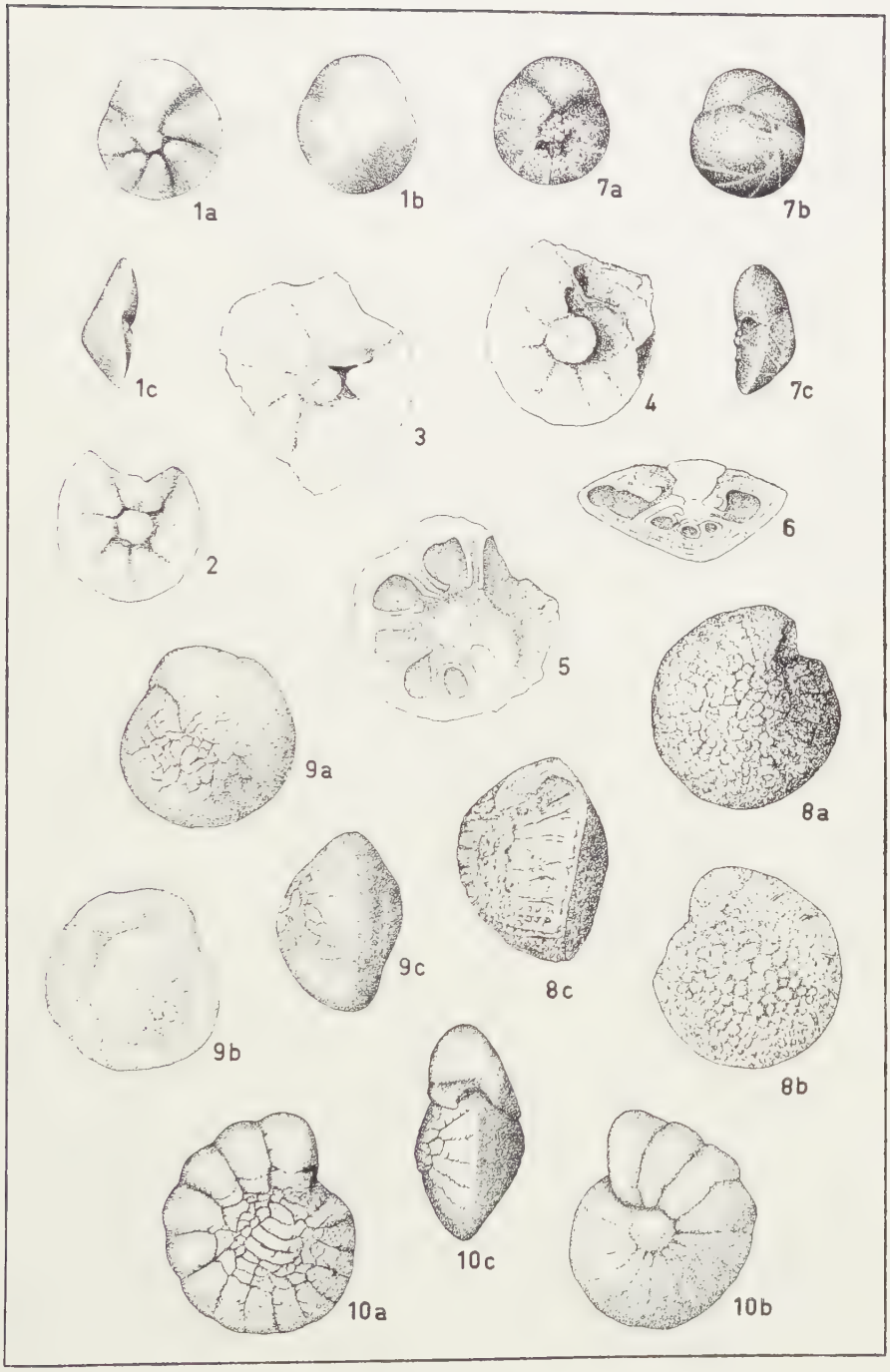

PLATE I

of narrow grooves into more or less polygonal, flattened pustules. These fissures commonly continue into those of the sutures. Some elongated pustules with fissures alongside may occur between the umbilical mass and the simple sutural groove. Especially towards the periphery the sutural furrows are often seen to send tiny shallow branches to either side some way over the outer surface of the chambers. In part of the specimens this feather-like structure is apparent from weak costae or elongated granules on the chambers alongside the sutures. On earlier chambers the grooves from anterior and posterior directions may join in a radial groove over the middle of the chamber wall.

The periphery is sharp to narrowly rounded. The surface of the test is smooth. Its finely granular appearance, especially of the ventral side, is probably due to fossilisation. The opaque walls are finely perforated.

The range of variation of the diameter of the test is not the same in all samples. As a whole it is from 0.40 mm to 1.10 mm; the corresponding thickness varies from 0.15 mm to 0.45 mm. In some samples (XF–TP, 34 m; XF–16, 81–82 m and 86.40 m) the average type is a little more compressed than it is in the other samples. The number of chambers in the final coil increases rapidly with increasing size, but for each size group it shows considerable variation. The average changes from about 12 at a diameter of 0.4 mm to about 25 at a size of 1.0 mm.

The axial and horizontal sections show that there are basal intercameral openings, which are median to ventral (at the least involute side). Such an opening was never clearly observed in a final chamber, which may be due to the state of preservation of the material, however. Dorsally the chamber cavities show much longer alar prolongations than they do on the ventral side. The septa are double. The ventral intraseptal fissures diminish rapidly in width towards the dorsal side, where they are either absent or so thin as to be no longer noticeable. The intraseptal fissures continue into the reticulate fissure pattern of the umbilical mass. The

PLATE 2

Storrsella haastersi (VAN DEN BOLD)

All figures × 45. *a*, ventral view; *b*, dorsal view; *c*, peripheral view.

Figs. 1*a*, *b*, *c*. Holotype of *Cibicides haastersi* VAN DEN BOLD. V 134, Paleocene-Lower Eocene series of Guatemala. Utrecht coll. no. S 12619.

Figs. 2*a*, *b*, *c*. Planoconvex individual. XF-TP, 34 m.

Figs. 3, 4. Ventral sides of biconvex individuals from XF-16, 81–82 m, and XF-TP, 34 m, respectively.

Fig. 5. Peripheral view of a broken specimen showing the intercameral foramen. XF-TP, 28 m.

Figs. 6–9. Horizontal half-sections at different heights of the spiral. All from XF-TP, 28 m.

Figs. 10, 11. Axial half-sections. Both from XF-TP, 28 m.

Figs. 12, 13. Oblique half-sections, more or less at right angles to the dorsal spiral wall. Both from XF-TP, 28 m.

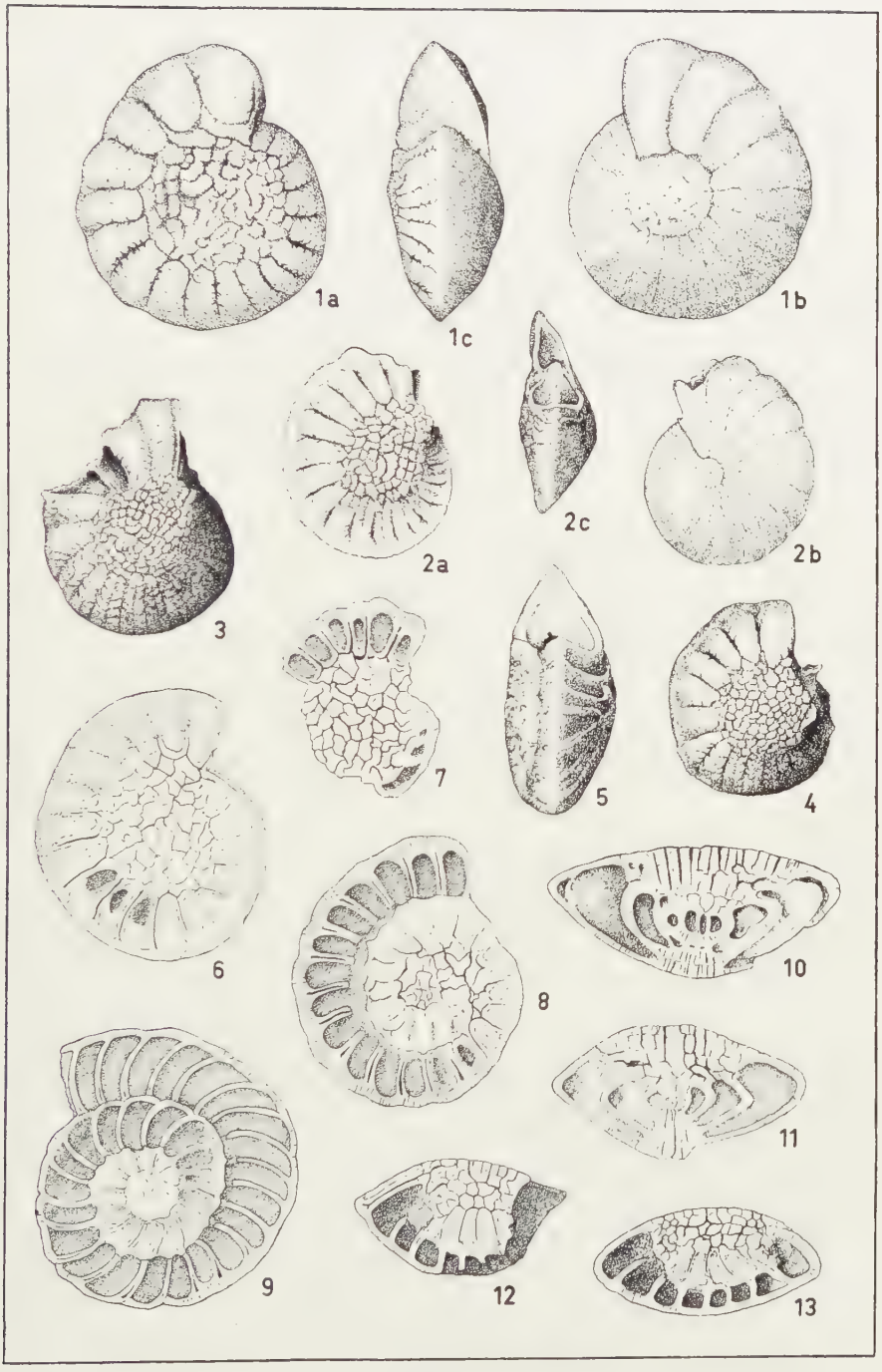

PLATE II

fissures of the latter are deep and continuous to the proximity of the chamber cavities, either uninterrupted throughout, or changing in position in the calcareous material of the successive whorls. Occasionally the fissures show a slight spiral arrangement in the outer part of the umbilical mass. It is not fully clear whether and in which way the chamber cavities communicate with the fissure system. Vertical sections often suggest that there are narrow elongated connections at the base of the chamber cavities, which may open sideways into the septal fissures. But such connections were not clearly discernible in the horizontal sections.

To neither side is there a prominent spiral canal. Some vertical sections suggest the presence of an umbilical flap or toothplate close to the umbilical mass, but there are only faint indications of a corresponding spiral canal. The excessive ornament of the umbilical region may obscure the astral furrow, which is clearly visible in some specimens from Guatemala.

The granules of the central part of the dorsal side appear to be superficial. The umbilical mass is fairly thick at this side too. It is not fissured, but it shows distinct pores, some of which become so wide towards the exterior as to deserve the name of vertical or radial canals.

Specific determination. The original material of *Cibicides haastersi*, stored in the paleontological collections of the State University of Utrecht, is of a different kind of preservation. The specimens are more worn, and thus nicely show the feathered sutural grooves and the umbilical fissures. The dorsal boss is generally bigger, more granular and often surrounded by a somewhat depressed spiral suture. The periphery is commonly more rounded. Again probably due to the worn character of the test the ventral pustules are usually more rounded or partly obscured, and less numerous. Some specimens show a shallow depression in the ventral chamber wall, which in other rotaliid species corresponds to the astral furrow, the place of infolding of the umbilical flap. In our Guyanese specimens this furrow is probably situated below the outermost fissures of the umbilical mass. The size of Van den Bold's specimens is comparable to that of the specimens from Guyana; the holotype is the biggest individual with a diameter of 0.88 mm and a thickness of 0.35 mm. Regarding the size, the number of chambers in the final convolution of 12 to 18 is also about identical. Also in the variation of the general shape there is a fair resemblance. Because of the scarce material no sections were made. Since most of the minor differences are probably due to differences of preservation, our Guyanese specimens are considered conspecific with those of Van den Bold.

Age. *Cibicides haastersi* has been described from the Paleocene-Lower Eocene series of Guatemala and British Honduras, and according to Van den Bold from the Early Eocene deposits. The latter narrower age determination is considered debatable since it was based on the knowledge

in 1946 of the stratigraphic distribution of some Ostracoda species. In our opinion there is no sufficient reason to exclude a Paleocene age for the occurrences in Guatemala and British Honduras, which age is considered the most likely one for the Guyanese fauna.

To be continued

SOME EARLY ROTALIID FORAMINIFERA. II

BY

C. W. DROOGER

(Communicated by Prof. G. H. R. VON KOENIGSWALD at the meeting of Febr. 27, 1960)

Genus **Lockhartia** DAVIES, 1932

Lockhartia haimei (DAVIES)

Pl. 3, fig. 1–10

Dictyoconoides haimei DAVIES, 1927, Quart. Jour. Geol. Soc., vol. 83, p. 280, pl. 21, fig. 13–15, pl. 22, fig. 6.
Lockhartia haimei (Davies), SMOUT, 1954, p. 49, pl. 2, fig. 1–14.

Occurrence. The species is rare in several samples of the borings XF–15 and XF–16, abundant only in XF–15 at 62.50 m.

Description. In sample XF–15, 61.50 m, the individuals have a diameter of 1.4–2.3 mm, with a thickness of 0.9–1.2 mm. The smaller specimens usually show an apical angle of 90–120° and a more or less flattened umbilical side. The bigger ones are rather irregularly biconvex, the dorsal cone being rounded and 120–160°, the umbilical side inflated with a more flattened central part.

This central part of the ventral side is occupied by numerous polygonal to rounded pustules with narrow fissures in between. In well-preserved specimens rounded openings can be observed in the fissures, commonly situated near the angles of the pustules. The size of the pustules (60–125 μ) shows little variation per individual; the average generally increases with the size of the specimens. Sometimes part of the pustules are vermicular. Along the periphery the umbilical side has a smooth band of variable width, showing some of the sutures between the chambers and the coarse perforation of the wall. In most individuals the final chambers have been broken off. In some big ones the end of the spiral is indistinct at this side, in others it is visible by a slight bulge. In complete specimens no basal aperture was observed.

The apical or dorsal side is generally more elevated and conical in smaller individuals than it is in bigger ones. The ornamentation is highly variable, also in each specimen from the centre to the periphery. Commonly the wall of the final whorl only shows coarse pores and distinct sutures. The latter are often marked by a series of larger pores to either side of an imperforated band. Following the coils towards the centre

the pores become larger, first of all those along the sutures. This finally results in an irregularly reticulate pattern of ridges and rounded pustules with large and deep depressions in between. The reticulation, coarsest near the centre, often becomes independent of the sutures, though part of the ridges and pustules may still be seen to have an arrangement along the spiral and chamber sutures.

In sample XF–15, 62.50 m, the more numerous, but smaller individuals range in diameter from 0.6 to 1.3 mm, and in thickness from 0.5 to 0.9 mm. Commonly they are biconvex to planoconvex; in very small specimens the ventral side may even be the most elevated one. The umbilical pustules are often rounded and smaller towards the periphery. The ornamentation well resembles that described for the individuals of the previous sample. Dorsally it occasionally reaches the periphery, a smooth band thus being absent. The sutures may be slightly depressed on both sides.

Broken individuals of both samples show an elongate, basal intercameral slit at the ventral side. Some ten specimens, the umbilical filling of which had been broken out, show the trochoid spiral. The protoconch is variable in diameter, from 175 to 300 μ; the number of coils of these relatively small specimens varies from one to two and a half. The number of chambers in the last coil varies from 9 to 14; this number somewhat increases with increasing diameter of the individuals. The thick spiral wall shows numerous distinct pores. There are no traces of intraseptal canals in these broken specimens. Intraseptal shallow fissures seem to be present only on the ventral side near the central mass. These open depressions continue into the fissures of the umbilical mass; they were observed in only some of the individuals and only between the last-formed chambers; those of earlier septa have evidently been filled or covered. Umbilical flaps are clearly present, leaving a spiral canal that is continuous with the umbilical cavities.

Several axial sections show that the trochoid spiral is arranged towards the dorsal surface. The cavities of the chambers, which are rounded to subquadrate in section, are evolute on both sides, most strongly so on the apical side. The umbilical mass has the same internal shape as the apical cone. It shows a fairly irregular system of cavities, among which horizontal and vertical directions are predominant. The cavities occupy about half of the total volume of the umbilical mass. They clearly communicate with the exterior through the rounded openings in the fissures of the central shield. Their connection with the chamber cavities is less clear. Some sections and broken specimens suggest that there are narrow communications at the base of the chambers below the umbilical flap; in some broken specimens a small number of larger pores were observed at this place, in others again nothing could be seen, which may be due to the state of preservation of the material.

Generic determination. This is the first time that the genus *Lockhartia* is clearly demonstrated from the western hemisphere. Up till now it had been known from Paleocene and Eocene deposits of southern Asia and eastern Africa.

Specific determination. A detailed thorough review of the *Lockhartia* species of India and Qatar was recently given by SMOUT (1954). The variation of our specimens overlaps that of three of SMOUT's species without the possibility of a definite choice. This mainly concerns *L. haimei* (DAVIES) and *L. diversa* SMOUT.

In our material the biconvex shape of *L. diversa* and the more planoconvex appearance of *L. haimei* are about equally represented. The reticulation of the dorsal side of *L. diversa* is found again in most of our individuals, but generally it does not cover the entire apical surface as it is typical for *L. diversa*. According to SMOUT such partly smooth surfaces were found in his material among the older, more primitive specimens of *L. diversa*. The dorsal spiral ornamentation of *L. haimei* is also represented, but it is never so clear and prominent as it was figured by SMOUT in his individuals of Qatar. The ornamentation of the umbilical side shows that of the types of both species; but there are never radiating bands on the last chamber, as there are in *L. diversa*. The pattern of the umbilical cavities in axial section is more or less intermediate, just as is the average angle (70°) between the septa and the spiral sutures. The ratio diameter/thickness is fairly high, which rather corresponds to that of *L. haimei*, whereas the diameter of the protoconch is closer to that of *L. diversa*.

All these differential features, mentioned by SMOUT for his two species occur in various combinations in our material. Hence, there is no variation from a *L. haimei* type to a *L. diversa* type, but a complex mixture of

PLATE 3

Lockhartia haimei (DAVIES)

All figures × 27. *a*, ventral view; *b*, dorsal view; *c*, peripheral view.

Figs. 1*a*, *b*, *c*; 2*a*, *b*, *c*; 3*a*, *b*, *c*. Individuals of different size from XF-15, 62.50 m.

Fig. 4. Ventral side of a big specimen showing the pores in the umbilical fissures. XF-15, 61.50 m.

Fig. 5. Ventral view of a specimen, the umbilical mass of which has been broken out. XF-15, 62.50 m.

Fig. 6. Peripheral view of a broken specimen showing the basal intercameral openings and some larger pores in the umbilical top of one of the chambers. XF-15, 61.50 m.

Fig. 7. Peripheral view of a broken specimen showing the irregular cavities of the umbilical mass. XF-15, 62.50 m.

Figs. 8–10. Axial half-sections showing the pattern of the umbilical cavities and their communications with the chambers and with the openings in the umbilical fissures. XF-15, 62.50 m.

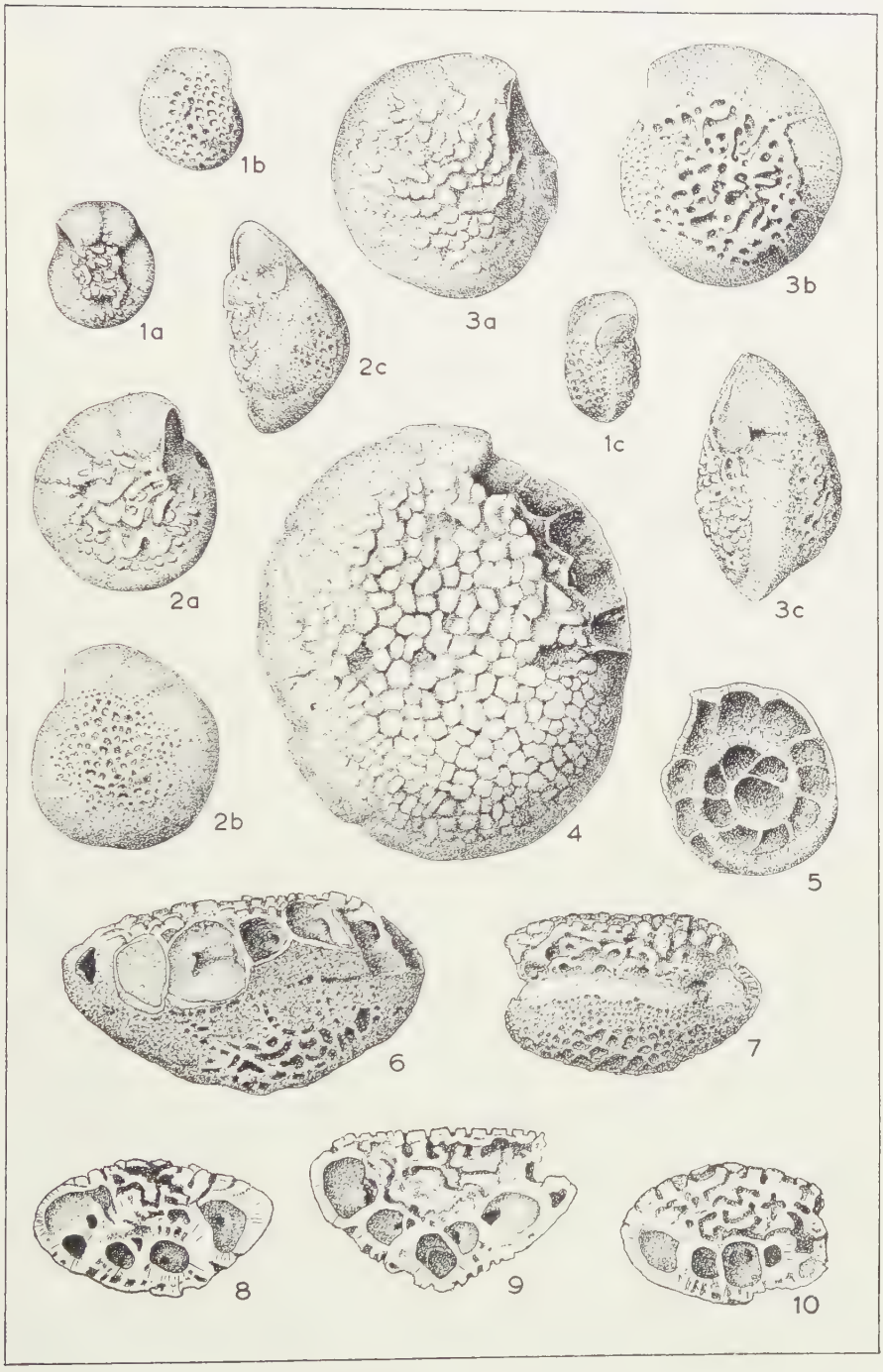

PLATE III

characteristics. It should be pointed out that most of our individuals are smaller than those from Qatar, which certainly influences the appearance of the characteristics, especially those of the axial sections. Also a number of features of *L. prehaimei* SMOUT seem to be present in our material. Evidently we are dealing with American populations, the variation of which more or less covers that of three of SMOUT's species. As specific name the earliest one has been chosen, which does not imply that the other two are considered to be synonyms or their individuals mere variants.

Age. *Lockhartia haimei* and *L. diversa* have exactly the same stratigraphic range in Qatar: Paleocene, zones 2 to 6. Their ancestor, *L. prehaimei* forms an intermediate population with them in zone 2, which population probably very much resembles those of our Guyanese samples. However, the distance between Qatar and Central America is considered too great for us to warrant the conclusion that our intermediate populations would be of exactly the age of zone 2 of the Paleocene of Qatar.

Genus **Smoutina** n.gen.

Type species. *Smoutina cruysi* n.sp.

Etymology. The genus is named in honour of Dr. A. H. SMOUT (London), whose publications clarified much of the complicated structure of rotaliid Foraminifera.

Diagnosis. Test trochoid with lamellar walls of radial structure. The simple trochoid spiral is dorsally evolute with several whorls showing. At the ventral side only the final coil is visible and the central area is occupied by an umbilical filling with, at least in the middle, a number of separate rounded to irregularly elongate openings. The ventral sutures show fissures which may superficially correspond with some of the openings of the umbilical mass. The septa are double and they contain the fissures only in their ventral parts. Towards the umbilicus these fissures connect with a mainly covered, branching, spiral canal system in the outer part of the umbilical mass. At their tops the chamber cavities also communicate with these spiral canals. Vertical canals, originating from the deeper parts of the spiral system, penetrate the central part of the umbilical mass, opening into the separate openings of its surface. There is an elongated intercameral foramen.

Remarks. The genus clearly belongs to the early rotaliid stock. It is morphologically intermediate between *Kathina* SMOUT and *Rotalia* LAMARCK. *Kathina* is different by the absence of any spiral canal system, while in *Rotalia* the umbilical mass is completely fissured. If our interpretation of some described species is correct, there is in the course of time a change within the genus *Smoutina* from *Kathina*-like forms to

Rotalia-like species. *Smoutina bermudezi* (Cole) from the Upper Cretaceous of Cuba only shows a faint development of the spiral canal, *S. cruysi* from the Paleocene of Guyana is the most typical, while in *S. cushmani* (Applin and Jordan) from the Middle Eocene of Florida the number of vertical canals is restricted and the spiral system is complex and of excessive width. Relations with typical *Rotalia* are considered to be remote. Descendents of the *Smoutina* group may have got the appearance of *Rotalia* or *Pararotalia*.

Age. Upper Cretaceous-Paleocene-Middle Eocene of tropical America.

Smoutina cruysi n.sp.

Pl. 4, fig. 1–13

Etymology. The species is named in honour of Dr. H. Cruys, geologist of the Bureau Minier Guyanais, who collected the material.

Occurrence. The species was found in most of the investigated samples of all three borings. It is rare to frequent, abundant only in XF–TP at 28 metres, and in XF–15 at 62.50 metres.

The holotype (coll. no S 12796) was derived from the sample at 62.50 metres of the boring XF–15, Basses Plaines formation (Paleocene), NW French Guyana (pl. 4, fig. 1). It is stored with the other material of this species in the paleontological collections of the Mineralogisch-Geologisch Instituut of the State University of Utrecht.

Description. The test is about equally biconvex. In sample XF–15, 62.50 m, the diameter varies between 0.7 and 1.3 mm, the corresponding thickness from 0.3 to 0.7 mm. In the other samples the dimensions are about equal, but occasionally the maximum size is considerably larger, up to 2.0 mm.

The smooth dorsal side has the shape of a low, somewhat rounded cone. In the apical part the sutures are indistinct by an evenly distributed lamellar thickening of the wall. Also the sutures of the later part are often hardly discernible. They are flush with the surface, those between the chambers are moderately curved backwards. The entire dorsal wall is finely perforated. Ventrally the last coil usually has the shape of a low, truncated cone. The ventral sutures are somewhat curved and slightly depressed in the later part. They usually show narrow fissures. The umbilical region, which has a diameter of about half of that of the entire test, is inflated to flattened with many, more or less regularly rounded depressions. Especially towards the border several depressions may coalesce to more elongate and tortuous ones, occasionally connected with those of the sutures.

Horizontal sections of some ten specimens from XF–15, 62.50 m, in the size range of 0.9–1.2 mm, show $2\frac{1}{4}$ to 4 coils with 18 to 25 chambers

in the last convolution. The first coil has 8 to 10 chambers, the second 13 to 17. The protoconch measures 45–65 μ in diameter. The double septa are regularly curved. The spiral wall is finely perforated. The pores appear much more distinctly than the lamellar structure of the wall.

Other horizontal sections, cut more towards the ventral surface, show the deep intraseptal fissures. Towards the dorsal surface these fissures are absent or they are so thin that they were no longer distinguishable. The umbilical mass contains a complex canal system. There is a distinct, ramifying spiral system below the chambers. These spiral canals communicate with the chamber cavities through narrow passages at the latter's umbilical ends. More towards the ventral surface there are also covered connections with the intraseptal fissures. All through the umbilical filling there are many vertical canals, which connect the spiral system with the depressions of the central surface.

Broken specimens show the intraseptal fissures and sometimes the open connections of the chamber cavities with the spiral canals at the umbilical end of the continuously sloping bottom of the chambers. Evidently the umbilical flap and lip of the chambers form together a solid structure bordering the distal part of the outer branches of the spiral canals. Openings underneath could not be observed for all chambers. Occasionally large pores were observed in the bottom of the chambers towards their umbilical ends.

The axial sections demonstrate that the chamber cavities are dorsally completely evolute. They are somewhat more involute on the ventral side, leaving an umbilical mass that is internally more convex than the dorsal surface of the test. The spiral is distinctly and moderately trochoid. The ventral and dorsal pores are fine and straight; in the central part of the dorsal side they may be slightly longer and coarser. The vertical canals of the ventral umbilical filling are usually straight. Close to the chambers they are mainly restricted to the horizontal layer which corresponds to the last whorl, but more towards the centre they are generally continuous through several such layers. Horizontal structures in the umbilical mass, which evidently belong to the spiral canals, are most distinct close to the chamber cavities, where they also show connections with the chamber tops. In these halfsections and in broken individuals an elongate, nearly basal intercameral opening is seen in the septa. It is not certain whether these openings are due to later resorption alone, since most specimens have some chambers broken off, so that there are no clear observations concerning the aperture.

Specific determination. There is much resemblance with *Kathina bermudezi* (Cole) (*Lockhartia bermudezi* Cole, 1942, Jour. Pal., vol. 16, p. 641, pl. 92, fig. 1–5; Applin and Jordan, 1950, Jour. Pal., vol. 24, p. 476, pl. 7, fig. 8, 9?, 10?; *Kathina bermudezi* (Cole), Smout, 1954, p. 61, pl. 7, fig. 9–13). A number of topotypes of this species from the Cuban

Upper Cretaceous were kindly sent by Prof. Cole. They confirm our opinion about the differences, already concluded from the published figures. In our specimens of *S. cruysi* the spiral is more trochoid and the chamber cavities are more evolute dorsally and more involute ventrally. Especially on the dorsal side the sutures are much more strongly curved, instead of being straight and nearly radial. In several of the topotype specimens of *Lockhartia bermudezi* the straight dorsal sutures between the chambers are slightly raised and sometimes even continuous to a slight apical knob. These features are absent in our individuals. However, most of our specimens are smaller than those of Cole's species (0.9–1.8 mm in diameter), which may accentuate some of the differences, though it can not account for all. According to the figures there is a fair resemblance between both species in the number of spiral chambers of corresponding coils. There are again considerable differences in the canal systems. Smout (1954) thought that there was no spiral canal in *Lockhartia bermudezi*, but in our sections of some topotype specimens we observed horizontal connections between the vertical canals in the border part of the umbilical mass close to the chambers of the last coil (pl. 4, fig. 14). Although much less developed, this is certainly comparable to the spiral system of *S. cruysi*. Probably *Lockhartia bermudezi* is intermediate in features between the typical species of the genera *Kathina* and *Smoutina*. Regarding the great resemblance and the relative age it is quite likely that *Smoutina bermudezi* is ancestral to *S. cruysi*.

Kathina jamaicensis (Cushman and Jarvis) (*Eponides jamaicensis* Cushman and Jarvis, 1931, Contrib. Cushman Lab. Foram. Res., vol. 7, p. 77, pl. 10, fig. 4) from Late Cretaceous beds of Jamaica, as re-figured by Brown and Bronnimann (1957, Micropaleont., vol. 3, p. 136, pl. 1, fig. 7–10) is similar to *S. cruysi* in the curved dorsal sutures and the ventrally more involute character of the chambers of the last coil. It is different from both *S. bermudezi* and *S. cruysi* in the greater number of spiral chambers, as may be concluded from the figures (27 corresponding to a diameter of 1.0 mm, and at least 32 with a diameter of 1.2 mm). Other important features of *Eponides jamaicensis* are as yet unknown, and hence its generic place. The figures of the ventral side (fig. 8 and 9 of Brown and Bronnimann), showing elongate depressions in the external part of the umbilical mass, suggest that a spiral canal system might be present. The identity of this Jamaican form with *S. bermudezi* is considered doubtful; it seems to be closer to our *S. cruysi*.

Another species, probably related to *S. cruysi* is *Lockhartia cushmani* Applin and Jordan (1945, Jour. Pal., vol. 19, p. 143, pl. 21, fig. 5; Applin and Jordan, 1950, Jour. Pal., vol. 24, p. 474–477, pl. 66, fig. 1–7; *Rotalia cushmani* (Applin and Jordan), Cole (not *Rotalia cushmani* Applin and Jordan, 1945, Jour. Pal., vol. 19, p. 143), 1947, Bull. Amer. Pal., no. 126, p. 15, pl. 5, fig. 2–8) from the Middle Eocene of Florida. Especially in the shape and the trochoid arrangement of the chambers there is a

fair resemblance with *S. cruysi*, but in individuals of comparable size the number of chambers per coil is distinctly lower and the number of vertical canals is much more restricted. In the umbilical mass there are horizontal connections between the vertical canals, but in addition this species has developed a complex spiral system of cavities encircling the central filling. A careful study of the figures given by Cole (1947) and Applin and Jordan (1950) give an idea of this spiral system. Newly formed chambers were very low, except for their peripheral part. About half way the distance to the umbilical mass there was a deeply depressed astral furrow, where a distinctly recurved umbilical flap (toothplate?) incompletely separated a fairly small chamber cavity from a more central cavity under a long, curved umbilical lip. The latter cavity communicated with the spiral spaces of the earlier whorls. Later lamellae only adhered to the peripheral parts of the ventral chamber walls, continuing straight to the umbilical mass and leaving wide spaces over the primary chamber and its lip. The septal flap only adhered to the dorsal part of the previous apertural face. Higher up it bent forward leaving a wide "intraseptal" space and over about the middle of the primary chamber this septal flap (or rather the outer primary wall) became more or less vertical, recurving at the place where it was joint by later lamellae. As a result there is, in addition to the more or less seperate cavities of the chambers and the lips, a considerable volume of intraseptal and spiral spaces, partly interrupted by the ventral vertical partitions. The septal fissures are narrow in the visible outer lamellae only, directly underneath they widen into the spiral spaces. There is a superficial resemblance of this set of cavities

Plate 4

Smoutina cruysi n. gen. n.sp.

All figures × 27, except fig. 6: × 55. *a*, ventral view; *b*, dorsal view; *c*, peripheral view.

Figs. 1*a*, *b*, *c*. Holotype. Utrecht coll. no. S. 12796. XF-15, 62.50 m.

Figs. 2*a*, *b*, *c*. One of the biggest specimens. XF-16, 90 m.

Fig. 3. Dorsal view. XF-TP, 28 m.

Figs. 4, 5. Axial half sections. XF-TP, 28 m.

Fig. 6. Oblique ventral view of a broken specimen showing various open parts of the canal system. XF-16, 81–82 m. × 55.

Fig. 7. Broken individual, the dorsal wall of which has been removed, showing the trochoid coil of curved chambers. XF-16, 90 m.

Figs. 8–11. Successive horizontal half-sections from the ventral to the dorsal side of four different specimens, showing the canal systems and their connections. 8–10 from XF-TP, 28 m; 11 from XF-15, 62.50 m.

Figs. 12, 13. Peripheral views of broken specimens, showing intraseptal and vertical canals, and the nearly basal intercameral foramen. 12 from XF-15, 62 m; 13 from XF-TP, 28 m.

Fig. 14. *Lockhartia bermudezi* Cole. Part of the ventral view of a topotype specimen. In the left half of the figure the umbilical centre has been slightly ground off showing tiny lateral communications of the vertical canals. Loc. B 537, Cuba (see Cole, 1942).

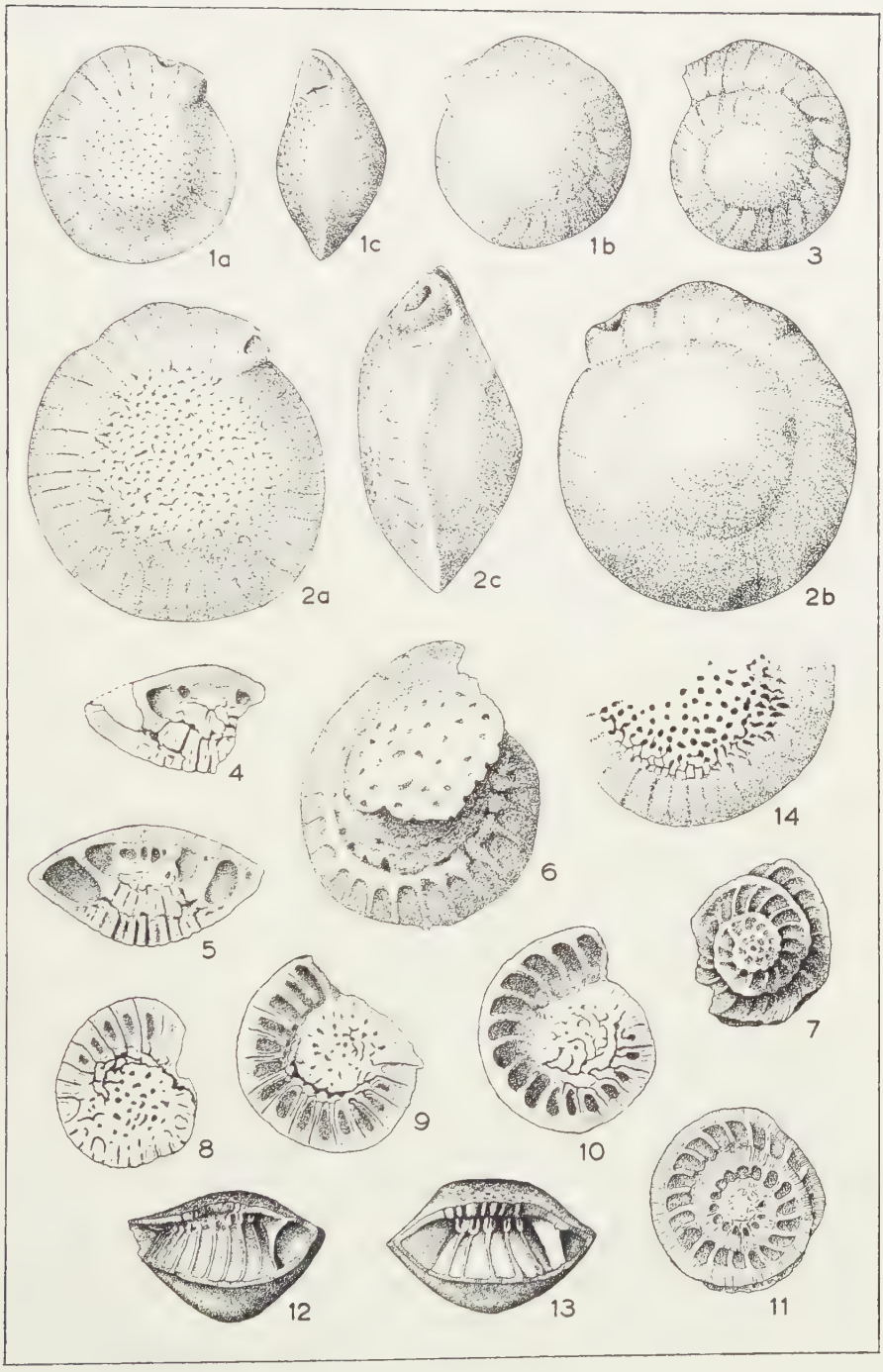

PLATE IV

with that of the more simple spiral canal in *Rotalia* s.str.. Nevertheless, a derivation of *Lockhartia cushmani* from a more typical *Smoutina* ancestor is thought to be more logical because of the resemblance of the structures of the umbilical mass. Evidently, the outer complex spiral system is a new addition.

Probably size of the individuals plays an important part in the external specific differences. In outer appearance our bigger specimens best resemble *S. bermudezi*, our smaller ones *S. cushmani*, without being fully identical. There is certainly no identity of all the populations of this group from the Late Cretaceous till the Middle Eocene. Ours are distinctly intermediate between the two extremes, and the canal systems evidently showed an enormous development within the group. Apart from the achieved complex spiral system possible descendents of this group would soon have resembled species of the genus *Rotalia* s.l.. This may have been the line of descent for one of the groups of this heterogeneous genus.

Age. Although *S. cruysi* is considered to be intermediate between a Late Cretaceous species and a Middle Eocene one, the suggestion of an intermediate age is in itself a weak support to our Paleocene age determination of the fauna.

Genus **Ranikothalia** Caudri, 1944

Ranikothalia soldadensis (Vaughan and Cole)

Pl. 5, fig. 1–14

Miscellanea soldadensis Vaughan and Cole, 1941, Geol. Soc. Am., Spec. paper no. 30, p. 36, pl. 4, fig. 8, 9; Vaughan, 1945, Geol. Soc. Am., Mem. 9, p. 30, pl. 5, fig. 2–5.

Ranikothalia soldadensis (Vaughan and Cole), Caudri, 1944, Bull. Am. Pal., vol. 28, no. 114, p. 23, pl. 4, fig. 19, pl. 5, fig. 24, 26.

Operculinoides georgianus Cole and Herrick, 1953, Bull. Am. Pal., vol. 35, no. 148, p. 52, pl. 1, fig. 1–21, pl. 2, fig. 1–3.

Occurrence. In the samples of XF–16 the species is rare. In XF–15 it is frequent at the depths of 61.50 m, 62 m, and 62.50 m. Part of the individuals from 62 m are exceptionally well-preserved.

Description. The numerous individuals of XF–15, 61.50 m are of greatly variable diameter, from 0.5 mm (rare) to 5.5 mm. Bigger specimens are the most common. The thickness range is from 0.3 to 0.8 mm. In the sample from 62.50 m of the same boring the equally numerous individuals range in diameter from 0.6 to only 2.0 mm; the variation of the thickness is identical to that in the previous sample. The dimensions of the individuals of the sample from 62 m in between are intermediate.

In particular the test of the larger individuals is very much flattened with roughly parallel sides. In small specimens the greatest thickness is usually in the centre, often with a thickened knob of variable size. If

such a knob is present the thickness of the test usually somewhat tapers off towards the periphery. Smaller specimens are sometimes strongly asymmetric. Especially in larger individuals the outline of the test may be irregular. The height of the coils increases rapidly and the evolute part of the chambers is twice to four times as high as broad.

The periphery is evenly rounded or somewhat truncated in section. The thickness of this marginal cord usually exceeds that of the adjoining parts of the chambers. It may even be the double. In larger specimens the marginal cord of the previous whorls forms an elevated spiral on the lateral surfaces. On the smooth surface the sutures are distinct, more or less radiating and often somewhat raised. Their curvature is strongest near the periphery. They are commonly continuous from the periphery to the centre, in larger specimens passing the elevated spiral suture without interruption. Occasionally they appear as a series of granules, in which cases such small knobs may also be present on the surface of the chambers in between. Also the central ornamentation may then consist of a number of closely set knobs. Especially the nicely preserved specimens of XF–15, 62 m, show a row of large pores to either side of the sutures.

The external surface of the marginal cord is fissured by many anastomosing grooves, which leave irregularly elongated islands in between. In larger specimens as many as 30 grooves were counted in transverse direction. Worn and broken specimens show that the grooves are fully open to the interior of the cord. In inward direction their pattern becomes simpler and they end in a set of straight longitudinal canals at the base of the fissure system and close to the top of the chamber cavities. Usually the external longitudinal canals are strongest. They clearly communicate with the intraseptal canals.

Horizontal sections show the double septa and the intraseptal canals which open into the spiral canals of the marginal cord, and which also communicate with the exterior through branches ending in the double series of pores along the sutures. The walls are finely perforate.

The protoconch of macrospheric individuals ranges from 165 μ to 325 μ in diameter. Occasional observations of microspheric individuals showed a protoconch diameter of about 15 μ. Corresponding with a diameter of the test of 1.5–2.8 mm there are one and three quarters to three coils with a total of 20 to 50 chambers. There are 8 to 10 chambers in the first coil and 15 to 22 in the second. In individuals with a size from 1.6 mm to 4.0 and 5.0 mm the number of chambers in the final coil increases from about 15 to about 30 (altogether some 30 observations).

Transverse sections show that the spiral wall is completely involute. Even in big specimens also the chamber cavities appear to be involute with very thin projections across the previous whorls.

Generic determination. In 1944 Caudri erected the genus *Ranikothalia* for the group of Caribbean and Indian *Nummulites*-like species,

which are characterized by "the bluntly rounded chamber tops in horizontal section" and "the thickness of the coarsely gutted supplementary skeleton as compared with the majority of other *Nummulites*". Since, many authors gave their opinion on the validity of this genus. Davies (1949) and Nagappa (1959b) supported Caudri's decision with arguments, others (Grimsdale, 1952) silently accepted it. A greater number of authors rejected *Ranikothalia*: Vaughan (1945), De Cizancourt (1948), Cole (1953), Smout (1954) and Hanzawa (1957), though there is no general agreement about the generic place of the species that have been variously assigned to *Miscellanea* Pfender, *Nummulites* Lamarck (or *Camerina* Bruguière), *Operculinoides* Hanzawa, *Operculinella* Yabe and *Operculina* d'Orbigny. Apart from obvious errors this shows that, once *Ranikothalia* is rejected, its homogeneous species group cannot be nicely fitted into a single other genus. Also opponents of the genus agree that the group is homogeneous and can be seperated without difficulty from other groups of nummulitic species (De Cizancourt: "Nummulites cordelées"). To the arguments advanced already by Caudri and Nagappa, may be added that of the presence of the coarse canal system, completely open to the exterior both in the marginal cord and through the double row of coarse pores along the sutures. The open marginal cord may be seen as morphologically intermediate between some rotaliid ancestor and typical *Nummulites*, though closest to the latter. The wide openings along the sutures (also observable in some published figures: Vaughan, 1945, pl. 5, fig. 2; De Cizancourt, 1948, pl. 1, fig. 2 and others) better resemble the characteristics of some rotaliid genera, such as *Elphidiella* Cushman and *Laffitteina* Marie. However, it must be remarked that such sutural openings, though of much thinner structure, were described and figured already by Carpenter (1862, p. 259, pl. 17) for recent *Operculina* specimens.

Cole (1953, p. 10) is perfectly right in stating that the difference between *Ranikothalia* and other nummulitic genera is one of degree. However, though possibly not different by a completely new structure, the absence of a general morphological intergradation between the species of the *Ranikothalia* group and those of *Nummulites* and *Operculina* is considered a sufficient basis for generic separation. The more so since the species are restricted in time (Paleocene-?Early Eocene) and space (southern Asia, Togoland, Caribbean). They represent a distinct off-shoot of the rotaliid stock, possibly ancestral to all or part of the early *Nummulites*, *Operculina* and *Assilina* of the Mediterranean and other areas. At least in America, *Ranikothalia* is not accompanied by other nummulitic genera; it may have originated in this area.

Specific determination. Sachs (1957) gave a detailed review of the American species of *Ranikothalia*. In several scatter diagrams this author shows that there is continuous variation in the measured features of the

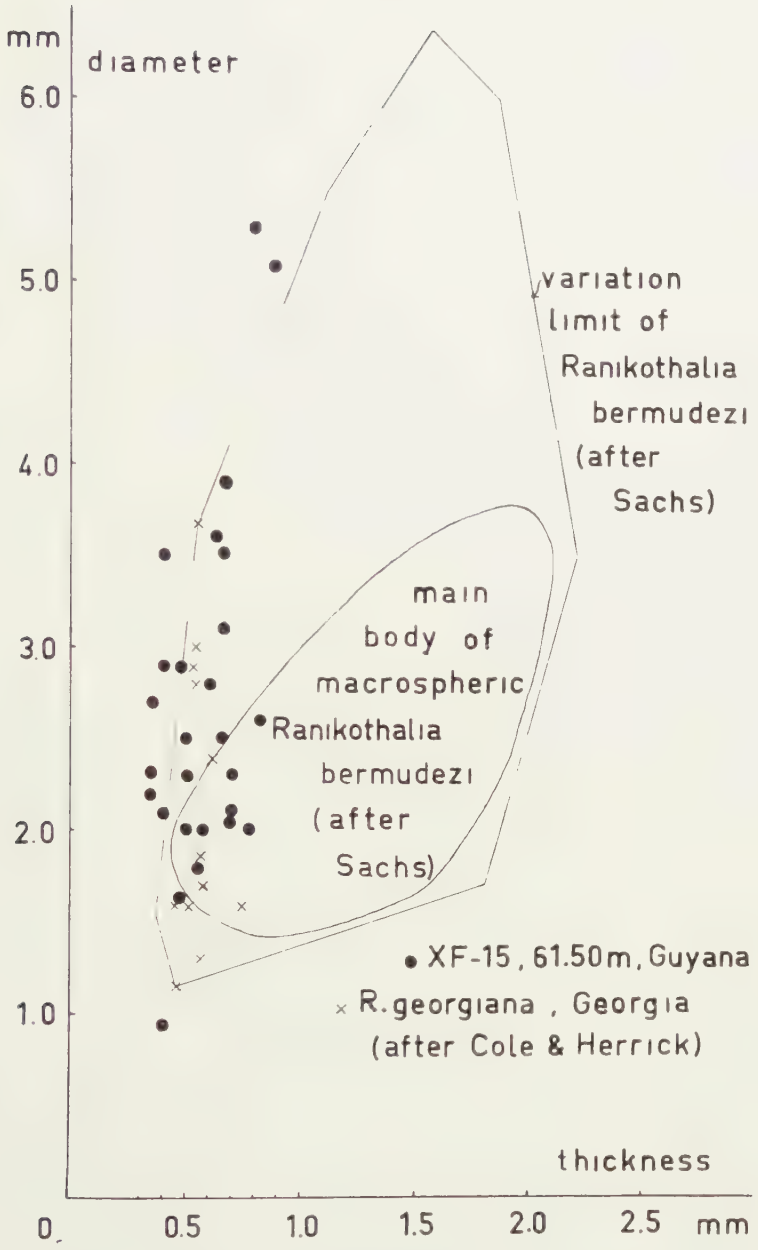

Fig. 2. Scatter diagram of the diameter/thickness ratio of the test of a number of specimens of *Ranikothalia soldadensis* (VAUGHAN and COLE) from sample XF-15, 61.50 m. The relative thinness of the test corresponds to the measurements of *R. georgiana*, given by COLE and HERRICK. From the data given by SACHS, it is apparent that most individuals of *R. bermudezi* are relatively thicker.

many described species. No doubt he is perfectly right in saying that too many specific names have already been introduced for this group. But it must be considered questionable whether they can all be united under

the single specific name *R. bermudezi* (PALMER). In this way this species gets a width of variation that is certainly not realized in our populations. It is true that most features of our Guyanese individuals do not allow separating them from *R. bermudezi*, but the ratio diameter/thickness of the test (fig. 2) clearly demonstrates that the entire group of our individuals is extreme by the relative thinness. In this respect our specimens would be identical with the typical representatives of *R. soldadensis* (VAUGHAN and COLE) and *R. georgiana* (COLE and HERRICK) (synonym). In the published details of the populations of *R. soldadensis* there are indications of variation to the thicker *R. bermudezi* type, but such variation seems to be absent in other populations, such as those of *R. georgiana* in the Georgia wells.

The absence of clear discontinuities between a fairly great number of populations is in itself not a sufficient reason to lump the entire wide variation under a single specific name. It will be hard to find a good example to prove that considerable differences between extreme populations are merely due to environmental factors, and even then there is a danger of generalization. Both in Guyana and in Georgia the populations consist of flattened individuals only. This is less certain for the original population of *R. soldadensis* from Soldado Rock. From Venezuela, Trinidad and Barbados this type is commonly reported together with thicker variants (VAUGHAN, CAUDRI, 1944, DE CIZANCOURT), so that populations with a wider variation may be the rule here. Since the name *R. soldadensis* is the oldest, it is chosen in preference to the more distinct *R. georgiana*, pending a revision of ample material from

PLATE 5

Ranikothalia soldadensis (VAUGHAN and COLE)

Figs. 1–3. Side views of specimens of different size. 1 and 2 from XF-15, 62.50 m; 3 from XF-15, 62 m. All three × 15.

Figs. 4*a*, *b*. *a*, side view of a large specimen showing the double row of pores along the sutures; *b*, peripheral view, showing the reticulate surface of the marginal cord and the more regular canals in the deeper parts. XF-15, 62 m. × 15.

Fig. 5. Part of peripheral view. In the upper part the reticulate surface pattern has been worn off, showing the underlying longitudinal canals of the marginal cord. XF-15, 62 m. × 30.

Fig. 6. Peripheral view of a worn fragment showing the longitudinal canals of the marginal cord and their connections with the intraseptal canals. XF-15, 62 m. × 15.

Figs. 7–10. Various fragments of the peripheral area with details of the marginal cord. All four from XF-15, 62 m. 7, × 15; 8, 9 and 10, × 30.

Fig. 11. Horizontal thin-section. XF-15, 61.50 m. × 15.

Fig. 12. Part of the thin-section of figure 11. × 40.

Fig. 13. Transverse thin-section. XF-15, 61.50 m. × 30.

Fig. 14. Transversely broken specimen showing an intercameral basal opening. XF-15, 62 m. × 15.

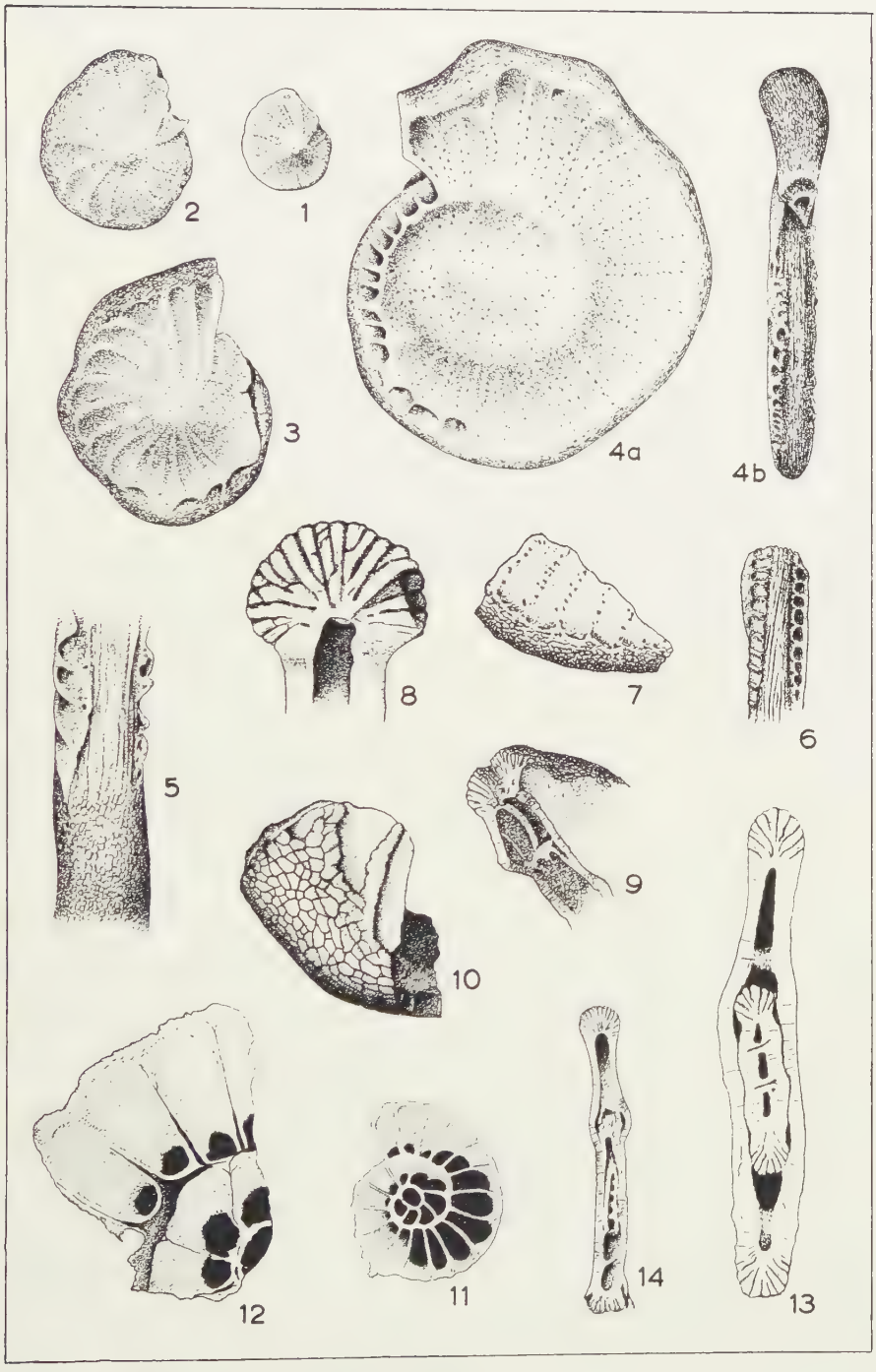

PLATE V

Soldado Rock. A still older name may be *R. catenula* (Cushman and Jarvis) (*Operculina catenula* Cushman and Jarvis, 1932, Proc. U.S. Nat. Museum, vol. 80, p. 42, pl. 12, fig. 13), but this species is solely known from its holotype (see Cole, 1953, p. 13). Cole (1959b) substituted *Operculina catenula* for the entire group of *R. bermudezi* in the sense of Sachs, which of course is a logical consequence from these authors' point of view on the observed variation.

Comparison of the Caribbean *Ranikothalia* species with those of India shows a striking similarity in features and variation. Already Davies (1927, p. 275) noted that "it is hard to resist that, at Thal, the Operculine (=*R. sindensis* (Davies)) only represents an extreme variant of the Nummulite (=*R. nuttalli* (Davies)). In Sind, however, the latter is less compressed, and so the two forms are more easily kept apart". Evidently again variation between the thick and the flattened type may be present or absent. Comparison of material from both regions may eventually even show that *R. soldadensis* is not specifically different from *R. sindensis*, or that *R. bermudezi* is conspecific with *R. nuttalli*.

Age. *R. soldadensis* is considered to be of Paleocene age at Soldado Rock, in the San Juan limestone of Venezuela, in the Upper Lizard Springs beds of Trinidad, and in the blocks of the mudflows of the Joes River, Barbados. Under the name of *R. georgiana* it has been described from borings in Georgia from beds that have been correlated with the Porters Creek clay of Midway age. In southern Asia, according to Nagappa (1959b), the *Ranikothalia* group is restricted to the Paleocene, possibly rarely extending into the Early Eocene.

To be continued

SOME EARLY ROTALIID FORAMINIFERA. III

BY

C. W. DROOGER

(Communicated by Prof. G. H. R. VON KOENIGSWALD at the meeting of Febr. 27, 1960)

CLASSIFICATION AND PHYLOGENY

Because some place was sought for our new Guyanese genera among the other representatives of the Rotaliidea, the various existing classifications were investigated in some detail. Phylogenetic relations of the genera of the superfamily Rotaliidea are partly very obscure, and correspondingly there is no clear, uniform classification. This is not only due to a lack of sufficient data on many of the genera, but also to the fact that no distinct hierarchy of characteristics is apparent from the development of the group.

After the recognition of the presence of the septal flap as a distinctive feature of the superfamily (SMOUT, 1954), new groupings have been proposed, which differ considerably from that of CUSHMAN (1948), which was the one most commonly used. The newer ideas are sometimes conflicting, depending on which features are given some prevalence over other, such as for instance toothplates (HOFKER), canals (SMOUT) or apertures (REISS and MERLING). At the moment it is really impossible to decide which is the best hierarchy of features, probably there is not a general one.

A discussion of various characteristics may review the possibilities accepted at present.

1. The arrangement of the chambers of simple spirals is mostly trochoid or planispiral. Reversed trochoid is added as a third possibility, which may be partly identical with secondary trochoid. The distinction of two different types of trochoid arrangement implies that a distinction can be made between both sides, the ventral and dorsal sides of common use. Umbilical and spiral are hardly better terms. In asymmetric forms, the ventral or umbilical side, of the Rotaliidea at least, is thought to be distinguishable by a greater size of the umbilical mass and also by the preference of the intercameral foramen to be situated at this side. Reversed trochoid is then characterized by dorsal prolongations of the open chamber cavities reaching farther towards the axis than do those of the ventral side (*Laffitteina*, *Storrsella*). There is no general trend in phylogeny between the three types. If the group is monophyletic, it is likely that the first representatives were slightly to moderately trochoid.

developing more trochoid as well as planispiral stocks. These changes were reversible, however, as may be seen from the development of planispiral from trochoid Miogypsinidae, and the reverse case from the rise of younger trochoid offspring (*Polystomellina*, etc.) from the planispiral *Elphidium* group. It is logical to suppose that reversed trochoid forms developed from planispiral ones (*Laffitteina*), but it is conceivable that they originated directly from normally trochoid ancestors.

2. The alar prolongations of the chambers are another feature in classification. Most genera have involute chambers, both their cavities and the walls. Since the outer wall of the test, with the forming of each new chamber, may be covered by a more or less thin layer, the walls are generally involute, though thickening is often hardly perceptible. The involute or evolute character of the chamber cavities is evidently more important in systematics. Chambers are said to be involute when their cavities reach the umbilical mass, and evolute when the earlier coils are visible, or at any rate not covered by the cavities of the later whorls over a considerable distance. It is clear that in practice these definitions are not tight. In distinctly trochoid forms the dorsal side is commonly evolute (*Rotalia*). In planispiral forms the cavities may be involute (*Nummulites*) or evolute (*Operculina*). A general trend is absent.

3. Deviations from the simple spiral type are always distinct one-way trends. The original spiral may become complicated by doubling one or several times, resulting in a multiple spiral (*Dictyoconoides*). Elongate chambers may become subdivided (*Heterostegina*), annular (*Cycloclypeus*), or meandrine with separate polar cavities (*Miscellanea*). Orbitoidal growth may develop (*Miogypsina*) or systems of lateral chambers may become added (*Pseudorbitoides*). Several of these trends often occur together.

4. The apertures are a subject to discussion and confusion. The presence of an intercameral foramen is a general feature, but especially for many fossil genera it is uncertain whether it was present as an aperture in the final chamber. Resorption of part of the septal wall between earlier chambers is known to occur in species which aleady have a distinct interiomarginal aperture of the final chamber (*Rotalia*). It is likely that in a number of genera the aperture in the last chamber is represented only by a few pores. The intercameral foramen may be interiomarginal (*Rotalia*), interiomarginal to areal (*Laffitteina*) or entirely areal (*Pararotalia* in its original sense). In planispiral forms it is about median, in others ventral or median to ventral. Since so much doubt exists about this structural element, its value for classification cannot be great at the moment.

There is equally much confusion about the openings of the chamber cavities in umbilical direction, which are either continuous or discontinuous with the interiomarginal opening. If present, they may open into the

umbilical fissure or canal, or in the sutural fissures, or directly to the exterior. Reiss and Merling (1958) described a set of labial apertures in some trochoid genera. If too much differentiation is being made, however, the systematic value decreases for fossil genera, in which such minute structures are often not observable.

5. Septal structures are a consequence of the septa being double for at least the greater part. If there are flattened spaces in between both lamellae, which open to the exterior along a considerable part of the sutural length, they are commonly described as fissures (*Fissoelphidium*). If their depth cannot be ascertained, they can be termed sutural grooves or furrows. A special character of such fissures is that they are often feathered, i.e. there are extensions of the fissures on the outer walls of the adjoining chambers, usually convergent to the periphery (*Storrsella*). Either these fissure branches or the small costae in between are prominent, which is often dependent on the state of preservation. Surface parts of the septal fissures may be closed, leaving intraseptal canals below, which generally open in sutural direction through ascending branches. In these cases the septa are usually mainly closed, leaving a row of openings (*Pseudorotalia*), which often is double to either side of a continuous straight bar of the sutures (*Ranikothalia*). The double rows are a consequence of the frequently observed bifurcation of the ascending canals, evidently a character corresponding to the feather structures in fissured forms. Yet another complication of the superficial covering of the sutures is the presence of retral processes (*Elphidium*), backward projections of the chamber cavities across the septa, enclosed by the septal flap. In the open parts in between again fissures or openings of ascending canals may be found. Finally the sutures may be entirely closed, though such conditions, when seen in fossil material, may be due to the state of preservation.

The intraseptal spaces and canals usually communicate with spaces and canals in the umbilical region, and occasionally with similar structures in the marginal area. They are used as important distinctive characters in classification at the generic level, though in fossil species they are often difficult to ascertain. Especially the differentiation between canals and fissures may be impossible. The open fissures might be thought to represent the most primitive condition, but the oldest known species suggest mainly closed sutures, which may be due to preservation, however. Closed sutures with pores are clearly derived, both from a morphological point of view and phylogenetically.

6. In many genera a spiral fissure or canal is clearly present in between the umbilical ends of involute chambers and the central umbilical mass. It is formed by spaces left between the umbilical, infolding parts of the chamber walls, the wall of the umbilical mass or of the previous coil, and the covering of umbilical lips and superficial lamellae corresponding

to later chambers. If the latter are partly or wholly absent, there is an umbilical fissure that is continuous with the septal fissures, if present. The umbilical infolding of the septal flap (umbilical flap) occurs at variable distances from the umbilical mass. Especially if this distance is considerable, the ventral wall of the primary chamber may continue in umbilical direction as the umbilical lip with or without infolding parts. The infolding umbilical flap joins the wall of the previous coil, usually extending in the ventral part only. Its internal end (toothplate) may adhere but partly to the previous coil, leaving openings to the spiral canal or fissure underneath. It may also be pierced by larger pores or single openings, thus furnishing connections between the various cavities of the test. The infolding of the umbilical flap may be sharp and close to the umbilical mass, leaving a narrow fissure often of zig-zag course (*Smoutina bermudezi*). It may be broad, thus bordering a broader and more continuous fissure. Of course the rounding of the umbilical mass also influences the width of the fissure. If the fissure is covered by later lamellae, which continue into the umbilical mass, a buried spiral canal is the result. If the primary chamber has a well developed umbilical lip with infolded parts, an intermediate cavity may be recognized: the astral lobe. It has been variously interpreted as part of the chamber cavity or as part of the spiral fissure or canal. This depends on the degree of development of the umbilical flap and of the lip. If such cavities are distinctly present they again may have openings in umbilical or sutural directions, the labial apertures (Reiss and Merling). Yet another complication is found when the later lamellae adhere only partly to the ventral walls of chamber and lip. This is very extreme in *Smoutina cushmani*, where the later lamellae only join the ventral chamber wall in its peripheral part, thus leaving an additional wide space over the chambers, continuous with the spiral and intraseptal spaces.

Although there are many misinterpretations, much stress has been laid in systematics on these spiral structures. They may be very thin, causing different opinions about their existence. Groups are known (Miogypsinidae) in which they have become greatly reduced or even disappeared during the phylogenetic development. Whether such a spiral structure is a primitive feature cannot be decided. Among the early genera some with a distinct spiral structure occur next to others in which it could not be proved.

Whether details of the spiral fissure or canal are of systematic value at the generic or higher levels has to remain as yet undecided. No studies have been made of the possible variation of these details, such as the toothplate and the umbilical lips with their respective openings. There is a tendency in the literature to generalize too few observations and to overstress their systematic importance. From the numerous broken specimens of *Smoutina cruysi* and of *Lockhartia haimei* we failed to observe a constant appearance of the toothplates in these populations. In the

type material of *Storrsella haastersi* many specimens show a distinct astral furrow, whereas this feature is indistinct in the Guyanese specimens. Regarding the species grouped in the genus *Smoutina* there is a very wide range of variation of the spiral structures. Of course, it is possible that our conclusions on relationships of the *Storrsella* assemblages and of those of *Smoutina* are not correct. Nevertheless some doubt may be expressed concerning the great systematic value of the details of the spiral structures.

7. Umbilical structures generally occur as more or less solid masses at at least the ventral side, but often at both. They fill the space between the umbilical ends of the chamber cavities and adjoining spiral spaces by adding successive lamellae of imperforate shell material. Only in some evolute genera can no umbilical mass be differentiated structurally from the surrounding wall. Described umbilical structures are many and their separation is often indistinct, possibly partly due to again a lack of a sufficient number of observations. The mass may be entirely solid or show superficial, rounded, pustules of the inflational type, or it may be more deeply fissured. It may be pierced by rounded vertical canals, originating from the chamber cavities, either directly or passing a spiral that may be simple or branching. Probably the vertical canals are partly modified, enlarged pores, especially if more than one is seen to originate from a single chamber cavity. In other cases they may be extensions of an originally umbilical opening of the chamber cavity so that there is but one per chamber (*Kathina*). The umbilical mass may also contain larger cavities between the lamellae, which usually communicate horizontally with the umbilical ends of the chamber cavities and vertically with the exterior through short vertical canals, and in both directions with one another (*Lockhartia*).

Possibly a more or less solid mass with a spiral fissure around it, or one without such a fissure but with enlarged vertical pores, are both primitive, though persistent features. Fissures, cavities, extended umbilical openings of the chambers, and additional branches of the spiral canals are probably all later acquirements, appearing rather unsystematically in various groups and sometimes getting lost again. If well recognizable they may be valuable features in systematics.

8. Wall structures. The surface of the chamber walls is often smooth. The possession of inflational pustules is generally accepted as a feature below the generic level. Their distinction from incised pillars (*Miscellanea*) is often unsharp. These pillar types may occur all over the surface, their pattern being confluent with that of the umbilical masses and also occurring on the periphery of the test. In these types the entire wall is thickened with, as a consequence, that part of the original pores tend to widen or unite to vertical canals over the entire wall. Considerable

thickening and fissuring of the wall is considered to be of generic value in some cases (*Miscellanea*).

9. Marginal structures occur especially if the thickening of the wall is strongest in the peripheral area (*Pseudosiderolites*), or is even practically restricted to it (*Nummulites*). This thickened marginal area may be simply pierced by radial canals (*Pseudosiderolites*), it may be coarse and fissured mainly longitudinally (*Ranikothalia*) or mainly vertically with a central groove (*Sulcoperculina*). Longitudinal canals in the basal part of this marginal cord, connecting with the intraseptal spaces are common. The superficial part of the fissures may be at least partly closed (*Nummulites*). Another marginal structure consists of outward directed spines, which are formed around radial extensions of the intraseptal canals (*Siderolites*). Shorter radial spines of the peripheral part of the chamber walls (*Pararotalia*) are considered to be of specific value only. In *Pellatispira* there is a thickened skeleton all over, possessing longitudinal rounded canals in the marginal area, connecting with the cavities of the test and with the exterior through rounded canals, probably enlarged pores.

In several of the discussed structural elements phylogenetic trends can be recognized, but in others they seem to be absent. As yet many of the described genera are insufficiently known and most often but one or a few of their species have been investigated in more detail. Fortunately the latter group includes the type species of many of the genera. The number of more detailed descriptions, though of much differing emphasis, has rapidly been increasing during the last few years (Hofker, Cole, Smout, Wade, Reiss and others). This enables us to repeat Smout's attempt (1955) to make a general survey.

Groupings in families and subfamilies will be entirely left out of discussion. Furthermore all age determinations from the literature, if not contradictory, are taken for granted. The same holds good for nearly all described genera. A discussion of possibilities of further splitting or lumping, which is certainly possible, would only cause complications, unnecessary for the attempted survey.

In establishing a classification it is a great help that several groups can be formed, and have actually been formed, because of one or more peculiar characteristics. However, especially for the genera of the Cretaceous and the Paleocene, the time of explosive development, groupings are much less distinct. For our scheme (fig. 3) we started from these early genera in order to detect whether some hierarchy of features could be found. This attempt failed because of our too scanty knowledge of the detailed structure of most of the species.

It is striking that among the Cretaceous genera a fully planispiral growth is very rare (*Fissoelphidium*). But there is a large group of species, which are slightly trochoid to planispiral. They generally have on both

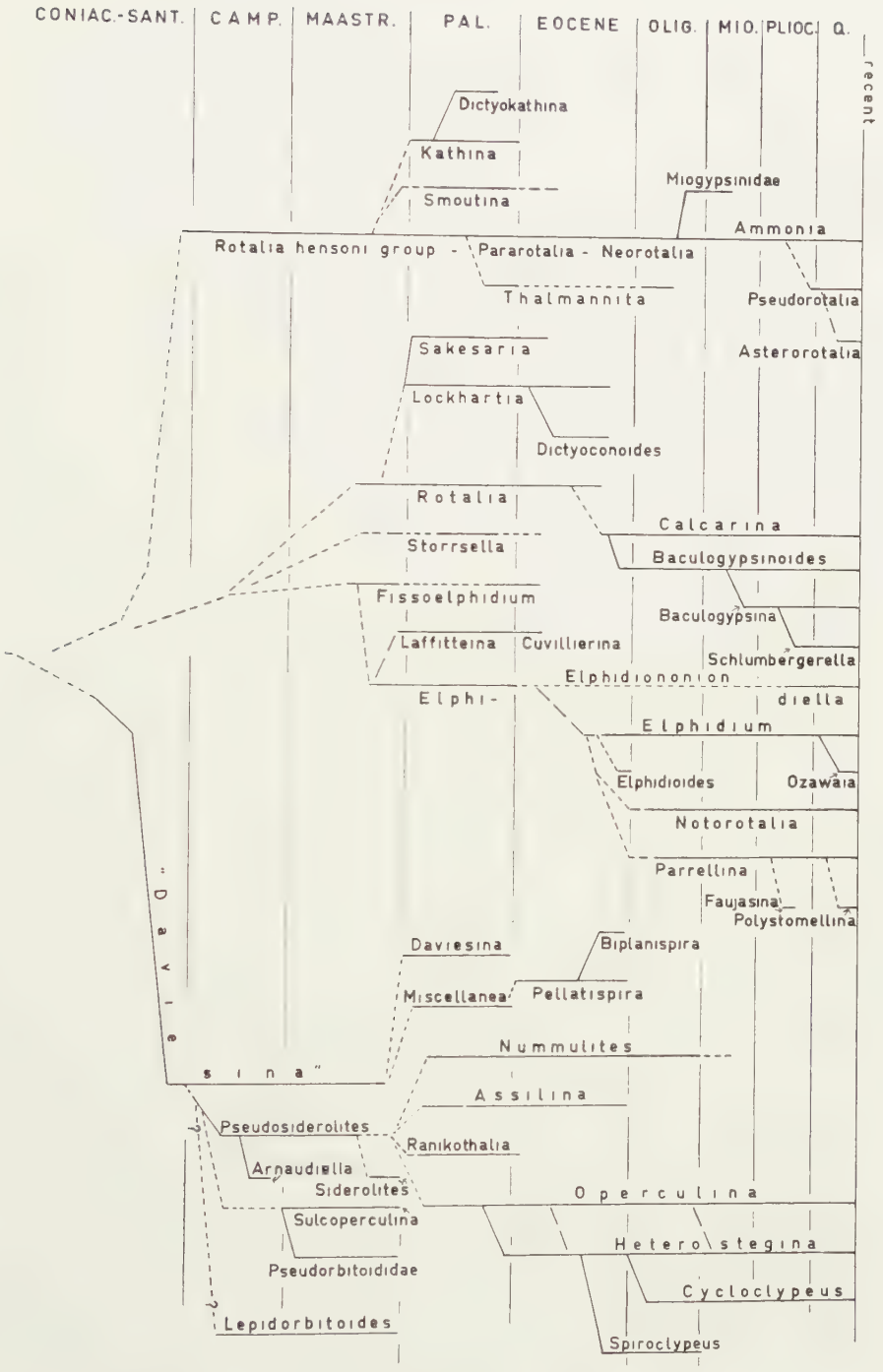

Fig. 3. Stratigraphic distribution and possible relations of the genera of the Rotaliidea. The horizontal scale is not considered proportional to the relative lengths of the time intervals. Vertical distances between genera are not necessarily a degree of supposed relationships.

sides a number of umbilical pustules, often also along the sutures and on the remaining parts of the outer surface. As far as could be found the oldest form is from the Santonian of Germany, described as *Lockhartia minuscula* by HOFKER (1957a). This author later (1958a) mentioned this species in connection with two similar forms of the genus *Daviesina* from the Campanian-Maastrichtian. All these species are slightly trochoid, with double septa, and they show at both sides umbilical masses of somewhat different size, which consist of inflated pillars, probably with some vertical canals in between. The Santonian species lacks sutural knobs. Whether there are other septal or umbilical structures is unknown. Certainly this looks like a basic type, though lack of knowledge may account for its general appearance.

In the Campanian probably at least two additional groups can be distinguished. In one we find a more trochoid character of the test without a distinct dorsal umbilical mass, together with the possession of ventral and spiral fissures (*Rotalia algeriana* MAGNÉ and SIGAL). There is a solid umbilical mass and the species, also of later time, show frequent thickenings of the inner ends of the ventral chamber tips. This is evidently the base of the persistent group, probably continuous up to the present day (*Rotalia hensoni* group, *Pararotalia*, *Neorotalia*, *Ammonia*). The question whether the *Pararotalia tuberculifera* group of the Maastrichtian and younger, claimed to have been derived from a *Globorotalia* species (HOFKER, 1957c), is an independent later addition, has to remain unsolved. Anyhow, it seems morphologically quite a step from the probably closed structure of *Daviesina minuscula* (HOFKER) to the open fissures of *Rotalia algeriana*. It has been remarked that *Pararotalia* specimens have been observed in the Coniacian-Santonian of SW Europe, but this is as yet of little use (REISS and MERLING).

Another group beginning in the Campanian, that of *Pseudosiderolites*, is different from Cretaceous *Daviesina* by a nearly planispiral growth and thick wall structures, especially so in the marginal area. All these secondary structures are pierced by radial canals. The morphological step from early *Daviesina* is probably not so great. It is considered likely that the ill-known *Arnaudiella* (Campanian) was derived from *Pseudosiderolites* by the addition of vacuoles or lateral chambers in the side walls. Also *Siderolites* of the Maastrichtian looks like a further development of a group of *Pseudosiderolites* in that it acquired radial spines.

A much greater step is needed to come to the important *Sulcoperculina* and its rich group of descendent Pseudorbitoididae, all from the Maastrichtian. Their typical marginal complications can hardly be compared with those of *Pseudosiderolites*, which nevertheless is the only other genus with definite marginal structures. The change from radial canals and spaces (see ARNI) to a system of vertical plates with a central groove, is considerable, though it is the most likely one.

Regarding the resemblance of the Campanian early *Lepidorbitoides* of

Austria with the accompanying *Pseudosiderolites* (Papp and Küpper, Papp, 1955, 1956), one is inclined to link this genus with its orbitoidal growth to the Rotaliidea. The generic determination of these early orbitoidal forms may be wrong, however.

During the Maastrichtian still more genera were added. There is *Fissoelphidium* with its bilateral symmetry and simple system of sutural and umbilical fissures. If the fissure systems are considered as important in phylogenetic relations, it is logical that *Rotalia* s.str. (Latest Cretaceous-Eocene) and *Storrsella* with possibly the same stratigraphic range have to be grouped with *Fissoelphidium*. Possibly they arose from the latter genus by restricting the fissure system to one side. An alternative solution is that these genera arose from the *Pararotalia* lineage by loss of the spiral groove and fissuring of the base. A third possibility would again be a direct derivation from some *Daviesina* ancestor.

It seems most logical to link the Maastrichtian-Paleocene representatives of *Elphidiella* with *Fissoelphidium*, which involves a partial closing of the septal fissures and a more complete closing of these fissures in the umbilical region. The derivation of *Laffitteina* and its Eocene end in *Cuvillierina* from *Elphidiella* is again quite plausible.

A final group arising in the Late Cretaceous is that of *Kathina*. One possible solution is again a direct derivation from *Daviesina*. However, closing of an umbilical spiral fissure might have caused the elongation of the umbilical openings of the chamber cavities as vertical canals. This suggests some derivation from the *Pararotalia* lineage. The Paleocene development of this group includes the acquiring of again strong spiral canals in *Smoutina* and the repeated doubling of the primary spiral in *Dictyokathina*.

Now shifting our attention to the Paleocene we find still more complications. Thus *Fissoelphidium* may have given rise to *Miscellanea* and *Pellatispirella* by thickening of the walls and more excessive fissuring, but these two hardly different genera might equally well have developed, at least partly, from the obscure *Daviesina* group. Regarding the Cretaceous species of the latter genus (Hofker, 1958a) and those of the Paleocene (Smout, 1954) one sees in both a trend from a trochoid to a more planispiral mode of growth. For this reason it might be considered likely that the Paleocene group is not a direct continuation of that of the Cretaceous. The insufficient detailed knowledge of all these *Daviesina* species may at the moment overstress their importance as the basal stock of all kinds of other genera.

One is at a loss where to link *Ranikothalia*, which is probably at the base of the entire *Nummulites* group. Derivation from the *Elphidiella-Laffitteina* group because of the sutural openings is considered the least likely one. Connection with *Daviesina* or *Miscellanea* is possible, but *Pseudosiderolites* is the only genus which already possessed a considerable thickening and complication of the marginal area. *Operculina*, *Nummulites*

and *Assilina* are possibly three independent offshoots of early *Ranikothalia*, all three with an advanced, less coarse development of the fissures and canal systems in addition to special characters of their own. The occasional morphological intergradation of these genera does not necessitate their lumping together. The repeated development of *Heterostegina* from *Operculina*, and the independent origins of *Spiroclypeus* and *Cycloclypeus* from *Heterostegina* are sufficiently well known.

The ventral fissured umbilical area of *Lockhartia* is highly reminiscent of that of *Rotalia* s.str. Descent of this genus with umbilical cavities from *Rotalia* is thought to be morphologically less complex than a derivation from the *Pararotalia* group. *Sakesaria* and *Dictyoconoides* developed from *Lockhartia* by elongation and by repeated doubling of the spiral, respectively.

Three more groups arose during the Eocene. It seems reasonable that *Elphidium* is related to early *Elphidiella*. Whether our recent *Elphidiella* species are direct descendents of the Paleocene forms is open to doubt. There is a group of *Elphidium*-like forms without retral processes, *Elphidiononion* Hofker (1951), which possibly bridges the gap in time. Trochoid younger genera with retral processes (*Faujasina*, *Polystomellina*) can only be connected with *Elphidium* or *Parrellina*, and the same is true for the uncoiling *Ozawaia*. Where the inadequately known *Elphidioides* Cushman of the Late Eocene fits in exactly, must be left undecided. The data on *Notorotalia* suggest an early differentiation of the *Elphidium* group, but Wade's remark on a very trochoid Eocene form still leaves the possibility of another derivation of this genus. Recently also *Sherbornina* (Eocene-Miocene) with later annular growth was added to the *Elphidium* group (Wade and Carter, 1957). Relations within this group are not yet very clear, notwithstanding the important paper by Wade (1957), who suggested that the retral processes are of minor systematic importance, thus placing *Elphidiella* in the synonymy of *Elphidium*.

The derivation of *Calcarina* and its offshoot of the Baculogypsinidae (Küpper, 1954) is still a problem. Smout (1955) advanced the idea of a direct descent from *Siderolites*, even suppressing the generic name *Calcarina* as a synonym of *Siderolites*. If on the other hand, the possession of radial spines is regarded as a renewed development in the Eocene, nearly everything is possible, though a descent from *Rotalia* s.str. or from the *Pararotalia* group is considered most likely because of the trochoid character of the test.

Another problem concerns the derivation of *Pellatispira*, and its descendent *Biplanispira*. Any suggested link is doubtful, also that with *Miscellanea*, which, amongst other things, involves a closing of the fissures of the latter. As a matter of fact *Pseudosiderolites* would be a more plausible ancestor, but here we meet with the difficulty of bridging the gap of the Paleocene.

Finally some complications of the *Pararotalia* lineage must be mentioned.

It is one of the least known groups, and it is probably heterogeneous. The mainly Cretaceous-Paleocene *Rotalia hensoni* group, the mainly Eocene *Pararotalia* and the mainly Oligo-Miocene *Neorotalia* groups, may constitute a single branching tree of relations, in which foreign, but resembling groups may be hidden. *Ammonia* is thought to be a Neogene offshoot, and also *Pseudorotalia* with the group of *Rotalia elphidioides* CAUDRI (1934) with its partly closed septal fissures on both sides and strong vertical umbilical canals chiefly on one side. *Asterorotalia* with its peculiarly covered sutures and occasional spines, probably again descended from *Pseudorotalia*. The development of the Miogypsinidae, which attain orbitoidal growth in the Oligo-Miocene, is well known. BERMUDEZ' *Thalmannita* may be a side group with again nearly bilateral symmetry.

This review is certainly not an exhaustive one and it is fully realized that rewriting it in another year may result in quite a different phylogeny and classification. However, it demonstrates the numerous deficiencies. apt to rouse still more general interest and investigation.

It is apparent from fig. 3 that some hierarchy of characteristics has been introduced more or less involuntarily. The correct succession in time has been taken as the primary condition, as indeed it should be. Apart from generally recognized groupings based on one or two diagnostic features (orbitoidal growth, retral processes, marginal plexus) some characteristics have been granted a greater diagnostic value because of assumed trends in phylogeny. They are a change from trochoid to planispiral, a change from open fissures to more closed structures, and a change towards a more thickened skeleton, especially in the marginal area. These are no general trends, as may be seen from the exceptions that have been made. On the other hand, apertures and to a lesser extent also canal systems, got much less weight. This is mainly because of our confused and insufficient knowledge.

KEY TO THE GENERA OF THE ROTALIIDEA

This key is one out of many that could be made. An easy method based on the clearest morphological differences has been given preference to a system that would better reflect the assumed phylogenetic relations.

1. Chamber arrangement a simple spiral. 2
   Chamber arrangement not a simple spiral. 17
2. Sutures without a series of separate openings or retral processes. . . . 3
   Sutures with a series of separate openings or retral processes. 9
3. Test trochoid without distinct dorsal umbilical mass.. 4
   Test slightly trochoid to planispiral with more or less developed umbilical masses at both sides. 5
   Test planispiral. 6
   Test reversed trochoid. Ventral mass and sutures simply fissured. . . .
   Storrsella

4. Ventral mass and sutures simply fissured. . . . . *Rotalia*
Ventral mass solid or with inflated pillars and occasional vertical canals.
Strong spiral fissure which may be partly covered. . . . . *Ammonia*
Pararotalia
Neorotalia
Ventral mass with umbilical cavities. Spiral broader than high. . *Lockhartia*
Ventral mass with umbilical cavities. Spiral higher than broad. . *Sakesaria*
Ventral mass with strong vertical canals only. . . . . *Kathina*
Ventral mass with strong vertical canals and ramifying spiral canals *Smoutina*
Test with thickened walls and marginal spines. . . . . *Calcarina*
5. Test with inflational pustules in the umbilical regions to all over the surface. Sometimes with vertical canals. . . . . *Daviesina*
Test with thickened walls, especially in the marginal area. Vertical canals all over. . . . . *Pseudosiderolites*
Test with thickened walls, especially in the marginal area. Vertical canals and radial spines. . . . . *Siderolites*
Test with thickened walls and incised to inflated pillars all over. Nearly completely planispiral. . . . . *Miscellanea*
Pellatispirella
Test with a marginal sulcus and vertical plates. . . . . *Sulcoperculina*
6. Without a marginal cord. 7
With a marginal cord. 8
7. With umbilical and sutural fissures. . . . . *Fissoelphidium*
With inflated pustules on both umbilical sides. . . . . *Thalmannita*
With fissured or pustulated walls all over. . . . . *Miscellanea*
Pellatispirella
With thickened walls all over. Numerous coarse radial and circular canals, in the outer wall suggesting the presence of a marginal cord. . *Pellatispira*
8. With extremely thickened marginal cord with fully open fissures. Chambers usually involute. . . . . *Ranikothalia*
Often with coarse marginal cord, the fissures of which are partly closed. Chambers mainly evolute. Whorls rapidly increasing in height. . *Operculina*
Fissures of the marginal cord partly closed. Chambers mainly evolute. Whorls slowly increasing in height. . . . . *Planocamerinoides (= Assilina)*
Fissures of the marginal cord partly closed. Chambers mainly involute. Whorls often, but not necessarily, slowly increasing in height.
Nummulites (= Camerina)
Operculinoides
Operculinella
9. With retral processes. 10
Without retral processes. 13
10. Test trochoid. 11
Test planispiral. 12
11. Test biconvex. Retral processes only ventrally, interrupted fissures in the dorsal sutures. . . . . *Elphidioides*
Test biconvex, ornamented with bars and ridges. . . . . *Notorotalia*
Test planoconvex. Dorsal side flat. . . . . *Faujasina*
Test planoconvex. Ventral side flat. . . . . *Polystomellina*
12. Test not uncoiling. . . . . *Elphidium*
Parrellina
Test uncoiling. . . . . *Ozawaia*
13. Test trochoid. 14
Test planispiral. 15
Test reversed trochoid. 16

14. With rows of simple openings in and along the sutures, both ventrally and dorsally. . . . . *Pseudorotalia*
With simple openings in and along the sutures, partly covered by thin plates with distal openings. . . . . *Asterorotalia*
15. Sutures with a single row of openings or with interrupted fissures. *Elphidiononion*
Sutures with a double row of openings. No marginal cord. . . . *Elphidiella*
Sutures with a double row of openings. Marginal cord highly developed. *Ranikothalia*
16. Sutures with one or two rows of openings. Umbilical radial canals, opening in rounded pores. . . . . *Laffitteina*
Sutures with one or two rows of openings. Walls thickened causing a reticulate surface pattern around the ends of the umbilical and sutural canals. . . . . *Cuvillierina*
17. In addition to an early more or less reduced spiral, some orbitoidal growth and often lateral chambers. Radial plates or rods in the median layer.
Pseudorbitoididae *(Sulcorbitoides, Vaughanina, Pseudorbitoides,* etc.*)*
In addition to an early more or less reduced spiral, orbitoidal growth and lateral chambers. Early stages fully central. (?) . . . . . *Lepidorbitoides*
In addition to an early more or less reduced spiral, orbitoidal growth and often lateral chambers. Early stages never fully central.
Miogypsinidae *(Miogypsina, Miogypsinoides,* etc.*)*
In addition to an early more or less reduced spiral, orbitoidal to acervuline growth. Radial spines present.
Baculogypsinidae *(Baculogypsinoides, Baculogypsina, Schlumbergerella)*
Later elongate chambers of the plane spiral subdivided. No lateral chambers or annular growth. . . . . *Heterostegina*
Grzybowskia
Later elongate chambers of the plane spiral subdivided. Lateral chambers present. . . . . *Spiroclypeus*
Later elongate chambers of the plane spiral and following annular chambers subdivided. No lateral chambers. . . . . *Cycloclypeus*
Later annular chambers not subdivided. . . . . *Sherbornina*
Lateral chambers in addition to a primary spiral with thickened marginal walls. . . . . *Arnaudiella*
A simple spiral, in the later stages doubling vertically. Thick walls with canals. . . . . *Biplanispira*
A simple spiral, repeatedly doubling in the plane of coiling. 18
A simple spiral, the later chambers of which are meandrine and form polar "chambers". 19
18. Spiral trochoid. Ventral umbilical mass with cavities and vertical openings. Umbilical surface fissured. . . . . *Dictyoconoides*
Spiral trochoid. Ventral umbilical mass with strong vertical canals. Umbilical surface with separate openings. . . . . *Dictyokathina*
Spiral plane, involute. . . . . *Nummulites* p.p.
19. Thickened wall with open fissures. No marginal cord. . . *Miscellanea* p.p.
Wall without open fissures. Marginal cord present. . . . . *Nummulites* p.p.
Paraspiroclypeus

REFERENCES

Applin, E. R. and L. Jordan, Diagnostic Foraminifera from subsurface formations in Florida. Jour. Pal., **19**, 129–148 (1945).

———, "*Lockhartia*" *cushmani* Applin and Jordan and notes on two previously described Foraminifera from Tertiary rocks in Florida. id., **24**, 474–478 (1950).

Arni, P., Eine neue *Siderolites* spezies (*S. Heracleae*) und Versuch einer Bereinigung der Gattung. Ecl. geol. Helv., **25**, 199–221 (1932).

Barker, R. Wright and T. F. Grimsdale, Studies of Mexican fossil Foraminifera. Ann. Mag. Nat. Hist., ser. 10, **19**, 161–178 (1937).

Batjes, D. A. J., Foraminifera of the Oligocene of Belgium. Verh. Kon. Belg. Inst. Natuurw., **143** (1958).

Bermudez, P. J., Estudio sistematico de los Foraminiferos rotaliformes. Bol. Geol. Venezuela, **2**, no. 4 (1952).

Bold, W. A. van den, Contribution to the study of Ostracoda. Acad. thesis Utrecht (1946).

Brown, N. K. and P. Bronnimann, Some Upper Cretaceous rotaliids from the Caribbean region. Micropaleont., **3**, 29–38 (1957).

Carpenter, W. B., Introduction to the study of the Foraminifera. London (1862).

Caudri, C. M. B., Tertiary deposits of Soemba. Acad. thesis Leiden (1934).

———, The larger Foraminifera from San Juan de los Morros, State of Guarico, Venezuela. Bull. Amer. Pal., **28**, no. 114 (1944).

Cizancourt, M. de, Nummulites de l'île de la Barbade. Mém. Soc. géol. France, n.ser., **27**, no. 57 (1948).

———, Grands Foraminifères du Paléocène, de l'Eocène inférieur et de l'Eocène moyen du Vénezuela. id., **30**, no. 64 (1951).

Cole, W. Storrs, *Lockhartia* in Cuba. Jour. Pal., **16**, 640–642 (1942).

———, Internal structure of some Floridan Foraminifera. Bull. Amer. Pal., **31**, no. 126 (1947).

———, Criteria for the recognition of certain assumed camerinid genera. id., **35**, no. 147 (1953).

———, The genera *Miscellanea* and *Pellatispirella*. id., **36**, no. 159 (1956).

———, Names and varaition in certain American larger Foraminifera, particularly the Camerinids—no. 2, id., **38**, no. 173 (1958).

———, Names of and variation in certain Indo-Pacific Camerinids. id., **39**, no. 181 (1959*a*).

———, Faunal associations and the stratigraphic position of certain American Paleocene and Eocene larger Foraminifera. id., **39**, no. 182 (1959*b*).

——— and S. M. Herrick, Two species of larger Foraminifera from Paleocene beds in Georgia. id., **35**, no. 148 (1953).

Cruys, H., Termes inférieures d'âge tertiaire et plio-quaternaire de la série sédimentaire côtière de la région Saint Laurent –Mana. Comm. 5. conf. géol. Guyanes, Georgetown, Octobre (1959).

Cushman, J. A., A foraminiferal fauna from the Twiggs clay of Georgia. Contrib. Cushman Lab. Foram. Res., **21**, 1–11 (1945).

———, Foraminifera ,their classification and economic use. Harvard Univ. Press, 4. ed. (1948).

——— and P. J. Bermudez, Some Cuban Foraminifera of the genus *Rotalia*. Contrib. Cushman Lab. Foram. Res., **23**, 23–29 (1947).

Davies, L. M., The Ranikot beds at Thal (Northwest Frontier Provinces of India). Quart. Jour. Geol. Soc., **83**, 260–290 (1927).

———, The genera *Dictyoconoides* Nuttall, *Lockhartia* nov. and *Rotalia* Lamarck. Trans. Roy. Soc. Edinb., **57**, 397–428 (1932).

———, *Ranikothalia* in East and West Indies. Geol. Mag., **86**, 113–116 (1949).

Drooger, C. W., Foraminifera from Cretaceous-Tertiary transitional strata of the Hodna Mountains, Algeria. Contrib. Cushman Found. Foram. Res., 3, 89–103 (1952).

Emberger, J., J. Magné, D. Reyre and J. Sigal, Note préliminaire sur quelques Foraminifères nouveaux ou peu connus dans le Crétacé supérieur de faciès sub-récifal d'Algérie. C.R. somm. Soc. géol. France, 110–113 (1955).

Frizzell, D. L. and A. Myra Keen, On the nomenclature and generic position of *Nautilus beccarii* Linné (Foraminifera, "Rotaliidae"). Jour. Pal., 23, 106–108 (1949).

Glaessner, M. F. and M. Wade, Revision of the foraminiferal family Victoriellidae. Micropaleont., 5, 193–212 (1959).

Grimsdale, T. F., Cretaceous and Tertiary Foraminifera from the Middle East. Bull. Brit. Mus. Nat. Hist., Geology, 1, 223–247 (1952).

Hanzawa, S., Cenozoic Foraminifera of Micronesia. Mem. Geol. Soc. Amer., 66 (1957).

Hofker, J., The Foraminifera of the Siboga expedition. Part I, Tinoporidae, Rotaliidae, Nummulitidae, Amphisteginidae. Ed. Brill, Leiden (1927).

———, id., Part III, Ordo Dentata (1951*a*).

———, The Toothplate-Foraminifera. Arch. Néerl. Zoologie, 8, 353–373 (1951*b*).

———, Foraminifera from the Cretaceous of southern Limburg, Netherlands, I. *Lockhartia roestae* (Visser). Natuurh. Maandbl., 44, 4–5 (1955*a*).

———, id., XI. *Rotalia trochidiformis* (Lamarck). 119–121 (1955*b*).

———, Foraminifera of Santa Cruz and Thatch-Island, Virginia Archipelago, West Indies. Skr. Univ. Zool. Mus. Köbenhavn, 15 (1956).

———, Foraminiferen der Oberkreide von Nordwestdeutschland und Holland. Beih. Geol. Jahrb., 27 (1957*a*).

———, Foraminifera from the Cretaceous of southern Limburg, Netherlands, XXIV. The development of *Pararotalia tuberculifera* (Reuss). Natuurh. Maandbl., 46, 32–39 (1957*b*).

———, id., XXVI. *Globorotalia praetuberculifera* nov. sp.. 59–60 (1957*c*).

———, *Daviesina voigti* n.sp., eine gesteinsbildende Foraminifere aus dem Campan der subherzynen Kreidemulde. Mitt. Geol. Staatsinst. Hamburg, 27, 69–73 (1958*a*).

———, Supplément sur quelques Rotalidés. Verh. Kon. Belg. Inst. Natuurw., 142 (1958*b*).

———, Les Foraminifères des Craies tuffoïdes de Charente et Dordogne de l'Aquitaine, France du Sud-Ouest. 84. Congr. Soc. Sav., Dijon, 253–368 (1959).

Kaasschieter, J. P. H., The microfauna of the Aquitanian-Burdigalian of south-western France, part 3. Smaller Foraminifera. Verh. Kon. Ned. Ak. Wetensch., afd Natuurk., ser. 1, 21, no. 2 (1955).

———, Foraminifera of the Eocene of Belgium. Verh. Kon. Belg. Inst. Natuurw. (1960 or 1961, in press).

Küpper, K., Note on *Schlumbergerella* Hanzawa and related genera. Contrib. Cushman Found. Foram. Res., 5, 26–30 (1954).

Loeblich, A. R. and H. Tappan, Morphology and taxonomy of the foraminiferal genus *Pararotalia* Le Calvez, 1949. Smiths. Misc. Coll., 135, no. 2 (1957).

Magné, J. and J. Sigal, Résultats géologiques et micropaléontologiques du sondage d'El Krachem (Hauts Plateaux algérois). Description des espèces nouvelles, 1. Foraminifères. Bull. Soc. géol. France, ser. 6, 3, 480–489 (1953).

Marie, P., Sur *Laffitteina bibensis* et *Laffitteina Monodi*, nouveau genre et nouvelles espèces du Montien. id., ser. 5, 15, 419–434 (1945).

Nagappa, Y., Foraminiferal biostratigraphy of the Upper Cretaceous-Eocene succession in the India-Pakistan-Burma region. Micropaleont., **5**, 145–192 (1959*a*).

———, Note on *Operculinoides* Hanzawa, 1935. Paleont., **2**, 156–160 (1959*b*).

Papp, A., Biostratigraphische Ergebnisse in der Oberkreide und Bemerkungen über die Lagerung des Eozäns. Sitzungsber. Österr. Ak. Wiss., Math.-naturw. Kl., Abt. 1, **164**, 317–334 (1955).

———, Die morphologisch-genetische Entwicklung von Orbitoiden und ihre stratigraphische Bedeutung im Senon. Pal. Zeitschr., **30**, 45–49 (1956).

———, and K. Küpper, Foraminiferen aus dem Campan von Silberegg. Sitzungsber. Österr. Ak. Wiss., Math.-naturw. Kl., Abt. 1, **162**, 345–357(1953).

Reiss, Z., Occurrence and stratigraphic significance of *Cuvillierina eocenica* Debourle. Bull. Geol. Survey Israel, **10**, 1–12 (1957).

———, Classification of lamellar Foraminifera. Micropaleont., **4**, 51–70 (1958).

———, and P. Merling, Structure of some Rotaliidea. Bull. Geol. Survey Israel, **21** (1958).

Sachs, K. N., Restudy of some Cuban larger Foraminifera. Contrib. Cushman Found. Foram. Res., **8**, 106–120 (1957).

Smout, A. H., Lower Tertiary Foraminifera of the Qatar peninsula. Publ. Brit. Mus. Nat. Hist. (1954).

———, Reclassification of the Rotaliidea (Foraminifera) and two new Cretaceous forms resembling *Elphidium*. Jour. Wash. Ac. Sc., **45**, 201–210 (1955).

Umbgrove, J. H. F., Het genus *Pellatispira* in het indo-pacifische gebied. Wetensch. Meded. Dienst Mijnb. Ned.-Indië, **10** (1928).

———, *Heterospira*, a new foraminiferal genus from the Tertiary of Borneo. Leidsche Geol. Meded., **8**, 155–159 (1936).

Vaughan, T. W., American Paleocene and Eocene larger Foraminifera. Mem. Geol. Soc. Amer., **9**, part I (1945).

Vella, P., Upper Miocene to recent species of the genus *Notorotalia*. Pal. Bull. New Zeal. Geol. Survey, **28**, part 2 (1957).

Wade, M., Morphology and taxonomy of the foraminiferal family Elphidiidae. Jour. Wash. Ac. Sc., **47**, 330–339 (1957).

———, and A. N. Carter, The foraminiferal genus *Sherbornina* in southeastern Australia. Micropaleont., **3**, 155–164 (1957).

THE INFLUENCE OF SURFACE TENSION ON THE SURFACE WAVES INDUCED BY A ROLLING THIN STRIP

BY

J. A. SPARENBERG

(Communicated by Prof. W. P. A. VAN LAMMEREN at the meeting of Febr. 27, 1960)

Summary

The waves caused by a thin strip rolling on the surface of water are considered, making allowance for surface tension. There are two types of waves denoted as gravity waves and tension waves. The first type causes radiation of energy to infinity while the amplitude of the second one tends to zero, when the distance to the strip increases.

1. *Introduction*

In general surface tension is neglected when the motion of water induced by some moving body is considered. The influence of surface tension, however, becomes important when the forces or moments exerted by the surface tension and those exerted by the pressure of the water become of the same order of magnitude. This may happen when the rolling of ship models is studied, hence it is possible that surface tension is one of the important factors causing scale effects [1], [2].

On the water surface we consider a horizontal infinitely long strip of zero thickness and finite width which sometimes is called a dock. This strip performs a harmonic rolling motion and induces surface waves. The effect of the surface tension is the same as the influence of a membrane without mass spread over the fluid. The tension of the membrane represents the surface tension.

Here we arrive at a difficulty. Our theory cannot give information about the direct interaction of the edge of the dock and the boundary of the membrane. This interaction is a molecular one and depends on the materials used, for instance a dock of paraffin wax or a dock of wood induce a different behaviour of the water surface in the neighbourhood of their edges. We consider two different cases, first the movement of the boundary of the membrane is prescribed, second, the angle under which the membrane meets the strip is given as a function of time. For instance, the first case happens when the boundary of the membrane is fixed to the dock, the second case, when there is no direct interaction between dock and membrane, then the tangent to the membrane is horizontal.

There occur two types of waves with different lengths. One can be considered as a gravity wave while the other is caused by the surface tension. The main difference between the two types can be seen by approaching the limit of zero surface tension. Then the gravity waves change gradually into the ordinary gravity waves while the tension waves disappear. It will also be seen that the gravity waves give rise to radiation of energy towards infinity while the amplitude of the tension waves tends to zero when the distance to the strip increases.

There are two well known mathematical methods for solving this type of problems. The most straight forward one, uses a Green function which is constructed by applying a periodical δ function pressure to the free surface without a dock. Then an integral equation with this Green function as kernel can be written down, which states the conditions for the displacements on the rolling dock. The kernel has an oscillatory character which can yield difficulties for numerical calculations when the waves are short. For the determination of the Green function we need to introduce some artificial damping or to consider a transient problem in order to make Fourier transforms convergent.

The second method, which we apply in this paper, uses a simple type of sectionally holomorfic functions in the complex domain. Here we do not need damping or transient phenomenae while we arrive at an integro-differential equation with a monotomic kernel. It can be proved that this integro-differential equation does not possess eigenfunctions. These theoretical advantages, however, are obtained at the cost of some greater complexity of the analysis.

In a future paper we hope to discuss the application of the first method and to compare the suitability of both methods for numerical calculations.

2. *Formulation of the problem*

The water occupies the lower half space. We use a Carterian coordinate system $\bar{x}, \bar{y}, \bar{z}$ of which the origin lies in the undisturbed water surface while the $\bar{y}$ axis is perpendicular to it and points out of the water. The

Fig. 1. The strip on the water surface.

dock extends from $-l \leqslant \bar{x} \leqslant l$, $\bar{y} = 0$, $-\infty < \bar{z} < +\infty$ and makes a periodical rolling motion defined by

$$\bar{y}(\bar{x}, \bar{t}) = \alpha \bar{x} \sin \omega \bar{t}. \tag{2.1}$$

We now give a slightly different formulation of the problem which will be used throughout the rest of the paper.

On the whole surface of the water $|\bar{x}|<\infty$ a membrane is spread with tension $\bar{\tau}$. For $|\bar{x}|\leqslant l$ we may apply an external pressure, which compels the membrane for $|\bar{x}|<l$ to behave as a rigid dock performing a rolling motion (2.1).

The water motion is assumed to be irrotational, two dimensional and simply periodic, hence we can introduce the velocity potential:

$$\bar{\theta}(\bar{x},\bar{y},\bar{t})=\bar{\vartheta}_1(\bar{x},\bar{y})\cos\omega\bar{t}+\sum_{n=2}^{N}\bar{\vartheta}_n(\bar{x},\bar{y})(a_{1,n}\cos\omega\bar{t}+a_{2,n}\sin\omega\bar{t}). \tag{2.2}$$

The first term on the right hand side of (2.2) is some solution of the inhomogeneous problem with $\alpha\neq 0$. The second part of the right hand side is a solution of the homogeneous problem with $\alpha=0$. These functions are necessary for satisfying the radiation condition at infinity and conditions imposed on the behaviour of the membrane at $\bar{x}=\pm l$. The velocities $\bar{u}$ and $\bar{v}$ in the $\bar{x}$ and $\bar{y}$ direction are given by

$$\bar{u}=\frac{\partial\bar{\theta}}{\partial\bar{x}}\quad,\quad \bar{v}=\frac{\partial\bar{\theta}}{\partial\bar{y}}. \tag{2.3}$$

For completeness we mention the derivation of the linearised boundary condition for the free water surface with surface tension. This derivation may be found, for instance, in reference [3]. From the equation of Bernoulli we have

$$\bar{P}_i=-\varrho\frac{\partial\bar{\theta}}{\partial\bar{t}}-g\varrho\bar{y}, \tag{2.4}$$

where $\bar{P}_i$ is the pressure inside the fluid, ϱ the density and g the acceleration due to gravity. The surface tension $\bar{\tau}$ (water 0,072 gramm/cm) yields the following relation between the pressure just inside the fluid $\bar{P}_i$ and the external pressure $\bar{P}_u$ exerted at the surface,

$$\bar{P}_u=\bar{P}_i+\bar{\tau}\frac{\partial^2\bar{y}_s}{\partial\bar{x}^2}=-\varrho\frac{\partial\bar{\theta}}{\partial\bar{t}}-g\varrho\bar{y}_s+\bar{\tau}\frac{\partial^2\bar{y}_s}{\partial\bar{x}^2}, \tag{2.5}$$

where $\bar{y}_s$ is the elevation of the surface. Differentiation of (2.5) with respect to $\bar{t}$ yields

$$\frac{\partial\bar{P}_u}{\partial\bar{t}}-\omega^2\varrho\bar{\theta}-g\varrho\frac{\partial\bar{\theta}}{\partial\bar{y}}+\bar{\tau}\frac{\partial^3\bar{\theta}}{\partial\bar{x}^2\partial\bar{y}}. \tag{2.6}$$

When we put $\bar{P}_u\equiv 0$ we arrive at the following boundary value problem

$$\frac{\partial^2\bar{\theta}}{\partial\bar{x}^2}+\frac{\partial^2\bar{\theta}}{\partial\bar{y}^2}=0, \tag{2.7}$$

$$\frac{\partial\bar{\theta}}{\partial\bar{y}}=\alpha\bar{x}\omega\cos\omega\bar{t},\ |\bar{x}|<l;\ \omega^2\varrho\bar{\theta}-g\varrho\frac{\partial\bar{\theta}}{\partial\bar{y}}+\bar{\tau}\frac{\partial^3\bar{\theta}}{\partial\bar{x}^2\partial\bar{y}}=0,\ |\bar{x}|>l,\bar{y}=0. \tag{2.8}$$

We now introduce the dimensionless quantities

$$\begin{cases} x=\bar{x}l^{-1},\ y=\bar{y}l^{-1},\ t=\bar{t}\omega,\ y_s=\bar{y}_s l^{-1},\ \theta=\bar{\theta}\cdot(\omega l^2)^{-1},\ \vartheta_n=\bar{\vartheta}_n\cdot(\omega l^2)^{-1},\\ \qquad\qquad \nu=\omega^2 lg^{-1},\ \tau=\bar{\tau}(g\varrho l^2)^{-1},\ P_u=\bar{P}_u\cdot(lg\varrho)^{-1}. \end{cases} \tag{2.9}$$

With these notations we have the following boundary value problems for the functions $\vartheta_n(x, y)$

$$\frac{\partial^2 \vartheta_n}{\partial x^2} + \frac{\partial^2 \vartheta_n}{\partial y^2} = 0. \tag{2.10}$$

$$\begin{cases} \dfrac{\partial \vartheta_n}{\partial y} = \begin{matrix} \alpha x, & n=1 \\ 0, & n>1 \end{matrix}, |x|<1; \nu\vartheta_n - \dfrac{\partial \vartheta_n}{\partial y} + \tau \dfrac{\partial^3 \vartheta_n}{\partial x^2 \partial y} = 0, \\ \qquad\qquad n=1,2\ldots N, |x|>1; y=0. \end{cases} \tag{2.11}$$

We introduce the harmonic functions

$$\varphi_n = \nu\vartheta_n - \frac{\partial \vartheta_n}{\partial y} + \tau \frac{\partial^3 \vartheta_n}{\partial x^2 \partial y}, \tag{2.12}$$

which have to satisfy the boundary conditions

$$\begin{cases} \nu \dfrac{\partial \varphi_n}{\partial y} - \dfrac{\partial^2 \varphi_n}{\partial x^2} + \tau \dfrac{\partial^4 \varphi_n}{\partial x^4} = \begin{matrix} \alpha\nu^2 x, & n=1 \\ 0, & n>1 \end{matrix}, |x|<1; \varphi_n = 0, \\ \qquad\qquad n=1,2\ldots N, |x|>1; y=0. \end{cases} \tag{2.13}$$

Using these functions we find from (2.6) after integrating over t

$$P_u = \sum_{n=1}^{N} \varphi_n(x, 0)(a_{1,n} \sin t - a_{2,n} \cos t),\ a_{1,1}=1,\ a_{2,1}=0. \tag{2.14}$$

a formula which will be used later.

The complex conjugated functions $\psi_n(x, y)$ of $\varphi_n(x, y)$ are defined by

$$\varphi_n(x, y) + i\psi_n(x, y) = Q_n(x+iy) = Q_n(z). \tag{2.15}$$

$$\frac{\partial \varphi_n}{\partial x} = \frac{\partial \psi_n}{\partial y}\ ,\ \frac{\partial \varphi_n}{\partial y} = -\frac{\partial \psi_n}{\partial x}. \tag{2.16}$$

As the space variable $\bar{z}$ will not be used in the following paragraphs, it will not be confusing when the symbol z is made to denote the complex variable $x+iy$.

Using the functions ψ_n we obtain for (2.13) after an integration over x,

$$\begin{cases} \nu\psi_n + \dfrac{\partial \varphi_n}{\partial x} - \tau \dfrac{\partial^3 \varphi_n}{\partial x^3} = \begin{matrix} -\alpha\nu^2 x^2/2, & n=1 \\ 0, & n>1 \end{matrix}, |x|<1; \dfrac{\partial \psi_n}{\partial y} = 0. \\ \qquad\qquad n=1,2\ldots N, |x|>1; y=0. \end{cases} \tag{2.17}$$

The constant of integration is taken equal to zero which is allowed because by (2.16) ψ_n is defined within a constant.

This is the final formulation of the boundary value problem that we are going to consider. It remains to remark that at infinity the functions φ_n and ψ_n have to be bounded.

3. *The integro differential equation for* φ

From (2.15) we have

$$\frac{\partial \psi_n}{\partial y} = \operatorname{Im} iQ_n'(z). \tag{3.1}$$

As $\dfrac{\partial \psi_n}{\partial y} = \dfrac{\partial \varphi_n}{\partial x} = 0$, $|x|>1$, $y=0$ it follows

$$iQ_{n+}'(x) - iQ_{n-}'(x) = -2i\frac{\partial \psi_n}{\partial y} = -2i\frac{\partial \varphi_n}{\partial x},\ |x|<1,\ y=0, \tag{3.2}$$

where Q_{n+}' and Q_{n-}' denote the limiting values of Q_n' when $y \to 0$ through positive respectively negative values of y. Hence [4]

$$Q_n'(z) = \frac{i}{\pi} \int_{-1}^{+1} \frac{\frac{\partial \varphi_n}{\partial x}(\xi)}{(\xi - z)} d\xi + i \sum_{m=1}^{M} \frac{A_m}{(1-z)^m} + i \sum_{m=1}^{M} \frac{B}{(1+z)^m}, \tag{3.3}$$

A_m and B_m are unknown constants which are real because $\operatorname{Im} iQ_n'(z) = 0$, $|x| > 1$, $y = 0$. It will be shown that for satisfying all our conditions at $x = \pm 1$ and the radiation condition at infinity, we need A_m and B_m with $m = 1$, 2 and 3. When in a function of the two variables x and y only x is mentioned it means that $y = 0$.

Integration of (3.3) with $M = 3$ yields

$$\begin{aligned} Q_n(z) = &-\frac{i}{\pi} \int_{-1}^{-1} \frac{\partial \varphi_n}{\partial x}(\xi) \ln (\xi - z)\, d\xi - iA_1 \ln (1-z) + iB_1 \ln (1+z) + \\ &+ \frac{iA_2}{(1-z)} - \frac{iB_2}{(1+z)} + \frac{iA_3}{2(1-z)^2} - \frac{iB_3}{2(1+z)^2} + C_1. \end{aligned} \tag{3.4}$$

By (2.14) we find

$$\begin{aligned} \varphi_n(x,y) = \operatorname{Re} Q_n(z) = &\frac{1}{\pi} \int_{-1}^{+1} \frac{\partial \varphi}{\partial x}(\xi)\, \chi(\xi, x, y)\, d\xi + A_1 \chi_1(x,y) + \\ &- B_1 \chi_2(x,y) - \frac{A_2 y}{(1-x)^2 + y^2} - \frac{B_2 y}{(1+x)^2 + y^2} - \frac{A_3 y (1-x)}{\{(1-x)^2 + y^2\}^2} + \\ &- \frac{B_3 y (1+x)}{\{(1+x)^2 + y^2\}^2} + C_2. \end{aligned} \tag{3.5}$$

$$\begin{aligned} \psi_n(x,y) = \operatorname{Im} Q_n(z) = \\ -\frac{1}{2\pi} \int_{-1}^{+1} \frac{\partial \varphi}{\partial x}(\xi) \ln \{(\xi - x)^2 + y^2\}\, d\xi - \frac{A_1}{2} \ln \{(1-x)^2 + y^2\} + \\ + \frac{B_1}{2} \ln \{(1+x)^2 + y^2\} + \frac{A_2 (1-x)}{(1-x)^2 + y^2} - \frac{B_2 (1+x)}{(1+x)^2 + y^2} + \frac{A_3 \{(1-x)^2 - y^2\}}{2\{(1-x)^2 + y^2\}^2} + \\ - \frac{B_3 \{(1+x)^2 - y^2\}}{2\{(1+x)^2 + y^2\}^2} + C_3, \end{aligned} \tag{3.6}$$

where C_2 and C_3 are the real and imaginary parts of C_1 and the angles $\chi \geqslant 0$, $\chi_1 \geqslant 0$ and $\chi_2 \leqslant 0$ are denoted in fig. 2. Because the functions ψ_n are even with respect to x we have $A_m = -B_m$.

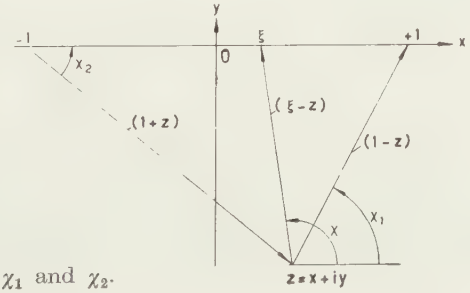

Fig. 2.
The angles χ, χ_1 and χ_2.

The formulae (3.5) and (3.6) are valid for each pair of conjugated functions φ_n and ψ_n when $\frac{\partial \varphi_n}{\partial x} = \frac{\partial \psi_n}{\partial y} = 0$ for $|x|>1$, $y=0$. However, the first equation in (2.17) yields a relation between φ_n and ψ_n in our case. Combining (2.17) and (3.6) we obtain for $|x|<1$, $y=0$,

$$\begin{aligned} & \frac{\partial \varphi_n(x)}{\partial x} - \tau \frac{\partial^3 \varphi_n(x)}{\partial x^3} - \\ & = \frac{\nu}{\pi} \int_{-1}^{1} \frac{\partial \varphi_n}{\partial x}(\xi) \ln |\xi - x| \, d\xi + \nu A_1 \ln (1-x) + \nu A_1 \ln (1+x) + \\ & - \frac{\nu A_2}{(1-x)} - \frac{\nu A_2}{(1+x)} - \frac{\nu A_3}{2(1-x)^2} - \frac{\nu A_3}{2(1+x)^2} - \nu C_3 \begin{cases} -\frac{\tau^2}{2} \cdot 3x^2 & n=1 \\ +0 & , n>1 \end{cases} \end{aligned} \tag{3.7}$$

where to each value of n we choose specific values of A_m, as will be discussed in para. 4.

This integro differential equation is the basis for our further investigations. A solution is defined when for instance the values of $\frac{\partial \varphi_n}{\partial x}(x)$, are prescribed for $x = \pm 1$.

In addition we shall use, in the next paragraph, the condition that

$$\int_{-1}^{1} \frac{\partial \varphi_n}{\partial x}(\xi) \, d\xi \tag{3.8}$$

must have some prescribed value. In order to be sure of the uniqueness of the solutions of the special cases of (3.7) we prove the following property.

When $\nu > 0$ and $\tau > 0$, for which regions these parameters have physical meaning, the equation

$$f(x) - \tau \frac{d^2}{dx^2} f(x) = \frac{\nu}{\pi} \int_{-1}^{+1} f(\xi) \ln |\xi - x| \, d\xi + C, \tag{3.9}$$

under the conditions

$$\int_{-1}^{+1} f(x) \, dx = 0 \ , \ f(\pm 1) = 0, \tag{3.10}$$

possesses the zero solution only.

This can be shown as follows. Multiply both sides of the integral equation in (3.9) by $f(x)$ and integrate over x, we find

$$\int_{-1}^{+1} f(x)^2 \, dx + \tau \int_{-1}^{+1} \left(\frac{d}{dx} f(x) \right)^2 dx = \frac{\nu}{\pi} \int_{-1}^{+1} \int_{-1}^{+1} f(\xi) f(x) \ln |\xi - x| \, d\xi \, dx. \tag{3.11}$$

The double integral is negative definite [5] hence the right hand side is negative definite while the left hand side is positive definite. The only possibility is $f(x) \equiv 0$.

4. *Discussion of the solutions of the integro-differential equation*

First we consider the solution $\frac{\partial \varphi_1}{\partial x}$ of (3.17) with $A_n = 0$,

$$(4.1)\quad \frac{\partial \varphi_1}{\partial x}(x) - \tau \frac{\partial^3 \varphi_1(x)}{\partial x^3} = \frac{\nu}{\pi} \int_{-1}^{+1} \frac{\partial \varphi_1}{\partial x}(\xi) \ln |\xi - x| \, d\xi - \frac{\alpha \nu^2}{2} x^2 - \nu C_{3,1}; \frac{\partial \varphi_1}{\partial x}(\pm 1) = 0.$$

The second index attached to C_3 denotes the function $\frac{\partial \varphi_1}{\partial x}$ to which this C_3 belongs, generally $C_{n,m}$ is the C_n which belongs to $\frac{\partial \varphi_m}{\partial x}$. Because we have $\varphi_1(x, 0) = 0$ for $x < -1$ we have by (3.5) and fig. 2, $C_{2,1} = 0$,

$$(4\ 2)\qquad \varphi_1(x, y) = \frac{1}{\pi} \int_{-1}^{-1} \frac{\partial \varphi_1}{\partial x}(\xi) \, \chi(\xi, x, y) \, d\xi.$$

Also we have the condition $\varphi_1(x, 0) = 0$, $x > 1$, hence we require

$$(4.3)\qquad \int_{-1}^{-1} \frac{\partial \varphi_1}{\partial x}(x) \, dx = 0.$$

This prescribes the constant $C_{3,1}$. The function $\psi_1(x, y)$ is determined by (3.6)

$$(4.4)\qquad \psi_1(x, y) = -\frac{1}{2\pi} \int_{-1}^{-1} \frac{\partial \varphi_1}{\partial x}(\xi) \ln \{(\xi - x)^2 + y^2\} \, d\xi + C_{3,1}.$$

By analogous reasoning we can determine four other independent solutions of (3.7). Systematically the functions $\frac{\partial \varphi_n}{\partial x}(x)$ are defined as follows

$$(4.5)\quad \begin{cases} \frac{\partial \varphi_1}{\partial x}(x);\ A_n = 0 & ;\ \frac{\partial \varphi_1}{\partial x}(\pm 1) = 0;\ C_{2,1} = 0;\ C_{3,1} \text{ from } \int_{-1}^{+1} \frac{\partial \varphi_1}{\partial x}(x) \, dx = 0, \\ \frac{\partial \varphi_2}{\partial x}(x);\ A_n = 0 & ;\ \frac{\partial \varphi_2}{\partial x}(\pm 1) = 1;\ C_{2,2} = 0;\ C_{3,2} \quad ,, \quad \int_{-1}^{+1} \frac{\partial \varphi_2}{\partial x}(x) \, dx = 0, \\ \frac{\partial \varphi_3}{\partial x}(x);\ A_1 = 1, A_2 = A_3 = 0;\ \frac{\partial \varphi_3}{\partial x}(\pm 1) = 0;\ C_{2,3} = \pi;\ C_{3,3} \quad ,, \quad \int_{-1}^{+1} \frac{\partial \varphi_3}{\partial x}(x) \, dx = -2\pi, \\ \frac{\partial \varphi_4}{\partial x}(x);\ A_2 = 1, A_1 = A_3 = 0;\ \frac{\partial \varphi_4}{\partial x}(\pm 1) = 0;\ C_{2,4} = 0;\ C_{3,4} \quad ,, \quad \int_{-1}^{+1} \frac{\partial \varphi_4}{\partial x}(x) \, dx = 0, \\ \frac{\partial \varphi_5}{\partial x}(x);\ A_3 = 1, A_1 = A_2 = 0;\ \frac{\partial \varphi_5}{\partial x}(\pm 1) = 0;\ C_{2,5} = 0;\ C_{3,5} \quad ,, \quad \int_{-1}^{+1} \frac{\partial \varphi_5}{\partial x}(x) \, dx = 0. \end{cases}$$

The uniqueness of the $\frac{\partial \varphi_n}{\partial x}(x)$, $n = 1, \ldots, 5$, which shall have to be determined by numerical means, follows from the end of para. 3. In the following we assume the φ_n and ψ_n to be known. It is clear that there are no more independent solutions.

Some characteristic properties of $\varphi_4(x, y)$ and $\varphi_5(x, y)$ are the following. When $x \to \pm 1$ and $y \to 0$ the function $\varphi_4(x, y)$ becomes infinite in such a way that for $y = 0$ it behaves as a δ function of Dirac. Because the functions $\varphi_n(x, y)$ are by (2.14) directly related to the external pressure P_u it follows that $\varphi_4(x, y)$ gives rise to singular external forces at $x = \pm 1$, $y = 0$. These forces cause discontinuities of the first derivative at $x = \pm 1$ of the elevation of the membrane.

At $x = \pm 1$, $y = 0$ the function $\varphi_5(x, y)$ possesses also a singularity which, however; is of a stronger type than the δ function of $\varphi_4(x, y)$, it corresponds to a singular moment. By this it is possible that the elevation of the membrane possesses a jump discontinuity at $x = \pm 1$.

5. *The determination of the velocity potential* ϑ_n

We discuss the calculation of ϑ_n from the functions φ_n. From equation (2.12) we have

$$\nu\vartheta_n - \frac{\partial \vartheta_n}{\partial \eta} + \tau \frac{\partial^3 \vartheta_n}{\partial x^2 \partial \eta} = \varphi_n. \tag{5.1}$$

This partial differential equation can easily be written in the form of an ordinary differential equation in the complex domain. Introducing

$$\vartheta_n(x, y) = \operatorname{Re} F_n(z); \quad \frac{\partial \vartheta_n}{\partial y}(x, y) = \operatorname{Re} i F_n'(z); \quad \frac{\partial^3 \vartheta_n}{\partial x^2 \partial y}(x, y) = \operatorname{Re} i F_n'''(z). \tag{5.2}$$

we can write (5.1) in the form

$$\nu F_n(z) - i F_n'(z) - i\tau F_n'''(z) = Q_n(z). \tag{5.3}$$

We may add an arbitrary imaginary constant to the right hand side of (5.3). This has as influence that the same constant must be added to the solution $F_n(z)$, hence by (5.2) ϑ_n does not change.

The general solution of (5.3) is

$$F_n(z) = \frac{i}{\tau} \int_0^z Q_n(\zeta) \left\{ \frac{e^{\lambda_1(z-\zeta)}}{(\lambda_1 - \lambda_2)(\lambda_1 - \lambda_3)} + \frac{e^{\lambda_2(z-\zeta)}}{(\lambda_2 - \lambda_3)(\lambda_2 - \lambda_1)} + \frac{e^{\lambda_3(z-\zeta)}}{(\lambda_3 - \lambda_1)(\lambda_3 - \lambda_2)} \right\} d\zeta + \sum_{m=1}^{3} E_{m,n} e^{\lambda_m z}, \tag{5.4}$$

where the $E_{m,n}$ are arbitrary complex constants and the λ_m are roots of

$$\nu - i\lambda + i\tau\lambda^3 = 0. \tag{5.5}$$

The λ_m can be written as

$$\lambda_1 = -i\beta_1; \quad \lambda_2 = \alpha_2 + i\beta_2; \quad \lambda_3 = -\alpha_2 + i\beta_2, \tag{5.6}$$

the α_n and β_n are real and without loss of generality we may assume $\alpha_2 > 0$. When the surface tension becomes zero we have $\lambda_1 = -i\nu$, hence λ_1 represents waves which can be looked upon as gravity waves. The waves which belong to λ_2 and λ_3 are caused by the surface tension and will be called tension waves.

To equation (5.5) we can apply the Nyquist criterium based on the

Cauchy principle [6] which gives information about the number of roots and poles of a function in a prescribed region. We find for $\nu > 0$ and $\tau > 0$

$$\beta_1 > 0, \quad \beta_2 > 0. \tag{5.7}$$

When τ is sufficiently small, which happens in general for ship models on water, the roots (5.6) can be written approximately as

$$\lambda_1 = -i\nu \; ; \; \lambda_{\frac{2}{3}} \approx \pm \tau^{-\frac{1}{2}} + \frac{i\nu}{2} + O(\tau^{\frac{1}{2}}). \tag{5.8}$$

This means that in this case the wave length of the tension waves is twice the wave length of the gravity waves.

The part of (5.4) with the exponent λ, z remains bounded at infinity, hence we first turn our attention to $E_{2,n}$ and $E_{3,n}$. We have two regions I and II (fig. 3) in which respectively Re $\lambda_2 z > 0$ and Re $\lambda_3 z > 0$. When

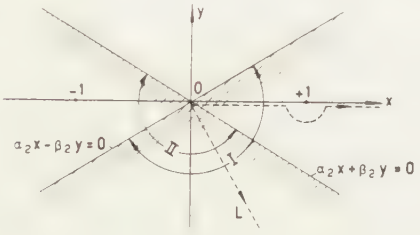

Fig. 3. The regions of exponentially increase.

the point z moves along a radius towards infinity within the region of overlapping of I and II we have to choose

$$E_{2,n} = -\frac{i}{\tau}\int_L \frac{e^{-\lambda_3\zeta}}{(\lambda_2-\lambda_3)(\lambda_1-\lambda_2)} Q_n(\zeta)\,d\zeta; \quad E_{3,n} = -\frac{i}{\tau}\int_L \frac{e^{-\lambda_2\zeta}}{(\lambda_3-\lambda_1)(\lambda_2-\lambda_3)} Q_n(\zeta)\,d\zeta, \tag{5.9}$$

where L denotes the path of integration.

The integrands in (5.9) are exponentially decreasing analytic functions hence it does not matter where we take the lines of integration within the corresponding regions I or II. When we choose the negative y axis which is in both regions, we find

$$E_{2,n} = -\bar{E}_{3,n}. \tag{5.10}$$

Hence we have to calculate one quantity only, for instance $E_{2,n}$. For this we take the positive x-axis, with an indentation at $x = 1$ in view of the singularities of $Q_4(z)$ and $Q_5(z)$, as the line of integration (fig. (3)). We introduce the notation

$$\begin{cases} (\lambda_1-\lambda_2)(\lambda_3-\lambda_1) = p_1; \quad (\lambda_2-\lambda_3)(\lambda_1-\lambda_2) = p_2 + iq_2; \\ \qquad\qquad\qquad\qquad\qquad\qquad (\lambda_3-\lambda_1)(\lambda_2-\lambda_3) = p_2 - iq_2. \end{cases} \tag{5.11}$$

Herewith we obtain

$$\begin{cases} E_{2,n} = -\bar{E}_{3,n} = \\ \quad = \dfrac{1}{\tau(p_2^2+q_2^2)} \displaystyle\int_0^\infty e^{-\alpha_2\xi}[\{-q_2\varphi_n(\xi) + p_2\psi_n(\xi)\}(\cos\beta_2\xi - i\,\sin\beta_2\xi) + \\ \quad -i\{p_2\varphi_n(\xi) + q_2\psi_n(\xi)\}(\cos\beta_2\xi - i\,\sin\beta_2\xi)]\,d\xi, \qquad n = 1, 2, 3. \end{cases} \tag{5.12}$$

The function $Q_4(z)$ possesses a pole at $z=1$ (3.4), (4.5), hence we have a contribution from the small semicircle around $z=1$

$$
\begin{aligned}
E_{2,3} &= -\bar{E}_{3,4} = \\
&\frac{1}{\tau(p_2^2+q_2^2)} \oint_0^{\sim} e^{-\alpha_2\xi}\left[\{-q_2\varphi_4(\xi)+p_2\psi_4(\xi)\}(\cos\beta_2\xi - i\sin\beta_2\xi) + \right. \\
&\left. i\{p_2\varphi_4(\xi)+q_2\psi_4(\xi)\}(\cos\beta_2\xi - i\sin\beta_2\xi)\right] d\xi \\
&- \frac{\pi e^{-\alpha_2}}{\tau(p_2^2+q_2^2)}\{(q_2\cos\beta_2 + p_2\sin\beta_2) + i(p_2\cos\beta_2 - q_2\sin\beta_2)\}.
\end{aligned} \tag{5.13}
$$

From the function $Q_5(z)$ we have to subtract the non integrable part, which follows from (3.4), (4.5) and we have a contribution of a pole at $z=1$,

$$
\begin{aligned}
E_{2,5} &= -\bar{E}_{3,5} = \\
&\frac{1}{\tau(p_2^2+q_2^2)} \oint_0^{\sim} e^{-\alpha_2\xi}\left[\{-q_2\varphi_5(\xi) - p_2\psi_5(\xi)\}(\cos\beta_2\xi - i\sin\beta_2\xi) - \right. \\
&- i\{p_2\varphi_5(\xi) + q_2\psi_5(\xi)\}(\cos\beta_2\xi - i\sin\beta_2\xi) + \\
&\left. - \frac{e^{-\alpha_2}}{2(1-\xi^2)}\{(p_2\cos\beta_2 - q_2\sin\beta_2) - i(q_2\cos\beta_2 + p_2\sin\beta_2)\}\right] d\xi + \\
&- \frac{e^{-\alpha_2}}{2\tau(p_2^2+q_2^2)}\{(p_2\cos\beta_2 - q_2\sin\beta_2)(1-\pi\beta_2 + i\pi\alpha_2) + \\
&\qquad + (q_2\cos\beta_2 + p_2\sin\beta_2)(\pi\alpha_2 - i + i\pi\beta_2)\}.
\end{aligned} \tag{5.14}
$$

The singular behaviour of $\vartheta_n(x, y)$ for $(x, y) \to (1, 0)$ follows from (5.4). We have the following relations

$$
\frac{\lambda_1^l}{(\lambda_1-\lambda_2)(\lambda_3-\lambda_1)} + \frac{\lambda_2^l}{(\lambda_2-\lambda_3)(\lambda_1-\lambda_2)} + \frac{\lambda_3^l}{(\lambda_3-\lambda_1)(\lambda_2-\lambda_3)} = \begin{matrix} 0 & l=0,1 \\ -1 & , l=2 \end{matrix} \tag{5.15}
$$

the cases $l>2$ can be reduced to (5.15) by the use (5.5). When $(z-\zeta)$ is sufficiently small we can expand the integrand in (5.4) and using (5.15) we find

$$
Q_n(\zeta)\{-\tfrac{1}{2}(z-\zeta)^2 + O(z-\zeta)^3\}. \tag{5.16}
$$

It follows that for $n=5$, in which case $Q_n(\zeta)$ possesses the strongest singularity, which is of the order $(1-\zeta)^{-2}$, the function $F_5(z)$ behaves as follows

$$
\lim_{z\to 1} F_5(z) \approx \text{const} + O((1-z)\ln(1-z)). \tag{5.17}
$$

From (5.17) we find that the derivatives of $\vartheta_5(x, y)$ and hence the velocities of the water in the neighbourhood of the points $x=\pm 1$, $y=0$ become infinite of logarithmic order. This is physically admissible because then there are no sinks or sources at these points.

It can be proved that we have more than boundedness of the sum of

the four terms in (5.4) with λ_2 and λ_3 in the exponent and that this sum tends to zero for $|z| \to \infty$. For $n = 1, 2, 3$ we find

$$(5.18)\quad \begin{cases} \lim\limits_{x \to +\infty} \vartheta_n(x, 0) = \\ \operatorname{Re} \lim\limits_{x \to +\infty} F_n(x) = \lim\limits_{x \to +\infty} \operatorname{Re}\Big[\dfrac{i}{p_1 \tau} \displaystyle\int_0^x Q_n(\xi)\, e^{\lambda_1 (x-\xi)}\, d\xi + E_{1,n}\, e^{\lambda_1 x}\Big], \quad n = 1, 2, 3. \end{cases}$$

When we put $E_{1,n} = T_{1,n} + i T_{2,n}$ it follows from ϑ_n and φ_n being odd functions and ψ_n being even with respect to x that $T_{1,n} = 0$. Hence we have

$$(5.19)\quad \begin{cases} \lim\limits_{x \to -\infty} \vartheta_n(x, 0) \\ \qquad - \dfrac{\cos \beta_1 x}{\tau p_1}\Big[\displaystyle\int_0^\infty \{\varphi_n(\xi, 0) \sin \beta_1 \xi + (\psi_n(\xi, 0) - C_{3,n}) \cos \beta_1 \xi\}\, d\xi\Big] + \\ \qquad + \dfrac{\sin \beta_1 x}{\tau p_1}\Big[\displaystyle\int_0^\infty \{\varphi_n(\xi, 0) \cos \beta_1 \xi - (\psi_n(\xi, 0) - C_{3,n}) \sin \beta_1 \xi\}\, d\xi + \\ - \dfrac{C_{3,n}}{\beta_1} + T_{2,n} \tau p_1\Big] = k_{1,n} \cos \beta_1 x + (k_{2,n} + T_{2,n}) \sin \beta_1 x, \qquad n = 1, 2, 3. \end{cases}$$

where we have introduced the abbreviations $k_{1,n}$ and $k_{2,n}$ and have subtracted from $\psi_n(\xi, 0)$ its asymptotical value $C_{3,n}$ in order to obtain convergent integrals.

For the functions $\vartheta_4(x, 0)$ and $\vartheta_5(x, 0)$ we find, when we take care of the singularities at $x = 1$, $y = 0$ the following

$$(5.20)\quad \begin{cases} \lim\limits_{x \to +\infty} \vartheta_4(x, 0) - \\ - \dfrac{\cos \beta_1 x}{\tau p_1}\Big[\oint\limits_0^\infty \{\varphi_4(\xi, 0) \sin \beta_1 \xi + (\psi_4(\xi, 0) - C_{3,4}) \cos \beta_1 \xi\}\, d\xi + \pi \sin \beta_1\Big] + \\ \qquad + \dfrac{\sin \beta_1 x}{\tau p_1}\Big[\oint\limits_0^\infty \{+\varphi_4(\xi, 0) \cos \beta_1 \xi - (\psi_4(\xi) - C_{3,4}) \sin \beta_1 \xi\}\, d\xi + \\ \qquad - \dfrac{C_{3,4}}{\beta_1} + \pi \cos \beta_1 + T_{2,4} \tau p_1\Big] = k_{1,4} \cos \beta_1 x + (k_{2,4} + T_{2,4}) \sin \beta_1 x, \end{cases}$$

$$(5.21)\quad \begin{cases} \lim\limits_{x \to -\infty} \vartheta_5(x, 0) - \\ - \dfrac{\cos \beta_1 x}{\tau p_1}\Big[\oint\limits_0^\infty \Big\{\varphi_5(\xi, 0) \sin \beta_1 \xi + (\psi_5(\xi, 0) - C_{3,5}) \cos \beta_1 \xi - \dfrac{\cos \beta_1}{2(1-\xi)^2}\Big\}\, d\xi + \\ \qquad - \Big(\dfrac{\pi \beta_1}{2} + \dfrac{1}{2}\Big) \cos \beta_1\Big] + \dfrac{\sin \beta_1 x}{\tau p_1}\Big[\oint\limits_0^\infty \Big\{\varphi_5(\xi, 0) \cos \beta_1 \xi + \\ \qquad - (\psi_5(\xi, 0) - C_{3,5}) \sin \beta_1 \xi + \dfrac{\sin \beta_1}{2(1-\xi)^2}\Big\}\, d\xi + \Big(\dfrac{\pi \beta_1}{2} + \dfrac{1}{2}\Big) \sin \beta_1 - \dfrac{C_{3,5}}{\beta_1} + \\ \qquad + T_{2,5} \tau p_1\Big] = k_{1,5} \cos \beta_1 x + (k_{2,5} + T_{2,5}) \sin \beta_1 x. \end{cases}$$

For the time dependent velocity potential (2.2) we obtain

$$
\begin{aligned}
(5.22)\quad \lim_{x\to\infty} \vartheta_n(x,0)(a_{1,n}\cos t + a_{2,n}\sin t) = \\
= \tfrac{1}{2}\{a_{1,n}k_{1,n} - a_{2,n}(k_{2,n}-T_{2,n})\}\cos(\beta_1 x + t) + \\
+ \tfrac{1}{2}\{a_{1,n}k_{1,n} + a_{2,n}(k_{2,n}+T_{2,n})\}\cos(\beta_1 x - t) + \\
+ \tfrac{1}{2}\{a_{1,n}(k_{2,n}+T_{2,n}) + a_{2,n}k_{1,n}\}\sin(\beta_1 x - t) + \\
- \tfrac{1}{2}\{a_{1,n}(k_{2,n}+T_{2,n}\} - a_{2,n}k_{1,n}\}\sin(\beta_1 x - t).
\end{aligned}
$$

The first and the third term of (5.22) represent waves which come in from infinity, the second and fourth term represent waves travelling towards infinity.

From above considerations it follows that only the gravity waves can reach infinity and radiate energy, the tension waves die out.

6. *Determination of the constants and the solution of the problem*

We now investigate which boundary conditions are satisfied by

$$
(6.1)\qquad \theta(x,y,t) = \sum_{n=1}^{5} \vartheta_n(x,y)(a_{1,n}\cos t + a_{2,n}\sin t),
$$

where $a_{1,1}=1$ and $a_{2,n}=0$. We first determine the number of unknown constants in $\theta(x,y,t)$. By (5.4) we see that each $\vartheta_n(x,y)$ can be written in the form

$$
(6.2)\qquad \vartheta_n(x,y) = \vartheta_n^*(x,y) + \operatorname{Re} E_{1,n}e^{\lambda_1 z} = \vartheta_n^*(x,y) - T_{2,n}\sin\beta_1 x\, e^{\beta_1 y}.
$$

Hence instead of (6.1) we have

$$
\begin{aligned}
(6.4)\quad \theta(x,y,t) = \sum_{n=1}^{5} \vartheta_n^*(x,y)(a_{1,n}\cos t + a_{2,n}\sin t) \\
+ e^{\beta_1 y}\sin\beta_1 x(\gamma_1\cos t + \gamma_2\sin t).
\end{aligned}
$$

$$
\gamma_1 = \sum_{n=1}^{5} a_{1,n}T_{2,n}\ ,\quad \gamma_2 = \sum_{n=1}^{5} a_{2,n}T_{2,n}.
$$

From this it follows that we have ten unknown constants γ_1, γ_2, $a_{1,n}$ and $a_{2,n}$, $n=2,\ldots,5$.

From (2.8) we find that $\theta(x,y,t)$ has to satisfy

$$
(6.5)\qquad \frac{\partial\theta}{\partial y} = \alpha x\cos t,\ |x|<1;\ \nu\theta - \frac{\partial\theta}{\partial y} + \tau\frac{\partial^3\theta}{\partial x^2\partial y} = 0;\ |x|>1;\ y=0.
$$

First it may be remarked that the condition of boundedness of $\theta(x,y,t)$ for $(x,y)\to\infty$ is satisfied. This follows from the way in which the constants $E_{2,n}$ and $E_{3,n}$ were determined. By equation (5.1), from which the functions ϑ_n were determined, we see that the second condition of (6.5) is satisfied, because $\varphi_n(x,y)$ is zero for $|x|>1$, $v=0$. It remains to consider the first condition in (6.5).

The only thing we know is that ϑ_n is related to φ_n by (5.1) and that

φ_n satisfies the first boundary condition in (2.13). This means that certainly

$$\nu^2\frac{\partial\theta}{\partial y}+\frac{\partial^3\theta}{\partial x^2\partial y}-2\tau\frac{\partial^5\theta}{\partial x^4\partial y}+\tau^2\frac{\partial^7\theta}{\partial x^6\partial y}=\alpha\nu^2 x\cos t,\ |x|<1;\ y=0. \tag{6.6}$$

This is an ordinary linear differential equation for $\frac{\partial\theta}{\partial y}$ when $y=0$. In order that the first condition of (6.5) is satisfied we have to demand

$$\left.\begin{aligned}&\frac{\partial\theta}{\partial y}(0,0,t)=0,\ \frac{\partial^2\theta}{\partial x\partial y}(0,0,t)=\alpha\cos t,\\ &\frac{\partial^3\theta}{\partial x^2\partial y}(0,0,t)=\frac{\partial^4\theta}{\partial x^3\partial y}(0,0,t)=\frac{\partial^5\theta}{\partial x^4\partial y}(0,0,t)=\frac{\partial^6\theta}{\partial x^5\partial y}(0,0,t)=0.\end{aligned}\right\} \tag{6.7}$$

However, the $\vartheta_n(x, y)$ are constructed as odd functions of x. This means that we only have to require

$$\frac{\partial^2\theta}{\partial x\partial y}(0,0,t)=\alpha\cos t,\ \frac{\partial^4\theta}{\partial x^3\partial y}(0,0,t)=\frac{\partial^6\theta}{\partial x^5\partial y}(0,0,t)=0. \tag{6.8}$$

As (6, 8) holds for all values of t these three conditions yield six equations separately for the cosine and sine coefficients. In addition the radiation condition at infinity must be satisfied, which states that the coefficients of the incoming waves $\sin(\beta_1 x+t)$ and $\cos(\beta_1 x+t)$ are zero. Together we have eight conditions for the ten unknown constants in (6.1).

These eight equations can be written in simple forms. In order to determine the three derivatives in (6.8) we first consider the corresponding derivatives of the functions $\vartheta_n(x, y)$. These can be calculated from (5.4) by means of

$$\frac{\partial^m}{\partial x^{m-1}\partial y}\vartheta_n=\operatorname{Re} iF_n^{(m)}(z). \tag{6.9}$$

For this calculation the relations (5.15) are useful. After some reductions we can write the equations (6.8) in the following form

$$\sum_{n=1}^{5}a_{\substack{1,n\\2}}\Big\{\operatorname{Re} i\sum_{m=2}^{3}E_{m,n}\lambda_m^2\Big\}+\gamma_{\substack{1\\2}}\beta_1^2=\begin{matrix}\alpha\\0\end{matrix}, \tag{6.10}$$

$$\sum_{n=1}^{5}a_{\substack{1,n\\2}}\Big\{-\operatorname{Re}\nu\sum_{m=2}^{3}E_{m,n}\lambda_m+\frac{\partial\varphi_n}{\partial x}(0)\Big\}-\gamma_{\substack{1\\2}}\nu\beta_1=\begin{matrix}-\alpha\\0\end{matrix}, \tag{6.11}$$

$$\sum_{n=1}^{5}a_{\substack{1,n\\2}}\Big\{\operatorname{Re} i\nu^2\sum_{m=2}^{3}E_{m,n}\Big\}-\gamma_{\substack{1\\2}}\nu^2=\begin{matrix}-\alpha\\0\end{matrix}. \tag{6.12}$$

The radiation conditions are easily formulated by means of (5.22), we obtain

$$\sum_{n=1}^{5}\{a_{1,n}k_{1,n}-a_{2,n}k_{2,n}\}-\gamma_2=0, \tag{6.13}$$

$$\sum_{n=1}^{5}\{a_{1,n}k_{2,n}+a_{2,n}k_{1,n}\}+\gamma_1=0. \tag{6.14}$$

We have still to find two more conditions. These come, as has been said in the introduction, from the prescription of the displacement $h(t)$ of the membrane or of its tangent $s(t)$ for $x \to 1$ from the right hand side (fig. 4). To find these two conditions we have to consider the elevation of the surface.

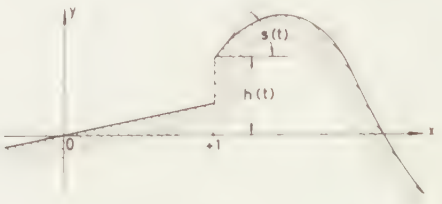

Fig. 4. The motion of the membrane in the neighbourhood of $x = +1$, $y = 0$.

From (2.5) when we introduce dimensionless coordinates we obtain

$$-y_s+\tau\frac{d^2y_s}{dx^2}=\nu\frac{\partial\theta}{\partial t}+P_u. \tag{6.15}$$

First we consider the case that the jump discontinuity Δ_1 of the membrane at $x=1$ is given. When $h(t)$ is given in the form

$$h(t)=\alpha_1\cos t+\alpha_2\sin t, \tag{6.16}$$

we obtain

$$\Delta_1=+\alpha_1\cos t-(\alpha_2-\alpha)\sin t. \tag{6.17}$$

This discontinuity is connected uniquely to the magnitude of the singular moment of the external pressure P_u. From the boundedness of y_s and $\frac{\partial\theta}{\partial t}$ at $x=1$, we find from (2.14), (3.5) by equating the derivatives of the δ functions at both sides of (6.15)

$$\left.\begin{aligned}&\tau\{+\alpha_1\cos t+(\alpha_2-\alpha)\sin t\}\frac{d}{dx}\delta(1-x)=\\&\qquad=(a_{1,5}\sin t-a_{2,5}\cos t)\frac{\pi}{2}\frac{d}{dx}\delta(1-x)\end{aligned}\right\} \tag{6.18}$$

or

$$a_{1,5}=\frac{2}{\pi}\tau(\alpha_2-\alpha)\ ,\ a_{2,5}=-\frac{2}{\pi}\tau\alpha_1. \tag{6.19}$$

Hence we have found two more equations and the problem is determined.

Next we consider the case that the right hand side derivative of the membrane at $x=1$ is prescribed. When $s(t)$ is given as

$$s(t)=\beta_1\cos t+\beta_2\sin t, \tag{6.20}$$

we find for the jump discontinuity Δ_2 of the tangent at $x=1$

$$\Delta_2=+\beta_1\cos t+(\beta_2-\alpha)\sin t. \tag{6.21}$$

Again from (2.14), (3.5) by comparing the δ functions singularities at both sides of (6.15) we find

$$\tau\{+\beta_1 \cos t+(\beta_2-\alpha)\sin t\}\,\delta(x)=(a_{1,4}\sin t-a_{2,4}\cos t)\,\pi\delta(x), \tag{6.22}$$

or

$$a_{1,4}=\frac{\tau}{\pi}(\beta_2-\alpha)\ ,\ a_{2,4}=-\frac{\tau}{\pi}\beta_1. \tag{6.23}$$

Hence we have found two extra equations and also in this case the solution is determined.

From (6.15) we can calculate the elevation of the free surface. The general solution of this equation is

$$\left.\begin{aligned} y_s(x,t)=D_1(t)\,e^{x/\sqrt{\tau}}+D_2(t)\,e^{-x/\sqrt{\tau}}+\\ +\frac{\nu}{2\sqrt{\tau}}\int_0^x\frac{\partial\theta}{\partial t}(\xi,0,t)\{e^{\frac{(x-\xi)}{\sqrt{\tau}}}-e^{\frac{-(x-\xi)}{\sqrt{\tau}}}\}\,d\xi. \end{aligned}\right. \tag{6.24}$$

Because this solution has to remain finite for $x\to+\infty$ we have from (6.1)

$$D_1(t)=\frac{-\nu}{2\sqrt{\tau}}\int_1^\infty\{\sum_{n=1}^{5}\vartheta_n(\xi,0)\,(-a_{1,n}\sin t+a_{2,n}\cos t)\}\,e^{-\frac{\xi}{\sqrt{\tau}}}\,d\xi. \tag{6.25}$$

When the elevation at $x=1$ of the membrane is given (6.16) we have

$$y_s(1,t)=D_1(t)\,e^{1/\sqrt{\tau}}+D_2(t)\,e^{-1/\sqrt{\tau}}=\alpha_1\cos t+\alpha_2\sin t. \tag{6.26}$$

When the discontinuity of the tangent at $x=1$ is prescribed (6.20) we have

$$\frac{d}{dx}y_s(1,t)=\frac{1}{\sqrt{\tau}}(D_1(t)\,e^{1/\sqrt{\tau}}-D_2(t)\,e^{-1/\sqrt{\tau}})=\beta_1\cos t+\beta_2\sin t. \tag{6.27}$$

Hence in both cases we have two equations for $D_1(t)$ and $D_2(t)$ and the surface is determined.

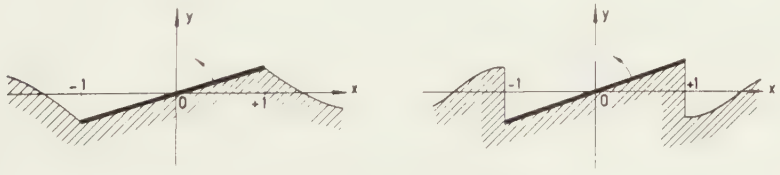

Fig. 5. The two special cases.

It is possible to consider two special cases, first there is no jump discontinuity of the elevation, then in (6.17) $\alpha_1=0$, $\alpha_2=\alpha$, second, the right hand sided derivative of the free surface for $x=1$ is zero, then in (6.20) $\beta_1=\beta_2=0$.

Both cases are drawn in fig. 5, in the first the membrane of the surface tension is connected to the dock, in the second, the edge of the dock and the boundary of the membrane have no direct interaction.

7. *The case of zero surface tension*

In this case we have $\tau = 0$ and hence the integro differential equation (3.7) becomes an ordinary integral equation of the second kind. This equation reads as follows

$$(7.1)\quad \begin{cases} \dfrac{\partial \varphi_n}{\partial x}(x) = \dfrac{\nu}{\pi}\displaystyle\int_{-1}^{+1} \dfrac{\partial \varphi_n}{\partial x}(\xi) \ln|\xi - x|\, d\xi + \nu A_1 \ln(1-x) + \\ \qquad + \nu A_1 \ln(1+x) - \nu \mathcal{C}_{3} \begin{cases} -\frac{\nu^2 \lambda^2}{2} & n=1 \\ 0 & n>1 \end{cases} \end{cases}$$

where it is now not allowed to prescribe boundary conditions for its solutions and where we have only considered the coefficients A_1 and B_1. The physical reason for this latter limitation is that because of the absence of the membrane we do not need singular forces and moments at the edge of the dock. It will be seen that a sufficient number of solutions are obtainable to meet all the conditions.

In this problem the function $\frac{\partial \varphi_2}{\partial x}(x)$ which is caused by the possibility of prescribing the boundary values for $x = \pm 1$ does not occur. Hence we have to consider only $\frac{\partial \varphi_1}{\partial x}(x)$ and $\frac{\partial \varphi_2}{\partial x}(x)$ which satisfy the equations

$$(7.2)\qquad \frac{\partial \varphi_1}{\partial x}(x) = \frac{\nu}{\pi}\int_{-1}^{+1} \frac{\partial \varphi_1}{\partial x}(\xi) \ln|\xi - x|\, d\xi - \frac{\alpha}{2}\nu^2 x^2 - \nu \mathcal{C}_{3,1},$$

$$(7.3)\quad \frac{\partial \varphi_3}{\partial x}(x) = \frac{\nu}{\pi}\int_{-1}^{+1} \frac{\partial \varphi_3}{\partial x}(\xi) \ln|\xi - x|\, d\xi + \nu \ln|1-x| + \nu \ln|1+x| - \nu \mathcal{C}_{3,3}.$$

The condition for the constants $C_{3,1}$ and $C_{3,3}$ are given in (4.5) and the functions φ_1, φ_2, ψ_1 and ψ_2 follow from (3.5) and (3.6).

The equation (5.3) for the function $F_n(z)$ changes into

$$(7.4)\qquad \nu F_n(z) - i F_n'(z) = Q_n(z).$$

From this equation follows

$$(7.5)\qquad \vartheta_n(x, y) = \operatorname{Re} F_n(z) = \operatorname{Re}\left\{ i \int_0 Q_n(\zeta)\, e^{-i\nu(z-\zeta)} d\zeta + E_{1,n}\, e^{\quad} \right\},$$

where the constant $E_{1,n}$ is imaginary because $\vartheta_n(x, y)$ is odd with respect to x. In the notation of para. 5, $E_{1,n} = iT_{2,n}$.

The boundary condition analogous to (6.6) which is satisfied by

$$(7.6)\quad \begin{cases} \theta(x, y, t) = \vartheta_1(x, y)\cos t + \vartheta_3(x, y)(a_{1,3}\cos t + a_{2,3}\sin t) = \\ \qquad = \vartheta_1^*(x, y)\cos t + \vartheta_3^*(x, y)(a_{1,3}\cos t + a_{2,3}\sin t) + \\ \qquad + e^{\beta_1 \nu} \sin \beta_1 x (\gamma_1 \cos t + \gamma_2 \sin t), \end{cases}$$

is

$$(7.7)\qquad \nu^2 \frac{\partial \theta}{\partial y} + \frac{\partial^3 \theta}{\partial x^2 \partial y} = \alpha \nu^2 x \cos t,$$

Hence we have to require

$$(7.8) \qquad \frac{\partial\theta}{\partial y}(0,0,t)=0\ ;\ \frac{\partial^2\theta}{\partial x\partial y}(0,0,t)=\alpha\cos t\ ;\ \frac{\partial^3\theta}{\partial x^2\partial y}(0,0,t)=0.$$

The first and third condition are satisfied automatically because $\theta(x, y, t)$ is ann odd function with respect to x, there remains the condition

$$(7.9) \qquad \frac{\partial^2\theta}{\partial x\partial y}(0,0,t)=\alpha\cos t.$$

Also we have the two radiation conditions. From these and from (7.9) it follows that we have to satisfy equation (6.10), (6.13) and (6.14), where now $a_{1,1}=1$, $a_{2,3}=a_{1,2}=a_{2,2}=a_{1,4}=a_{2,4}=a_{1,5}=a_{2,5}=E_{2,n}=E_{3,n}=0$. These are four linear equations for the four unknown constants.

Hence the solution of the rolling dock on the water surface without tension is determined.

8. *Concluding remarks*

It is our aim to consider the rigid dock rolling on the surface of the water, whereas on the free part of the surface a membrane is spread. In para. 2 we converted this problem into a problem for a membrane spread over the whole surface. At the place of the dock it was allowed to apply external pressures P_u (2.14) to the membrane so that this behaved as a rigid strip. Next we determined the velocity potential of the fluid motion, by which also the external pressure P_u, expressed in the functions φ_n, is known. This external pressure, however, does not yield after integration the moment we have to exert on the rigid dock, in order to obtain the desired fluid motion. We consider separately the two cases, drawn in fig. 5.

In the first case, that with the membrane fixed to the edge of the dock, we find a singular force acting at the edge $x=1$. This force is caused by the vertical components of the tension in the membrane at both sides of $x=1$. However, in the case of the rigid dock the tension for $|x|<1$ does not exist at all, hence we have to reduce the singular force by the amount

$$(8.1) \qquad -\alpha\tau\sin t.$$

In the second case the singular force has to be neglected completely on base of the preceeding argument. Here, however, singular moments arise from the tearing up of the membrane at $x=1$. These moments do not exist in the problem we want to solve, they originate from the formulation in terms of the two sided infinite membrane, hence they have to be neglected.

Netherlands Ship Model Basin,
Wageningen

REFERENCES

1. Ueno, K., Influence of the surface tension of the surrounding water upon the free rolling of model ships. Mem. Fac. Eng. Kyushu University, Japan, **XII**, 1 (1950).
2. Vossers, G., Fundamentals of the behaviour of ships in waves. Intern. Shipbuilding Progress, **6** and **7**, 1959 (1960).
3. Kotchin, N. J., J. A. Kibel and N. W. Rose, Theoretische Hydromechanik, Akademie Verlag, Berlin, 410 (1954).
4. Muskhelishvily, N. J., Singular integral equations, P. Noordhoff, Groningen, 43 (1953).
5. Sparenberg, J. A., Applications of the Hilbert problem to problems of mathematical physics, thesis Delft, 49 (1958).
6. Whittaker, E. I. and G. N. Watson, A course of modern analysis, Cambridge University Press, Cambridge, 119 (1958).

USE OF ANOMALOUS SCATTERING IN X-RAY ANALYSIS OF PROTEINS

CORRECTION FOR ANOMALOUS SCATTERING FROM LIGHT ATOMS

BY

A. DE VRIES [1])

(Communicated by Prof. J. M. BIJVOET at the meeting of February 27, 1960)

The anomalous scattering effects, being used more and more during recent years in the analysis of relatively small molecules, appear to be useful also in the study of protein crystal structures.

However, as BLOW (1958) has pointed out, it is no longer possible to neglect the anomalous effect of the light atoms when studying a protein to which some heavy atoms are attached, especially not when the protein contains sulfur or iron. This will be clear from the comparison of the r.m.s. values of the anomalous scattering amplitudes of the different components of $\frac{1}{2}$ molecule of a Hg-haemoglobin compound (BLOW, 1958) in table I.

TABLE I

Anomalous scattering in Hg-haemoglobin

Components of $\frac{1}{2}$ molecule	$\sqrt{\sum \Delta f''^2}$		
	CrKα	CuKα	– radiation –
1580 C + 397 N + 439 O atoms	0.84	0.60	
7 S atoms	2.6	1.5	
2 Fe atoms	1.3	4.8*	
0.65 Hg atoms	9.8*	5.2*	

* The table given by BLOW (1958) contains some errors (BLOW, 1960). Furthermore BLOW emphasized that the contribution for Hg, occupying one single position, should be calculated as $\sum \Delta f''$, rather than $\sqrt{\sum \Delta f''^2}$.

In his calculations on the anomalous effect BLOW takes into account only one of the three terms involved. Therefore it seemed useful to look for the result when all three correction terms are considered.

1. *Notation and general formulas*

$f_i + i\Delta f_i''$ scattering factor of atom i

$\boldsymbol{F}_H$ structure factor of the heavy atoms only

$\boldsymbol{F}_L$ structure factor of the light atoms only

$\boldsymbol{F}$ structure factor of all atoms

[1]) Laboratorium voor Kristalchemie der Rijksuniversiteit, Catharijnesingel 51, Utrecht, The Netherlands (permanent address) and temporarily Biophysics Department, Roswell Park Memorial Institute, 666 Elmstreet, Buffalo 3, N.Y., U.S.A.

F_H, F_L modulus of $\sum f_i \exp\{i\varphi_i\}$, the sum taken over only heavy or light atoms respectively

F_H'', F_L'' idem for $\sum \Delta f_i'' \exp\{i\varphi_i\}$

A cosine part of an F

B sine part of an F

φ phase angle of an F

Considering a structure containing both heavy and light atoms, with a centrosymmetric array of the heavy atoms and a non-centrosymmetric array of the light atoms, the following formulas are obtained for the different structure factors:

$$F_H = \sum (f_i + i\Delta f_i'') \cos \varphi_i = A_H + iA_H''$$

$$F_L = \sum (f_j + i\Delta f_j'') \exp\{i\varphi_j\} = A_L + iB_L + iA_L'' - B_L''$$

$$F = F_H + F_L = (A_H + A_L - B_L'') + i(A_H'' + A_L'' + B_L)$$

From the last formula the difference between $F^2(hkl)$ and $F^2(\bar{h}\bar{k}\bar{l})$ is

$$\Delta F^2 = 4B_L A_H'' + 4B_L A_L'' - 4B_L'' A_H - 4B_L'' A_L \tag{1}$$

When the anomalous effect of the light atoms is negligible, this formula is reduced to

$$\Delta F^2 = 4B_L A_H''$$

ΔF^2 can be measured and, the array of the heavy atoms being known, A_H'' can be calculated. Thus from this formula B_L can be calculated, and from this in turn the phase angle φ_L of F_L (apart from the ambiguity between φ_L and $\pi - \varphi_L$). More particularly the sign of B_L can be calculated from the relation

$$\text{sign of } B_L = \text{sign of } \Delta F^2 \times \text{sign of } A_H'' \tag{2}$$

2. *Statistical evaluation of the effect of the light atoms*

In proteins, however, where the anomalous effect of the light atoms is not negligible, the following correction terms can be seen to appear in the right hand side of (1):

$$4B_L A_L'' - 4B_L'' A_L - 4B_L'' A_H \equiv 4C \tag{3}$$

And when we still want to determine the sign of B_L from (2), because the value of the correction terms cannot be calculated, we will find the wrong sign for B_L when C and $B_L A_H''$ have different signs when $|C| > |B_L A_H''|$. To calculate the probability that this will happen, the expression (3) is rewritten:

$$C = F_L F_L'' (\sin \varphi_L \cos \varphi_L'' - \sin \varphi_L'' \cos \varphi_L) - A_H F_L'' \sin \varphi_L''$$

$$C = F_L F_L'' \sin(\varphi_L - \varphi_L'') - A_H F_L'' \sin \varphi_L'' \tag{4}$$

As further calculations depend on the relation between φ_L and φ_L'', two cases will be considered separately.

2a. Systematic equality of φ_L and φ_L''

This situation will occur when both F_L and F_L'' are practically determined by atoms with about the same value of $f/\Delta f''$, for instance when all light atoms are equal. With the relations $\varphi_L'' \approx \varphi_L$ and $F_L''/F_L \approx \Delta f_L''/f_L$ formula (1) is now reduced to

$$\begin{aligned}\Delta F^2 &= 4F_L A_H'' \sin \varphi_L - 4A_H F_L'' \sin \varphi_L \\ &= 4F_L \sin \varphi_L (A_H'' - A_H \Delta f_L''/f_L)\end{aligned}$$

From this formula we can again calculate φ_L both in sign and in magnitude, so in this case the anomalous scattering from the light atoms gives no difficulties.

2b. Complete independence of φ_L and φ_L''

This situation will be encountered in such compounds as haemoglobin, where F_L is almost completely determined by the C, N and O atoms, whereas the Fe and S atoms are responsible for the major part of F_L''.

The ratio between the mean values of the terms in the right hand side of (4) is determined now only by the ratio between the mean values of A_H and F_L, which is rather small in the case under consideration: a few heavy atoms and many light ones (with Hg-haemoglobin

$$\sqrt{\overline{A_H^2}}/\sqrt{\overline{F_L^2}} = \tfrac{1}{6} \text{ for } \sin \theta/\lambda = 0.05)$$

Therefore the distribution function for C can be approximated very well by that for the first part of the right hand side of (4). Moreover, as we are considering the case that φ_L and φ_L'' are independent, the distribution functions for $\sin(\varphi_L - \varphi_L'')$ and $\sin \varphi_L''$ are the same and so the probability that $|C| > |B_L A_H''|$ equals the probability that

$$F_L F_L'' \,|\sin \varphi_L''| > |B_L A_H''|$$

or that

$$|B_L''| > |A_H'' \sin \varphi_L|$$

or that

$$\left|\frac{B_L''}{\sin \varphi_L}\right| > |A_H''|.$$

We shall now omit for convenience the index L of $\sin \varphi_L$ and use the symbol S for $B_L''/\sin \varphi$.

To calculate the distribution function for S we shall assume that B_L'' has a normal probability distribution. Of cause this is only true when a large number of atoms is contributing to B_L'' and therefore this assumption is probably not always valid: for instance, when haemoglobin is irradiated with CuKα radiation the major contribution to B_L'' comes from eight Fe atoms per unit cell, of which only two are independent. However, it seems to be the best assumption that can be made. So the

normalized distribution function for B_L'' is given by

$$\psi(B_L'') = \frac{1}{\sqrt{2\pi}R''} \exp\left\{-\frac{B_L''^2}{2R''^2}\right\} \tag{5}$$

with $R'' = \sqrt{\overline{B_L''^2}}$. From this the probability that S lies between S and $S + dS$ while $\sin\varphi$ is constant is

$$\psi(S)_{\sin\varphi}\, dS = \frac{|\sin\varphi|}{\sqrt{2\pi}R''} \exp\left\{-\frac{S^2\sin^2\varphi}{2R''^2}\right\} dS$$

the probability that S lies between S and $S - dS$ while $\sin\varphi$ lies between $\sin\varphi$ and $\sin\varphi + d\sin\varphi$ is

$$\psi(S, \sin\varphi)\, dS\, d\sin\varphi \quad \frac{|\sin\varphi|}{\sqrt{2\pi}R''} \exp\left\{-\frac{S^2\sin^2\varphi}{2R''^2}\right\} \frac{1}{\pi|\cos\varphi|} dS\, d\sin\varphi$$

and the probability that S lies between S and $S - dS$ with no restrictions on $\sin\varphi$ is

$$\psi(S)\, dS = \frac{2dS}{\pi R''\sqrt{2\pi}} \int_0^1 \frac{x}{\sqrt{1-x^2}} \exp\left\{-\frac{S^2x^2}{2R''^2}\right\} dx.$$

with $x = \sin\varphi$

The probability of finding the wrong sign for B_L from (2) is given by the probability that $|S| > |A_H''|$ while S and A_H'' have different signs, so by

$$P = \frac{2}{\pi R''\sqrt{2\pi}} \int_{|A_H''|}^{\infty} dS \int_0^1 \frac{x}{\sqrt{1-x^2}} \exp\left\{-\frac{S^2x^2}{2R''^2}\right\} dx,$$

or, changing the sequence of integration, by

$$P = \frac{2}{\pi\sqrt{2\pi}} \int_0^1 \frac{dx}{1-x^2} \int_{H_x}^{\infty} \exp\left\{-\frac{y^2}{2}\right\} dy. \tag{6}$$

with $y = \frac{Sx}{R''}$ and $H = \frac{|A_H''|}{R''}$ — the "heaviness" of the heavy atoms compared with the light atoms in relation to the anomalous effect.

The integral over y is tabulated for instance by HALD (1952) and then the integral over x can be evaluated numerically to give P as a function of H. In fig. 1 P as a function of H is compared with the probability calculated from Blow's formula as a function of H as well as of $\sqrt{\frac{1}{2}}H$ [1]).

It can be seen that for all values of H our function gives a higher probability of finding the wrong sign. This might explain why BLOW (1958), even with the wrong R'', found the disagreement between the Cu and the Cr measurements to be slightly higher than calculated.

[1]) The value of R'' used by BLOW in his paper (1958) was erroneously $\sqrt{2}$ times the correct value (BLOW, 1960). So to compare his results with ours we have to plot his formula as a function of $\sqrt{\frac{1}{2}}H$.

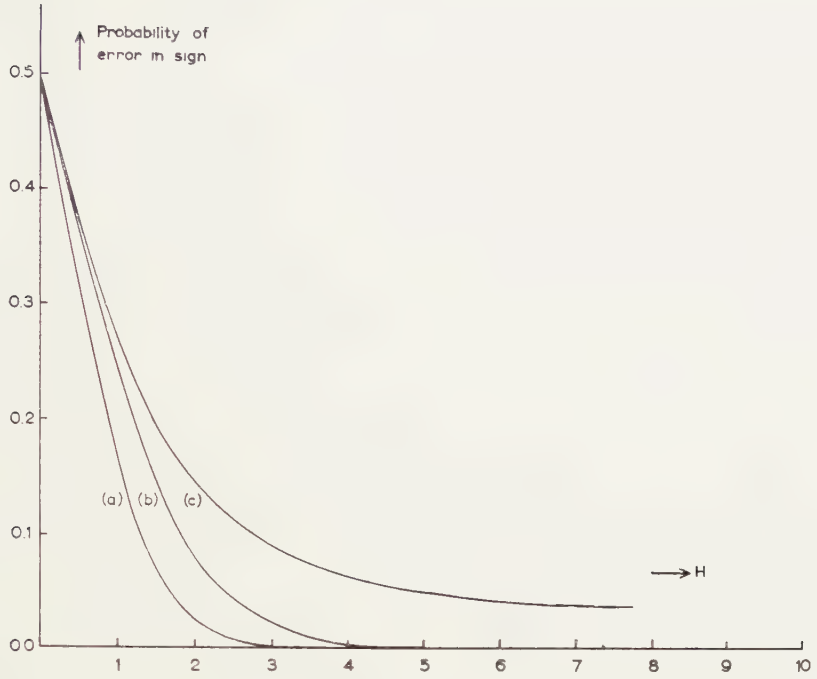

Fig. 1. Probability of error in the sign of B_L determined from the anomalous effect when the contribution of the light atoms is ignored, plotted against H = the anomalous effect of the heavy atoms compared to that of the light atoms

a) $P = \frac{1}{\sqrt{2\pi}} \int_{H}^{\infty} \exp\left\{-\frac{x^2}{2}\right\} dx$ b) $P = \frac{1}{\sqrt{2\pi}} \int_{\frac{1}{2}H}^{\infty} \exp\left\{-\frac{x^2}{2}\right\} dx$

c) P according to formula (6).

3. *Measurement of the effect of the light atoms*

However, another and more general way to determine the sign of φ_L can be found, not so dependent on the value of A_H'' or the relation between φ_L and φ_L''.

It is evident that correction for the anomalous scattering of the light atoms is necessary only when this anomalous scattering can surpass that of the introduced heavy atoms. Thus, for the reflections concerned, it would be possible to measure the anomalous effect of the isomorphous unsubstituted compound also. This leads us to consider such case more detailedly. From (1) it can be seen that the anomalous effect for the light atom compound is given by

$$\Delta F_L^2 = 4B_L A_L'' - 4B_L'' A_L$$

and using this result in (1) we obtain for the anomalous effect of the compound containing both heavy and light atoms

$$\Delta F^2 = 4B_L A_H'' + \Delta F_L^2 - 4B_L'' A_H,$$

or

$$\Delta F^2 - \Delta F_L{}^2 = 4B_L A_H'' - 4B_L'' A_H \tag{7}$$

If it be allowed to neglect the term $4B_L'' A_H$, this formula would provide us again with a means to determine the sign of B_L, by the relation

$$\text{sign of } B_L = \text{sign of } (\Delta F^2 - \Delta F_L{}^2) \times \text{sign of } A_H'' \tag{8}$$

The correctness of the result from this relation depends on the probability of finding the same sign for $B_L'' A_H$ and $B_L A_H''$ when

$$B_L'' A_H \quad B_L A_H''$$

or

$$|B_L''| > \left| B_L \frac{A_H''}{A_H} \right|.$$

As a distribution function for B_L'' we shall use again (5), and because A_H''/A_H is known the distribution function for $B_L A_H''/A_H$ is the same as that for B_L, which is of the same kind as that for B_L''. So the probability of finding the same sign for $B_L'' A_H$ and $B_L A_H''$ when $|B_L''$ is larger than some fixed value of $|B_L A_H''/A_H|$ is

$$\frac{1}{\sqrt{2\pi} R''} \int_{|B_L A_H''/A_H|}^{\infty} \exp\left\{ -\frac{B_L''^2}{2R''^2} \right\} dB_L'',$$

and this, multiplied by the distribution function for $B_L A_H''/A_H$ and integrated over all values of B_L gives us Q, the probability of finding the wrong sign for B_L:

$$Q = \frac{1}{2\pi R R''} \int_{-\infty}^{+\infty} \exp\left\{ -\frac{B_L^2}{2R^2} \right\} dB_L \int_{|B_L A_H''/A_H|}^{\infty} \exp\left\{ -\frac{B_L''^2}{2R''^2} \right\} dB_L'',$$

with $R = \sqrt{\overline{B_L^2}}$. With $\frac{A_H'' R}{A_H R''} = \alpha$, $\frac{B_L}{R} = x$ and $\frac{B_L''}{R} = y$ this gives

$$Q = \frac{1}{\pi} \int_0^{\infty} \exp\left\{ -\frac{x^2}{2} \right\} dx \int_{\alpha x}^{\infty} \exp\left\{ -\frac{y^2}{2} \right\} dy.$$

The integral over y can again be found in tables and then the integral over x can be evaluated numerically, giving Q as a function of α, which in turn is a function of θ and of the compound used. If we again take as an example the Hg-haemoglobin with CrKα radiation the values of α are 29, 20 and 18 for $\frac{\sin\theta}{\lambda} = 0.00$, 0.05 and 0.10 respectively, and with these values of α we get for Q: 0.012, 0.016 and 0.018 respectively. So with all the reflections in this region (up to spacings of 5 Å) the probability of finding the right sign for B_L with this method of calculation is higher than 98 %, independent of the value of A_H'', while the other method

gives results with a probability of 90 % or more only when H is at least 2.75 (this corresponds to $A_H'' = 16.8$ for Hg-haemoglobine.)

Of course the practical applicability of this method is seriously limited by the accuracy of the measurements and by the degree of isomorphism between the heavy atom and the non-heavy atom compounds. This last demand, however, is not as heavy in this case as in the case of isomorphous replacement, as ΔF_L^2 in general is only a small correction on ΔF^2.

In theory at least it will even be possible to determine B_L quantitatively from the relation

$$\Delta F^2 - \Delta F_L^2 \approx 4 B_L A_H''$$

The error in this formula is given by $4 B_L'' A_H$. With $\alpha = 18$ the probability that $B_L'' A_H$ is larger than 10, 17, 22 or 50 % of $B_L A_H''$ is 15, 10, 8 or 3 % respectively. To be able to calculate φ_L from this result it is necessary to determine first the sign of A_L from the intensity change in the isomorphous replacement.

The author wishes to express his gratitude towards Professor Dr. J. M. Bijvoet, Drs. J. van Laar and Professor Dr. D. Harker for their critical remarks. He also wishes to express his appreciation to the National Science Foundation the support of which made possible the completion of this work at the Roswell Park Memorial Institute.

REFERENCES

Blow, D. M., Proc. Roy. Soc. A, **247**, 323–325 (1958).

—— —, Personal communication, 1960.

Hald, A., Statistical Tables and Formulas, John Wiley and Sons, N.Y., 34–35 (1952).

THE CONDENSATION AND DE-CONDENSATION OF SILICA

I. VISCOSITY AND ELECTROPHORESIS STUDIES

BY

J. H. DE BOER, B. G. LINSEN AND C. OKKERSE

(Communicated at the meeting of March 26, 1960)

1. *The formation of polymeric silica from monomeric silicic acid*

A solution of monomeric silicic acid – $Si(OH)_4$ – may be prepared by a carefully controlled hydrolysis either of silicon tetrachloride [1], tetra aethyl orthosilicate [2] or tetramethyl orthosilicate [3] or by a careful decomposition of a solution of sodium metasilicate by either acid [4, 3], or by means of a cation exchange resin in its H-form [5]. If the temperature is kept low – e.g. 0° C – and the pH of the solution is in the neighbourhood of 2 or 3, this monomeric acid is relatively stable and it does not readily react in itself to form condensation products of high molecular weight [6].

At pH-values higher than 3 or lower than 2, and at a concentration higher than 0.01 %, hydroxyl groups of monomeric silicic acid react, at room temperature, according the scheme:

$$(HO)_3Si(OH) + (HO)Si(OH)_3 \rightarrow (HO)_3Si{-}O{-}Si(OH)_3 + H_2O,$$

or generally:

$$|SiO_pH_q|_n \quad SiOH \quad HOSi \quad |SiO_rH_s|_m \;\; + \;\; |SiO_pH_q|_n \quad Si\ O\ Si \quad |SiO_rH_s|_m \quad H_2O$$

In literature this reaction is often referred to as a polymerization reaction [6]. We prefer to adhere to the name condensation reaction, because the formation of every new Si O Si link is accompanied by the liberation of one molecule of water. One might consider to use the term condensation polymerization. The advantage of this more cumbersome name is, however, not great enough to warrant its use.

As a result of the condensation reaction an irregular three-dimensional network of irregular SiO_4 tetrahedrons is formed, each silicium atom being linked to four oxygen atoms and each oxygen atom being linked to two silicium atoms [1]).

[1]) Sometimes the silicium atoms are described as fourfold positively charged silicium ions and the oxygen atoms as doubly negative ions [7]; although the silicium atoms will, undoubtedly, on the average, have an excess of positive charge and the oxygen atoms an excess of negative charge, we must, however, consider the links as mainly covalent bonds.

At those – arbitrary – spots where the condensation reaction has stopped, silicium atoms will be found, still carrying three, two or one OH-groups [8]. Fig. 1 gives a very rough schematic picture (two-dimensional) of a – very small – particle of such condensed $[SiO_{(2-x)}(OH)_{2x}]_n$, with $n = 20$, $x = 0.9$; in this drawing there are still 3 Si-atoms with 3 OH-groups, 12 with 2 OH-groups, 3 with 1 OH-group, whereas only 2 Si-atoms are devoid of OH-groups. As long as such condensed polymeric particles are in (colloidal) solution or in the state of a hydrogel, numerous water molecules are bound by the numerous OH-groups of the structure.

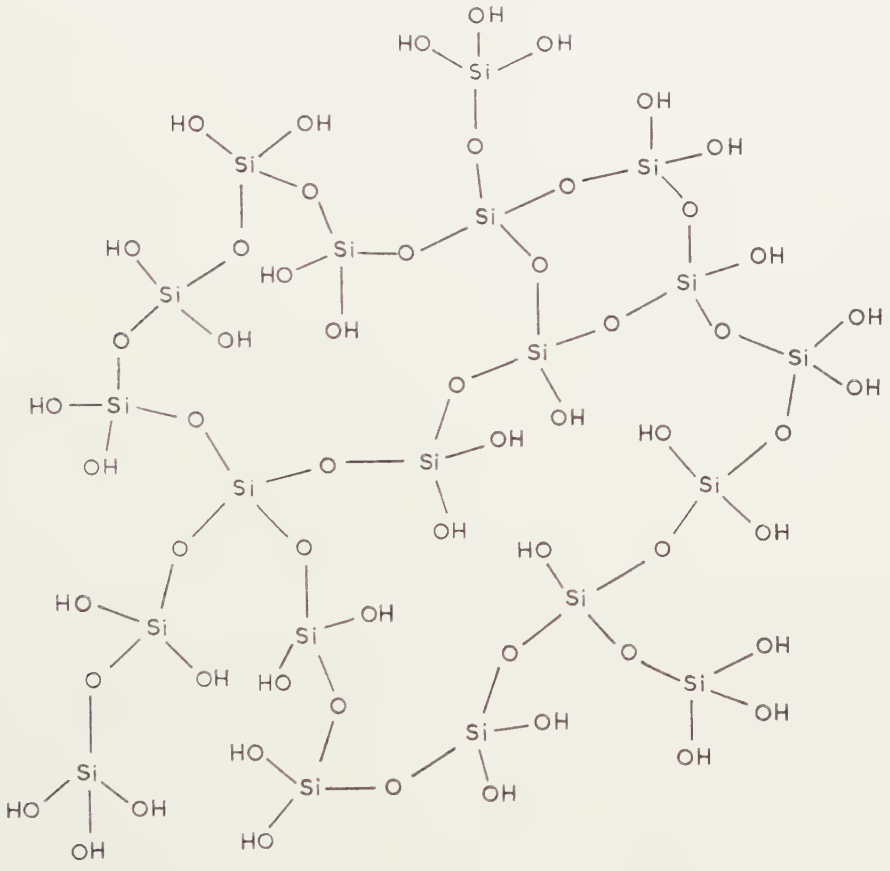

Fig. 1

At the moment that, as a result of the proceeding condensation reaction in a silica sol gelation sets in, the gel particles consist of macromolecules, which have, mostly, larger values of n and lower values of x than those corresponding with fig. 1. During gelation and during the drying of the gel the condensation reaction proceeds, until the gel is dry and a so-called xero-gel has been obtained [8]. During these various stages the condensation reaction takes place between Si–OH groups of the same macromolecule or of different macromolecules in the same gel particle, or between

the OH-groups of different macromolecules of different particles, thus strengthening the coherence of the grains.

Reversely when water is brought into contact with a dried xero-gel, water molecules attack Si–O–Si bonds and convert them into Si–OH groups. Consequently, small molecules, such as having, say, $n=1$ to 5 and $x=2$ to 1.2, may enter into solution. They may redeposit, by means of the condensation reaction, at such places where the surface energy of the particles is high enough, but a certain amount of low molecular weight silica (monomeric $Si(OH)_4$ included) stays in solution, in equilibrium with the silica particles. This solution represents a metastable equilibrium, because the non-crystalline silica is not the stable form at room temperature. However, the de-condensation process, just described, leads to a definite saturation value for the solubility of amorphous silica [9]. The solubility data, reported in literature, vary between 0.009 [10] and 0.015 % [11], at room temperature. These values depend on the surface energy of the specimen of silica which is used for its determination; they are definitely higher than the figures found for quartz, viz. 0.0011 % [12].

The solubility of silica is – in the pH-range up to about 8 – independent of the pH [11]. The rate of dissolution (de-condensation), however, depends largely on pH. In this and subsequent papers we shall discuss the rates of condensation and of de-condensation of silicium hydroxide and of silica respectively, in aqueous media and it shall be shown that the rates of these reactions are catalytically increased by hydrogen- and by hydroxyl ions.

2. *Viscosity measurements*

The formation of polymeric condensation products of increasing molecular weights leads to an increase of the viscosity of the solutions. Kruyt and Postma [13] studied this increase as a function of time. We repeated some of these experiments and extended them largely by studying the influence of pH. The solutions were made by mixing 50 ml of a solution of crystallized sodium metasilicate ($Na_2SiO_3 \cdot 9\,H_2O$) in distilled water, of such a strength that it contained 1 % SiO_2, and 50 ml of a solution of hydrochloric acid of such a concentration that, after mixing, a pre-calculated pH value was obtained. The viscosity of these solutions was measured at regular time intervals by means of an Ostwald-viscosimeter in a thermostat at 20° C. The reproducibility of the measurements is about 1 ‰, as is shown in fig. 2, where the kinematic viscosities are given for 0.5 % SiO_2 sols, as a function of pH, after 4 days and after 13 days.

Despite the relatively large spreading in the measurements it is clear that both the viscosity and the relative change of viscosity are minimal in the neighbourhood of pH 2.

A 1 % SiO_2 sol was then prepared at pH 3 and kept for 10 days at this pH value, in order to produce relatively large silica sol particles.

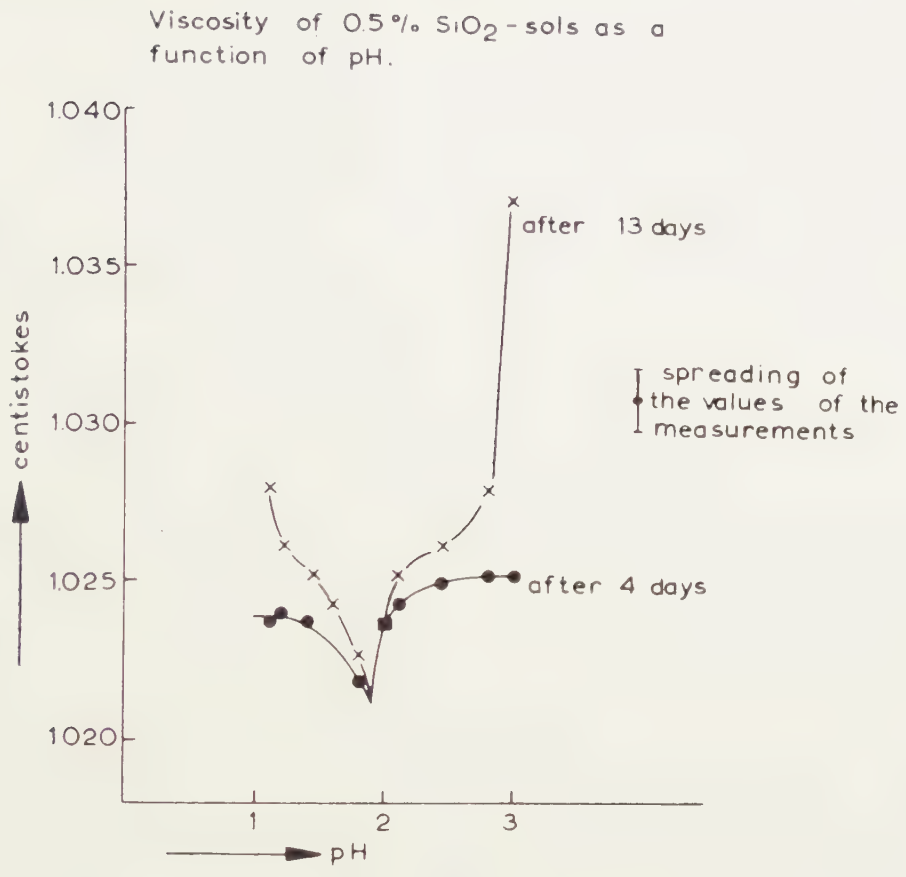

Fig. 2

By dilution of this aged sol 0.5 % sols of different pH values were then prepared. These latter sols were then kept at their pH-values and their viscosities were measured after various time intervals. The results are shown in fig. 3.

3. *The isoelectric point of silica*

It is obvious to try and correlate the above data with the isoelectric point of colloidal silica. Various authors [14] report the isoelectric point of silica to be in the neighbourhood of pH 2, though some confusion seems to exist as to even the region of pH values where it may be expected to be. As quartz suspensions show an isoelectric point at a pH value, somewhat higher than pH 1 [15], we may expect the isoelectric point of silica to be in the same neighbourhood.

In order to determine the sign of the charge of the particles in the sols of the present study, some simple electrophoresis experiments were made. The sols were dialysed in "Nalon" sausage skins, resulting in very pure sols of low conductivity. A 1 % silica sol of pH 1, obtained by mixing

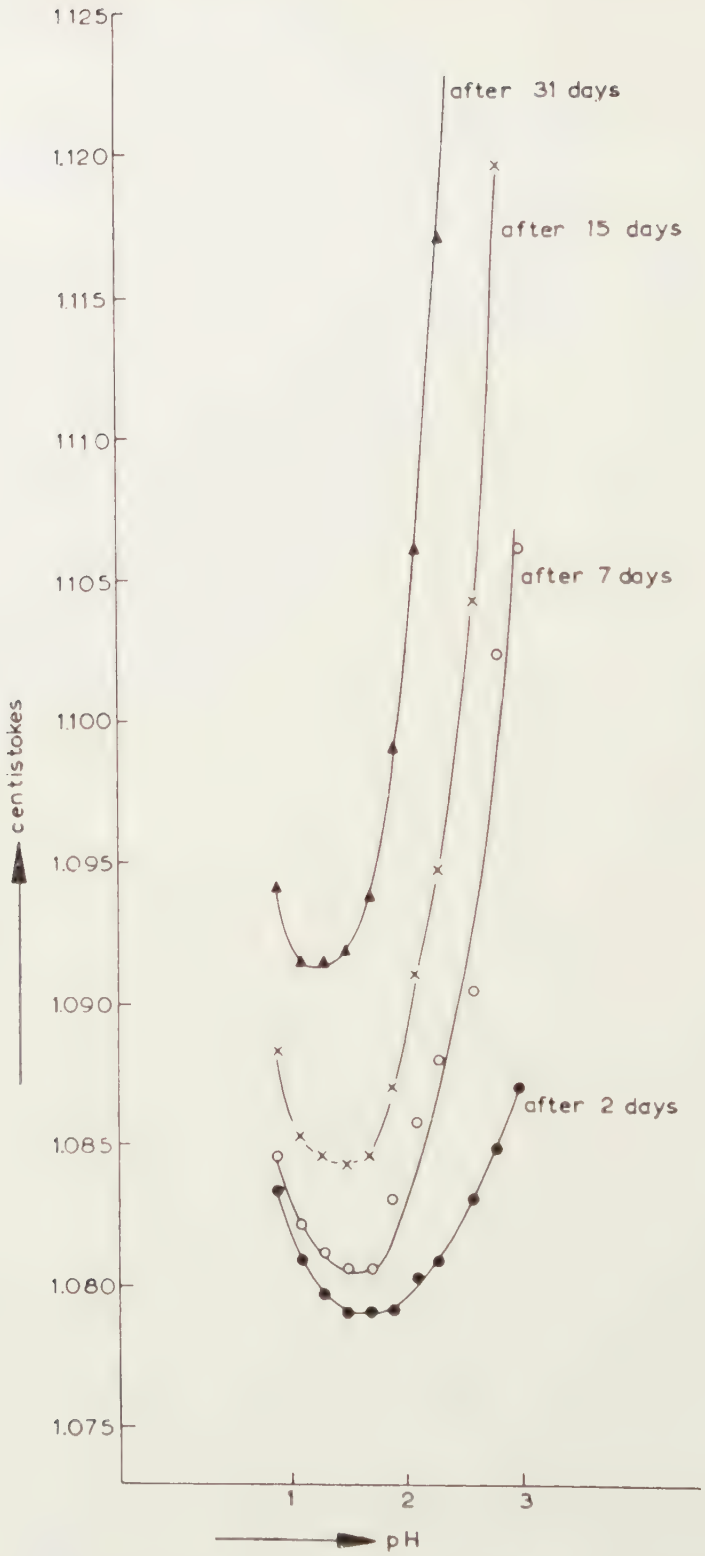

Fig. 3. Viscosity of 0.5 % SiO_2-sols as a function of pH. (The sols have been prepared by dilution of a 1 % SiO_2-sol, aged at pH = 3 during 10 days).

a solution of sodium metasilicate and a solution of hydrochloric acid at constant pH, was dialysed for two days. The final pH was about 5.5 and the final percentage of silica was 0.5 %. From this dialysed sol other sols were made with varying pH-values (pH from 1 to 4) by adding an adequate number of drops of hydrochloric acid.

The electrophoresis experiments showed that the sol particles have a positive charge at pH values lower than 1 and a negative charge at pH-values higher than 1.5. The isoelectric point of a 1 % sol, therefore, seems to be in between pH 1 and pH 1.5.

In a similar way it was found that the isoelectric point of a 0.26 % sol, obtained by dilution of the 0.5 % sol, seems to be at about pH 2. It appears that dilution may move the isoelectric point to higher pH values as already indicated by the work of LOSENBECK [14].

The minimum in the viscosity curves seems to be related to the minimum of charge of the sol particles. Fig. 3 shows that the viscosity minimum shifts slightly towards lower pH values when the condensation reaction proceeds. This observation tallies well with the result of VERWEY [15], who found that larger particles of a quartz suspension show a stronger tendency to assume a negative charge than smaller ones and also with the observation by GRUNDMANN [16], who found that his positively charged silica sols became negative after ageing. Apparently larger particles are isoelectric at somewhat lower pH-values than smaller particles.

The difference in the rate of growing of the particles at different pH-values could, qualitatively, also be demonstrated by dialysing 1 % silica sols of pH values 1, 2 and 3. After a dialysis of about 27 hours, the decreases in concentration were 27.3, 30.5 and 16.2 % respectively.

4. *The catalysing ions for the condensation reaction*

H^+ and OH^- ions are the potential determining ions of silica sol particles. The observations, described above, indicate that the same ions may have a catalysing effect on the rate of condensation of silica. In 1902 FLEMMING [17] derived a similar conclusion with respect to gel formation. He observed that the rate of gelling of a silica sol was minimal at a pH value of approximately 1.5.

In fig. 4 we show the variation with pH of the gelling time of 5 % silica sols; the maximum is clearly demonstrated. In the experiments of fig. 4 we considered the sol to be gelled when the gel fulfilled the criterion proposed by HURD and MILLER [20], viz. that a glass rod of a certain size, put in the gel at an angle of 20°, does not fall over. In older literature gelling was, sometimes, considered as being strongly related to flocculation; if this were so, the gelling rate would be expected to be maximal at the isoelectric point, hence at about pH = 2. If, however, with CARMAN [18], gelling is considered as a normal consequence of the proceeding condensation reaction, the minimal rate of gelling – maximal time before gelling sets in – is easily understood.

It looks, therefore, as if the potential determining ions, viz. H^+ and OH^- ions, or the net charges which they produce, are also the catalysts for the condensation reaction. There are, as already stated, also various statements in literature, indicating this effect. However, ILER [19] recently suggested OH^- and F^- to be the catalysing ions in the high pH and low pH regions, respectively. In subsequent articles of this series we intend to show that, although F^- ions may catalyse the condensation reaction, H^+ and OH^- ions must be considered as the normal catalysts.

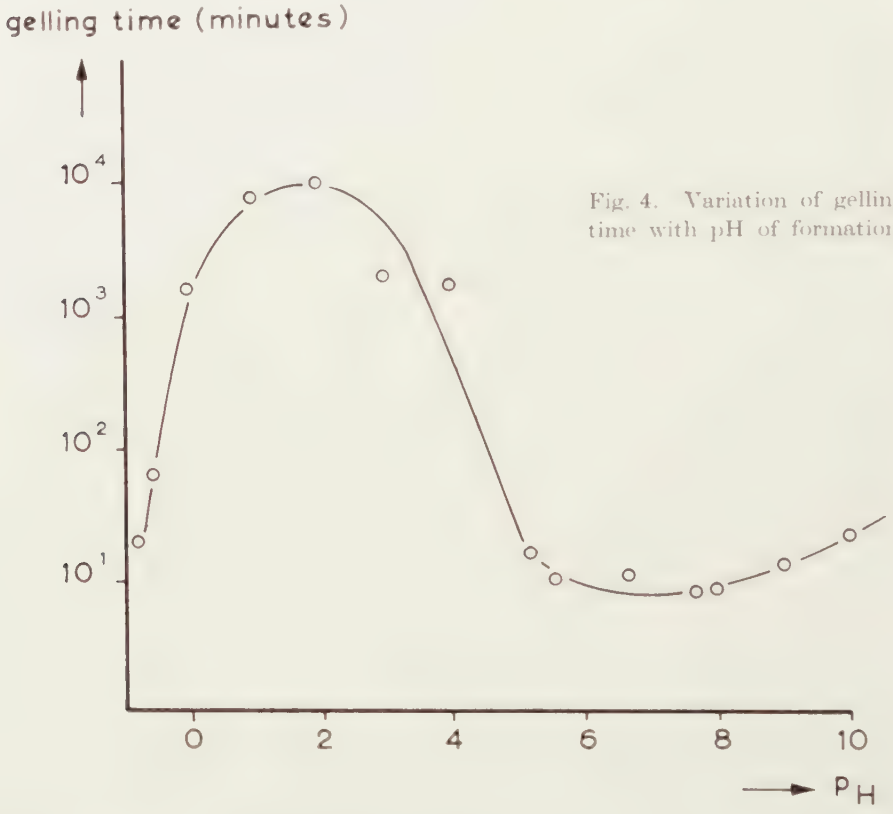

Fig. 4. Variation of gelling time with pH of formation.

5. *Summary*

Silica sols are positively charged at pH-values below – roughly – 2, they are negatively charged at pH-values higher than this figure. This isoelectric point is shifted to somewhat higher pH-values when the sol is diluted. Larger particles show an isoelectric point at somewhat lower pH-values.

The potential determining ions – H^+ and OH^- ions, or the net charges they produce – catalyse the condensation reaction of – SiOH groups. This condensation is, consequently, minimal at the isoelectric point.

Centraal Laboratorium,
Staatsmijnen in Limburg, Geleen,
and Technische Hogeschool, Delft

REFERENCES

1. Willstätter, R., H. Kraut and K. Lobinger, Ber. d. Deutschen Chem. Ges. **58 B**, 2462 (1925); **61**, 2280 (1928); **62**, 2027 (1929).
   Gruner, E. and J. Elöd, Z. anorg. allgem. Chem. **208**, 317 (1932).
2. Brintzinger, H. and B. Troemer, Z. anorg. allgem. Chem. **181**, 237 (1929).
3. Weitz, E., H. Franck and M. Schuchard, Chem. Ztg. **74**, 256 (1950).
4. Kraut, H., Ber. d. Deutschen Chem. Ges. **64 B**, 1709 (1931).
5. Alexander, G. B., J. Am. Chem. Soc. **75**, 2887 (1953).
6. For further literature see: R. K. Iler, The Colloid Chemistry of Silica and Silicates, Cornell Univ. Press, Ithaca, New York, 1955, Ch. III.
7. See e.g. W. A. Weyl, A new approach to surface chemistry and to heterogeneous catalysis, Mineral Industries Emp. Sta. Bull. No. 57; State College, Pa; Penn. State College, 1951.
8. See e.g. J. H. de Boer, M. E. A. Hermans and J. M. Vleeskens, Proc. Kon. Ned. Akad. Wet. **B 60**, 45 (1957); J. H. de Boer and J. M. Vleeskens, Proc. Kon. Ned. Akad. Wet. **B 60**, 54 (1957); **B 60**, 234 (1957); **B 61**, 2 (1958); **B 61**, 85 (1958).
9. See Iler, lit. 6., Ch. I.
10. Alexander, G. B., J. Phys. Chem. **61**, 1563 (1957).
11. ————, W. M. Heston and R. K. Iler, J. Phys. Chem. **58**, 453 (1954).
12. Lier, J. A. van, Thesis, Utrecht, 1959.
13. Kruyt, H. R. and J. Postma, Rec. trav. Chim. **44**, 765 (1925).
14. Losenbeck, O., Kolloid chem. Beih. **16**, 27 (1922).
    Gordon, N. E., Colloid Symposium Monograph, (Chemical Publ. Co., New York) **2**, 114 (1925). For further literature see ref. 6., Ch. V.
15. Verwey, E. J. W., Rec. trav. chim. **60**, 625 (1941).
16. Grundmann, W., Kolloid chem. Beih. **18**, 197 (1924).
17. Flemming, W., Z. physik. Chem. **41**, 427 (1902).
18. Carman, P. C., Trans. Faraday Soc. **36**, 964 (1940).
19. Iler, R. K., J. Phys. Chem. **56**, 680 (1952).
20. Hurd, C. B. and P. S. Miller, J. Phys. Chem. **36**, 2194 (1932).

TERTIARY FORAMINIFERA FROM N.W. DUTCH NEW GUINEA

BY

W. P. F. H. DE GRAAFF

(with 1 plate and 2 sketch maps)

(Communicated by Prof. I. M. VAN DER VLERK at the meeting of March 26, 1960)

Dr. G. J. H. MOLENGRAAFF, former leader of the "Mijnbouwkundige en geologische onderzoekingen in Nederlands Nieuw-Guinea", sent a number of *foraminifera*-containing limestones from the river-basin of the Moon and Koor (northern part of the "Vogelkop") and from the islands Doom, Salawati, Batanta and Kofiau, to the Rijksmuseum van Geologie en Mineralogie.

The director of the museum, Dr. I. M. VAN DER VLERK, gave these samples to me for determination. Since it proved to be impossible to separate the *foraminifera* from the matrix, the determinations had to be based on non-orientated thin sections. As, however, the limestones originate from regions that previously have not been explored geologically, a publication of the results of these investigations seems to be justified.

I. *Northern part of the Vogelkop: river-basin of the Moon and Koor.*

No. 315b $2\frac{1}{2}$ km West of Valse Kaap.
A limestone breccia with augite andesite components, containing: *Austrotrillina howchini* (SCHLUMBERGER) (plate, fig. 1), *Heterostegina borneënsis* VAN DER VLERK, *Spiroclypeus* sp., *Neoalveolina* sp. (plate, fig. 2), *Quinqueloculina* sp. (plate, fig. 3), *Rotalidae*, *Orbulina* sp., *Globigerina* sp., corals (very numerous), *algae* (numerous).

No. 806 Upper course of the Soengo River (southern part of the Tosem Mountains). Massive fine-grained light coloured limestone, containing: *Lepidocyclina sumatrensis* (BRADY) (plate, fig. 4), ?*Miogypsinoïdes*, *Heterostegina* sp., *Gypsina* sp., *Globigerina* sp., corals, *algae*.

No. 660 Soejouw River (right tributary of the Koor River).
Light coloured limestone (boulder), containing:
Lepidocyclina cf. *parva* OPPENOORTH, *Lepidocyclina* sp., *Operculina* sp., *Heterostegina* sp., *Amphistegina* sp., *Gypsina globulus* REUSS, *Marginopora vertebralis* (QUOY and GAIMARD), *Globigerina* sp., *algae*.

No. 380a Quarry at the lower course of the Remoe River (the mouth of the Remoe River lies 4 km S.E. of Sorong).

Limestone breccia (Jefman breccia), containing:
Lepidocyclina cf. *sumatrensis* (Brady), *Lepidocyclina* cf. *parva* Oppenoorth, *Miogypsina* s.str. sp., *Austrotrillina howchini* (Schlumberger), *Heterostegina* sp., *Flosculinella bontangensis* L. Rutten, *Operculina* sp., *Marginopora vertebralis* (Quoy and Gaimard), *algae*, corals, *Globigerina* sp.

II. *The isle of Doom.*

No. 222c Garden and 25 m north of the garden of the former house of the resident of N.W. New Guinea.
Sandy part of limestone in conglomerate, light grey limestone, containing:
Miogypsinoïdes sp., *Lepidocyclina* sp., *Heterostegina borneënsis* Van der Vlerk (plate, fig. 5), *Miogypsina* s.str., sp., *Cycloclypeus* sp., *Amphistegina* sp., *Orbulina* sp., *Gypsina* sp., corals (very numerous), *Lithophyllum* sp. (numerous).

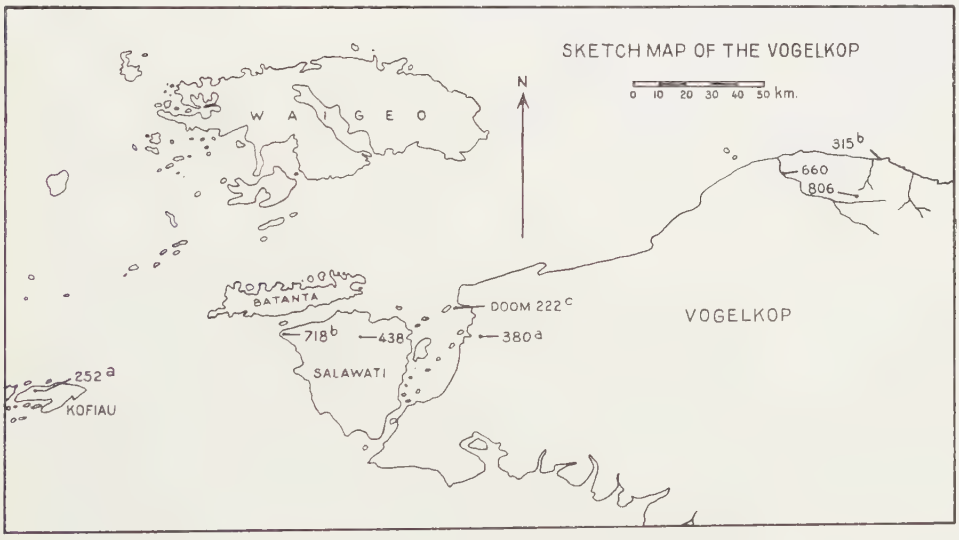

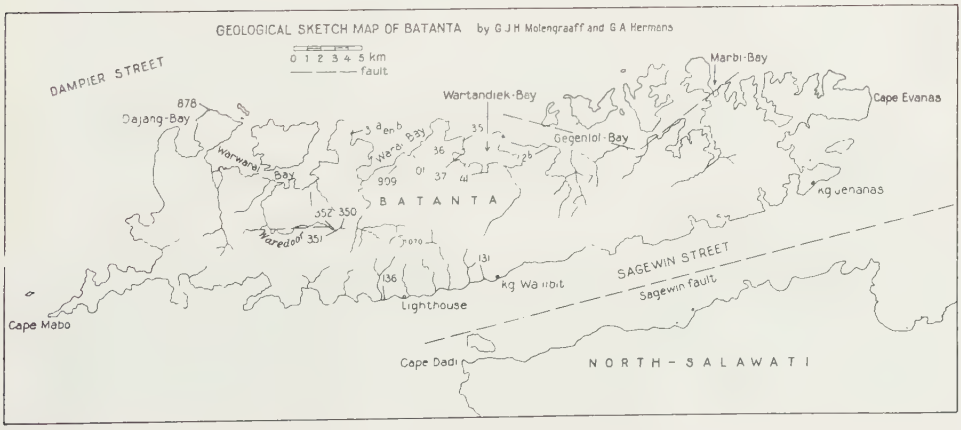

III. *The isle of Salawati.*

No. 438 Out of the Waidjang River.
Massive grey limestone (boulder), containing:
Lepidocyclina sp. sp., *Katacycloclypeus* sp. (plate, fig. 6), *Planorbulina larvata* (PARKER and JONES), *Rotalidae*, *Amphistegina* sp., *Cycloclypeus* sp., *algae*, *Globigerina* sp. (very numerous).

No. 718b Salawati (900 m east of Cape Dadi).
Fine-grained dark coloured limestone, containing:
Lepidocyclina parva OPPENOORTH (plate, fig. 7), *Miogypsina* s.str., sp., *Operculina* sp., *Amphistegina* sp., *Orbulina* sp., *Globigerina* sp. (very numerous), *algae*.

IV. *The isle of Batanta.*

No. 01 North Batanta (east side of Warai Bay, 1½ km N.E. of No. 909).
Light coloured *Operculina* limestone (Warai limestone) (boulder), containing:
Lepidocyclina sp., *Operculina* sp. (very numerous), *Planorbulina* sp., *Orbulina* sp., *Heterostegina* sp.

No. 2b South-west coast of Gegenlol Bay.
Massive yellow-brown limestone (Warai limestone), containing:
Lepidocyclina (*Nephrolepidina*) sp., *Operculina* sp., *Amphistegina* sp., *Rotalidae*, *Globigerina* sp. (numerous), *algae*.

No. 7 South coast of Gegenlol Bay.
Fine-grained grey limestone (Warai limestone), containing:
Eulepidina sp., *Amphistegina* sp., *Operculina* sp., *Globigerina* sp., *algae*.

No. 31a North Batanta (north-west side of Warai Bay).
Light limestone (Warai limestone), containing:
Lepidocyclina japonica YABE (plate, figs. 8 and 9), *Operculina* sp., *Rotalia* sp., *Heterostegina* sp., *Amphistegina* sp., *Alveolinella* sp., *Planorbulina larvata* (PARKER and JONES), *Globigerina* sp., *algae*.

No. 31b North Batanta (north-west side of Warai Bay).
Light coloured limestone (Warai limestone), containing:
Lepidocyclina sp., *Lepidocyclina* with *trybliolepidine nucleoconch* (plate, fig. 10), *Flosculinella bontangensis* L. RUTTEN, *Rotalia* sp.,

Fig. 1: *Austrotrillina howchini* (SCHLUMB.) (30 ×); Fig. 2: *Neoalveolina* sp. (30 ×); Fig. 3: *Quinqueloculina* sp. (30 ×); Fig. 4: *Lepidocyclina sumatrensis* (BRADY) (16 ×); Fig. 5: *Heterostegina borneënsis* VAN DER VLERK (30 ×); Fig. 6: *Katacycloclypeus* sp. (30 ×); Fig. 7: *Lepidocyclina parva* OPPENOORTH (30 ×); Figs. 8 and 9: *Lepidocyclina japonica* YABE (30 ×); Fig. 10: *Lepidocyclina* sp. (30 ×); Fig. 11: *Miogypsina* s. str. sp. (30 ×); Fig. 12: *Lepidocyclina ferreroi* PROVALE (30 ×); Fig. 13: *Alveolinella quoyi* (D'ORBIGNY) (12 ×).

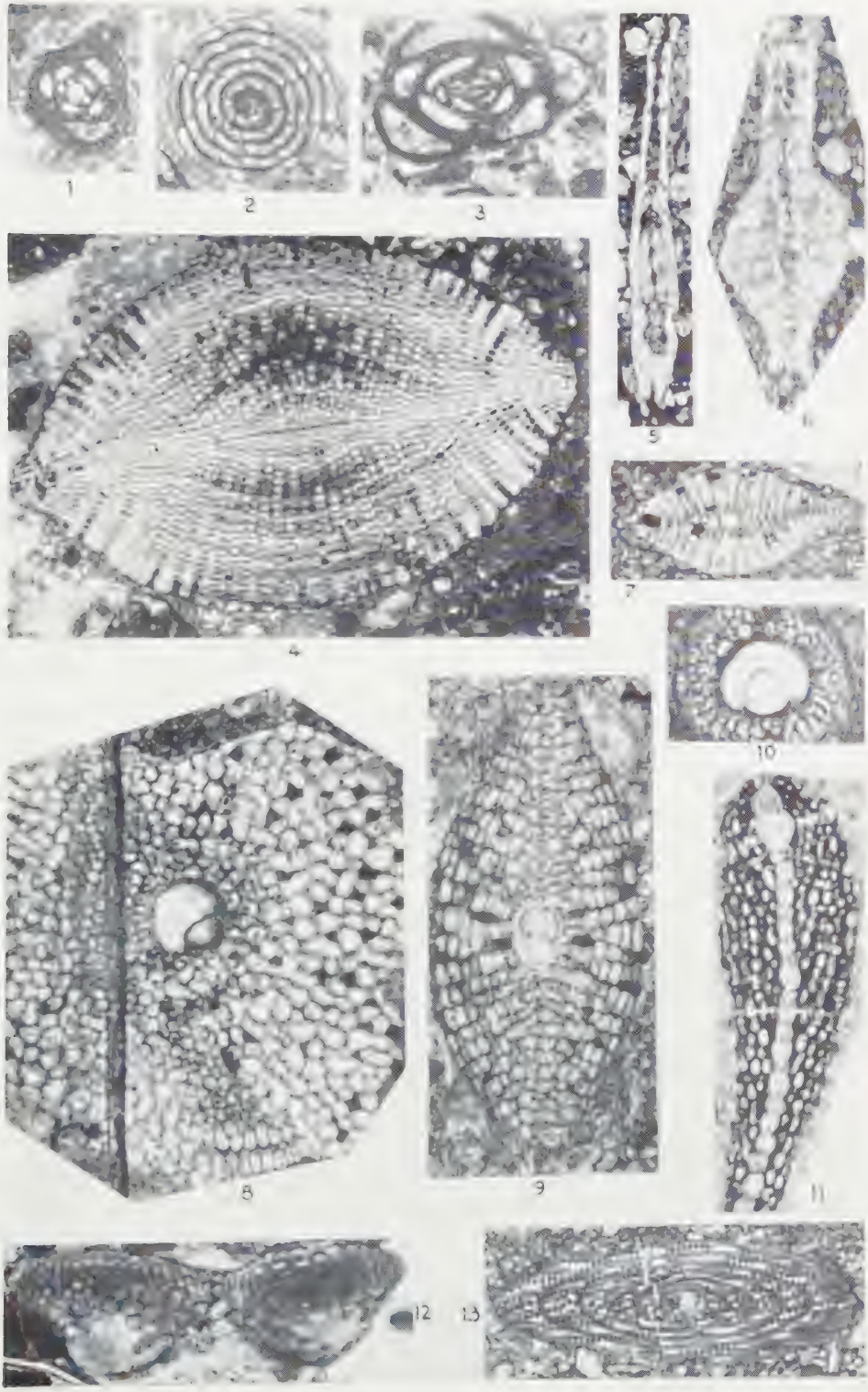
1
2
3
4
5
6
7
8
9
10
11
12
13

Heterostegina sp., *Operculina* sp., *Orbulina* sp., *Marginopora vertebralis* Quoy and Gaimard, *Amphistegina* sp., *Lithophyllum* sp., corals, *Globigerina* sp., *bryozoa*.

No. 35 West coast of Wartandiek Bay.
Light yellow limestone (Warai limestone), containing:
Lepidocyclina sp., *Operculina* sp., *Gypsina globulus* Reuss, *algae*, corals, *Globigerina* sp. (numerous).

No. 36 West coast of Wartandiek Bay.
Coarse-grained limestone (Warai limestone), containing:
Amphistegina sp., *Operculina* sp., *Planorbulina* sp., *Gypsina globulus* Reuss, *Globigerina* sp., corals, *algae*.

No. 37 West coast of Wartandiek Bay (North Batanta).
Light coloured limestone breccia (Warai limestone), containing:
Lepidocyclina sp., *Amphistegina* sp., *Operculina* sp., ? *Gypsina*, *Globigerina* sp., corals, *algae*.

No. 41 North Batanta, south coast of Wartandiek Bay.
Light coloured, rather coarse-grained limestone (Warai limestone), containing:
Miogypsina s. str. sp. (plate, fig. 11), *Katacycloclypeus* sp., *Flosculinella bontangensis*, L. Rutten, *Lepidocyclina* sp., *Amphistegina* sp., *Operculina* sp., ? *Cycloclypeus* sp., corals, *Globigerina* sp., *algae*.

No. 131 South coast of Batanta (1 km west of kg Wailibit).
Fine-grained yellow-brown limestone in coarser dark-grey limestone (Warai limestone), containing:
Miogypsina s. str. sp., *Lepidocyclina parva* Oppenoorth, *Gypsina globulus* Reuss, *Operculina* sp., *Amphistegina* sp., corals, *Globigerina* sp. (numerous), *algae*.

No. 136 South Batanta (1½ km north of the lighthouse).
Light grey limestone, containing:
Lepidocyclina sp., *Spiroclypeus* sp., *Eulepidina* sp., *Cycloclypeus* sp., *Rotalia* sp., *Amphistegina* sp., *Cymopolia* sp., corals (very numerous), *Lithophyllum* sp., *bryozoa*.

No. 350 West Batanta (upper course of the Warédoor River).
Fine-grained grey limestone (*Globigerina* limestone, Warai limestone), containing:
Miogypsina s. str. sp., *Lepidocyclina* sp., *Gypsina globulus* Reuss, *Cycloclypeus* sp., *Amphistegina* sp., *Globigerina* sp. (very numerous), *algae*.

No. 351 West Batanta (upper course of the Warédoor River).
Massive light brown limestone (Warai limestone), containing:
Eulepidina formosa Schlumberger, *Lepidocyclina* cf. *sumatrensis* (Brady), *Miogypsina* s. str. sp., *Heterostegina* sp., *Globigerina* sp. (numerous), *algae*.

No. 352 West Batanta (upper course of the Warédoor River).
Dark grey limestone (Warai limestone), containing:
Miogypsina s. str., sp., *Lepidocyclina ferreroi* PROVALE (plate, fig. 12), *Lepidocyclina* sp., *Cycloclypeus* sp., *Amphistegina* sp., *Planorbulina* sp., ? *Operculina*, corals, *algae*, *bryozoa*, *Globigerina* sp.

No. 878 N.W. Batanta (north point of the peninsula between Dajang Bay and Warwarai Bay).
Porous yellow-white fine-grained limestone (Dajang limestone), containing:
Miogypsina s. str. sp., *Operculina* sp., *Planorbulina* sp., *Orbulina* sp., *Rotalidae*, corals.

No. 909 North Batanta (east side of Warai Bay, 1½ km S.W. of No. 01).
Very light-coloured *Operculina* limestone (Warai limestone), containing:
Lepidocyclina sp., *Operculina* sp. (very numerous), *Heterostegina* sp., *Amphistegina* sp., *Globigerina* sp.

V. *The isle of Kofiau.*

No. 252a Kofiau, west of Salawati (north-eastern part of the Monges Hills).
Compact light-coloured limestone, containing:
Alveolinella quoyi (D'ORBIGNY) (plate, fig. 13), *Marginopora vertebralis* (QUOY and GAIMARD), *Cycloclypeus* sp., *Rotalia* sp., *Archaias* sp., *Globigerina* sp., *Amphistegina* sp., corals.

From these determinations the following conclusions can be drawn:
The oldest sample is number 222c. It is to be placed in the lower part of Tertiary e. Numbers 315b and 136 belong to Tertiary e and No. 136 perhaps to upper e. The limestones numbered 806, 380, 2b, 7, 35 and probably also the numbers 36 and 37 are formed during the upper e or lower f. Those numbered 660, 718b, 31a, 41, 131, 350, 351, 352 and 909 belong to upper e or f. For numbers 660, 41 and 909, and f-age is very probable. Also the numbers 878, 01, 31b are from the last-mentioned age. Number 252a, however, is probably younger.

Rijksmuseum van Geologie en Mineralogy, Leiden

LITERATURE

BAKX, L., De genra *Fasciolites* en *Neoalveolina* in het Indo-Pacifische gebied. Verh. Geol. Mijnb. Gen. Ned. en Kol., Geol. Ser. **IX** (1932).

BURSCH, JAC. GEORGE, Mikropaläontologische Untersuchungen des Tertiärs von Gross Kei (Molukken). Inaugural-dissertation. Basel 1947.

CAUDRI, B., Lepidocyclinen von Java. Verh. Geol. Mijnb. Gen. Ned. Kol. Geol. Ser. **XII** (1939).

Cole, W. S., Larger *Foraminifera* from Eniwetok atoll drill holes, U.S. Geol. Survey, Prof. paper, 260-V (1957).

————, Larger *Foraminifera* and smaller diagnostic *Foraminifera* from Bikini drill holes, U.S. geol. Survey, Prof. paper 260-0 (1954).

————, Geology of Saipan (Mariana Islands), chapter I: Larger *Foraminifera*, U.S. Geol. Survey, Prof. paper 280-E-J (1957).

———— and J. Bridge, Geology and Larger *Foraminifera* of Saipan Island, U.S. Geol. Survey, Prof. paper 253 (1953).

Hanzawa, Shoshiro, Cenozoic *Foraminifera* of Micronesia, Geol. Soc. of Am., Memoir 66 (1957).

Reichel, M., Sur la structure des Alvéolines, Eclogae geologicae Helvetiae, 24, 2 (1931).

Silvestri, A., Intorno all'*Alveolina Melo* d'Orbigny (1846), Riv. Ital. Pal. XXXIV (1928).

Vlerk, I. M. van der, Het genus *Lepidocyclina* in het Indo-Pacifische gebied. Wetensch. Meded. v.d. Dienst v.d. Mijnbouw in Ned.-Indië, No. 8 (1928) (also: Eclogae geologicae Helvetiae 21, 1 1928).

————, Correlation of Tertiary of the Far East and Europe. Micropaleontology, 1, 1, 72–75 (1955).

Yabe, H. and S. Hanzawa, *Lepidocyclina* from Naka-Kosaka, province of Kozuke, Japan. Jap. Journ. of Geol. and Geograph., 1, 1 (1922).

POSSIBLE INTERMEDIATES IN THE BIOSYNTHESIS OF PROTEINS: THE OCCURRENCE OF NUCLEOTIDE-BOUND CARBOXYL ACTIVATED PEPTIDES IN PREPARATIONS OF RIBONUCLEIC ACIDS FROM SOLUBLE AND PARTICULATE FRACTIONS OF YEAST CELLS

A PRELIMINARY NOTE [1] [2]

BY

S. R. DE KLOET, A. H. W. M. SCHUURS,
V. V. KONINGSBERGER AND J. TH. G. OVERBEEK

(Communicated at the meeting of March 26, 1960)

1. *Introduction*

The occurrence of dialysable carboxyl-activated peptide-nucleotide compounds in extracts of ether-CO_2 frozen baker's yeast was reported by a group of investigators from this laboratory about three years ago (1). During a study on the occurrence and the composition of these activated compounds, it was found (2–6) that they can be isolated from both the 100.000 g supernatant- and the microsomal RNP particulate fractions of yeast cells. Their probable chemical structure can be indicated as follows (4):

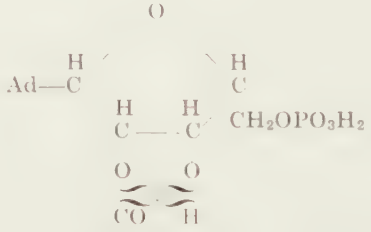

The isolation of similar peptide-nucleotide compounds from various tissues and microorganisms was described by a number of other authors (6–16, 19).

Regarding the reported rather general occurrence of peptide-nucleotide compounds in cells synthesizing proteins, it was considered of interest to

[1] This work was supported by the Netherlands Organization for Pure Research (Z.W.O.).

[2] The following abbreviations will be used: RNA, ribonucleic acid; RNP, ribonucleoprotein; Ad, adenine; AMP, adenosine monophosphate; ATP, adenosine triphosphate; PP, inorganic pyrophosphate.

obtain more experimental data on the origin of these compounds in the cell. In this paper, preliminary data are presented indicating the occurrence of carboxyl-activated nucleotide-bound peptides in preparations of ribonucleic acids (RNA) from both the 100.000 g supernatant (s-RNA)- and the microsomal RNP-particulate (m-RNA) fractions from cells of baker's yeast. Attention should be given to the fact, that the activated peptides occurring in preparations of RNA are not dialysable, in contradistinction to the activated peptides in yeast dialysate (1–6). This may be seen as an indication that they are bound to more than one nucleotide.

2. *Material and methods of preparation*

In most experiments, freshly obtained commercial baker's yeast ("koningsgist", Gist- en Spiritusfabriek, Delft) was used. The cells were broken up by grinding with carborundum; they were extracted with a 0.005 molar phosphate buffer pH 6.8 containing 3 μ mol Mg^{++} per ml. Whole cells, cellwalls and larger particles were spun off at 12.000 g in a refrigerated centrifuge: 100.000 g supernatant-and microsomal RNP-particulate fractions were obtained from the remaining extracts according to the method of Fu-Chuan Chao and Schachman [16]. RNA was isolated from these fractions by the phenol extraction method as described by Kirby [17]. As it has been stated [18] that the active RNA from yeast 100.000 g supernatant does not precipitate at pH 5, the extraction was performed without any preceding precipitations. The s- and m-RNA preparations were dialysed against water for 24 hours in the cold and concentrated by freeze-drying.

An instantaneous and very distinct ferric hydroxamate colour was observed when s-RNA preparations were incubated for a few minutes or less with 2 m salt-free hydroxylamine at 30° C, followed by the addition of an acidified (0.67 N HCl, 5 % TCA) $FeCl_3$ solution. With m–RNA preparations, the same procedure would yield hardly any distinguishable colour. Better results were obtained when the freeze-dried reaction mixture of m–RNA and hydroxylamine was subjected to paperelectrophoresis, the hydroxamate colour being developed by spraying the paper with the $FeCl_3$ solution.

The applied analytical reagents and procedures were essentially the same as have been described before (2, 4, 5); s–RNA and m–RNA preparations and the products of their reaction with salt-free hydroxylamine were subjected to paperelectrophoresis and paperchromatography.

3. *Paperelectrophoresis*

Preparations of s–RNA and of m–RNA were subjected to paperelectrophoresis on Whatman No. 3 paper in 0.02 m citrate buffer pH 3 and pH 4.1 and in 0.02 m phosphate buffer pH 6.2. The results of some representative experiments are shown in figs. 1 and 2. Measurements of the 260 mμ extinction indicated the presence of at least three nucleotide components in the s–RNA preparations. A distinct peak was found in the 260 mμ absorption in the direction of the cathode, at the spot where ninhydrin positive carboxyl activated compounds could be located by

spraying with 2 m salt-free hydroxylamine, heating to dryness (80° C) and subsequent spraying with $FeCl_3$ solution. Furthermore, a striking similarity was noticed between our present results with undialysable s-RNA and those with the carboxyl activated nucleotide-bound peptides from freeze-dried yeast dialysate (2–6), the main difference being the larger amount of nucleotide material in s-RNA.

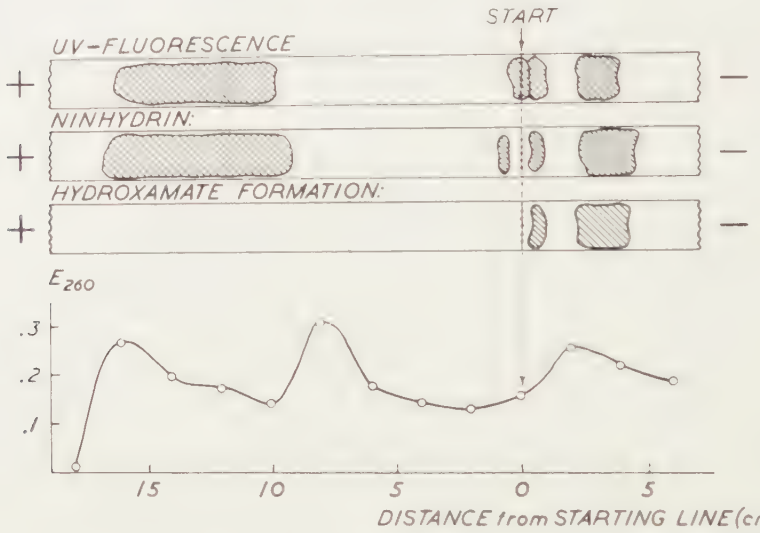

Fig. 1. Schematic outline of a paperelectrophoresis experiment with s-RNA, showing the spots with blue and violet fluorescence in U.V. light, a positive ninhydrin reaction, hydroxamate forming material and the course of the absorption at 260 mμ. Electrophoresis at 8 V cm^{-1} for 17 hours in 0.02 m phosphate buffer pH 6.2.

Hardly any fluorescence and no distinct hydroxamate colour could be observed when m-RNA preparations were subjected to paperelectrophoresis (fig. 2).

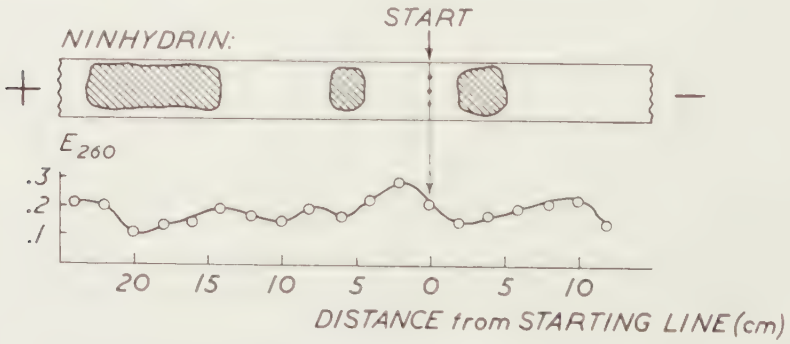

Fig. 2. Outline of a paperelectrophoresis experiment with m-RNA, showing ninhydrin positive spots and the course of the absorption at 260 mμ. Hardly any fluorescence was observed and the carboxyl-activated compounds could not be located. Electrophoresis at 8 V cm^{-1} for 17 hours in 0.02 m phosphate buffer pH 6.2.

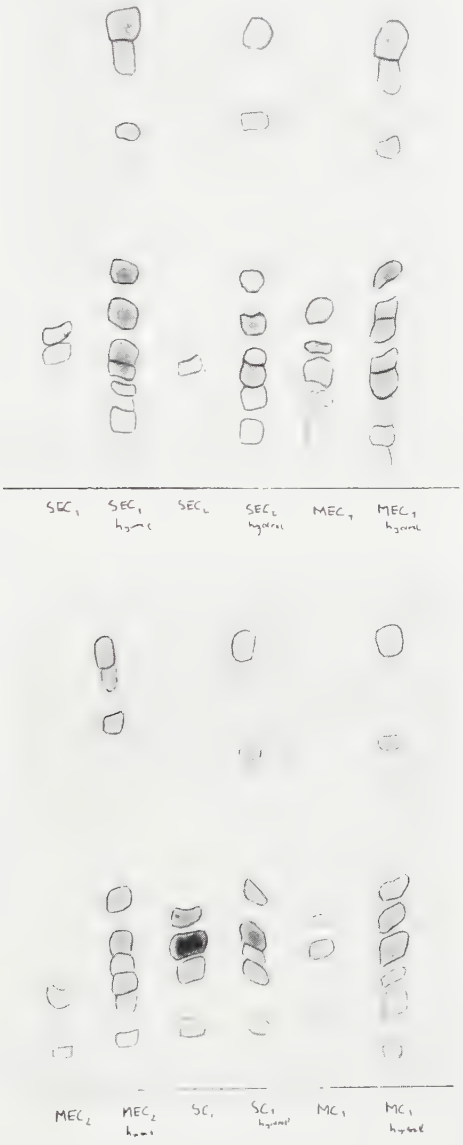

Fig. 3. Ninhydrin-sprayed chromatograms of hydrolysed and un-hydrolysed hydroxamic acids prepared from s-RNA and m-RNA preparations: see text and table I.

At least four peaks in the 260 mμ extinction indicated that the m–RNA preparation was also rather heterogeneous.

However, a distinct ferric hydroxamate colour and some blue-violet fluorescence was observed when the reaction mixture of m–RNA and 2 m salt-free hydroxylamine was subjected to electrophoresis after being kept at 30° C for 5 minutes and subsequent freeze-drying.

Hydroxamic acids from s–RNA and m–RNA preparations moved with the same velocity into the direction of the cathode and showed a similar blue-violet fluorescence in U.V. light. They were eluated and chromatographed in order to study their composition.

4. *Paperchromatography*

The following mixtures and compounds were subjected to paperchromatography on Whatman No. 1 filterpaper with n–butanol–acetic acid-water (9:1:1) as the solvent.

1. Preparations of s–RNA and of m–RNA were incubated for 5 minutes at 30° C with 2 m salt-free hydroxylamine, freeze-dried and extracted with a mixture of 50 % ethanol-50 % H_2O. Paperchromatograms of these extracts showed 3 (m–RNA) – 5 (s–RNA) spots with blue and violet fluorescence in U.V. light. Both preparations yielded only one spot showing a distinct ferric hydroxamate colour: this spot was eluated, one half being kept as a blank, the other half being hydrolysed with 6 N HCl. The hydrolysates and their blanks were run in separate chromatograms.
2. Hydroxamic acids from s–RNA and from m–RNA were subjected to paperelectrophoresis in 0.02 m citrate buffer pH 3. The zones containing the hydroxamic acids were eluated and chromatographed after freeze-drying. With both preparations, two spots showing a distinct ferric hydroxamate colour were obtained. These spots were eluated, treated as has been described above and re-chromatographed.

The results of our experiments are summarized in table I and illustrated in fig. 3.

TABLE 1

R_F values of hydroxamic acids from s-RNA and m-RNA in *n*-butanol-acetic acid-H_2O (9:1:1)

Spot	Hydroxamic acid from	Purified by	R_F
SC_1	s-RNA	single chromatography of 50 % EtOH-50 % H_2O extract	.23
MC_1	m-RNA	same as SC_1	.24
SEC_1	s-RNA	paperelectrophoresis at pH 3, followed by chromatography	.23
MEC_1	m-RNA	same as SEC_1	.24
SEC_2	s-RNA	same as SEC_1	.54
MEC_2	m-RNA	same as SEC_1	.55

The results with hydroxamic acids showing a low R_F are not conclusive for the presence of activated peptides (see fig. 3); both amino acyl– and peptide hydroxamates may be involved. The results obtained with the hydroxamic acids having a rather high R_F (SEC_2 and MEC_2) strongly suggest the presence of carboxyl-activated peptides in our preparations of both s– and m–RNA.

The sedimentation of both s– and m–RNA preparations has been studied in a SPINCO analytical ultracentrifuge. At least three peaks were obtained with our s–RNA preparations, showing sedimentation constants of 5, 2 and <1 Svedberg units. The m–RNA preparation showed four peaks with sedimentation constants of 5, 14, 20 and 30 Svedberg units. It is rather striking to notice the qualitative similarity of the hydroxamic acids that were isolated from these apparently different RNA preparations.

Our present knowledge about the biosynthesis of cytoplasmic proteins may be briefly outlined as follows:

1. Individual amino acids are activated (e.g. 20) according to:
   $R\text{–}HCNH_2\text{–}COOH + ATP + E(nzyme) \leftrightarrows E\text{–}AMP\text{–}CO\text{–}HCNH_2R + PP.$
2. Enzyme-bound carboxyl-activated amino acids are transferred to ribonucleic acids from the soluble fraction of the cell (e.g. 21, 22):
   $E\text{–}AMP\text{–}CO\text{–}HCNH_2\text{–}R + s\text{–}RNA \leftrightarrows s\text{–}RNA\text{–}CO\text{–}HCNH_2R + E + AMP$
3. The final condensation of carboxyl-activated protein precursors to proteins occurs in microsomal and other particulate fractions.

With regard to this knowledge, attention may be drawn to:

1. The probable structure of the carboxyl-activated peptides, which seem to be bound to one or more nucleotides.
2. The reported general occurrence of peptide-nucleotide compounds in cells synthesizing proteins.
3. The presence of carboxyl-activated peptide-nucleotide compounds in preparations of both s– and m–RNA, as well as in isolated microsomal RNP particles.

In our opinion, this experimental evidence suggests the occurrence of a "pre-particulate" condensation of s–RNA bound carboxyl-activated amino acids to specific nucleotide-bound activated peptides.

5. *Summary*

Ribonucleic acids have been isolated from 100.000 g supernatant- and microsomal ribonucleoprotein particulate fractions of baker's yeast. Experimental evidence is presented, indicating the presence of carboxyl-activated peptide compounds in both ribonucleic acid preparations. The possible bearing of these activated compounds on the biosynthesis of proteins is briefly discussed.

REFERENCES

1. Koningsberger, V. V., Chr. O. van der Grinten and J. Th. G. Overbeek, Proc. Kon. Ned. Akad. Wetensch. **B 60**, 144 (1957).
2. ———, ——— and ———, Biochim. Biophys. Acta **26**, 483 (1957).
3. Grinten, Chr. O. van der, A. H. W. M. Schuurs and V. V. Koningsberger, IVth Int. Congr. Biochem., Abstracts 30 (1958).
4. ———, Thesis, Utrecht (1959).
5. Koningsberger, V. V., 10 Coll. d. Gesellschaft f. physiol. Chemie, Mosbach, 50 (Springer Verlag, Berlin, 1959).
6. Weil, J. H., G. Dirheimer and J. P. Ebel, IVth Int. Congr. Biochem., Abstracts 21 (1958).
7. Brown, A. D., Biochim. Biophys. Acta **30**, 447 (1958).
8. Harris, G., J. W. Davies and R. Parsons, Nature **182**, 1565 (1958).
9. Gilbert, D. A. and E. W. Yemm, Nature **182**, 1745 (1958).
10. Bergkvist, R., Acta Chem. Scand. **12**, 364 (1958).
11. Ebel, J. P., 10 Coll. d. Gesellschaft f. physiol. Chemie, Mosbach, 70 (Springer Verlag, Berlin, 1959).
12. Mandel, P., ibidem 71 (1959).
13. Harris, G., Nature **184**, 788 (1959).
14. Hase, E. and S. Mihara, Arch. Biochem. Biophys. **83**, 170 (1959).
15. ——— and ———, Biochim. Biophys. Acta **32**, 298 (1959).
16. Fu-Chuan Chao and K. H. Schachman, Arch. Biochem. Biophys. **61**, 220 (1956).
17. Kirby, K. S., Biochem. J. **64**, 405 (1956).
18. Osawa, S. and E. Otaka, Biochim. Biophys. Acta **36**, 549 (1959).
19. Habermann, V., Biochim. Biophys. Acta **32**, 297 (1959).
20. Davie, E. W., V. V. Koningsberger and F. Lipmann, Arch. Biochem. Biophys. **65**, 21 (1956).
21. Hoagland, M. B., P. C. Zamecnik and M. L. Stephenson, Biochim. Biophys. Acta **24**, 215 (1957).
22. ———, ——— and ———, Symp. Mol. Biol. at Chicago, 104 (1959).

DICERORHINUS KIRCHBERGENSIS IN THE TIGLIAN?

BY

H. LOOSE

(Communicated by Prof. I. M. VAN DER VLERK at the meeting of March 26, 1960)

In 1927 J. J. A. BERNSEN described a maxillar dentition of *Dicerorhinus kirchbergensis* from the Tiglian. This identification has since been accepted and copied in all lists of European quaternary faunas. Now in recent years all other old pleistocene finds of *D. kirchbergensis* have been shown either to represent *D. etruscus* or to be of younger date. Therefore the arguments advanced by BERNSEN will be reexamined in the following.

BERNSEN described a maxillar dentition of "*Rhinoceros Mercki*" lacking the right P^2 and the greater part of the left P^3 (only fragments of the outer ectoloph wall are present). The right P^3 has no outer wall so that here too exact dimensions can not be given. The animal was of considerable age, its teeth show considerable wear.

BERNSEN writes:

"The great wear of the upper dentition has caused many characters, among which the primary character, to disappear. The remaining ones do not point to *Rh. etruscus*, but to *Rh. Mercki*, viz:

1. The exceedingly weak development of the inner cingulum in premolars and molars.
2. The direction of this cingulum in the pm 2 and 1 (P^3, P^4).
3. The great gradient of the anterior cingulum.
4. The V-shaped entrance to the medisinus of the molars, which, though comparatively wide in mol. 2, falls within the limits of variation of the *Mercki* forms studied by me.
5. The curved outer surface in mol. 3.
6. The thick cement covering of the outer wall of the molars.
7. The size of the separate teeth which exceeds that of all *etruscus* forms".

On reexamination of these seven points the following is seen:

(Point 1) The dentition has worn down close to the cingulum. This, and the fact that the enamel curves in on the lingual side of the chewing surface, makes it extremely difficult to say how much of a cingulum there actually was. Furthermore the argument loses much weight when BERNSEN writes a few lines lower:

"The dentition in Maastricht Museum possesses characters pointing in the direction of *Rh. Mercki*, as the development of the inner cingulum, which is insignificant for *Rh. etruscus*."

Nevertheless BERNSEN gives its determination as *Rh. etruscus*.

(Point 2) Both P^3 and P^4 have worn to such a degree that it is impossible to evaluate the exact development of the inner cingulum. BERNSEN's statement that the inner cingulum is absent on the anterior part of the right P^3 is not supported by examination of his specimen. The same holds for the right and left P^4.

(Point 3) BERNSEN here refers to the fact that the anterior cingulum of the M^1 and M^2 on the lingual side does not turn up at an angle, but sharply downwards. This is a situation which on the evidence of other molars of D. etruscus probably is a result of heavy wear. The upward curve which should be found on the lingual side of the protoloph is absent. Intermediate forms can be found in etruscus molars showing less wear.

(Point 4) Here again BERNSEN makes a risky assumption on the basis of a feature which he should not use in an absolute sense but only comparatively.

The shape of the medisinus entrance (protoloph sloping, metaloph steep, the medisinus rather wide, rounded, on the border between protoloph and metaloph a shallow incision) in the dentition from Steyl does not differ significantly from that of other molars from the Tegelen area.

(Point 5) Marked cases of this may also be found in *D. etruscus* molars. Only heavy wear makes the curvature look more pronounced.

(Pint 6) The thickness of the cement covering in the fossil depends on the degree of conservation. Other molars from Tegelen show quite definitely thar the cement covering was lost in preparation. Other etruscus molars (in the Leiden Museum for instance the molars described by STROMER VAN REICHENBACH 1899) show appreciable cement covering.

(Point 7) The principal argument of BERNSEN: the size of the molars. BERNSEN measured the molars stuck together with a bituminous substance. For all measurements and comparisons he always used complete dentitions or rows of elements. Obviously, reliable results cannot be obtained this way.

After separation and thorough cleaning, the following dimensions have been obtained (figures between brackets are those given by BERNSEN): (see table).

Dimensions by and large fall within the range indicated for *D. etruscus* from Mosbach (larger molars from other localities are known).

BERNSEN states that the molars from Steyl are *smaller* than the *R. megarhinus* (= *D. kirchbergensis*) molars from Grays and Ilford, Essex,

TABLE 1

		Tegelen (Steyl)		D.etruscus Mosbach	D.kirchbergensis (Schroeder '30)
		sin.	dext.		
length ectoloph	P^2	32 (32)	—	30–35	32–36
width protoloph		37 (39)	—	34–42	34–43
	P^3	—	—	33–36	36–46
		—	—	49–53	55–70
	P^4	ca. 41 (ca. 40)	38 (39)	36–41	40–53
		61 (62)	57 (57)	55–64	55–74
	M^1	ca. 47 (ca. 43)	ca. 45 (ca. 43)	42–49	47–60
		61 (63)	62 (63)	53–63	63–72
	M^2	52 (55)	52 (55)	46–51*)	52–63
		63 (64)	62 (64)	57–62	63–73
	M^3	60 (65)	59.5 (62)	51–61	61–71
		59 (62)	58 (61)	50–58	58–70

*) FREUDENBERG, 1914, mentions a specimen with Length 55.

and the *Rh. leptorhinus Owen* (= *D. hemitoechus Falc.*) molars from Barrington, all in the British Museum. They are about the same size as the molars of *Rh. leptorhinus Owen* (= *D. hemitoechus*) from Ilford, Essex and Peckham and the *Rh. Mercki* (= *D. kirchbergensis*) molars from Mosbach described by SCHROEDER 1903, page 108.

They are *larger* than all other *Rh. leptorhinus* molars in the British Museum and some molars of *Rh. Mercki* described by SCHROEDER 1903, pp. 106 en 133. These are the conclusions given by BERNSEN.

The new measurements show:

The molars from Steyl fall within the range of *D. etruscus*. They are too small for *D. kirchbergensis*. The measurements in the table for this species are taken from SCHROEDER, who did not recognize *D. hemitoechus* as a separate species. His *Rhinoceros Mercki* (and BERNSEN's) is a combination of *D. hemitoechus* and *D. kirchbergensis*. As the teeth of *D. hemitoechus* are on the average smaller than those of *D. kirchbergensis* the minimum values for the latter should actually be higher than those given in the table. There remains no argument not to attribute the Steyl dentition to *D. etruscus*.

Rijksmuseum van Geologie en Mineralogie, Leiden

LITERATURE

BERNSEN, J. J. A., The Geology of the Teglian Clay and its Fossil Remains of *Rhinoceros* (1927).

FREUDENBERG, W., Die Säugetiere des älteren Quartärs von Mitteleuropa. Geologische und Pal. Abhandl. N.F. 12, 4/5 (1914).

SCHROEDER, H., Die Wirbelthierfauna des Mosbacher Sandes, I Gattung *Rhinoceros*. Abh. K. Pr. Geol. Landesanst. N.F. Heft 18 (1903).

STROMER VON REICHENBACH, E., Über *Rhinoceros*-Reste im Museum zu Leiden. Samml. des Geol. Reichs-Museums in Leiden, N.F. II, II (1899).

CONTENTS

PRINTED IN THE NETHERLANDS
DRUKKERIJ HOLLAND N.V., AMSTERDAM